

Copyright is owned by the Author of the thesis. Permission is given for a copy to be downloaded by an individual for the purpose of research and private study only. The thesis may not be reproduced elsewhere without the permission of the Author.

HEAT TRANSFER DURING FREEZING OF FOODS AND
PREDICTION OF FREEZING TIMES

A thesis presented in partial fulfilment of the requirements for the degree of Doctor of Philosophy in Biotechnology at Massey University.

ANDREW CHARLES CLELAND

1977

HEAT TRANSFER DURING FREEZING OF FOODS AND
PREDICTION OF FREEZING TIMES

ABSTRACT

A study of methods for predicting the freezing time of foods was made. Four shapes - finite slabs, cylinders, spheres and rectangular bricks were considered.

For each shape experimental measurements of the freezing time were made over a wide range of conditions using Karlsruhe test substance, a defined analogue material. Experiments with slabs of minced lean beef and mashed potato were also conducted.

Practical food freezing problems, where the material is initially superheated above its freezing point and the third kind of boundary condition (convective cooling) is applied, have not been solved analytically because of the non-linear boundary conditions. Food materials when freezing release latent heat over a range of temperature which further complicates any attempt at solution.

The accuracy of the various solutions to the freezing problem proposed in the literature was evaluated by comparison of the various calculated freezing times with the experimentally determined values over a total of 187 freezing experiments.

For those solutions requiring numerical evaluation, the best was found to be a three-level finite difference scheme which generally gave a prediction of the freezing time to within $\pm 9\%$ of the experimental values with 95% confidence. With the regular geometric shapes investigated finite elements have no advantage over finite differences and were not considered.

For the existing exact and approximate analytical solutions, it is shown that these do not give accurate prediction of the freezing time for any of the four shapes,

mainly because all but two of these solutions do not take account of initial superheat in the material to be frozen, and these two solutions are for initial superheat in a semi-infinite slab, not a finite slab.

For the existing empirically modified solutions and empirical relationships, it is shown that they do not give accurate prediction of freezing time; at best the 95% confidence limits of the percentage difference between the calculated and experimental freezing times are 0% to +20% for slabs, cylinders and spheres.

All solutions for freezing of rectangular bricks with the third kind of boundary condition use the geometric factors derived by Plank. These factors are shown to be subject to error, the error increasing as the ratios of the two larger dimensions to the smallest increase.

A group of formulae is proposed which are simple to use and give accurate prediction of freezing time. They modify the geometric factors in Plank's equation, taking initial superheat into account, and in the case of rectangular bricks correct the errors inherent in these geometric factors. This group of simple formulae are shown to predict the freezing time with 95% confidence to within 5% of the experimental values for slabs, to within 7% for cylinders and spheres, and to within 10% for rectangular bricks.

The prediction accuracy of the simple formulae and the three level finite difference scheme are similar but the simple formulae can be calculated quickly without the use of a computer which is a big advantage. In addition to simplicity and accuracy the simple formulae are also versatile, and by use of suitable approximations can handle some practical problems in which conditions change with time.

ACKNOWLEDGEMENTS

I wish to acknowledge the following:-

- Professor R.L. Earle for his supervision and assistance.
- Dr. S.H. Richert and Dr. R.H. Villet for their supervision.
- Hoechst New Zealand Limited for supplying methylcellulose samples.
- Dr. I.F. Boag for valuable assistance in the statistical analysis of data.
- Mr. J.T. Alger and Mr. D.W. Couling for their assistance in building and maintaining equipment.
- Rosemary for moral support and for proof reading.

CONTENTS

	<u>ABSTRACT.</u>	2
	<u>ACKNOWLEDGEMENTS.</u>	4
	<u>CONTENTS.</u>	5
	<u>LIST OF FIGURES.</u>	10
	<u>LIST OF TABLES.</u>	14
1	<u>INTRODUCTION.</u>	16
2	<u>LITERATURE REVIEW.</u>	18
2.1	Problem Definition.	18
2.1.1	Definition of freezing time.	18
2.1.2	Boundary conditions.	19
2.1.3	Initial conditions.	20
2.2	Solutions Using the Assumption of a Unique Freezing Temperature.	21
2.2.1	Exact solutions for slabs.	21
2.2.2	Approximate solutions for slabs.	21
2.2.2.1	Integral profile and variational techniques.	21
2.2.2.2	Solutions for alloy solidification.	22
2.2.2.3	Other analytical approaches.	23
2.2.2.4	Solutions for aqueous systems.	23
2.2.3	Solutions for other shapes.	23
2.2.4	Empirical relationships.	24
2.2.5	Use of analogues.	25
2.2.6	Numerical solutions.	26
2.3	Solutions Using Changing Apparent Specific Heat Capacity and Varying Thermal Conductivity.	26
2.4	Summary.	28
3	<u>PRELIMINARY CONSIDERATIONS</u>	30

4	<u>COLLECTION OF EXPERIMENTAL DATA.</u>	32
4.1	Introduction.	32
4.2	Choice of Freezing Material.	32
4.3	One-Dimensional Heat Transfer in Slabs.	34
4.3.1	The equipment.	34
4.3.2	Dimensional measurement and control.	35
4.3.3	Temperature measurement and control.	38
4.3.4	Measurement and control of the surface heat transfer coefficient.	39
4.3.5	Analysis of heat transfer in slabs.	41
4.4	Radial Heat Transfer in Cylinders and Spheres.	45
4.4.1	The equipment.	45
4.4.2	Dimensional measurement and control.	55
4.4.3	Temperature measurement and control.	55
4.4.4	Measurement and control of the surface heat transfer coefficient.	55
4.4.5	Analysis of heat transfer in radial geometry.	58
4.5	Three-Dimensional Heat Transfer in Rectangular Bricks.	65
4.5.1	The equipment.	65
4.5.2	Dimensional measurement and control.	66
4.5.3	Temperature measurement and control.	67
4.5.4	Measurement and control of the surface heat transfer coefficient.	67
4.5.5	Analysis of heat transfer in rectangular bricks.	68
5	<u>EXPERIMENTAL DESIGN AND RESULTS.</u>	71
5.1	Introduction.	71
5.2	Slabs.	71
5.3	Cylinders and Spheres.	73
5.4	Rectangular Bricks.	74

6	<u>PREDICTION OF FREEZING TIME BY NUMERICAL METHODS</u>	93
6.1	Slabs.	93
6.1.1	Selection of numerical method.	93
6.1.2	Selection of finite difference approach.	95
6.1.3	Comparison of finite difference schemes.	96
6.2	Cylinders and Spheres.	105
6.2.1	Selection of numerical method.	105
6.2.2	Selection of finite difference approach.	106
6.2.3	Comparison of finite difference schemes.	106
6.3	Rectangular Bricks.	112
6.3.1	Selection of numerical method.	112
6.3.2	Selection of finite difference method.	112
6.3.3	Use of the finite difference scheme.	113
6.4	Summary.	119
7	<u>PREDICTION OF FREEZING TIME BY SIMPLE FORMULAE.</u>	121
7.1	Thermal Data.	121
7.2	Slabs.	121
7.2.1	Solutions for the first kind of boundary condition.	123
7.2.2	Solutions for the third kind of boundary condition.	123
7.2.3	Empirical modifications and formulae.	128
7.2.4	Present developments.	129
7.3	Cylinders and Spheres.	131
7.3.1	Solutions for the first kind of boundary condition.	131
7.3.2	Solutions for the third kind of boundary condition.	134

7.3.3	Empirical modifications and formulae.	134
7.3.3.1	Cylinders.	134
7.3.3.2	Spheres.	135
7.3.4	Present developments.	136
7.4	Rectangular Bricks.	137
7.4.1	Existing formulae.	137
7.4.2	Present developments.	141
8	<u>COMPARISON OF NUMERICAL AND SIMPLE METHODS FOR PREDICTING FREEZING TIMES.</u>	145
9	<u>PREDICTION OF FOOD FREEZING TIMES FOR SITUATIONS WITH NON-CONSTANT CONDITIONS.</u>	161
9.1	Introduction.	161
9.2	Varying Ambient Temperature.	161
9.3	Non-Uniform Initial Temperature.	162
9.4	Changing Surface Heat Transfer Coefficient.	163
9.5	Irregular Geometry.	164
9.6	Non-Homogeneous Food Material.	165
9.7	Summary.	165
10	<u>CONCLUSIONS.</u>	167
	<u>NOMENCLATURE.</u>	169
	<u>REFERENCES.</u>	172
	<u>APPENDICES.</u>	
1	General Description of Finite Difference Programs.	185
2	One-Dimensional Finite Difference Programs.	194
3	Two- and Three-Dimensional Finite Difference Programs.	204
4	Radial Finite Difference Program.	217
5	Derivation of Mellor's Formula.	222

6	Investigation of Changing Ambient Temperature.	225
7	Investigation of Non-Uniform Initial Temperature.	231

LIST OF FIGURES

4.1	Schematic outline of the experimental plate freezer.	36
4.2	Test slabs.	37
4.3	Typical temperature/time profiles for thermocouples placed at, or near, the surface of a freezing slab.	46
4.4	Schematic outline of the experimental liquid immersion freezer.	47
4.5	The sample oscillator used in liquid immersion freezing experiments	48
4.6	Schematic outline of the system used to oscillate cylinders in the liquid immersion freezer	49
4.7	Arrangement of the polystyrene foam caps and thermocouple leads for cylinders.	50
4.8	Insertion of thermocouples in the spheres.	53
4.9	Schematic outline of the experimental air blast freezer.	54
4.10	Typical finite difference results for freezing of a sphere.	61
4.11	Typical experimental results for air blast freezing of a cylinder.	62
4.12	Attachment of lids to the plastic boxes.	63
4.13	Typical polypropylene containers used in the experimental investigation into freezing of rectangular bricks.	64

5.1	Typical temperature curves for freezing of a slab of Karlsruhe test substance (Run F17).	86
5.2	Typical temperature curves for freezing of a slab of Karlsruhe test substance (Run F14).	87
5.3	Typical temperature curves for freezing of a cylinder of Karlsruhe test substance (Run C3).	88
5.4	Typical temperature curves for freezing of a sphere of Karlsruhe test substance (Run S1).	89
5.5	Typical temperature curves for freezing of a rectangular brick of Karlsruhe test substance (Run B72).	90
5.6	Typical temperature curves for freezing of a rectangular brick of Karlsruhe test substance (Run B55).	91
5.7	Typical temperature curves for freezing of a rectangular brick of Karlsruhe test substance (Run B43).	92
6.1	Thermal property curves used to approximate freezing at a unique phase change temperature.	98
6.2	The finite difference grid at the surface of a freezing slab.	98
6.3	Thermal conductivity data.	99
6.4	Apparent specific heat capacity data for Karlsruhe test substance.	99
6.5	Apparent specific heat capacity data for minced lean beef.	100
6.6	Apparent specific heat capacity data for mashed potato.	100

- 6.7 Frequency diagram of the percentage differences between experimental freezing times for slabs, and times calculated by finite differences. 104
- 6.8 Typical temperature and thermal conductivity profiles through a freezing sphere or cylinder showing the effect of a linear approximation of the thermal conductivity. 109
- 6.9 Frequency diagram of the percentage differences between experimental freezing times for cylinders, and times calculated by finite differences. 110
- 6.10 Frequency diagram of the percentage differences between experimental freezing times for spheres, and times calculated by finite differences. 110
- 7.1 Frequency diagram of the percentage differences between experimental freezing times for slabs, and times calculated by solutions with the first kind of boundary condition. 125
- 7.2 Frequency diagram of the percentage differences between experimental freezing times for slabs, and times calculated by solutions with the third kind of boundary condition. 125
- 7.3 Schematic diagram showing the heat to be removed in freezing of slabs. 126
- 7.4 Frequency diagram of the percentage differences between experimental freezing times for slabs, and times calculated by empirical modifications and formulae. 127

7.5	Frequency diagram of the percentage differences between experimental freezing times for cylinders, and times calculated by various methods.	133
7.6	Frequency diagram of the percentage differences between experimental freezing times for spheres, and times calculated by various methods.	133
7.7	Plot of the average prediction error (when comparing calculated freezing times to experimental results for rectangular bricks) versus number of equivalent heat transfer dimensions.	140
8.1	Frequency diagram of the percentage differences between experimental freezing times, and calculated freezing times.	146
A5.1	Schematic representation of typical temperature profiles within a freezing material where freezing occurs at a unique phase change temperature T_f .	223
A6.1	Ambient temperature profiles.	226

LIST OF TABLES

5.1	Typical conditions in food freezers.	76
5.2	Design of the factorial experiment for investigation of the freezing times of slabs of Karlsruhe test substance.	77
5.3	Experimental data for freezing of slabs of Karlsruhe test substance.	78
5.4	Experimental data for freezing of minced lean beef (M) and mashed potato (P) in slabs.	80
5.5	Experimental data for freezing of cylinders of Karlsruhe test substance.	81
5.6	Experimental data for freezing of spheres of Karlsruhe test substance.	82
5.7	Experimental data for freezing of rectangular bricks of Karlsruhe test substance.	83
6.1	Comparison of results from the three-dimensional program to a known analytical solution for cooling of a cube.	116
6.2	Results from the finite difference simulation of the freezing of rectangular bricks.	117
7.1	Thermal data for freezing food materials.	122
7.2	Comparison of experimental freezing times with times calculated by Neumann's method.	124
7.3	Prediction of freezing times of slabs of minced lean beef and mashed potato by equations 7.4 and 7.5.	132

7.4	Means and 95% confidence limits for the applicability of equations 7.19 to 7.27 to the experimental data.	144
8.1	Experimental and calculated freezing time data for all shapes.	151
8.2	Means and standard deviations of the percentage differences between experimental freezing times, and times calculated from (a) the three-level finite difference scheme, (b) equations 7.19 to 7.27.	158
8.3	Comparison of methods for prediction of food freezing times.	159
A6.1	Conditions used for the investigation of the effect of changing ambient temperature on freezing time.	228
A6.2	Results of the finite difference simulation of freezing of a slab subject to a cycling ambient temperature.	229
A6.3	Results of the finite difference simulation of freezing of a slab subject to an exponential fall in ambient temperature.	230
A7.1	Results from the finite difference simulation of freezing of a slab of Karlsruhe test substance with non-uniform initial temperature.	232

1 INTRODUCTION

With the development of agricultural efficiency in rural regions and the concentration of the world's population in urban areas, there is an increasing need for efficient food transportation from the production area to the market. In order to minimise quality losses in transport and distribution a variety of means for food preservation are used. Low temperature is one of the most important means as it retains, more closely than any other means, the "fresh" quality of the food.

Because of the importance of food freezing and chilling there has been a considerable amount of research into the physical, chemical and biological changes that occur in these processes, and how these affect the organoleptic appeal of the food. The major emphasis in this research has been to find a set of chilling or freezing conditions that minimises damage to the food product. Another important aspect of the research is gathering of data for the design of freezing and chilling equipment.

In order to be able to build a satisfactory food freezer the engineer must be able to predict the rate of freezing. He must be able to predict how long it takes for a package of food to freeze under various possible conditions so that the freezing process can be optimised.

In spite of extensive research into the physical aspects of food freezing there is, up to the present, no totally satisfactory method for predicting the freezing time of foods. The economic importance, especially to a country such as New Zealand, of being able to design food freezers accurately warranted further research to see if any reliable method for freezing time prediction does indeed exist. Accurate freezer design will reduce the costs to New Zealand of producing frozen foods for export, and hence the benefit from selling agricultural produce overseas will increase. Also, if the physics of a freezing

process are well understood biological and chemical changes can be correlated more easily with the conditions of freezing.

2 LITERATURE REVIEW

2.1 PROBLEM DEFINITION

2.1.1 Definition of Freezing Time

The problem of predicting the time for a material to freeze under a given set of conditions is classed physically as one of heat conduction with change of phase. This situation is described by the partial differential equation of heat conduction, subject to boundary conditions and initial conditions according to the particular circumstances:

$$C(T) \frac{\partial T}{\partial t} = \frac{\partial}{\partial x} \left(k(T) \frac{\partial T}{\partial x} \right) + \frac{\partial}{\partial y} \left(k(T) \frac{\partial T}{\partial y} \right) + \frac{\partial}{\partial z} \left(k(T) \frac{\partial T}{\partial z} \right) \quad (2.1)$$

Foods when freezing release latent heat over a range of temperature (Rolfe 1968) so that there is no sharp transition between the frozen and unfrozen material, but rather an intermediate "mushy" zone, the size of which depends on the freezing conditions. It is the presence of this zone and the resulting variation in the thermal properties of the partially frozen material, together with the non-linear boundary conditions that make the prediction of food freezing times so difficult.

The change of phase can be taken into account in two different ways. It can be assumed that all the latent heat is released at a unique freezing temperature at which a step change in thermophysical properties occurs (Carslaw and Jaeger 1959, p282). Alternatively, the release of latent heat over a range of temperature can be taken into account by using changing apparent specific heat capacity $C(T)$, and varying thermal conductivity $k(T)$ (Comini and Bonacina 1974a). The first method has been used extensively, even though variation in thermal properties means that a freezing foodstuff will fit a solution only approximately. The substantial and irregular way in which specific heat capacity and thermal conductivity change with temperature for foods limits the use of the second,

but more physically correct, method to numerical treatment.

This latter method also introduces a problem in defining the completion of freezing. Whereas freezing is deemed complete when the phase change front reaches the thermodynamic centre of the material in the first method, the presence of the mushy zone precludes the use of such a definition. Instead, the material is considered frozen when its thermodynamic centre attains a certain temperature; -5°C , -10°C and -18°C have been commonly used (Rolfe 1968; International Institute of Refrigeration 1972, p36; James et al 1976). An appreciable amount of latent heat is released in the temperature range -5°C to -10°C for most common food products, but there is little latent heat released between -10°C and -18°C (Rolfe 1968). Consequently a final centre temperature of -10°C will be used as an index of the completion of freezing for both experimental and theoretical estimations of freezing time, except in cases where a sharp phase change front is postulated.

2.1.2 Boundary Conditions

There are three boundary conditions of importance in food freezing problems. These are traditionally called the first, third and fourth kinds of boundary condition. The first kind of boundary condition is also known as a prescribed surface temperature :

$$T_s = T_a \quad \text{for } t > 0 \quad (2.2)$$

where T_s = surface temperature ($^{\circ}\text{C}$)

T_a = external medium temperature ($^{\circ}\text{C}$)

t = time (s)

The third kind of boundary condition is the case where Newton's law of cooling, or convective cooling, occurs :

$$h(T_a - T_s) = -(k(T) \frac{\partial T}{\partial x})_{x=0} \quad \text{for } t > 0 \quad (2.3)$$

where $k(T)$ = thermal conductivity ($W/m^{\circ}C$)
 h = surface heat transfer coefficient ($W/m^2^{\circ}C$)
 x = displacement from the surface (m)

The fourth kind of boundary condition is where the surface temperature is an arbitrary function of time :

$$T_s = f(t) \quad \text{for } t > 0 \quad (2.4)$$

The first kind of boundary condition can be treated as a special case of either the third kind (by setting $h = \infty$), or of the fourth kind (where $f(t) = T_a$). In practical problems h is never infinite as there are always resistances to heat transfer, for example imperfect thermal contact in plate freezing, and the film coefficient in liquid immersion freezing. The form of the function $f(t)$ can only be found by experiment in most practical situations, and so this boundary condition is not useful for prediction of food freezing times. Therefore the third kind of boundary condition is the most important as it takes account of those cases that approximate the first kind of boundary condition and, in general, describes the way in which the surface temperature varies with time.

2.1.3 Initial Conditions

Both constant and non-constant initial temperature distributions occur in practice. Generally, analytical solutions to freezing problems can only be found if a uniform initial temperature throughout the material is used. Numerical solutions can handle either type of initial distribution. Use of a mean bulk temperature allows a non-constant initial temperature distribution to be approximately related to a constant one, and then the simpler solutions based on uniform initial temperature can be used.

In most food freezing problems the material is initially superheated, that is initially at a temperature above that at which it starts to freeze.

2.2 SOLUTIONS USING THE ASSUMPTION OF A UNIQUE FREEZING TEMPERATURE

2.2.1 Exact Solutions for Slabs

Even with the assumption that all latent heat is released at a moving boundary in the cooling material, analytical solution of freezing problems is very difficult because of the non-linear boundary conditions. Therefore no general analytical solution has been found. Often simplifying assumptions have been made to enable an approximate solution to be derived. There are only two exact solutions, these are for slabs and are due to Stefan and Neumann (Carslaw and Jaeger 1959, p282-286). Both solutions are for the first kind of boundary condition at the surface of a semi-infinite body. Neumann's solution takes account of initial superheat but Stefan's solution, a special case of Neumann, assumes that the material is initially at the fusion temperature. Neither solution applies to problems in finite bodies with a significant heat transfer resistance at the surface, but they may give a reasonable approximation when the surface heat transfer coefficient is high. They are however the only exact analytical solutions to freezing problems. All other solutions involve approximations.

2.2.2 Approximate Solutions for Slabs

Muehlbauer and Sunderland (1965 - with 149 references) and Bankoff (1964 - with 157 references) have produced literature reviews covering this area. Those of importance to food freezing problems are conveniently classified into four groups.

2.2.2.1 Integral Profile and Variational Techniques The first group comprise the integral profile technique of Goodman (1964) and the variational technique of Biot (1957) which reduce the set of partial differential equations that define the problem to a set of simpler ordinary

integro-differential equations. For very simple boundary and initial conditions that are rarely if ever encountered in practice these can be solved analytically, but for most practical problems in food freezing the equations must be solved numerically, usually by computer (Goodman and Shea 1960; Lappadula and Mueller 1966; Hills and Moore 1967; Hills 1969; Imber and Huang 1973; Chung and Yeh 1975; Chung and Yeh 1976). Goodman (1958) has presented a solution for the third kind of boundary condition, but no initial superheat, that does not require numerical solution.

2.2.2.2 Solutions for Alloy Solidification In metal alloy solidification both solidus and liquidus fronts move through the solidifying material with a mushy zone between them. For simple cases (the first kind of boundary condition) analytical solutions can be found (Tien and Geiger 1967; Cho and Sunderland 1969), but for cases of more practical importance numerical evaluation is necessary, or the analytical solution is tedious to use because of its complexity (Tien and Geiger 1968; Tien and Koump 1968; Muehlbauer et al 1973). Generally these solutions involve Goodman's integral profile technique with a quadratic approximation to the temperature distribution. Goodman (1964) has shown that this leads to errors of the order of 9%. For application to freezing foods there is an additional difficulty because further approximations are necessary to relate the type of phase change in freezing foods to that found in alloy solidification. These differ because of the different distributions of latent heat across the phase change region.

Geuze et al (1972) have applied this type of method to the freezing of an agar gel with the first kind of boundary condition in a semi-infinite slab, and found reasonable agreement. Bakal and Hayakawa (1973) attempted to apply this form of approach to the freezing of meat with the third kind of boundary condition but were unable to find a suitable solution for the phase change region.

2.2.2.3 Other Analytical Approaches The third group are those solutions which, by a variety of simplifying assumptions and mathematical techniques, arrive at a simple formula, a convergent series solution, or a set of ordinary integro-differential equations. This group includes analytical iteration methods and perturbation (Danckwerts 1950; Boley 1963; Hamill and Bankoff 1963; Hamill and Bankoff 1964; Jackson 1964; Siegel and Savino 1966; Westphal 1967; Lock et al 1969; Patel and Boley 1969; Savino and Siegel 1969; Hirai and Komori 1971; Komori and Hirai 1972; Pedroso and Domoto 1973a; Pedroso and Domoto 1973b; Selim and Seagrave 1973a; Cho and Sunderland 1974; Huang and Shih 1975a; Huang and Shih 1975b). None of these was applied to food freezing problems.

2.2.2.4 Solutions for Aqueous Systems This group of solutions take advantage of the fact that in aqueous systems the ratio of the latent heat to the specific heat capacity is large. Hence it is possible to either ignore the sensible heat below the freezing point or take account of it in a simple fashion (Plank 1941; London and Seban 1943; Kreith and Romie 1955). These solutions take account of the third kind of boundary condition but none considers effect of initial superheat. For problems where there is initial superheat these solutions will always give a low prediction of freezing time.

An interesting method due to Hrycak (1963,1967) takes account of initial superheat in a semi-infinite slab in both stratified and homogeneous materials. Application of this solution to the freezing of finite slabs leads to over-estimation of the freezing time.

2.2.3 Solutions for Other Shapes

Whilst the majority of research has centred on the freezing of semi-infinite slabs, and to a lesser extent finite slabs, work has also been done on spheres, cylinders and regular two- and three-dimensional shapes. In the

case of radial heat flow in cylinders and spheres no analytical, or approximate analytical solutions exist that take account of initial superheat. Some solutions assume that the material is initially at the fusion temperature, and the boundary condition is of the first kind (Pekeris and Slichter 1939; Poots 1962a; Langford 1966; Cho and Sunderland 1970; Komori and Hirai 1970; Theofanous and Lim 1971; Pedroso and Domoto 1973c; Pedroso and Domoto 1973d; Riley et al 1974), or of the third kind (Plank 1941; London and Seban 1943; Kreith and Romie 1955; Shih and Chou 1971; Shih and Tsay 1971; Selim and Seagrave 1973b). All of these will give a low prediction of freezing time when there is initial superheat. Those solutions that only take account of the first kind of boundary condition will give low answers when applied to problems where the resistance to heat transfer from the surface of the body is significant.

Very few approximate analytical solutions exist for other geometries where heat is transferred in more than one direction. Such solutions are limited to regular shapes because of the mathematical complexity in handling other configurations. There are several solutions for problems where there is no initial superheat and the first kind of boundary condition is applied (Poots 1962b; Jiji et al 1970; Rathjen and Jiji 1971; Budhia and Kreith 1973; Riley and Duck 1977a; Riley and Duck 1977b), but these are of limited practical importance because initial superheat and resistance to heat transfer from the surface are so often encountered. Plank (1941), by use of appropriate geometric factors has found a solution for the infinite rectangular rod and brick shapes subject to the third kind of boundary condition. Tanaka and Nishimoto (1959, 1964) have extended the method of Plank to find related solutions for conical and trapezoidal bodies.

2.2.4 Empirical Relationships

The last group of important solutions other than numerical ones are the modified analytical solutions, and

related empirical formulae. Many of these are modifications to the equation of Plank (1941). In some cases these have arisen from the need to conform to experimental data (Rutov 1936; Nagaoka et al 1955), whilst in others they have been prompted by apparent shortcomings in the derivation of the formula (Cochran 1955; Cowell 1967; Mellor 1976). Other formulae have also been suggested. Charm (1971, p242) suggests a modification to Neumann's solution to enable it to be applied to the third kind of boundary condition. Kern (1977) has suggested a group of solutions which are designed never to give a low prediction for a group of freezing problems : the only one of these formulae applicable to foodstuffs ignores the effect of initial superheat. Khatchaturov (1958) has derived a formula for freezing of fish partly on theoretical grounds, and partly on experimental data. Mott (1964) developed a calculation procedure based on dimensional analysis which showed a linear relationship between the freezing time and the frozen depth. As this is known to be unjustified the solution has limited applicability. Baxter (1962) examined freezing with the third kind of boundary condition, but no initial superheat, by finite differences. He then fitted a simple regression line through his finite difference results for slabs and cylinders. Tao (1968) studied the same problem in the same way, and derived different regression equations for slabs, cylinders and spheres.

2.2.5 Use of Analogues

Muehlbauer and Sunderland (1965) in their review produced a summary of work done with electrical analogues. Because the establishment of an electrical analogue to take account of practical boundary and initial conditions is very time consuming, and the same problem is easily programmed on the more versatile digital machine, electrical analogues of freezing processes are now very rare.

Hashemi and Sliepcevich (1967a) suggest a diffusion analogue where mass transfer between two phases is used to

simulate the freezing process. Application to the first kind of boundary condition was simulated, but there was a difficulty in matching the thermal properties of the freezing material to those of the analogue. For this reason, and because of the comparative simplicity of using a digital machine, analogues of this and other types have not been more widely used.

2.2.6 Numerical Solutions

The last important types of solution which assume that all the latent heat is released at a unique freezing temperature at which a step change in thermal properties occurs, are finite difference and finite element solutions. In these the third kind of boundary condition is easily taken into account, as is initial superheat. These solutions are very similar to each other, being broadly based on the work of Dusinberre (1945), but differing in how the position of the phase change front is found. Some use a heat balance (Seider and Churchill 1965; Tao 1967; Charm et al 1972), whilst others interpolate temperatures on either side of the interface to fit the moving boundary condition and the temperature gradients on either side of the boundary (Ehrlich 1958; Murray and Landis 1959; Lazaridis 1970; Padmanabhan and Subba Raju 1975).

Freezing foods do not exhibit a sharp phase change of this nature so this group of solutions departs substantially from the physics of the situation, and the fit of data reflects this (Charm et al 1972).

There are also two graphical methods due to Ede (1949) and Longwell (1958). These are no longer of practical importance with the greater availability of digital computers.

2.3 SOLUTIONS USING CHANGING APPARENT SPECIFIC HEAT CAPACITY AND VARYING THERMAL CONDUCTIVITY

The second way that phase change in freezing foods can

be taken into account is by use of the varying thermal conductivity $k(T)$, and the apparent specific heat capacity $C(T)$ which is found from :

$$C(T) = \frac{dH}{dT} \quad (2.5)$$

where H = enthalpy of the food material (J/m^3)

As latent heat is released over a range of temperature the enthalpy/temperature graph is always differentiable. The irregular shape of the functions $k(T)$ and $C(T)$ for common foods precludes any analytical solution of the general problem :

$$C(T) \frac{\partial T}{\partial t} = \frac{\partial}{\partial x} (k(T) \frac{\partial T}{\partial x}) + \frac{\partial}{\partial y} (k(T) \frac{\partial T}{\partial y}) + \frac{\partial}{\partial z} (k(T) \frac{\partial T}{\partial z}) \quad (2.1)$$

subject to the appropriate boundary and initial conditions.

Several finite difference and finite element solutions have been developed for this approach to the problem. It is a more versatile approach than that of section 2.2.6 because solutions of this type can be made to approximate to the problem solved in section 2.2.6 by appropriate choice of $k(T)$ and $C(T)$ (Comini et al 1974c). Solutions based on these methods show a wide range of complexity. There are simple explicit finite difference formulae (Allada and Quan 1966; Earle and Earl 1966; Cullwick 1967; Mawson 1969; Bailey et al 1974; Chattopadhyay et al 1975), fully implicit and Crank-Nicolson finite difference schemes (Eyres et al 1946; Crank and Nicolson 1947; Albasiny 1956; Lockwood 1966; Hashemi and Slipecevich 1967b; Fleming 1971a; Joshi and Tao 1974; Shamsundar and Sparrow 1975; Tao 1975; Shamsundar and Sparrow 1976), three time-level finite difference schemes (Bonacina and Comini 1971; Bonacina and Comini 1973), and more recently finite element solutions (Comini et al 1974c; Baerdmaeker et al 1977).

Most workers have checked their numerical programs against known analytical solutions from Carslaw and Jaeger (1959). However real systems depart so substantially from

such solutions (which require constant thermal conductivity and specific heat capacity and no phase change) that there is no adequate check except by experiment, and in many cases where experimental verification has been sought the conditions have been limited and ill-defined. Fleming (1971b) showed the applicability of his scheme to immobilised ice/water systems, and Comini et al (1974b) have shown that their program based on the three level finite difference scheme of Lees (1966) gives good agreement to experiments with the fourth kind of boundary condition for a range of food materials. Bonacina and Comini (1973) have shown that their program can be extended to take account of the third kind of boundary condition but have checked the accuracy of the scheme only over a narrow range.

Finite differences and finite elements are closely related techniques with the latter being better suited to irregular geometry (Comini et al 1974c). For regular shapes they are no more accurate than finite differences (Myers 1971, p339), but are more difficult to program on a computer. Finite elements have not been widely used in freezing problems.

2.4 SUMMARY

There is a wide range of solutions to freezing problems, but very few of these apply to the most important situation with the third kind of boundary condition and initial superheat. For regular geometric shapes - slabs, cylinders, spheres and rectangular bricks, a variety of approximate analytical solutions and empirically modified analytical solutions give freezing time predictions, for which the accuracy depends on the assumptions made in the derivation of the formula. Versatile finite difference and finite element methods can handle irregular geometry as well as the regular shapes.

To date, there has not been a general critical survey published to show the accuracy of the various solutions to

the freezing problem when compared against experimental data collected over a wide range of conditions.

3 PRELIMINARY CONSIDERATIONS

The aim of the present research was to find an accurate prediction equation that can be used in food freezer design. Desirable criteria for a suitable solution are :

1. Sufficient accuracy for engineering purposes.
2. Applicability to a wide range of sizes, shapes and food materials.
3. Simplicity.
4. Applicability to the common practical situation of the third kind of boundary condition.
5. Applicability to problems where the material is initially superheated above its freezing point.
6. Minimal need for thermal property data.

The need for the sixth criterion arises from the fact that there is a lack of detailed measurements of thermal properties of foods. Commonly, only a few values at different temperatures and water contents are known for any food-stuff. Hence it is clearly an advantage if the design equation does not require detailed information on the thermal properties.

Analytical solution of freezing problems with the third kind of boundary condition and initial superheat is very difficult because of the non-linear boundary conditions, but there are a number of approximations to the solutions of problems of this type. It was decided to examine, critically, available solutions to see if any are sufficiently accurate, with or without modification, for design purposes. Only regular geometric shapes were considered in detail because limitations on time prevented a full survey being made. The steps involved in the investigation were as follows :

1. Collection of accurate experimental data for freezing of food materials over a wide range of conditions with four different shapes - slabs, cylinders, spheres and rectangular bricks.

2. For each shape, investigation of available solutions to see which, if any, give accurate prediction of freezing time over a range of conditions when compared to the experimentally measured freezing times. These solutions were divided into two groups.
 - (i) Those requiring a computer for calculation of the freezing time. This group includes solutions requiring numerical integration, and finite difference and finite element solutions.
 - (ii) Those sufficiently simple to allow hand calculation, hereafter referred to as "simple formulae". This group mainly comprises the approximate analytical solutions and the empirically modified formulae.

The division of the solutions into two categories was based on relative simplicity. Many engineers in a position where they must predict a food freezing time do not have access to a computer and must therefore rely on simple formulae. On the other hand, a person with a computer available will use a computer-based solution if it is more accurate than a simple formula.
3. The best solutions in each of the two categories for the various shapes were considered to see which is the superior method for predicting the freezing times of food materials.
4. Finally, although it was not possible to study irregular shapes in detail, the trends found in the investigation of freezing time calculations for regular shapes were applied to irregular shapes on a theoretical basis. The results of this should provide a guideline to the design engineer attempting to predict the freezing time of an irregularly-shaped package of food.

4 COLLECTION OF EXPERIMENTAL DATA

4.1 INTRODUCTION

As well as depending on the thermal properties of the material the freezing time of a package of food is influenced by five major factors.

1. Size of the object (as defined in the dimension D (m)).
2. Temperature of the external cooling medium (T_a ($^{\circ}\text{C}$)).
3. Initial temperature of the material (T_i ($^{\circ}\text{C}$)).
4. The resistance to the removal of heat from the surface of the freezing material (as defined in the surface heat transfer coefficient h ($\text{W}/\text{m}^2\text{C}$)).
5. The geometric arrangement of the material. For regular shapes this includes slabs, cylinders, spheres and rectangular bricks.

The accuracy of any experimental data collected is dependent on the ability to be able to measure and control accurately these five factors, and also on the homogeneity of the freezing material.

4.2 CHOICE OF FREEZING MATERIAL

Food materials are rarely themselves homogeneous, and it is difficult to achieve good repeatability of freezing experiments because there are structural changes in food materials during freezing and thawing. Also, for a large number of freezing experiments the cost of food materials, used only once, can be prohibitive. For these reasons a number of analogue materials have been considered (Riedel 1960a; Lentz 1961; Geuze et al 1972; Badari Narayana and Krishna Murthy 1975). The widely used "Karlsruhe test substance" was developed by Riedel (1960a), but is now commonly referred to by its trade name as "Tylose". It is a defined 23% methylcellulose gel. The enthalpy/temperature data for this gel are very similar to those for lean beef

(74% water), but the thermal conductivity is slightly different (Riedel 1960a; Morley 1972; Comini 1976).

Because of its gel nature it is easily formed into different shapes, but it was found in practice that it is difficult to totally exclude air pockets and to obtain 100% contact to any surface. The volume of air entrained is very difficult to evaluate, but it is estimated as less than 0.2% of the total gel volume. Contact onto a surface can be estimated by breaking the contact and examining the surface; in all cases there was found to be better than 90% contact. Ultimately these factors are only important in so far as they affect the heat transfer behaviour of the system. They will be discussed in conjunction with temperature measurement errors for each shape.

An investigation of commercially available methylcellulose powders was conducted. Attributes sought were pliability for moulding purposes, and a lack of air entrainment after mixing the gel. Tylose MH1000 (a product marketed by Hoechst New Zealand Limited) was found to be the best methylcellulose available. Riedel (1960a) suggests adding salt to the gel to get exactly the same initial freezing point as lean beef. He gives data for Karlsruhe test substance without added salt, which show that the difference in the enthalpy/temperature relationship between gels with and without salt is small. Because equipment was not available to make the accurate freezing point measurements that are necessary to determine the salt to be added, Karlsruhe test substance without added salt, but with 0.005% copper sulphate incorporated to inhibit fungi, was used.

Errors in making the gel due to inhomogeneity and varying moisture content are small. It was found that the water content in the gel equilibrated over a period of several days leading to a very homogeneous material. Errors in measuring out the components led to a moisture content of $77.0 \pm 0.2\%$ in the final gel.

The enthalpy/temperature data of Riedel (1960a) is considered accurate because of his great experience and care in measuring such data. Thermal conductivity data was obtained from Comini (1976). The density of the gel does not alter significantly on freezing and, like Comini (1976), a constant value was used. Comini and Bonacina (1974b) have shown that the shape of the thermal property functions, $C(T)$ and $k(T)$, need be known only approximately in the region -10°C to 0°C , and as long as the total enthalpy change is preserved significant errors will not arise. Taking these factors into account the overall error in the thermal property data was estimated at less than 1%.

For the reasons of homogeneity, repeatability and cost the bulk of the experimental work was done using Karlsruhe test substance. To show that the results obtained using this material are consistent with the freezing of real foods, experiments were also conducted with mashed potato and minced lean beef.

For the lean beef, all visible connective tissue and fat was removed prior to mincing. Duplicate drying tests were carried out to obtain the moisture content (74.0%). Enthalpy/temperature data were obtained from Riedel (1957) and thermal conductivity data from Morley (1972). These data are considered reliable and accurate.

The moisture content of the mashed potato was 82.0%. Only limited thermal data are available (Riedel 1960b), and so values were estimated by the method of Comini and Bonacina (1974b). The accuracy of this data is approximately $\pm 3\%$, which is of less precision than the data obtained for lean beef and Karlsruhe test substance.

4.3 ONE-DIMENSIONAL HEAT TRANSFER IN SLABS

4.3.1 The Equipment

To help ensure one-dimensional heat transfer in a small

slab so that it approximates to an infinite slab, all experimental work for this shape was done in a plate freezer. Figure 4.1 shows the experimental apparatus. The plates were cooled by a 29% calcium chloride brine pumped at a rate of approximately 1 kg/s from a well mixed tank. This tank has a refrigerated jacket. The plates can be lowered to accommodate thicknesses up to 0.10m which is the limit of the apparatus, and thermal contact was improved by exerting pressure on the plates.

For each slab thickness a mould was made by cutting a 0.23m diameter hole in the centre of a 0.38m x 0.38m piece of polystyrene foam board of the appropriate thickness. Two sheets of aluminium foil and one of brown paper were used to cover one side of the mould, and it was then filled from the opposite side taking care to avoid air entrainment. Copper/constantan thermocouples were inserted, three on each surface, and three at the centre of the slab. All thermocouples were run through isothermal regions to minimise errors. Two layers of aluminium foil and one of brown paper were then fixed to the second face to give a filled mould as shown in Figure 4.2. This wrapping adds a negligible heat transfer resistance but prevents dehydration of the surface of the material. The brown paper, placed between the two layers of aluminium foil so that it remains dry, provides structural strength to the wrapping.

4.3.2 Dimensional Measurement and Control

The slab thickness was measured with the material both frozen and unfrozen. Because the density of Karlsruhe test substance does not change appreciably there was no difference between the measurements in the two states. The thickness was found to vary by up to 0.5mm across each slab, with the largest variations being found at the edges of the material. Because all temperature measurements were taken towards the centre of the 0.23m diameter slab to avoid edge effects in heat transfer, the error in control and measurement of the thickness was most important in this region, and was estimated at $\pm 0.3\text{mm}$.

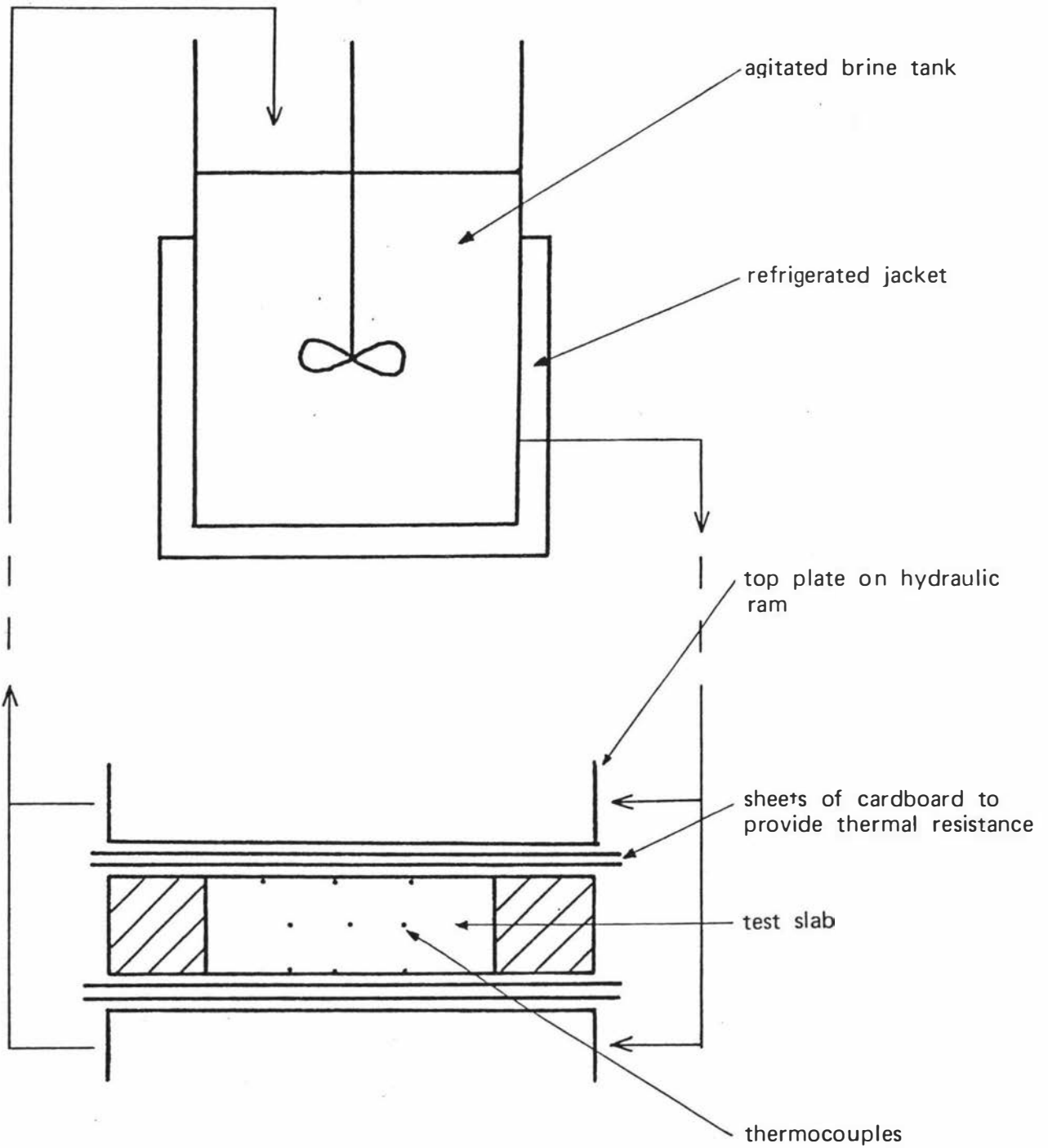
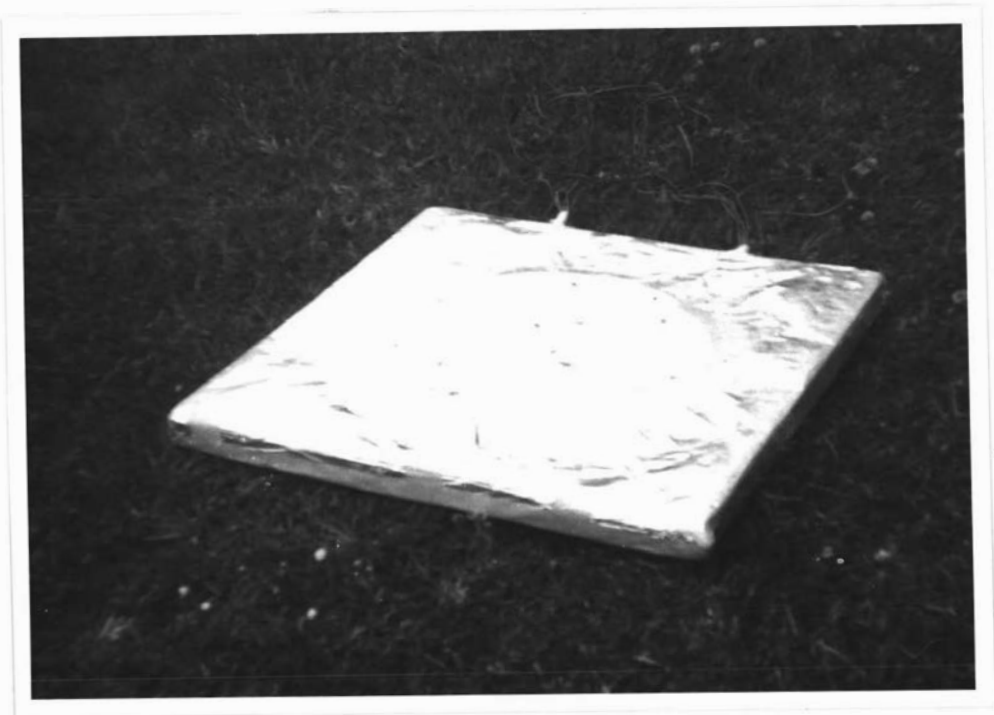


Figure 4.1 Schematic outline of the experimental plate freezer. Not to scale.



a



b

Figure 4.2 Test slabs.

- a. removed from its mould with thermocouples still in place
- b. in finished state

4.3.3 Temperature Measurement and Control

All temperature measurements were made with 24 gauge (United States Standard wire gauge) copper/constantan thermocouples connected to a 12 point Honeywell-Brown recording potentiometer operating on a 30 second print cycle. The error in the calibration of the machine was found to be less than 0.2°C .

Prior to freezing the slabs of Karlsruhe test substance were kept in constant temperature rooms for long enough to attain uniform temperature throughout. Pieces of 0.04m thick polystyrene foam board were used to insulate the faces of the slab during the time from removal of the slab from the constant temperature room to the onset of freezing. Under these conditions the maximum variation in the initial temperature across the slab was found to be $\pm 0.2^{\circ}\text{C}$ on either side of the mean value.

The temperature of the cooling medium (29% calcium chloride brine) was measured by two thermocouples in the jacketed tank. One of these was located in the return stream from the plates, and the other in the bulk medium. The difference in temperature between these two thermocouples was generally less than 0.1°C , although during the initial stages of some freezing experiments the difference was up to 0.3°C . This was due to very high initial heat fluxes which can occur for large surface heat transfer coefficients and large initial superheat, but only for very short times. Consequently the effect of the large initial heat flux over the full time of the freezing experiment was small, and the change in the circulating brine temperature was almost always less than 0.1°C .

The brine temperature was controlled by an on/off type of controller on the refrigeration unit, actuated by the temperature of a copper/constantan thermocouple in the brine tank. As the cooling capacity of the refrigeration unit was large compared to the heat capacity of the brine

tank, overshoot of the set-point was a problem. By adjusting the set-point the brine temperature was controlled to $\pm 0.5^{\circ}\text{C}$ of the required value. In Appendix 6 it is shown that an ambient temperature cycling around the mean value approximates to a constant ambient temperature with less than 0.5% error for fluctuations up to $\pm 2.5^{\circ}\text{C}$. Therefore cycling of the ambient temperature will not introduce a significant error. Taking calibration errors into account, the error in temperature measurement and control was estimated at $\pm 0.5^{\circ}\text{C}$.

4.3.4 Measurement and Control of the Surface Heat Transfer Coefficient

Surface heat transfer coefficients that occur in plate freezing are generally large because heat transfer resistances between the material and the cooling medium are small. To alter the surface heat transfer coefficient varying numbers (0 to 10) of waxed cardboard sheets were put on either side of the test block before it was inserted in the freezer. By altering the number of sheets of cardboard different surface heat transfer coefficients were obtained.

Details of the methods used to measure the surface heat transfer coefficient can be found elsewhere (Cleland and Earle 1976a). Briefly, these depend on measurement of surface temperature as it varies with time, and use of this data to calculate the surface heat transfer coefficient by the three methods given in the paper. The first method uses a finite difference approximation for the surface temperature. Instead of a value of the surface heat transfer coefficient being supplied and the new surface temperature calculated, the surface temperature at the next time step T_0^{i+1} is obtained from the experimental data, and a value of the surface heat transfer coefficient calculated from the rearranged finite difference equation for the surface temperature:

$$h = \frac{k (2 T_1^i + (M-2) T_0^i - M T_0^{i+1})}{2 \Delta x (T_0^i - T_a)} \quad (4.1)$$

$$\text{where } M = \frac{C(\Delta x)^2}{k \Delta t}$$

A value of h is calculated at each time step and these are arithmetically averaged.

The second method is an extension of the integral profile technique of Goodman (1964); it only applies for short times up to the time that the centre temperature starts to change, but it is convenient to use.

$$\frac{4}{3} \frac{h^2}{k C} = \frac{d}{dt} \left(\frac{1}{2Y^2} - \frac{1}{2} + \ln Y \right) \quad (4.2)$$

where $Y = (T_s - T_a)/(T_i - T_a)$ at time t .

Using the experimental data $(\frac{1}{2Y^2} - \frac{1}{2} + \ln Y)$ is plotted against time, and from the slope the surface heat transfer coefficient can be calculated.

The third method is a heat balance where the integral of the surface heat flux with respect to time is compared to the enthalpy change in the slab.

$$h \int_{t_1}^{t_2} (T_s - T_a) dt = \left[\int_0^{\frac{D}{2}} H dx \right]_{t_2} - \left[\int_0^{\frac{D}{2}} H dx \right]_{t_1} \quad (4.3)$$

For all sets of experimental data there was no significant difference between values of the surface heat transfer coefficient calculated from the three methods. Therefore all calculated values of the surface heat transfer coefficient were used in a calculation to find the least squares regression line relating external heat transfer resistance ($\frac{1}{h}$) to the number of sheets of cardboard present. From this line average values of h for different numbers of cardboard sheets were found. Error in the methods is discussed in some detail in the published paper (Cleland and Earle 1976a), and it is shown that the 95% confidence limits, which vary from $\pm 5\%$ up to $\pm 10\%$ in some cases, almost certainly overestimate the real error. A truer indication of the actual error can be obtained from five

replicate freezing experiments which gave freezing times varying by only $\pm 1.3\%$ from their mean value. For this degree of repeatability to be obtained the maximum error in the control and measurement of surface heat transfer coefficients was estimated at $\pm 2\%$.

Variation in the surface heat transfer coefficient between different regions on the surface of the slab is shown by any difference in the surface temperature at these places. In all cases the differences were found to be small; different thermocouples agreed within 0.5°C of each other, which is very close to the limit of sensitivity of the measurements made. Hence non-uniformity of the surface heat transfer coefficient was not a problem.

4.3.5 Analysis of Heat Transfer in Slabs

In a true one-dimensional slab there is no heat transfer in the other two directions. In practice this is impossible to achieve, but it is possible to reduce heat transfer in the other two directions to an insignificant amount. This was achieved by making the other two dimensions larger than the thickness, which is the critical dimension, by a ratio varying from 2.3:1 to 9:1 depending on the slab thickness; and by ensuring that each slab was surrounded on the edges by at least 0.08m polystyrene foam insulation. Under these conditions the edge heat flow was in the range 0.006 to 0.04 $\text{W}/^{\circ}\text{C}$, whereas the heat flow through the slab faces was in the range 1.6 to 36 $\text{W}/^{\circ}\text{C}$, that is always at least 150 times greater than the unwanted edge effects. Temperature measurements taken near the centre of each slab were unaffected by edge effects because of these precautions.

Air entrainment and less than perfect thermal contact were mentioned in section 4.2. The latter problem did not occur in the experimental work with slabs because the lowering of the plates to clamp the slab tightly in place was found to ensure good contact. When a frozen slab was

removed from the freezer its protective layer of aluminium foil was always tightly and completely bound to the freezing material. Air entrainment in packing the gel is only important if it affects the heat transfer characteristics of the material. The total void volume was estimated as less than 0.2%, and the voids were generally less than 1mm in their largest dimension. Whilst it was impossible to estimate the heat transfer characteristics of each void, they need only be considered if they affect the overall heat transfer behaviour of a slab. It has been shown (Cleland and Earle 1977b) that the experimental surface and centre temperature profiles can be followed very closely by profiles calculated using finite differences. This implies that the heat transfer effects of the voids must be negligibly small.

There are also errors consequent on thermocouple placement. These can be classified into three groups - heat conduction along the thermocouple wire, the inhomogeneity created by the presence of the thermocouple wire, and errors in the placement of the thermocouples.

All thermocouples were introduced parallel to the heat transfer surface through isothermal regions. Therefore there was no temperature gradient for conduction along the thermocouples.

Of the total area normal to the direction of heat transfer at each surface, and at the centre, only 0.3% was covered by thermocouple wires and their plastic insulation. The thermal resistance across the leads was almost totally due to the plastic insulation because the thermal conductivity of copper is large. The thermal conductivity of the plastic is approximately one quarter that of Karlsruhe test substance, so the thermal resistance across the leads was greater than the resistance for the equivalent amount of Karlsruhe test substance. This greater thermal resistance applied for only 0.3% of the area normal to heat transfer at only three places in the slab, and therefore did not

affect the heat flow significantly. As the thermocouple leads occupied only approximately 0.01% of the gel volume and have no latent heat effects the overall heat capacity of the gel was not significantly affected by their presence.

The last important consideration is error in the placement of thermocouples. Measurements were taken of the two most important temperatures, the surface and centre temperatures. The former is very sensitive to changes in the external heat transfer conditions, and so was used in the estimation of the surface heat transfer coefficient. The latter is needed to measure the freezing time. Because equal heat transfer occurs from both faces of the slab the geometric and thermodynamic centres will coincide, and hence during freezing any thermocouple not at the geometric centre will be at a lower temperature than the centre of the slab. Therefore the last thermocouple to reach -10°C will give the most accurate estimate of the freezing time provided heat transfer is homogeneous over the full surface of the slab. In practice, the centrally placed thermocouples reached -10°C in times that agreed within 2% of each other, and the last thermocouple to reach this temperature was taken as the best estimate of the slab centre temperature.

Because of the way the test slabs were held in the freezer it was impossible for a thermocouple to be above the surface. A true estimate of surface temperature would be where one side of the thermocouple was touching the aluminium foil protective layer, but in practice this was very hard to achieve. Provided heat transfer is homogeneous across the surface, a faster cooling thermocouple will probably give a better estimate of the surface temperature than a slower cooling one which is likely to be below the surface. However this does not allow an evaluation of homogeneity of heat transfer across the surface, so another criterion is needed. Supercooling must occur before freezing (Rolfe 1968, p170-183) and the first supercooling, and hence the first freezing, must occur at the surface. Once an ice front has formed in a non-cellular material such

as Karlsruhe test substance no further supercooling for ice crystal nucleation is necessary, although it may occur if the rate of cooling is sufficiently fast. The supercooling of the surface can be used to indicate the position of a thermocouple. Figure 4.3 shows typical profiles for different surface thermocouples.

Curve 1 is typical of a thermocouple that is well placed at the surface. It has supercooled below the freezing point, but upon the release of latent heat the surface temperature has still remained below the initial freezing temperature. Curve 2 is also a well placed thermocouple. Upon the release of latent heat the temperature has risen briefly above the freezing point. This could be because the rate of heat removal from the surface is insufficient to prevent the temperature rising this much, or because the thermocouple is fractionally below the surface. Curves 3 and 4 are typical of what happens when a thermocouple is below the surface. When ice crystal nucleation occurs at the surface and latent heat is released the material is warmed slightly, even several millimetres in from the surface. Hence a pseudo-supercooling curve occurs, but it is easily distinguished from the true supercooling curve by the temperature at which the peak occurs, and by the fact that the peak is generally flatter without an abrupt change in the temperature/time graph. Curve 5 is a very bad case where the thermocouple is well below the surface and is not affected by the surface supercooling, but the rate of temperature change with time is slowed by the release of latent heat.

Clearly, this criterion does not provide a sharp division between good and bad thermocouple placements, but differences in temperature between profiles of types 1 and 2 were in practice small. Using this criterion to delete badly placed thermocouples it was found that the surface temperature of the slab varied by less than 0.5°C around the mean value. Typically four or five out of six surface thermocouples were found to be sufficiently well placed for use.

The supercooling effect lasts for times of the order of 100 to 300 seconds, and its effect on the overall surface heat flux ($Q = hA(T_a - T_s)$) is small because the integral of $(T_a - T_s)$ with respect to time is very little different to what would be expected if no supercooling occurred. Consequently supercooling does not have a significant effect on the heat transfer characteristics, or the freezing time of a finite slab.

4.4 RADIAL HEAT TRANSFER IN CYLINDERS AND SPHERES

4.4.1 The Equipment

It is more difficult to obtain constant heat transfer conditions around a cylinder or sphere than it is on the two opposite faces of a slab. A system with a fluid flowing over the object is most common. Surface heat transfer coefficients in an air blast freezer vary greatly depending on the degree of exposure to the air flow. The variation of the surface heat transfer coefficient around an object is much less in a liquid immersion freezer. For this reason a liquid immersion freezer was built. It is shown diagrammatically in Figure 4.4.

The impeller circulates 29% calcium chloride brine around the freezer. The brine passes over the refrigeration coils and then through two mesh screens (aperture size 1mm x 1mm) which provide sufficient head loss to equalise any unevenness in the liquid flow profile. The liquid then flows through the experimental section (0.5m x 0.6m x 0.8m) and back to the impeller. The freezer can operate as low as -40°C , but its useful range is restricted to temperatures above -34°C by mechanical problems.

For reasons discussed in section 4.4.5 it was found necessary to oscillate the test samples. The sample oscillator is shown in Figures 4.5 and 4.6. Each sample was turned through an angle of 180° every six seconds approximately.

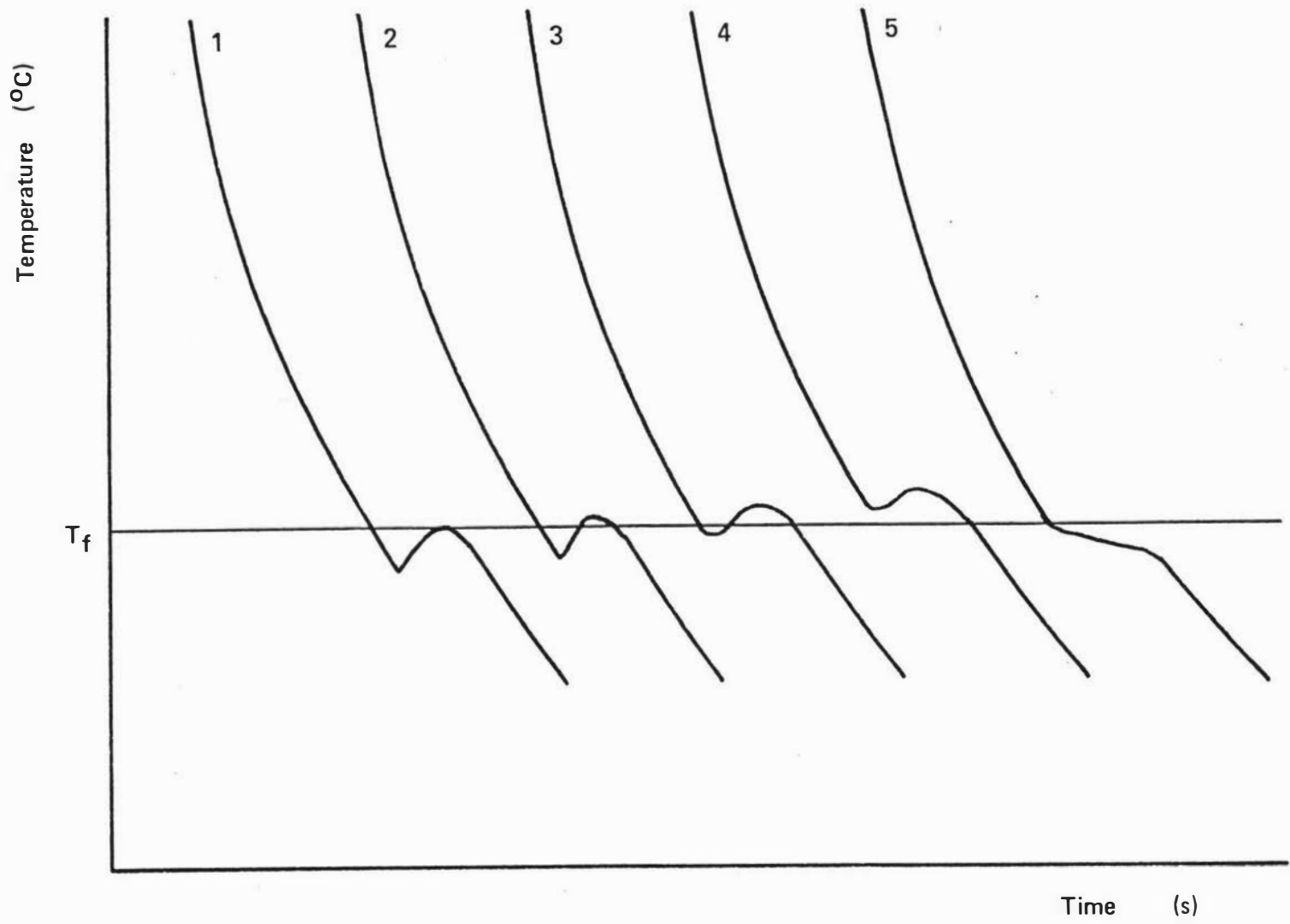


Figure 4.3 Typical temperature/time profiles for thermocouples placed at, or near the surface of a freezing slab.

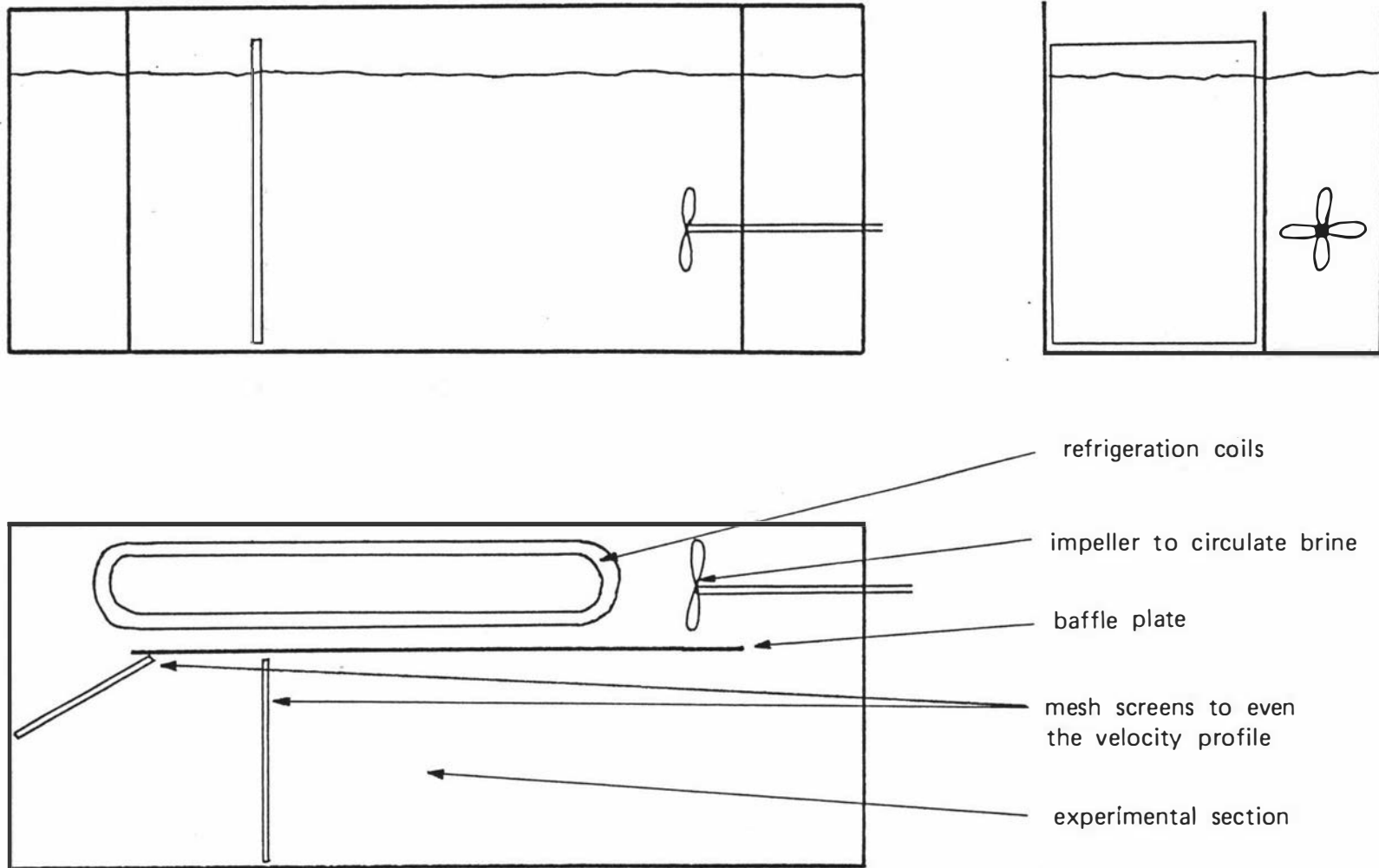


Figure 4.4 Schematic outline of the experimental liquid immersion freezer. Approximate scale 1 : 15.



a



b

Figure 4.5 The sample oscillator used in liquid immersion freezing experiments.
a. attachment of spheres
b. attachment of cylinders

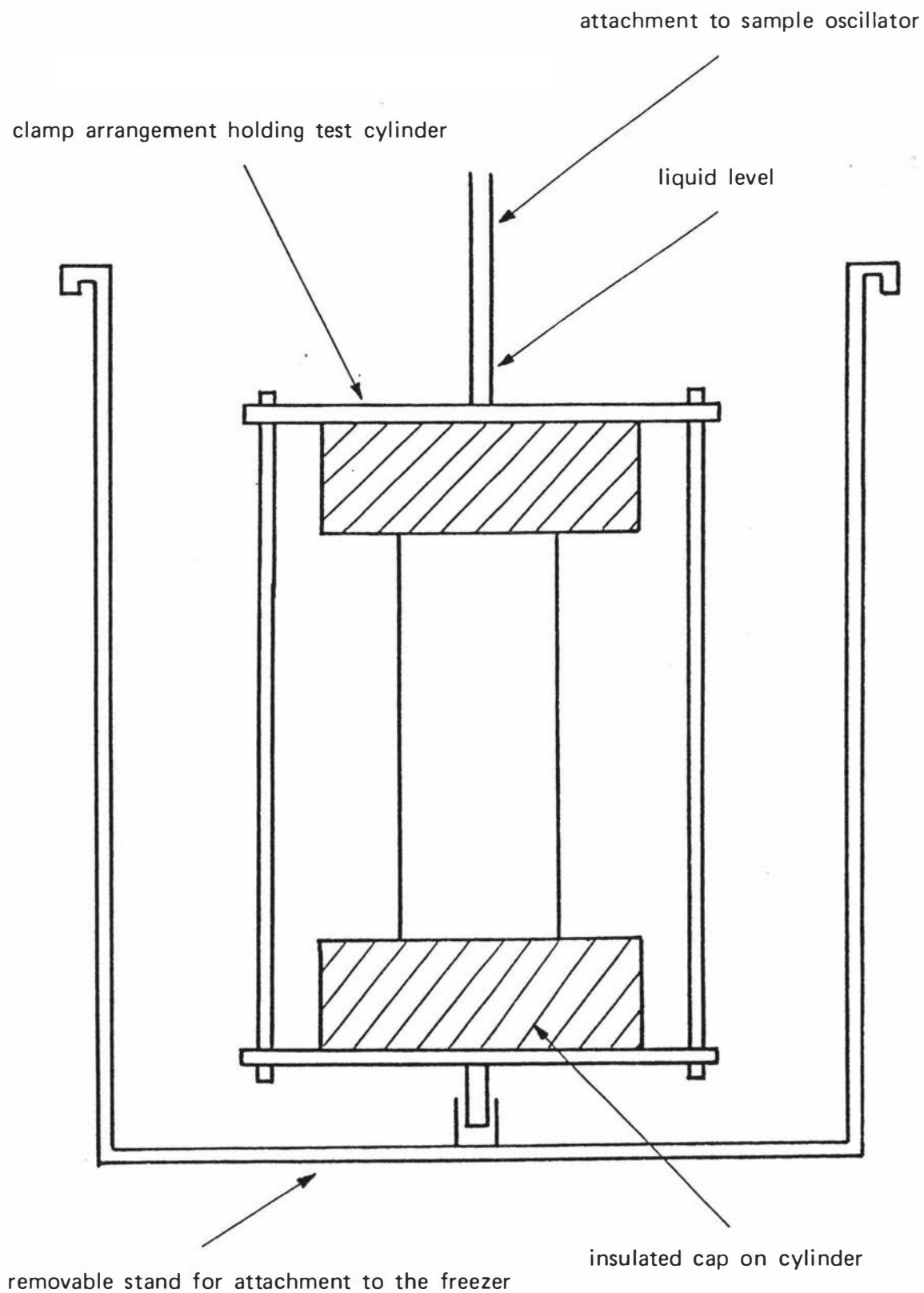


Figure 4.6 Schematic outline of the system used to oscillate cylinders in the liquid immersion freezer.

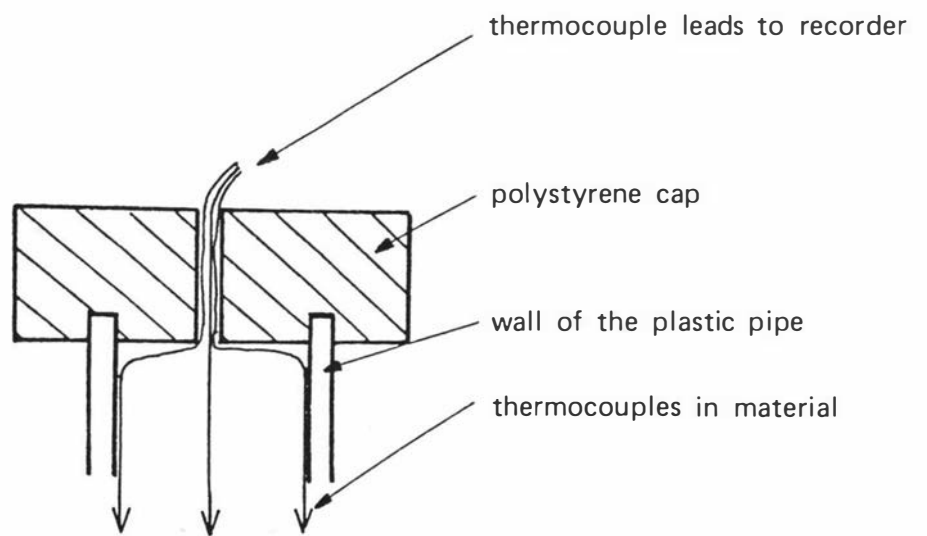


Figure 4.7 Arrangement of the polystyrene foam caps and thermocouple leads for cylinders.

In order to simulate infinitely long cylinders, lengths of polyvinyl chloride plastic pipe 0.45m long, and approximately 0.15m, 0.10m and 0.05m in diameter were used. These had different wall thicknesses to give different external heat transfer resistances. To reduce end effects in order to better simulate an infinite cylinder, caps of polystyrene foam insulation were put on the end of each cylinder in the manner shown in Figure 4.7.

The cylinders were packed with Karlsruhe test substance and thermocouples were introduced at the surface and centre positions through isothermal regions. In each case three thermocouples were used on the central axis and five at the surface. The thermocouples were led through a sealed hole in the top cap to enable connection to the recording potentiometer. Each cylinder could then be clamped into the sample holder as shown in Figure 4.6, and frozen.

Hollow rubber and vinyl balls were used to obtain spherical geometry. Three sizes, approximately 0.15m, 0.10m and 0.05m in diameter were used. These had different wall thicknesses to give different surface heat transfer coefficients. A bolt was glued to the surface of each ball to enable connection to be made to the sample holder as in Figure 4.5. This bolt added a heat transfer resistance of $0.0003 \text{ m}^2\text{C/W}$ to a fraction of the surface area ranging from 0.2% to 0.5%. The overall heat transfer resistance to the surface of the freezing material was in the range 0.0190 to $0.0375 \text{ m}^2\text{C/W}$, which is much higher. Therefore the bolt did not affect the heat transfer behaviour of the spheres significantly.

In order to fill the balls with Karlsruhe test substance an X-shaped incision about 30mm across was made in each of the two larger balls. After the balls were filled thermocouples were introduced on the surface (five thermocouples), and at the centre (one thermocouple) by the method shown in Figure 4.8. A 1mm diameter hole was made with a metal rod and the plastic coated thermocouple pushed

down it until contact with the surface was made. The centre thermocouple was marked before insertion to ensure that it was not pushed past the centre of the ball.

The smallest sphere was made by cutting the ball into two hemispheres, filling these, and then inserting thermocouples (four at the surface and one at the centre), before glueing the two hemispheres together.

Problems caused by voids and imperfect thermal contact are discussed in section 4.4.5. The disruption to the skin of the ball needed for filling affected 0.2% of the surface area of the largest ball, 0.5% of the medium sized ball, and 3.1% of the area of the smallest ball. This disruption is only important because of its affect on the heat transfer behaviour of the spheres, and is discussed in section 4.4.5.

Because of limitations in the range of wall thicknesses in the balls and pipes it was found that the use of liquid immersion freezing alone would not give a wide range of heat transfer resistances at the surface of the freezing material. In order to extend the range of heat transfer conditions some experimental work was carried out in an air blast freezer. The design of the freezer is shown in Figure 4.9. The air speed was set at a constant value of approximately 3 m/s for all runs. In spite of the air turning vanes the air flow through the working section (0.6m x 0.6m x 0.4m) was not completely even. Because of the unevenness in the heat transfer conditions around the freezing object it was considered desirable to oscillate the object through 180° , so that on average, all parts of the surface would be exposed to average heat transfer conditions. The design of the air blast freezer prevented the use of an oscillating device of the type used with the liquid immersion freezer. The small number of experiments conducted in the blast freezer did not justify an alternative mechanised sample oscillation. Instead, the spheres and cylinders were rotated 90° by hand approximately 10 to 20

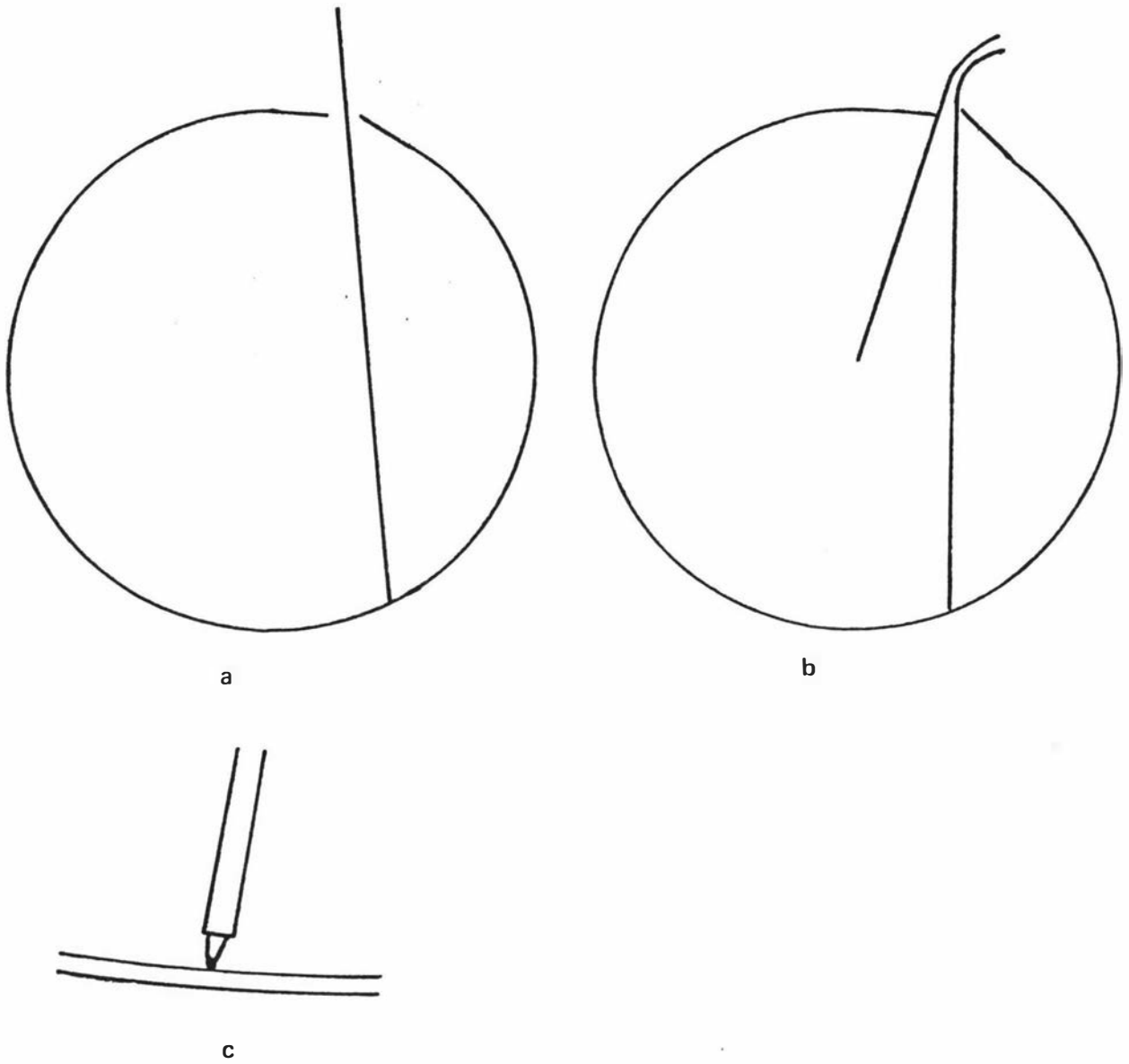


Figure 4.8 Insertion of thermocouples in the spheres.

a – a 1mm metal rod is used to make a path for insertion of the thermocouple wire.

b – two thermocouples inserted.

c – magnified sketch of a thermocouple at the surface.

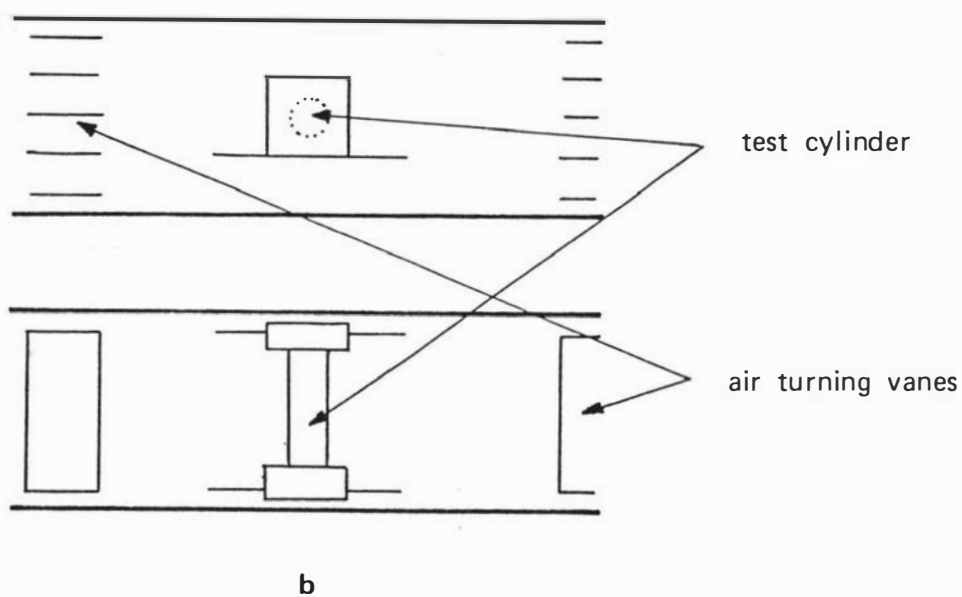
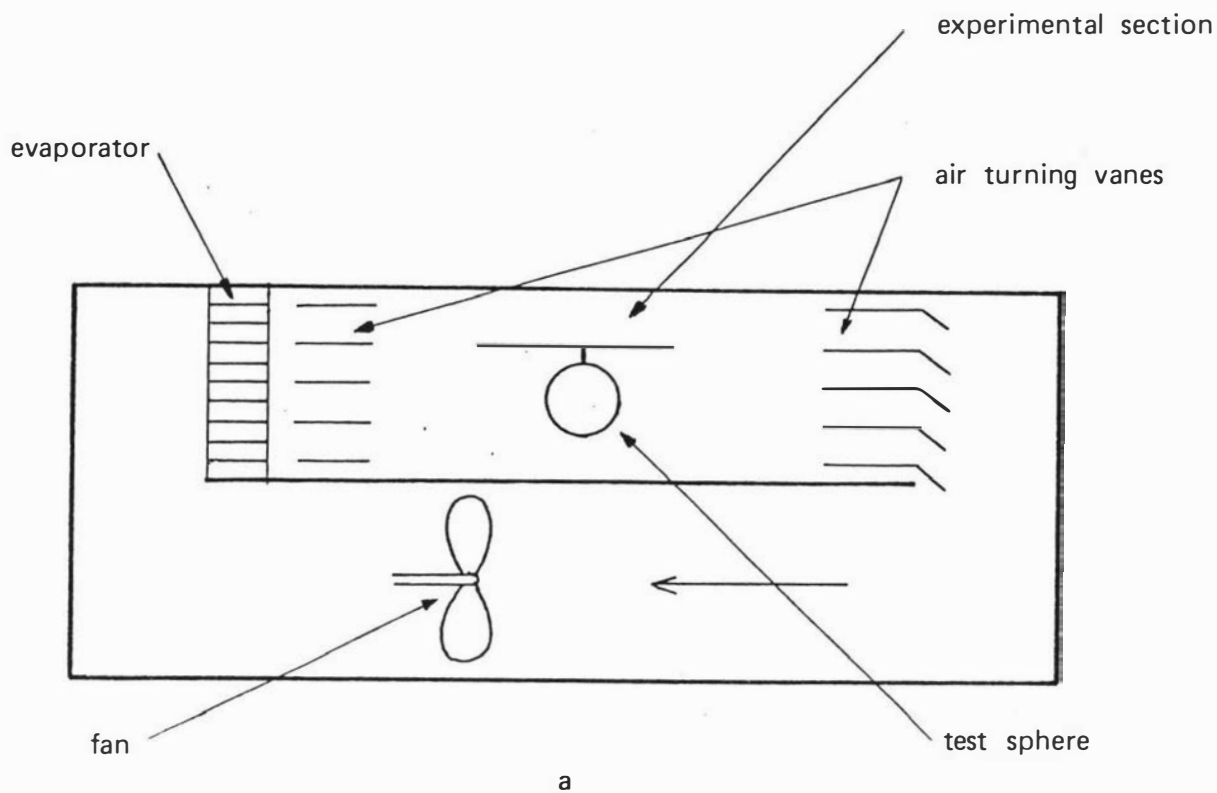


Figure 4.9 Schematic outline of the experimental air blast freezer.
 a. a sphere in the experimental section.
 b. the experimental section with a cylinder in place.

times in the course of each freezing experiment. The effect of turning the samples in this way is considered in section 4.4.5.

4.4.2 Dimensional Measurement and Control

Similarly to the slabs, there was no significant difference in diameter measurements between the frozen and unfrozen states for cylinders and spheres. The rigidity of the cylinders allowed diameter measurement to an accuracy of $\pm 0.5\text{mm}$. Because of the flexibility in the walls of the balls there was some variation in the measured diameter of the spheres. The precision to which measurements could be made was $\pm 1.5\text{mm}$.

4.4.3 Temperature Measurement and Control

The temperature recording system was the same as that used for slabs except that different numbers of thermocouples were used. The cylinders and spheres were wrapped in insulating material for transfer from the constant temperature rooms to the freezer. The initial temperature varied by up to $\pm 0.5^{\circ}\text{C}$ around the mean value under these conditions.

The brine and air temperatures were controlled using the same control system as was used for the plate freezer. The temperature of the brine was controlled to $\pm 0.5^{\circ}\text{C}$ of the mean value, but this precision was not obtainable in the air blast freezer. Because of the low thermal capacity of the air blast system there was considerable overshoot beyond the set point and the air temperature cycled by $\pm 1^{\circ}\text{C}$ around the mean value. This should not significantly affect the accuracy of the results as it has been shown (Appendix 6) that an arithmetic average is valid in this situation.

4.4.4 Measurement and Control of the Surface Heat Transfer Coefficient

The methods used to measure the surface heat transfer coefficient in radial heat flow were very similar to those used for slabs. Measured data of surface temperature as it varied with time was used in each of three ways.

Firstly, an explicit finite difference scheme was manipulated to provide an estimate of the surface heat transfer coefficient at each time step. The general equation for radial heat conduction is :

$$C(T) \frac{\partial T}{\partial t} = \frac{\partial}{\partial r} (k(T) \frac{\partial T}{\partial r}) + \frac{a k(T)}{r} \frac{\partial T}{\partial r} \quad (4.4)$$

where $a = 1$ for a cylinder.

$a = 2$ for a sphere.

The basic finite difference scheme used was similar to that of Albasy (1960) :

$$C_m^i \frac{T_m^{i+1} - T_m^i}{\Delta t} = \frac{k_{m+\frac{1}{2}}^i (T_{m+1}^i - T_m^i) - k_{m-\frac{1}{2}}^i (T_m^i - T_{m-1}^i)}{(\Delta r)^2} + \frac{a k_m^i (T_{m+1}^i - T_{m-1}^i)}{2 m (\Delta r)^2} \quad (4.5)$$

where $m\Delta r = r$ is the distance from the centre of the region. The boundary condition at the surface :

$$h (T_a - T_s) = k(T) \frac{\partial T}{\partial r} \quad \text{at } r = R \quad (4.6)$$

was substituted into equation 4.4, and a finite difference approximation of the type used in equation 4.5 was taken. Setting $M\Delta r = R$; $T_{M+1}^i = T_a$; and $k_{M+\frac{1}{2}}^i = h\Delta r$ in the resulting equation and rearranging to find h the following was derived :

$$h = \left[\frac{C_M^i}{\Delta t} (T_M^{i+1} - T_M^i) + \frac{k_{M-\frac{1}{2}}^i}{(\Delta r)^2} (T_M^i - T_{M-1}^i) \right] \frac{(\Delta r)}{(T_a - T_M^i) \left(\frac{a}{M} + 1 \right)} \quad (4.7)$$

An estimate of the surface heat transfer coefficient was calculated at each time step by use of experimentally determined values of the surface temperature at both the

(i) and (i+1) time levels in equation 4.7. The estimates of h were then arithmetically averaged.

For slabs the second method used to measure the surface heat transfer coefficient was based on Goodman's integral profile technique (Goodman 1964). This type of approach is not suitable for radial geometry (Lardner and Pohle 1961). Consequently another related approach was sought. The analytical solutions for heat conduction with convection at the surface for a cylinder and sphere with constant thermal properties (Carslaw and Jaeger 1959, p202, p238) can be used to estimate the surface heat transfer coefficient. The main difficulty with using these series solutions is that they are slow to converge at short times. Therefore six terms in the series were retained in each case; this gave convergence to better than 1% with the correct solution for Fourier numbers of 0.02 or greater. Because the sign of the series alternates it was found that convergence was improved if only 0.5 times the sixth term was used. A computer program was written that accepted values of the surface temperature at any time, under any set of conditions, and used an iterative procedure to find the value of the surface heat transfer coefficient that would give that surface temperature at that time. Approximately ten data pairs of surface temperature and time were used per freezing experiment, and the calculated values of the surface heat transfer coefficient averaged.

For slabs the third method used to measure the surface heat transfer coefficient was a heat balance. This method is equally applicable to radial geometry. The change in the enthalpy of a body must equal the integral of the surface heat flux with respect to time :

$$h A \int_{t_1}^{t_2} (T_s - T_a) dt = \left[\int_0^R 4\pi r^2 H dr \right]_{t_2} - \left[\int_0^R 4\pi r^2 H dr \right]_{t_1} \quad (4.8)$$

All terms except h can be found from the experimental data.

The beginning and end of the freezing process are convenient times to take as t_1 and t_2 ; using this data h can be calculated.

The difference between the results from the three methods was not significant at the 99% level of confidence. Experiments were conducted in the liquid immersion freezer at -20°C and -33°C . The liquid velocity used was the same at both temperatures, but the transport properties of the brine were different. These changes would alter the film coefficient by up to 10%, and hence change the overall heat transfer coefficient to the surface of the freezing material. However the bulk of the resistance to heat transfer is in the ball skin, or pipe wall, and this damps the effect of the altered film coefficient to such an extent that no statistically significant difference, at the 99% level, could be found between the surface heat transfer coefficients at the two temperatures. A similar effect was observed in air blast freezing: differences in the film coefficient at -40°C and -24°C were not large enough to give a significant difference in the measured overall heat transfer coefficient to the surface of the freezing material. For each sample an average heat transfer coefficient was used for all liquid immersion freezing experiments, and a different average value was used for all air blast freezing.

The errors in measuring and controlling the surface heat transfer coefficient were much greater than in plate freezing, and the repeatability of freezing experiments was not as good. Replicate freezing experiments varied by $\pm 2\%$ around the mean value in immersion freezing, and $\pm 3.5\%$ in air blast freezing. Taking these factors and the range of experimentally determined values into account, the error in the values of the surface heat transfer coefficient was estimated as $\pm 4\%$ for immersion freezing, and $\pm 7\%$ for air blast freezing.

4.4.5 Analysis of Heat Transfer in Radial Geometry

The problems encountered in radial geometry were similar to those found for slabs. In order to approximate an infinitely long cylinder the length of the test cylinders was always greater than the diameter by a factor of three or more. Addition of insulating caps reduced the heat flow through the ends to values in the range 0.0016 to 0.0140 W/°C which was always at least 400 times smaller than the heat flow through the radial surface which was in the range 1.66 to 7.31 W/°C. Therefore the test cylinders approximated infinite cylinders very closely.

Whilst end effects did not occur in spherical geometry there were errors due to cutting of the ball surface to allow filling. For the two larger spheres less than 0.5% of the surface area was disrupted so any effect on the centre temperature was negligible, but there could have been some localised effect on the temperature near the surface around the incisions. The extent of this could not be assessed, but the surface thermocouples were situated well away to avoid any errors introduced. The small sphere had approximately 3% of its surface area affected by cutting. Because the two hemispheres were glued back together very carefully the inhomogeneity should have been no greater than for the larger spheres. Again surface thermocouples were kept away from this region. The small inhomogeneities at the surface should not have altered measurements of the centre temperature or the freezing time.

Voids and imperfect thermal contact were also problems. Voids that occurred were no larger than those found in slabs so their effect would not be expected to be any more significant than the effect of the voids in the slabs. This was discussed in section 4.3.5. Thermal contact was in all cases better than 90%. Where perfect thermal contact did not occur a very small gap was present between the skin and the freezing material. This would not be expected to be any more significant than any other void in the overall heat transfer behaviour of the freezing material. The mode of heat transfer across these voids would be natural

convection. Because the voids were ill-defined it was impossible to evaluate the heat transfer resistance across them. The upper bound in this case would be where conduction alone occurred. For a 0.5mm void this would lead to a heat transfer resistance of $0.025 \text{ m}^2\text{C/W}$ which is significant. The actual heat transfer resistance due to natural convection would be less than this, but how much less cannot be predicted. However the extra heat transfer resistance applied to less than 10% of the heat transfer surface, and would only be important if the overall heat transfer characteristics of the sphere or cylinder were altered. In Chapter 6 it will be shown that finite differences accurately predict the surface and centre temperatures so the overall effect of voids at the surface appears to be small.

Errors due to the inhomogeneity created by the presence of thermocouple wires were of similar magnitude to those found for slabs, and were similarly negligible. Errors in placement of surface thermocouples were assessed by the same methods used for slabs. Because accurate placement was more difficult, a greater proportion were too badly placed for use. Centre thermocouples in the cylinders were placed on the central axis, and the one which cooled most slowly used as the best estimate of the centre temperature. In spheres the thermodynamic and geometric centres coincided at a single point, meaning that only one thermocouple could be placed at this position. Figure 4.10 shows typical finite difference results for freezing of a sphere. If the thermocouple was placed 10% of the sphere radius in error the measured freezing time would be 0.6% in error. Consequently any error in the placement of the centre thermocouple was highly damped in its effect on the measured freezing time, and did not significantly increase the overall error.

In the cylinders the thermocouples were introduced through isothermal regions to minimise conduction along them. This was not possible for spheres. Heat conduction will only be significant along the wire, not along the insulation. The cross-sectional area of each thermocouple

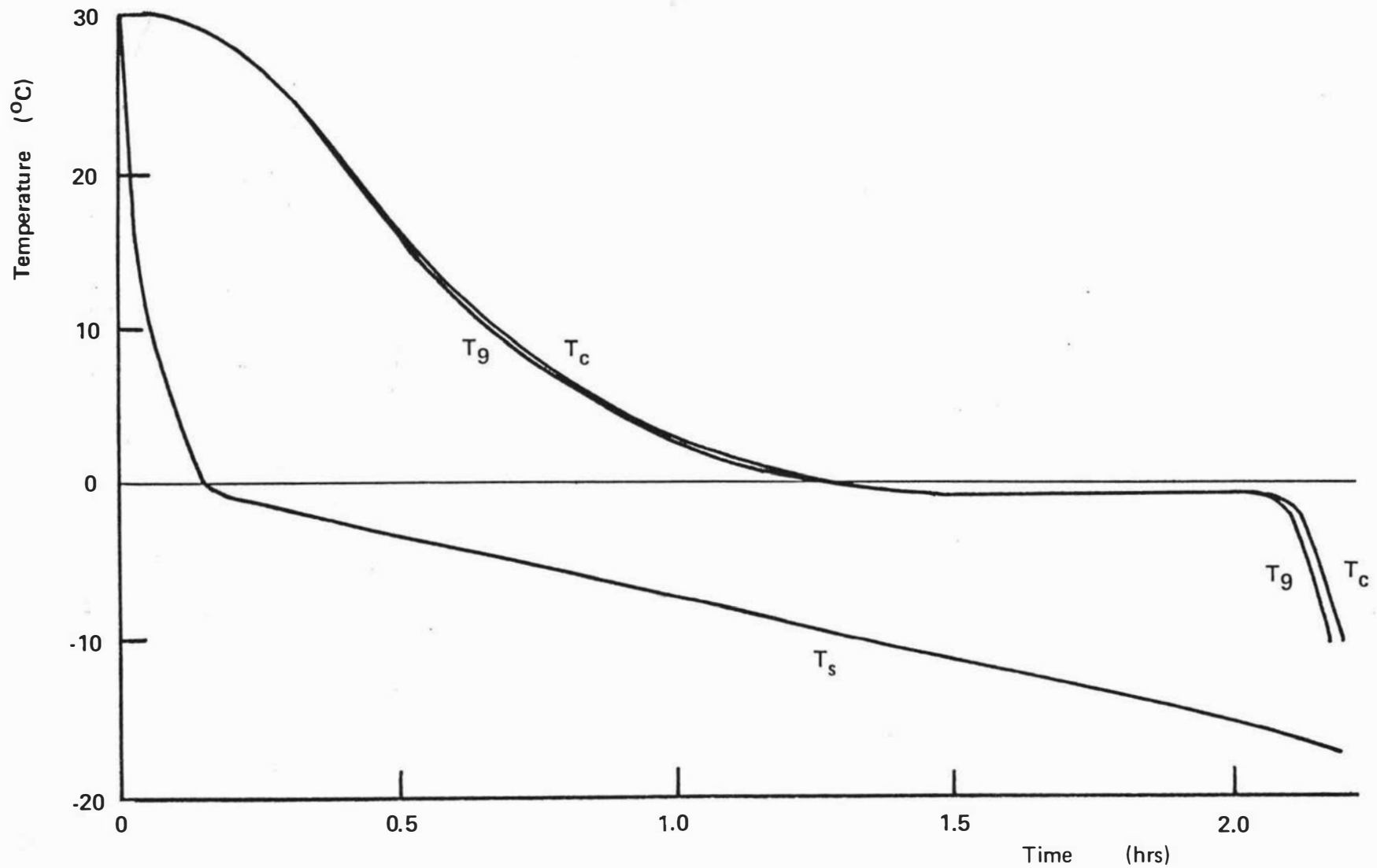


Figure 4.10 Typical finite difference results for freezing of a sphere. $D = 0.0905\text{m}$; $h = 53.0 \text{ W/m}^2\text{°C}$; $T_a = -20.0\text{°C}$; $T_i = 30.0\text{°C}$. T_c = centre temperature; T_g = temperature at a point 0.1R metres from the centre of the sphere; T_s = surface temperature.

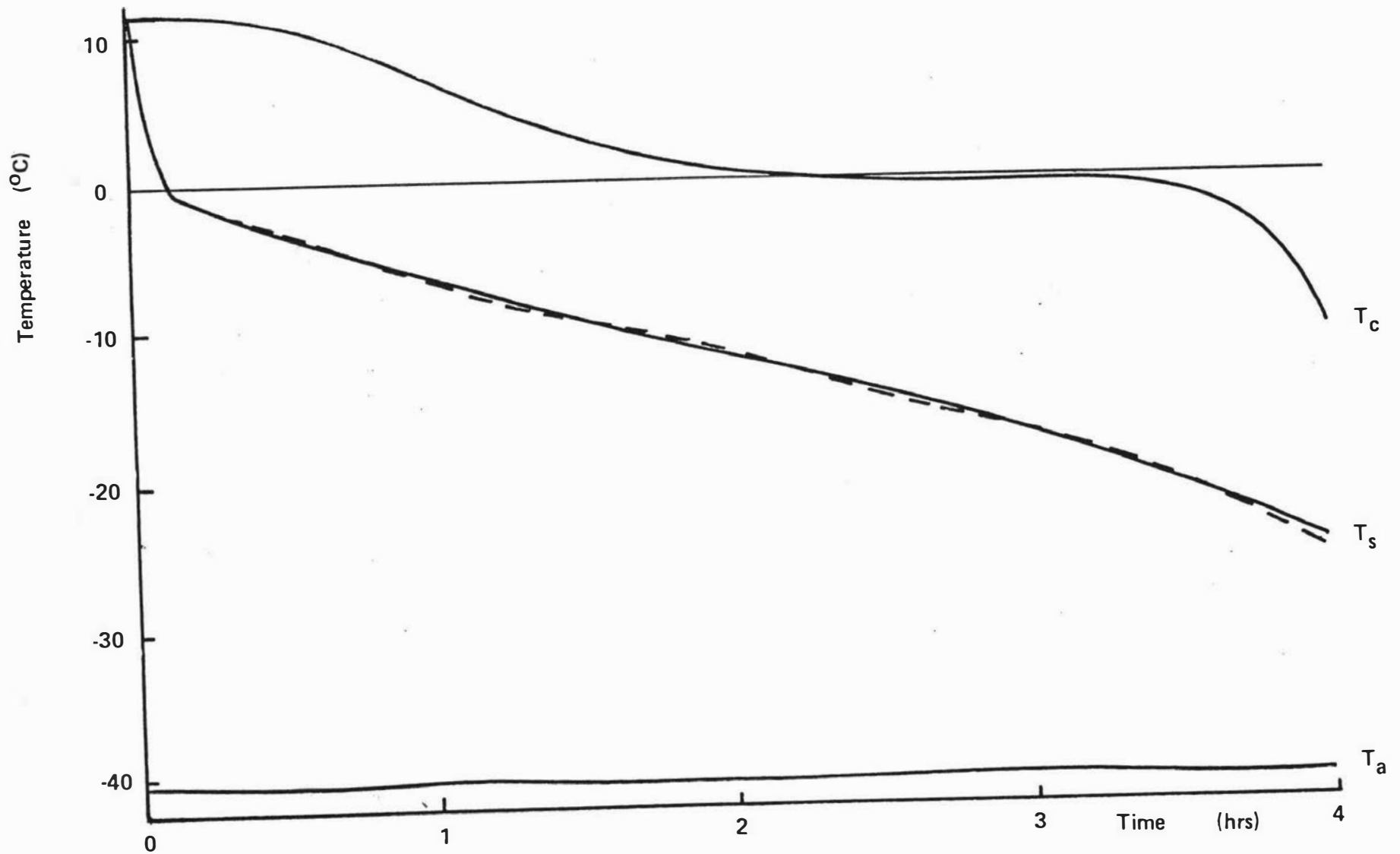


Figure 4.11 Typical experimental results for air blast freezing of a cylinder. $D = 0.1045\text{m}$; $h = 17.2 \text{ W/m}^2\text{°C}$;
 $T_a = -40.3^\circ\text{C}$; $T_i = 11.6^\circ\text{C}$.

(- - -) Temperature at a single point on the surface cycling around the average surface temperature.



Figure 4.12 Attachment of lids to the plastic boxes.
a. commercial food containers.
b. desirable arrangement.

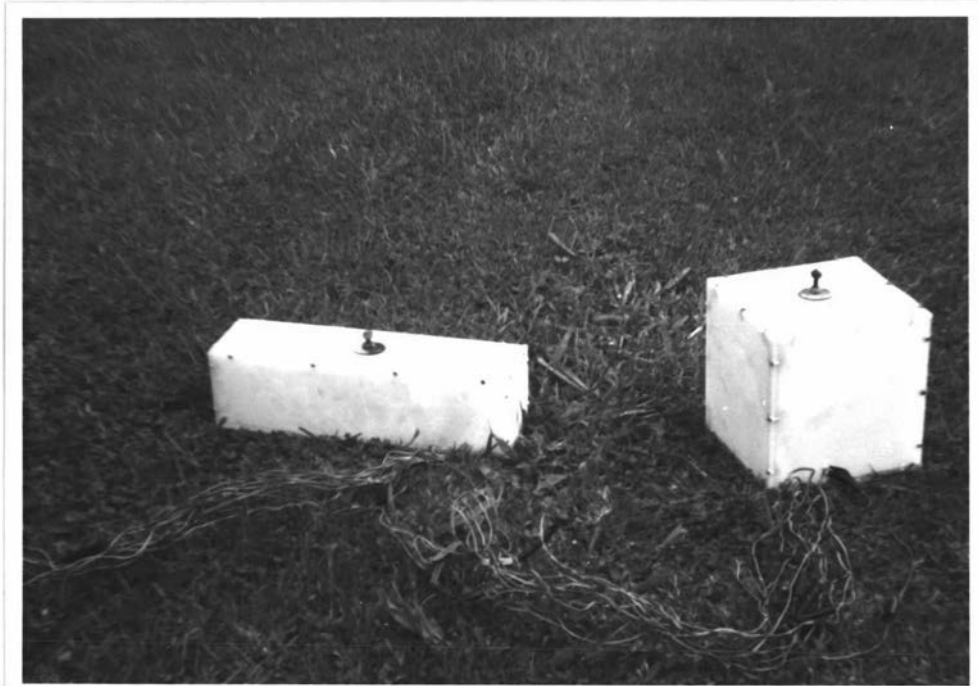


Figure 4.13 Typical polypropylene containers used in the experimental investigation into freezing of rectangular bricks.

wire was $2 \times 10^{-7} \text{ m}^2$, and heat flows along the wires would be typically $0.0002 \text{ W/}^\circ\text{C}$. There were ten wires per sphere, so conduction along the thermocouple wires would be in the range 0.02% to 0.16% of the total heat flow from each sphere. This is not significant.

In the air blast freezer additional errors were introduced because of the external heat transfer resistance varying around the body. Significant differences in surface temperature were found. Figure 4.11 gives typical results. On average each part of the surface was evenly exposed to the air flow, but the frequency of oscillations was too low to prevent cycling of the surface temperature. There was therefore additional error for the air freezing experiments as is indicated by the lower accuracy ($\pm 7\%$) to which the surface heat transfer coefficient is known compared to liquid immersion freezing ($\pm 4\%$). It is possible that the geometric and thermodynamic centres did not correspond under these conditions. However the surface temperature at any point cycles around the mean value which implies that approximately equal heat fluxes occurred from all points on the surface. In these circumstances the geometric and thermodynamic centres would be very close together if they did not coincide exactly.

4.5 THREE-DIMENSIONAL HEAT TRANSFER IN RECTANGULAR BRICKS

4.5.1 The Equipment

Both air blast and liquid immersion freezers were used. Rectangular plastic boxes were used with a 4mm diameter hole cut in them to allow a bolt to be inserted to hold them onto the sample oscillator in the same way as used for spheres. Up to 0.1% of the surface of each box was affected in this way, an insignificant amount. Two types of rectangular box were used :

1. Commercially available food containers. A wide range of shapes and sizes was available. The

important considerations were wall thickness, shape and type of lid. Whilst most of these containers slope out at the top it was possible to get some which were very close to rectangular, and only this latter type were used. Different wall thicknesses were wanted to give different external heat transfer resistances, but because it is in the manufacturers' interest to make the walls as thin as possible, the range of wall thicknesses available was insufficient to give a wide range of heat transfer conditions. Lids of these boxes were secured as shown in Figure 4.12a. The effect of the overlap in terms of the surface heat flux is very small as the fraction of the surface area affected is insignificant. The overall effect would be very close to what would be found in the ideal situation (Figure 4.12b).

2. Polypropylene boxes. To extend the range of heat transfer resistances some thick-walled plastic boxes were made from polypropylene sheet plastic with all the joints screwed together. This type of box is shown in Figure 4.13. The presence of the screws alters the heat transfer resistance of a small part (0.1% to 0.4%) of the surface area, depending on the box. The effect of this is insignificant and the corners approximated very closely to the desirable type of joint shown in Figure 4.12b.

Thermocouples were positioned at the centre of each brick, and at different places on the surface during packing of the boxes. The lids of the commercial food containers were glued in place and the lids of the polypropylene containers screwed down.

4.5.2 Dimensional Measurement and Control

The dimensions of each brick were measured in both the

frozen and unfrozen state. Allowing for variation in thickness as well as measurement inaccuracies all dimensions were accurate to $\pm 1\text{mm}$.

4.5.3 Temperature Measurement and Control

Exactly the same system of temperature measurement and control was used as for the experiments in radial geometry. This was discussed in detail in section 4.4.3. For the experimental investigation of the freezing of rectangular brick shapes the error in temperature measurement and control was $\pm 0.5^\circ\text{C}$ in the liquid immersion freezer, and $\pm 1^\circ\text{C}$ in the air blast freezer.

4.5.4 Measurement and Control of the Surface Heat Transfer Coefficient

In a brick shaped object heat transfer at any point on the surface can be treated as one-dimensional until the time that the heat penetration front from one or both of the other two dimensions reaches the point. This means that the methods developed for the measurement of surface heat transfer coefficients in slabs can be applied at short times whilst heat transfer in the other two directions is still insignificant. In section 4.3.4 it was shown that the three methods used for slabs were equally accurate. Therefore only one of these, that based on Goodman's integral profile technique (Goodman 1964), was used to calculate the surface heat transfer coefficient at short times. This method was chosen because it is the easiest of the three methods to use.

The analytical solution for heat conduction in three dimensions with the third kind of boundary condition and constant thermal properties (Newman 1936) was also used to estimate the surface heat transfer coefficient. This solution is only applicable for times before the onset of phase change. A similar computer program to that written for radial heat transfer was used. The program accepted values

of time, surface temperature and positional co-ordinates for the position where the measurement was made, and used an iterative loop to find the surface heat transfer coefficient needed to attain that temperature, at that time, in that position. Six terms of the heat conduction equation were used in each direction. This gave accuracy of better than $\pm 1\%$ for Fourier numbers greater than 0.02.

There was no statistically significant difference, at the 99% level of confidence, between the results from the two methods used to calculate the surface heat transfer coefficient, so the results from the two methods were averaged for each run. The measurements made on the polypropylene boxes in the immersion freezer agreed within 2.3% of the mean value with 95% confidence, whereas in the air blast freezer the 95% confidence limits were $\pm 5.2\%$. There was no statistically significant difference between values obtained at different temperatures of the cooling medium. Because the mean and 95% confidence limits for both air blast and immersion freezing were based on 8 sets of experimental data they give a good estimate of the error in measurement and control of the surface heat transfer coefficient.

For the commercial food containers 95% confidence limits were found after normalisation of the data set. The limits were $\pm 4\%$ in immersion freezing, and $\pm 7\%$ in air blast freezing. The results were less accurate than those found for the polypropylene containers because the surface heat transfer coefficients were generally larger, and consequently the time from the onset of cooling to the beginning of freezing was shorter than for the polypropylene containers. Values of the surface heat transfer coefficient are therefore based on less data, and their accuracy reflects this.

4.5.5 Analysis of Heat Transfer in Rectangular Bricks

Errors in calculations for bricks arise from similar sources to those for other shapes. Voids and imperfect thermal contact occur to the same extent as in spheres and

cylinders, and would not be expected to be any more significant for brick shapes than they were for the radial cases. Similarly any inhomogeneity caused by the presence of thermocouple wires would have a negligible effect.

Suitable isothermal regions for thermocouple lead location do not occur in brick shaped objects. Thermocouples were introduced through regions as near isothermal as possible to minimise conduction along the wires. Typical heat fluxes along the wires would therefore be similar to, or less than those occurring in spheres, and were hence insignificant.

Errors in the placement of surface thermocouples were assessed in the same way as for other shapes. The geometric and thermodynamic centres coincide at a single point and, similarly to a sphere, only one thermocouple could be placed here. Because of easy packing conditions it could be placed accurately, so error in the measurement of the centre temperature, and hence the freezing time, was small.

Errors due to inconsistencies in heat transfer within each brick were small, but in air blast freezing there were significant errors due to variation in the surface heat transfer coefficient around the faces of the brick. The bricks were rotated by hand in a similar fashion to that used for spheres and cylinders, and hence the overall error introduced would be of the same order. Temperatures at points on the surface which should be at the same temperature cycled around their mean value, but on average the points were exposed to the same heat transfer conditions. This effect did not occur in immersion freezing so there was clearly more error associated with the air blast system. This is indicated in the wider error bounds on the heat transfer coefficient in air blast freezing. As in radial geometry, each part of the surface received on average, the same exposure to the air flow, so the thermodynamic centre was very close to, or coincided exactly with the geometric centre where measurements of temperature were

made. These measurements of centre temperature would therefore be expected to be accurate.

5 EXPERIMENTAL DESIGN AND RESULTS

5.1 INTRODUCTION

In order to investigate the accuracy of methods for predicting the freezing time of foods, experiments must be conducted across a wide range of conditions covering those that occur in practical freezing problems. The four most important variables are the size of the object to be frozen, its initial temperature, the surface heat transfer coefficient, and the cooling medium temperature. These are defined in three dimensionless numbers, the Biot, Stefan and Plank numbers. The Biot number :

$$Bi = \frac{h D}{k_s} \quad (5.1)$$

takes account of the size of the object and the surface heat transfer coefficient; the Stefan number :

$$Ste = \frac{C_s (T_f - T_a)}{\Delta H} \quad (5.2)$$

takes account of the cooling medium temperature; and a new number :

$$\frac{C_l (T_i - T_f)}{\Delta H} \quad (5.3)$$

which it seems convenient and appropriate to call the Plank number, takes account of initial superheat. Table 5.1 shows typical values of these parameters for different food freezers. As well as these variables, shape factors are important for problems where heat transfer is in three dimensions.

An experimental design was sought in which these factors were varied over as wide a range as possible within the limitations of the experimental equipment.

5.2 SLABS

Apart from the relevant thermal properties, the four factors that affect the freezing time of a slab are the slab thickness D , ambient temperature T_a , initial temperature T_i and the surface heat transfer coefficient h . An orthogonal factorial experiment was performed with two levels of each of these variables plus centrepoints as shown in Table 5.2.

The freezing time was found to be a complex interaction of these factors. Because the four variables are all dimensional it was not possible to evaluate their effect on the freezing time without reference to the thermal properties of the material except by using dimensional coefficients. Therefore a set of dimensionless numbers were sought that totally defined the freezing conditions. Those chosen were the Fourier number :

$$Fo = \frac{k_s t}{C_s D^2} \quad (5.4)$$

the Stefan number, the Biot number and the Plank number. The Stefan and Plank numbers use ΔH , the enthalpy change in the phase change region. For cases where it is assumed that all latent heat is released at a unique freezing temperature it is the latent heat of freezing, but otherwise, it is defined as the enthalpy change between the initial freezing temperature and the final centre temperature.

The full functional dependence of the freezing time on the conditions and thermal properties is given by :

$$Fo = f(Bi, Ste, Pk) \quad (5.5)$$

When the previous factorial experiment was expressed in terms of these dimensionless numbers it was no longer orthogonal. Further experimental work was planned to extend the range of values of Bi , Ste and Pk under study. As the experimental design was no longer orthogonal there was no advantage in seeking to obtain precisely predetermined levels of each dimensionless number. Instead, provided a value close to the pre-selected level was obtained it was

considered satisfactory, and care was then taken to hold the experimental conditions as close to this value as possible. A set of 22 freezing experiments was conducted in this fashion. Table 5.3 gives the full set of results, and some typical freezing curves are shown in Figures 5.1 and 5.2.

Six experiments were conducted with each of minced lean beef and mashed potato to check that freezing experiments with Karlsruhe test substance gave results consistent with those for real foodstuffs. Table 5.4 gives the results of these experiments.

5.3 CYLINDERS AND SPHERES

Thirty freezing experiments were conducted with cylinders of Karlsruhe test substance, and the same number with spheres. Within these sets Bi , Ste and Pk were varied. It was possible to obtain an orthogonal design for the two factors Ste and Pk , but very difficult to obtain evenly spaced values of the Biot number over a wide range because Bi incorporates the effect of both the surface heat transfer coefficient and the diameter. Physical limitations in ball skin and pipe wall thickness were such that only a small range in the Biot number could be obtained using the liquid immersion freezer alone. Because surface heat transfer coefficients were lower in the air blast freezer the range of Biot numbers covered was increased by the use of this freezer, but an orthogonal experimental design was no longer feasible.

The design was set up to cover a wide range of conditions using four levels of Ste (corresponding to values of T_a of -20°C , -25.5°C , -33°C and -40°C); three levels of Pk (corresponding to values of T_i of 4°C , 17°C and 30°C); and six levels of Bi (resultant on three different diameter and wall thickness combinations, each frozen in both liquid immersion and air blast freezers). Because the experimental design was no longer orthogonal each freezing

experiment was conducted in the same way as used for some of the slab freezing experiments. For each factor, provided a value close to the preselected level was obtained it was considered satisfactory.

The full set of experimental results is given in Tables 5.5 and 5.6. Figures 5.3 and 5.4 show typical freezing curves.

5.4 RECTANGULAR BRICKS

As well as the three dimensionless numbers Bi , Ste and Pk , the freezing time of a brick shaped object depends on the ratio of the two longer sides to the shortest. This introduces two new factors that must be included in the experimental design. Because of practical difficulties in obtaining suitable boxes it was not possible to set up an orthogonal experiment in all five factors. Therefore the experiment was designed to give as wide as possible coverage over all five factors. Four levels of the Stefan number (corresponding to values of T_a of -20°C , -24°C , -30°C and -40°C); three levels of the Plank number (corresponding to values of T_i of 4°C , 17°C and 30°C); twenty-two levels of the Biot number (arising from eleven different wall thickness and box size combinations, each used in both liquid immersion and air blast freezers); and eleven different combinations of the geometric factors (from eleven differently shaped boxes) were used. Again, because the design was not orthogonal the pre-determined level of each variable was not sought exactly. Provided the actual value was known accurately, and it was close to the planned level it was considered satisfactory.

A total of 72 freezing experiments were conducted with Karlsruhe test substance, the results of which are given in Table 5.7, and typical freezing curves are shown in Figures 5.5, 5.6 and 5.7. No experiments were conducted with real food materials because the applicability of Karlsruhe test substance as an analogue should not depend

on the geometry. Having found slabs of food to freeze in a manner consistent with the slabs of Karlsruhe test substance there is no reason to expect inconsistencies in other shapes if accurate thermal data are available.

Table 5.1Typical conditions in food freezers

		Freezer Type		
		Air	Plate	Immersion
T_a	(°C)	-15 to -40	-15 to -35	-15 to -30
Ste		0.12 to 0.35	0.12 to 0.30	0.12 to 0.25
T_i	(°C)	0 to 40	0 to 40	0 to 40
Pk		0 to 0.60	0 to 0.60	0 to 0.60
D	(m)	0.001 to 0.5	0.02 to 0.2	0.01 to 0.2
h	(W/m ² °C) (no packaging)	10 to 50	200 to 500	100 to 600
Bi	(no packaging)	0.05 to 20	2.5 to 60	0.4 to 60
h	(W/m ² °C) (with packaging)	7 to 30	20 to 200	50 to 200
Bi	(with packaging)	0.05 to 10	0.3 to 10	0.2 to 10

Table 5.2

Design of the factorial experiment for investigation of the freezing times of slabs of Karlsruhe test substance

	D (m)	$\frac{1}{h}$ (m ² °C/W)	T _i (°C)	T _a (°C)
high level	0.0720	0.0193	30.0	-20.0
low level	0.0250	0.0463	10.0	-40.0
centrepoint level	0.0485	0.0327	20.0	-30.0

$\frac{1}{h}$ is used as a measure of the external heat transfer resistance in preference to the surface heat transfer coefficient.

Table 5.3

Experimental data for freezing of slabs of Karlsruhe test substance

Run Number	D (m)	h (W/m ² °C)	T _i (°C)	T _a (°C)	t _{exp} (hrs)	± err (hrs)
F1	0.0250	51.9	30.0	-40.0	0.64	± 0.04
F2	0.0720	51.9	30.0	-40.0	2.62	± 0.10
F3	0.0250	21.6	30.0	-40.0	1.42	± 0.07
F4	0.0720	21.6	30.0	-40.0	4.74	± 0.18
F5	0.0250	51.9	10.0	-40.0	0.56	± 0.04
F6	0.0720	51.9	10.0	-40.0	2.22	± 0.10
F7	0.0250	21.6	10.0	-40.0	1.26	± 0.07
F8	0.0720	21.6	10.0	-40.0	4.02	± 0.17
F9	0.0250	51.9	30.0	-20.0	1.26	± 0.07
F10	0.0720	51.9	30.0	-20.0	4.80	± 0.22
F11	0.0250	21.6	30.0	-20.0	2.74	± 0.14
F12	0.0720	21.6	30.0	-20.0	8.96	± 0.38
F13	0.0250	51.9	10.0	-20.0	1.12	± 0.07
F14	0.0720	51.9	10.0	-20.0	4.50	± 0.20
F15	0.0250	21.6	10.0	-20.0	2.44	± 0.13
F16	0.0720	21.6	10.0	-20.0	7.96	± 0.34
F17	0.0485	30.6	20.0	-30.0	2.74	± 0.12
F18	0.0485	30.6	20.0	-30.0	2.66	± 0.12
F19	0.0485	30.6	20.0	-30.0	2.70	± 0.12
F20	0.0485	30.6	20.0	-30.0	2.74	± 0.12
F21	0.0485	30.6	20.0	-30.0	2.74	± 0.12
F22	0.0250	90.0	11.0	-20.0	0.74	± 0.04
F23	0.0485	410	11.0	-21.0	1.00	± 0.05
F24	0.0720	90.0	11.0	-21.7	3.02	± 0.14
F25	0.1000	320	28.0	-21.0	4.28	± 0.18
F26	0.0250	400	21.6	-22.0	0.32	± 0.03
F27	0.0720	410	3.0	-22.0	1.92	± 0.09
F28	0.0485	90.0	34.5	-22.0	2.04	± 0.08
F29	0.0485	90.0	13.7	-24.3	1.54	± 0.07
F30	0.0720	330	10.5	-24.5	1.82	± 0.09

... continued

Table 5.3 continued

Run Number	D (m)	h (W/m ² °C)	T _i (°C)	T _a (°C)	t _{exp} (hrs)	± err (hrs)
F31	0.0250	430	3.0	-19.0	0.34	± 0.03
F32	0.1000	310	3.0	-23.0	3.46	± 0.15
F33	0.0485	360	3.0	-23.5	0.88	± 0.05
F34	0.0250	90.0	28.0	-24.0	0.68	± 0.04
F35	0.0250	16.7	3.0	-24.5	2.40	± 0.11
F36	0.0485	13.6	3.0	-26.0	5.34	± 0.20
F37	0.0720	13.6	3.0	-26.0	8.42	± 0.33
F38	0.0250	16.7	28.7	-26.0	2.68	± 0.13
F39	0.0485	16.7	15.3	-25.3	5.26	± 0.20
F40	0.0250	13.6	22.0	-25.3	3.10	± 0.12
F41	0.0720	16.7	28.0	-26.7	8.50	± 0.35
F42	0.0250	13.6	5.8	-29.6	2.32	± 0.10
F43	0.0485	13.6	28.6	-29.5	5.82	± 0.23

Table 5.4

Experimental data for freezing of minced lean beef (M)
and mashed potato (P) in slabs

Run Number	D (m)	h (W/m ² °C)	T _i (°C)	T _a (°C)	t _{exp} (hrs)	± err (hrs)
M1	0.0720	220	28.0	-25.0	2.32	± 0.12
M2	0.0720	51.9	3.0	-23.9	3.84	± 0.18
M3	0.0485	90.0	30.0	-25.4	1.68	± 0.08
M4	0.0485	21.6	3.0	-28.4	3.30	± 0.17
M5	0.0250	30.6	28.5	-25.7	1.54	± 0.07
M6	0.0250	16.7	16.4	-28.8	2.34	± 0.12
P1	0.0720	90.0	28.0	-24.3	3.20	± 0.16
P2	0.0720	51.9	11.8	-24.9	3.72	± 0.19
P3	0.0485	90.0	18.3	-26.7	1.58	± 0.09
P4	0.0485	21.6	15.0	-25.0	4.48	± 0.23
P5	0.0250	30.6	28.4	-25.9	1.76	± 0.10
P6	0.0250	13.6	4.7	-25.9	3.02	± 0.16

Table 5.5

Experimental data for freezing of cylinders of Karlsruhe test substance

Run Number	D (m)	h (W/m ² °C)	T _i (°C)	T _a (°C)	t _{exp} (hrs)	± err (hrs)
C1	0.1535	36.4	28.4	-21.0	8.36	± 0.46
C2	0.1045	27.2	30.0	-20.3	6.14	± 0.40
C3	0.0520	35.5	28.0	-19.9	2.16	± 0.17
C4	0.1535	36.4	21.0	-20.0	8.30	± 0.47
C5	0.1045	27.2	19.0	-20.0	5.82	± 0.38
C6	0.0520	35.5	19.7	-20.0	1.98	± 0.16
C7	0.1535	36.4	4.8	-21.1	7.50	± 0.39
C8	0.1045	27.2	5.8	-20.5	5.30	± 0.33
C9	0.0520	35.5	5.8	-20.2	1.84	± 0.14
C10	0.1535	36.4	27.2	-33.5	6.10	± 0.24
C11	0.1045	27.2	27.8	-33.1	4.10	± 0.23
C12	0.0520	35.5	26.8	-33.4	1.28	± 0.08
C13	0.1535	36.4	16.2	-33.6	5.56	± 0.23
C14	0.1045	27.2	16.5	-33.4	3.64	± 0.19
C15	0.0520	35.5	17.2	-33.2	1.18	± 0.08
C16	0.1535	36.4	10.8	-33.5	5.48	± 0.23
C17	0.1045	27.2	4.4	-34.0	3.44	± 0.21
C18	0.0520	35.5	4.8	-33.2	1.08	± 0.07
C19	0.1535	36.4	26.7	-19.8	8.90	± 0.46
C20	0.1535	36.4	27.6	-19.8	9.36	± 0.47
C21	0.0520	35.5	4.3	-33.5	1.06	± 0.07
C22	0.0520	35.5	4.0	-33.7	1.04	± 0.07
C23	0.1045	27.2	20.1	-25.6	4.56	± 0.27
C24	0.1045	27.2	19.6	-25.8	4.74	± 0.27
C25	0.1535	21.0	13.0	-40.5	5.86	± 0.37
C26	0.1045	17.8	14.6	-39.6	4.14	± 0.31
C27	0.0520	23.9	15.4	-40.2	1.34	± 0.13
C28	0.1535	21.0	4.0	-39.8	5.70	± 0.31
C29	0.1045	17.8	11.5	-39.9	3.96	± 0.37
C30	0.0520	23.9	25.3	-30.2	2.10	± 0.19

Table 5.6

Experimental data for freezing of spheres of Karlsruhe test substance

Run Number	D (m)	h (W/m ² °C)	T _i (°C)	T _a (°C)	t _{exp} (hrs)	± err (hrs)
S1	0.1575	45.9	28.5	-20.9	5.18	± 0.33
S2	0.0905	53.0	30.0	-19.9	2.28	± 0.18
S3	0.0535	46.7	27.2	-19.9	1.20	± 0.11
S4	0.1575	45.9	18.7	-20.0	5.14	± 0.32
S5	0.0905	53.0	18.7	-20.0	2.12	± 0.19
S6	0.0535	46.7	23.8	-20.0	1.14	± 0.11
S7	0.1575	45.9	4.9	-20.8	4.50	± 0.28
S8	0.0905	53.0	5.7	-20.5	1.92	± 0.16
S9	0.0535	46.7	3.2	-20.4	0.96	± 0.10
S10	0.1575	45.9	28.2	-33.2	3.38	± 0.19
S11	0.0905	53.0	30.4	-33.6	1.40	± 0.11
S12	0.0535	46.7	29.6	-33.4	0.80	± 0.08
S13	0.1575	45.9	16.0	-33.2	3.02	± 0.17
S14	0.0905	53.0	15.8	-33.2	1.30	± 0.10
S15	0.0535	46.7	15.8	-32.9	0.74	± 0.07
S16	0.1575	45.9	1.5	-32.6	2.70	± 0.17
S17	0.0905	53.0	11.4	-33.5	1.22	± 0.10
S18	0.0535	46.7	6.1	-33.4	0.68	± 0.05
S19	0.1575	45.9	29.3	-21.1	5.16	± 0.33
S20	0.1575	45.9	29.6	-20.8	5.24	± 0.33
S21	0.0535	46.7	4.7	-33.6	0.66	± 0.05
S22	0.0535	46.7	4.6	-33.7	0.66	± 0.05
S23	0.0905	53.0	20.8	-26.0	1.68	± 0.13
S24	0.0905	53.0	22.1	-26.0	1.68	± 0.13
S25	0.1575	26.9	13.0	-39.9	3.48	± 0.24
S26	0.0905	28.9	13.7	-39.6	1.62	± 0.17
S27	0.0535	27.3	13.0	-39.6	0.84	± 0.10
S28	0.1575	26.9	4.6	-39.7	3.30	± 0.24
S29	0.0905	28.9	4.0	-29.3	1.94	± 0.19
S30	0.0535	27.3	29.1	-29.3	1.26	± 0.15

Table 5.7

Experimental data for freezing of rectangular bricks of Karlsruhe test substance

Run Number	D_x (m)	D_y (m)	D_z (m)	h ($W/m^2 \cdot ^\circ C$)	T_i ($^\circ C$)	T_a ($^\circ C$)	t_{exp} (hrs)	\pm err (hrs)
B1	0.061	0.065	0.115	109	28.4	-20.5	1.34	\pm 0.10
B2	0.061	0.065	0.115	109	4.3	-19.7	1.20	\pm 0.10
B3	0.061	0.065	0.115	109	28.3	-30.0	0.92	\pm 0.07
B4	0.061	0.065	0.115	109	4.3	-29.8	0.80	\pm 0.07
B5	0.061	0.065	0.115	30.5	18.0	-40.3	1.28	\pm 0.10
B6	0.061	0.065	0.115	30.5	15.3	-25.0	2.02	\pm 0.16
B7	0.099	0.139	0.198	96.2	29.0	-20.2	3.90	\pm 0.26
B8	0.099	0.139	0.198	96.2	4.6	-20.6	3.40	\pm 0.24
B9	0.099	0.139	0.198	96.2	29.1	-30.2	2.80	\pm 0.15
B10	0.099	0.139	0.198	96.2	1.0	-29.9	2.32	\pm 0.14
B11	0.099	0.139	0.198	29.4	16.7	-40.3	3.32	\pm 0.24
B12	0.099	0.139	0.198	29.4	17.5	-23.4	5.76	\pm 0.46
B13	0.081	0.194	0.259	83.5	28.8	-20.0	4.10	\pm 0.26
B14	0.081	0.194	0.259	83.5	4.2	-20.6	3.46	\pm 0.24
B15	0.081	0.194	0.259	83.5	28.8	-29.8	3.04	\pm 0.17
B16	0.081	0.194	0.259	83.5	1.0	-29.8	2.32	\pm 0.16
B17	0.081	0.194	0.259	28.1	15.8	-39.7	3.50	\pm 0.27
B18	0.081	0.194	0.259	28.1	15.9	-24.7	5.72	\pm 0.48
B19	0.105	0.237	0.237	260	28.4	-20.0	4.90	\pm 0.26
B20	0.105	0.237	0.237	260	4.0	-20.1	4.24	\pm 0.24
B21	0.105	0.237	0.237	260	29.0	-29.9	3.40	\pm 0.16
B22	0.105	0.237	0.237	260	4.3	-29.9	2.90	\pm 0.16
B23	0.105	0.237	0.237	37.5	8.8	-39.0	4.02	\pm 0.26
B24	0.105	0.237	0.237	37.5	20.8	-25.0	6.76	\pm 0.52
B25	0.072	0.116	0.166	96.3	28.0	-20.3	2.44	\pm 0.18
B26	0.072	0.116	0.166	96.3	4.2	-20.2	2.16	\pm 0.17
B27	0.072	0.116	0.166	96.3	30.0	-30.2	1.70	\pm 0.12
B28	0.072	0.116	0.166	96.3	4.3	-29.7	1.48	\pm 0.11
B29	0.072	0.116	0.166	29.4	10.8	-39.6	2.06	\pm 0.16
B30	0.072	0.116	0.166	29.4	11.9	-24.2	3.44	\pm 0.24

... continued

Table 5.7 continued

Run Number	D_x (m)	D_y (m)	D_z (m)	h (W/m ² °C)	T_i (°C)	T_a (°C)	t_{exp} (hrs)	\pm err (hrs)
B31	0.086	0.115	0.219	92.0	27.0	-20.8	3.06	\pm 0.21
B32	0.086	0.115	0.219	92.0	4.2	-20.0	2.78	\pm 0.20
B33	0.086	0.115	0.219	92.0	31.4	-30.0	2.20	\pm 0.14
B34	0.086	0.115	0.219	92.0	3.6	-29.0	1.94	\pm 0.13
B35	0.086	0.115	0.219	29.0	18.5	-39.6	2.86	\pm 0.21
B36	0.086	0.115	0.219	29.0	15.2	-24.6	4.30	\pm 0.31
B37	0.085	0.192	0.263	98.5	27.8	-21.3	4.02	\pm 0.25
B38	0.085	0.192	0.263	98.5	4.7	-20.3	3.72	\pm 0.24
B39	0.085	0.192	0.263	98.5	31.2	-30.0	3.02	\pm 0.16
B40	0.085	0.192	0.263	98.5	4.6	-29.3	2.52	\pm 0.15
B41	0.085	0.192	0.263	29.6	18.5	-39.6	3.90	\pm 0.28
B42	0.085	0.192	0.263	29.6	16.8	-25.0	5.70	\pm 0.48
B43	0.135	0.164	0.164	260	26.8	-20.3	4.56	\pm 0.21
B44	0.135	0.164	0.164	260	4.0	-20.2	4.08	\pm 0.19
B45	0.135	0.164	0.164	260	31.3	-29.6	3.24	\pm 0.14
B46	0.135	0.164	0.164	260	4.6	-30.1	2.82	\pm 0.13
B47	0.135	0.164	0.164	37.5	12.0	-40.2	3.56	\pm 0.20
B48	0.135	0.164	0.164	37.5	18.1	-24.4	5.76	\pm 0.34
B49	0.075	0.075	0.075	41.0	29.5	-20.6	2.32	\pm 0.17
B50	0.075	0.075	0.075	41.0	4.0	-19.9	2.04	\pm 0.15
B51	0.075	0.075	0.075	41.0	28.9	-29.9	1.60	\pm 0.11
B52	0.075	0.075	0.075	41.0	4.6	-29.9	1.36	\pm 0.10
B53	0.075	0.075	0.075	22.1	16.9	-39.6	1.66	\pm 0.13
B54	0.075	0.075	0.075	20.5	19.6	-24.7	2.72	\pm 0.22
B55	0.150	0.150	0.150	41.0	30.8	-20.9	6.90	\pm 0.38
B56	0.150	0.150	0.150	41.0	4.6	-20.9	6.04	\pm 0.32
B57	0.150	0.150	0.150	41.0	29.4	-30.6	4.88	\pm 0.26
B58	0.150	0.150	0.150	41.0	4.6	-30.0	4.16	\pm 0.27
B59	0.150	0.150	0.150	20.5	16.8	-39.6	4.84	\pm 0.26
B60	0.150	0.150	0.150	20.5	16.7	-24.6	7.48	\pm 0.48
B61	0.075	0.075	0.300	41.0	32.1	-20.1	3.30	\pm 0.22
B62	0.075	0.075	0.300	41.0	4.1	-20.5	2.68	\pm 0.20

... continued

Table 5.7 continued

Run Number	D_x (m)	D_y (m)	D_z (m)	h (W/m ² °C)	T_i (°C)	T_a (°C)	t_{exp} (hrs)	\pm err (hrs)
B63	0.075	0.075	0.300	41.0	31.6	-31.1	2.20	\pm 0.13
B64	0.075	0.075	0.300	41.0	4.7	-29.9	1.86	\pm 0.12
B65	0.075	0.075	0.300	20.5	19.3	-40.7	2.38	\pm 0.19
B66	0.075	0.075	0.300	20.5	18.4	-24.8	3.68	\pm 0.34
B67	0.050	0.200	0.200	41.0	29.7	-20.1	3.46	\pm 0.26
B68	0.050	0.200	0.200	41.0	5.9	-20.1	2.86	\pm 0.23
B69	0.050	0.200	0.200	41.0	31.0	-30.8	2.30	\pm 0.16
B70	0.050	0.200	0.200	41.0	4.7	-30.0	1.88	\pm 0.13
B71	0.050	0.200	0.200	20.5	18.6	-40.0	2.62	\pm 0.24
B72	0.050	0.200	0.200	20.5	16.2	-24.6	4.10	\pm 0.38

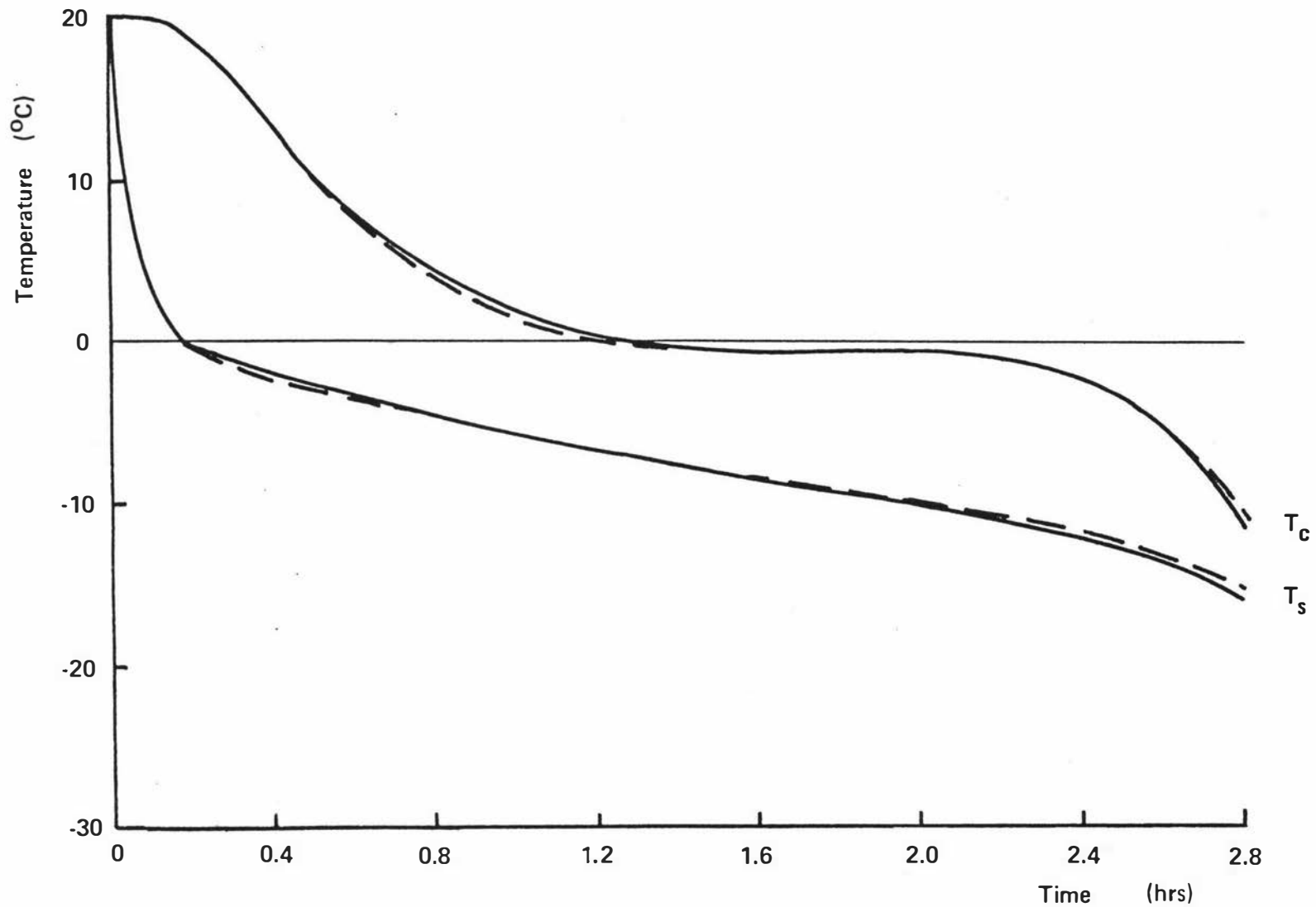


Figure 5.1 Typical temperature curves for freezing of a slab of Karlsruhe test substance (Run F17). $D = 0.0485\text{m}$; $h = 30.6 \text{ W/m}^2\text{°C}$; $T_a = -30.0\text{°C}$; $T_i = 20.0\text{°C}$.

(——) experimental results

(---) results from finite difference simulation (see section 6.1.3)

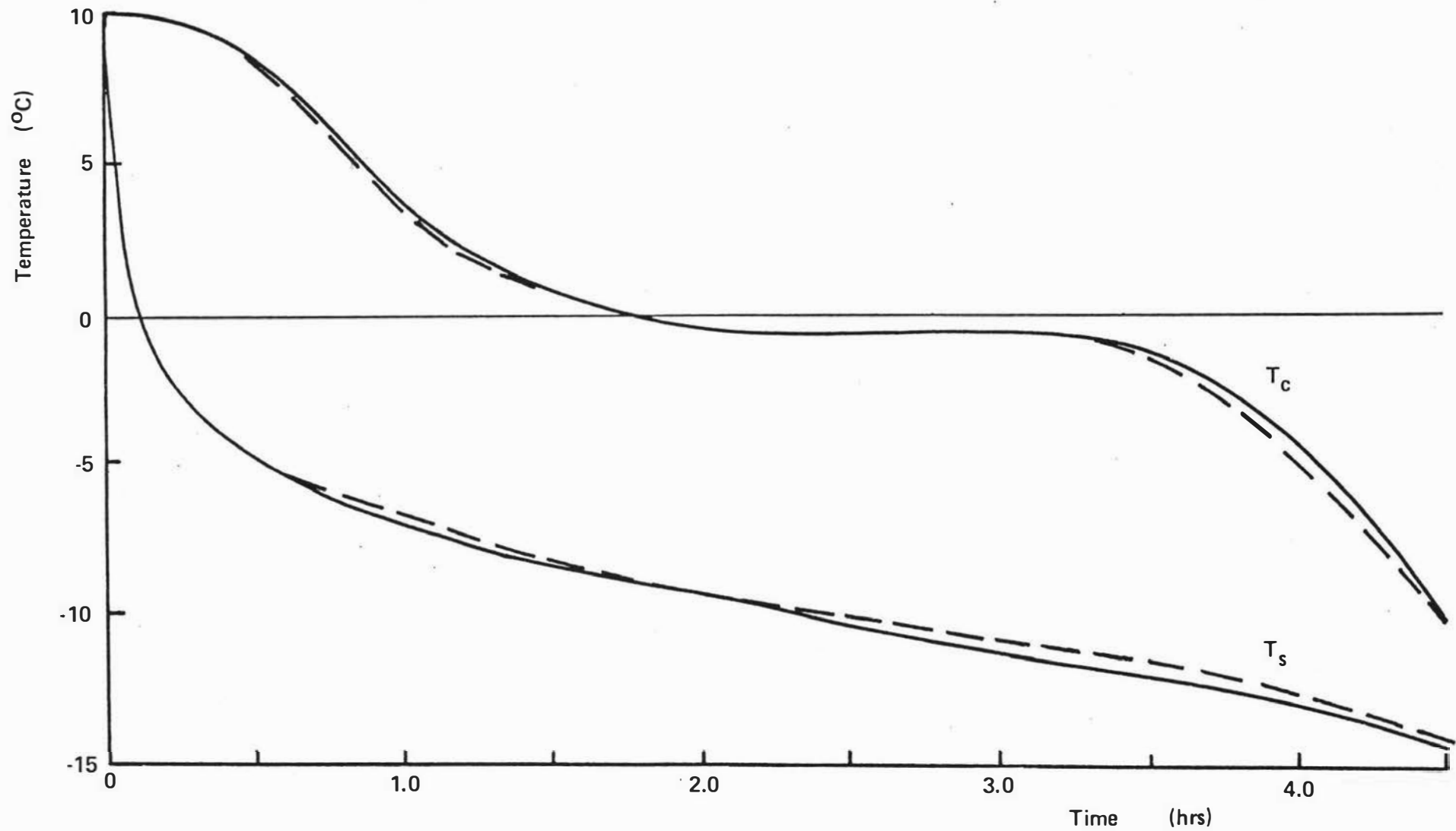


Figure 5.2 Typical temperature curves for freezing of a slab of Karlsruhe test substance (Run F14). $D = 0.0720\text{m}$;
 $h = 51.9 \text{ W/m}^2\text{°C}$; $T_a = -20.0\text{°C}$; $T_i = 10.0\text{°C}$.

(——) experimental results

(- - - -) results from finite difference simulation (see section 6.1.3)

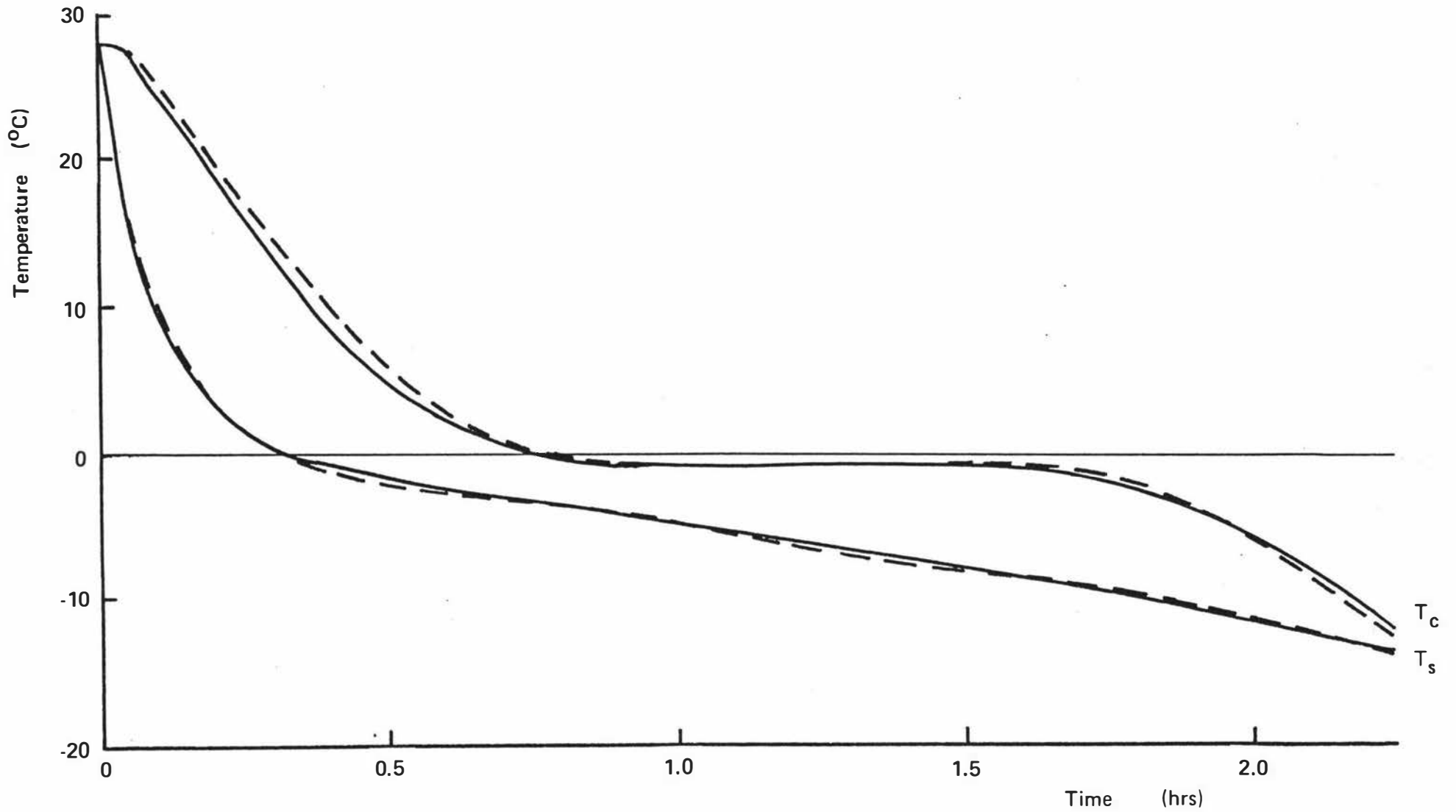


Figure 5.3 Typical temperature curves for freezing of a cylinder of Karlsruhe test substance (Run C3). $D = 0.0520\text{m}$;
 $h = 35.5 \text{ W/m}^2\text{°C}$; $T_a = -19.9\text{°C}$; $T_i = 28.0\text{°C}$.

(——) experimental results

(---) results from finite difference simulation (see section 6.2.3)

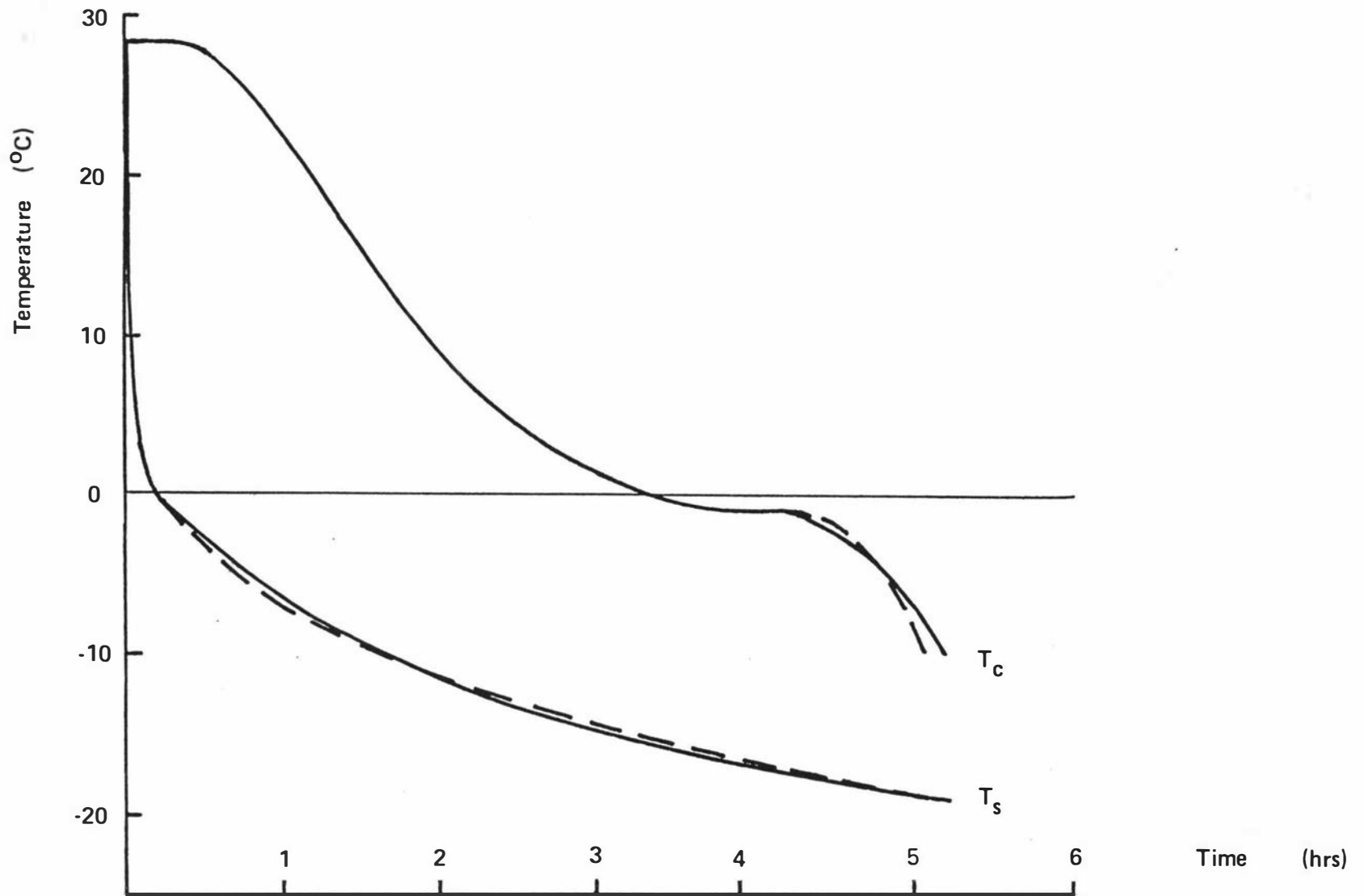


Figure 5.4 Typical temperature curves for freezing of a sphere of Karlsruhe test substance (Run S1). $D = 0.1575\text{m}$; $h = 45.9 \text{ W/m}^2\text{°C}$; $T_a = -20.9\text{°C}$; $T_i = 28.5\text{°C}$.
 (—) experimental results
 (- - -) results from finite difference simulation (see section 6.2.3)

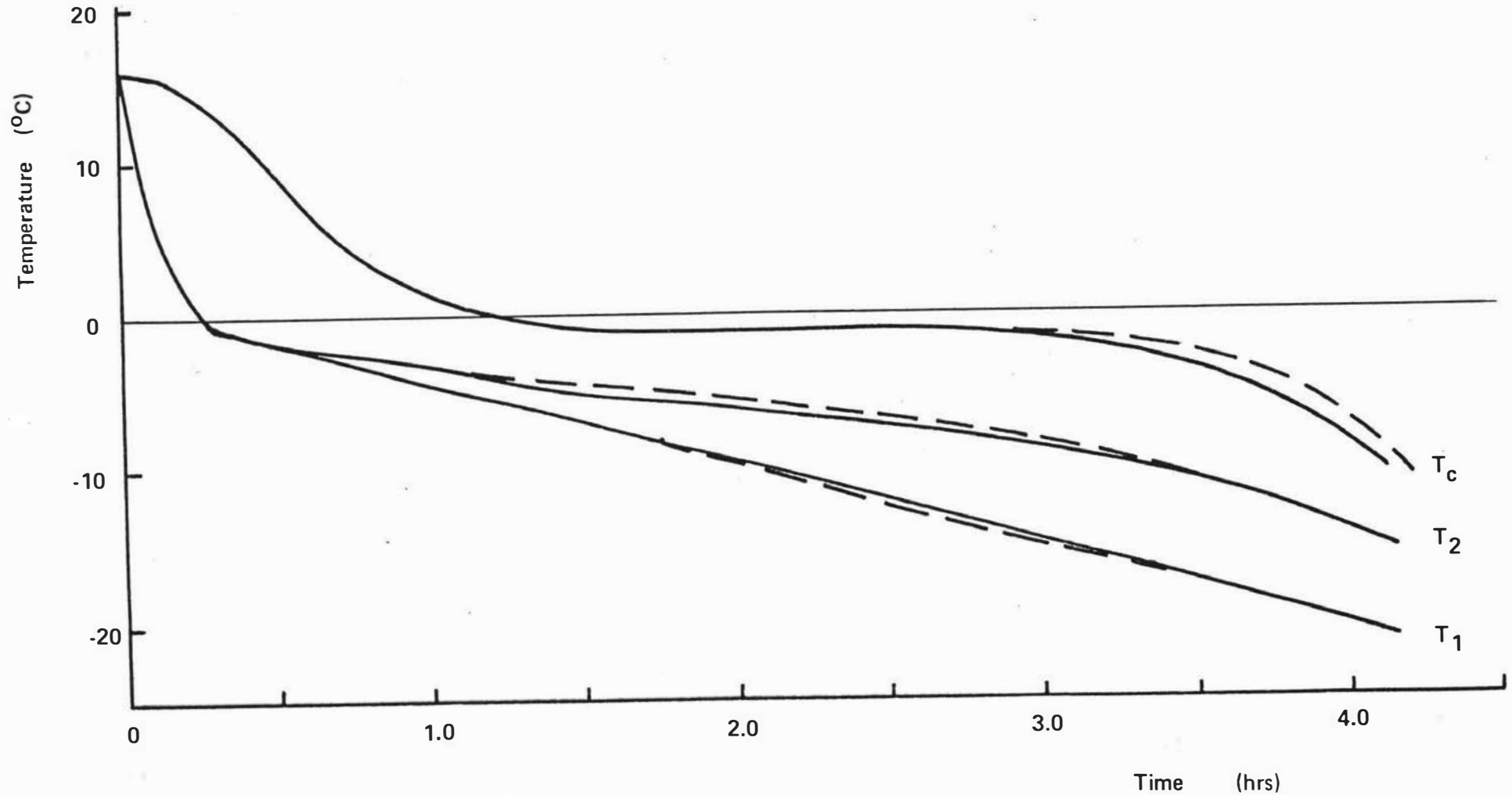


Figure 5.5 Typical temperature curves for freezing of a rectangular brick of Karlsruhe test substance (Run B72). Brick dimensions $0.050\text{m} \times 0.200\text{m} \times 0.200\text{m}$; $h = 20.5 \text{ W/m}^2\text{°C}$; $T_a = -24.6\text{°C}$; $T_i = 16.2\text{°C}$.
 T_1 = surface temperature at dimensionless point $(0,1,0)$. T_2 = surface temperature at dimensionless point $(1,0.4, 0)$.
 (—) experimental results
 (- - -) results from finite difference simulation (see section 6.3.3)

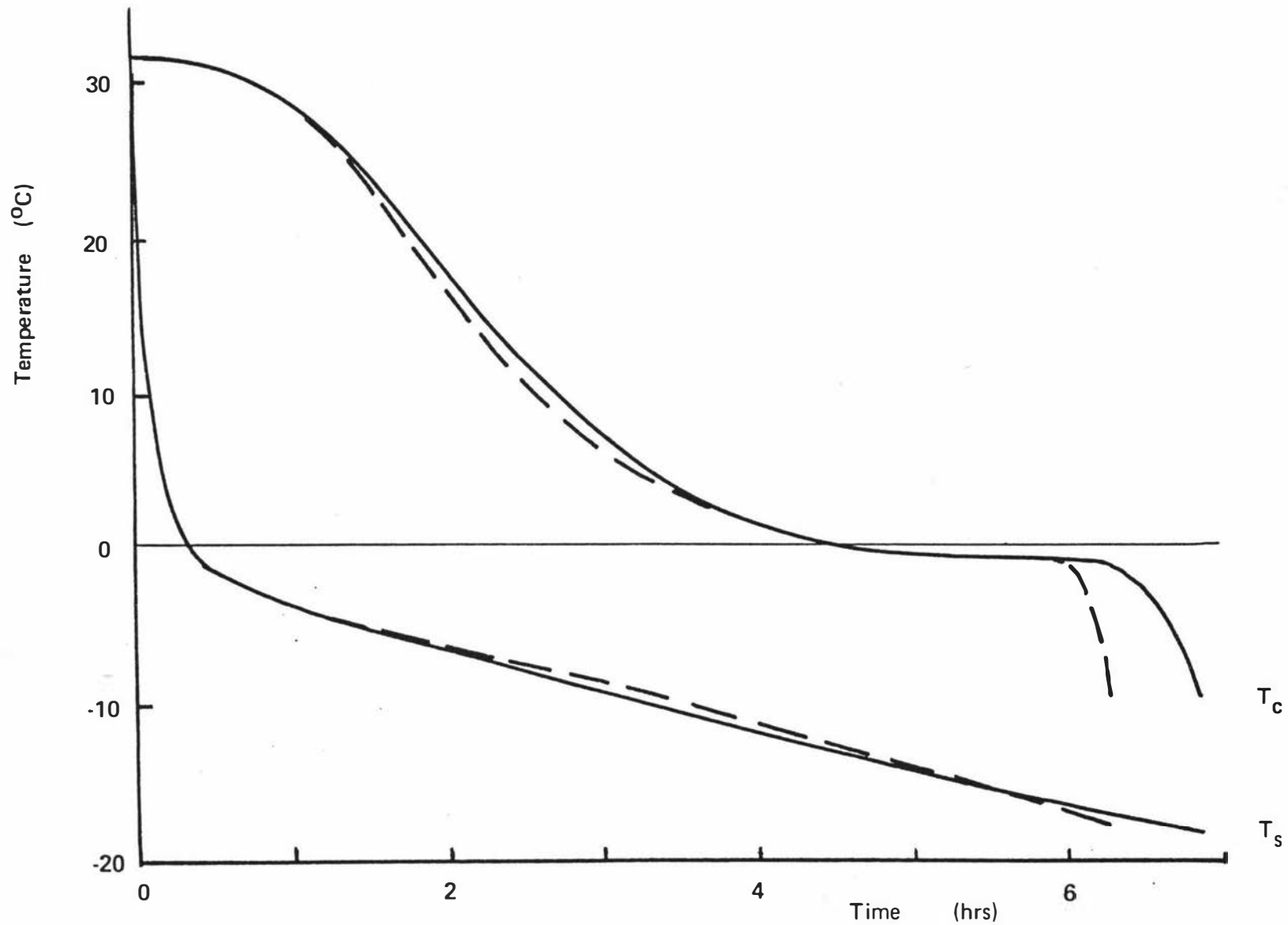


Figure 5.6 Typical temperature curves for freezing of a rectangular brick of Karlsruhe test substance (Run B55). Brick dimensions 0.150m x 0.150m x 0.150m; $h = 41.0 \text{ W/m}^2\text{°C}$; $T_a = -20.9\text{°C}$; $T_i = 30.8\text{°C}$; T_s = surface temperature at dimensionless point (0,1,0).

(—) experimental results

(---) results from finite difference simulation (see section 6.3.3)

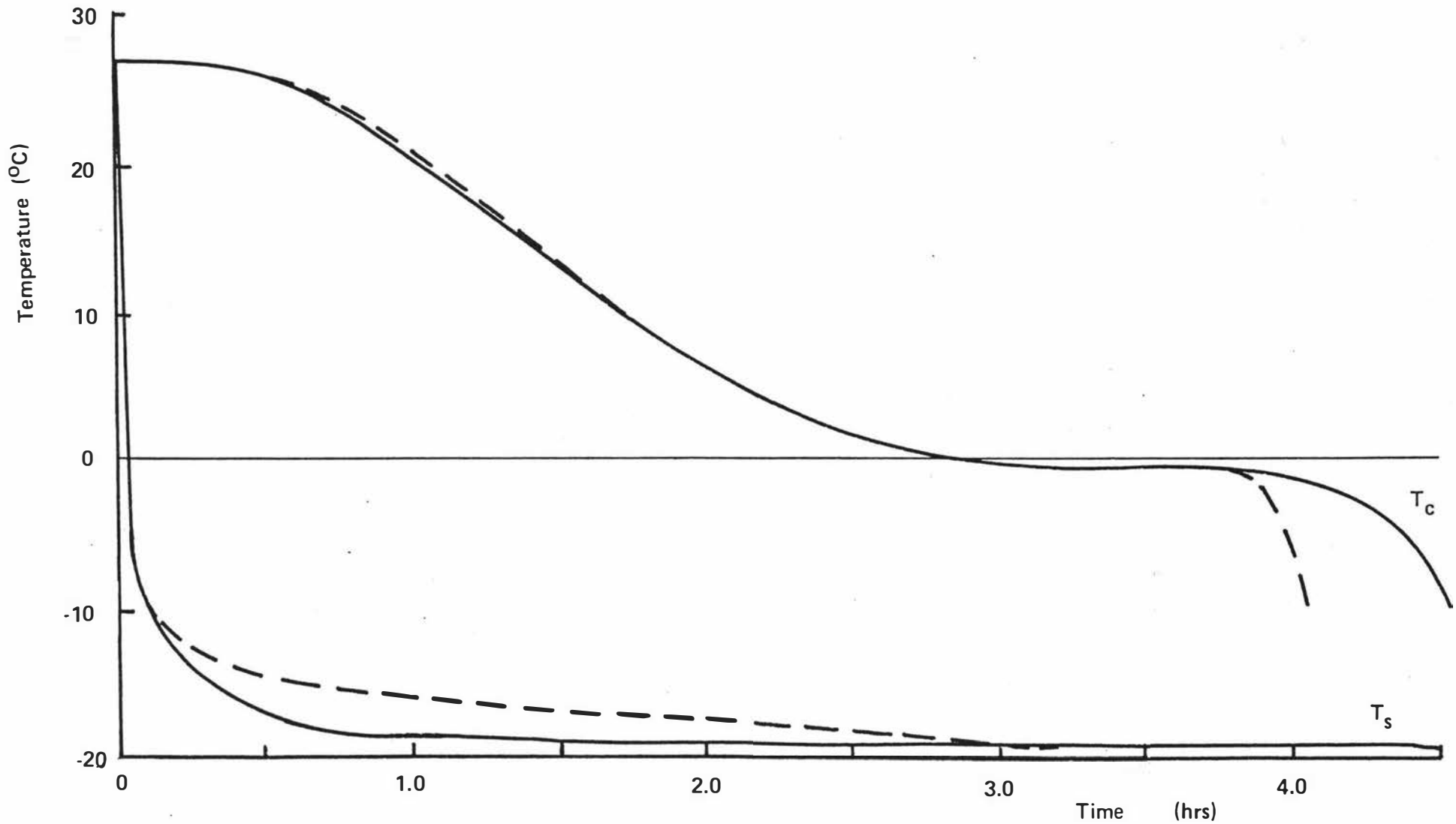


Figure 5.7 Typical temperature curves for freezing of a rectangular brick of Karlsruhe test substance (Run B43). Brick dimensions 0.136m x 0.164m x 0.164m; $h = 260 \text{ W/m}^2\text{°C}$; $T_a = -20.3\text{°C}$; $T_i = 26.8\text{°C}$. T_s = surface temperature at dimensionless point (0,1,0).
 (—) experimental results
 (- - -) results from finite difference simulation (see section 6.3.3)

6 PREDICTION OF FREEZING TIME BY NUMERICAL METHODS

6.1 SLABS

6.1.1 Selection of Numerical Method

There is a wide range of numerical solutions to freezing problems as discussed in Chapter 2. These fall into two groups :

1. Finite difference and finite element techniques.
2. Numerical integration and differentiation of ordinary integro-differential equations.

A number of solutions to slab freezing problems have been derived by the use of simplifying assumptions to reduce the partial differential equations to ordinary integro-differential equations. These were discussed in section 2.2.2. For the important third kind of boundary condition only three solutions of this kind are available. Those of Hills and Moore (1967) and Chung and Yeh (1975) are only applicable to problems where there is no initial superheat. The third method (Selim and Seagrave 1973a) uses integral transforms to solve the same problem with no initial superheat, but differs in that results are presented diagrammatically for dimensionless freezing time as a function of the Biot and Stefan numbers. The results agree within 3% of results calculated from Plank's equation (1941), and values read from the charts of Tao (1968). Therefore the complex methods requiring numerical integration are no more accurate than the simpler solutions, and because they do not take account of initial superheat they have serious shortcomings if applied to practical problems where superheat occurs.

Muehlbauer et al (1973) have produced a solution for a finite slab initially superheated and subject to the third kind of boundary condition. Latent heat is released over a range of temperature, and is taken into account as a constant apparent specific heat capacity evenly distributed

across the temperature range over which phase change occurs. The method relies on the use of Goodman's integral profile technique with binomial approximations, a method which is only accurate to 8-10% (Goodman 1964). This, together to the crude approximation to the specific heat capacity limit the accuracy of the solution. It does not rely on numerical integration, but rather several parameters must be found implicitly by iterative procedures. This means that the solution is very time-consuming to use by hand. For this reason it has been included in the group of methods requiring a computing device for solution. When the method was applied to the solidification of alloy mixtures large deviations from experimentally determined values were found (Muehlbauer et al 1973). No application of this method to the freezing of foods has been made, but another attempt to develop a solution of this type for freezing of foods was not successful (Bakal and Hayakawa 1973). Thus the method has no apparent advantages to recommend it in preference to either finite differences or finite elements for use in predicting the freezing time of foods.

The greatest advantage of finite difference and finite element methods is that they can take account of a variety of boundary and initial conditions, an attribute that no simple solution has. They have been shown to give very good agreement (within 2%) to a known exact solution to a freezing problem (Comini et al 1974c), and would be expected to give similar accuracy when applied to other food freezing problems. For these reasons methods of this type are superior to those requiring numerical integration, and therefore the latter group need not be considered any further.

Finite difference and finite element techniques both rely on approximations to the governing partial differential equations over small intervals. The errors in the two methods are of the same order (Myers 1971, p339), and the principle practical difference between them is in the way that the space grid is defined. Finite elements are more

versatile, and are the easier method to use for irregular shapes (Comini et al 1974c). For regular geometry (slabs, cylinders, spheres and rectangular bricks) there is nothing to choose between the two methods. For this reason the slightly simpler and better documented finite difference method has been chosen.

6.1.2 Selection of Finite Difference Approach

Because of their versatility finite differences can take account of phase change at a unique temperature, or over a range of temperature. The thermal properties of common foods are known to change continuously with temperature. The change in phase can be taken into account by use of an apparent specific heat capacity $C(T)$, and a temperature dependent thermal conductivity $k(T)$, in the general heat conduction equation :

$$C(T) \frac{\partial T}{\partial t} = \frac{\partial}{\partial x} (k(T) \frac{\partial T}{\partial x}) \quad (6.1)$$

subject to the appropriate boundary and initial conditions (see section 2.3). This model is physically correct, and the only errors are those in the data for $k(T)$ and $C(T)$, and errors in the finite difference approximation. Solutions of this type accurately simulate the temperature in a freezing object subject to the fourth kind of boundary condition (Bonacina and Comini 1971), and although not tested over a wide range of conditions were also found to be accurate for the third kind of boundary condition (Bonacina and Comini 1973).

The other method used to take account of phase change is to assume that all the latent heat is released at a unique freezing temperature with the thermal properties of the frozen and unfrozen phases constant, but different for each phase. This method is not as physically correct as the first method, and the position of the freezing front between nodes can only be determined approximately (Murray and Landis 1959). Because of these extra errors this type

of finite difference scheme does not predict temperature as a function of time as accurately as the other type of finite differences. In fact, the shape of the calculated temperature/time profiles is quite different from experimental freezing curves (Charm et al 1972). For these reasons this type of finite difference scheme is not as useful for predicting the freezing times of foods as the first type.

By choice of the functions $C(T)$ and $k(T)$ as shown in Figure 6.1 the more versatile programs can also be made to approximate to freezing at a unique phase change temperature (Comini et al 1974c). Consequently only this type of finite differences need be considered any further.

6.1.3 Comparison of Finite Difference Schemes

Of the large number of finite difference schemes that have been developed to take account of phase change in the functions $k(T)$ and $C(T)$ several are based on an erroneous premise. The general heat conduction equation :

$$C(T) \frac{\partial T}{\partial t} = \frac{\partial}{\partial x} (k(T) \frac{\partial T}{\partial x}) \quad (6.2)$$

can only be reduced to :

$$C(T) \frac{\partial T}{\partial t} = k(T) \frac{\partial^2 T}{\partial x^2} \quad (6.3)$$

if $k(T)$ is not a function of position. If $k(T)$ varies with temperature, and temperature varies with position, then thermal conductivity is position dependent and the simplification cannot be made. Finite difference schemes based on this simplification (Earle and Earl 1966; Cullwick 1967; Mawson 1969; Bailey et al 1974; Joshi and Tao 1974; Chattopadhyay et al 1975) therefore lead to erroneous results. Typically, results from the scheme of Cullwick (1967) were found to overpredict the freezing time by up to 50% when compared to experiment. Bonacina and Comini (1971) made a study of finite difference methods and found that the

scheme of Lees (1966), hereafter referred to as the "Lees scheme", was best. This is a three time-level scheme :

$$C_m^i \frac{T_m^{i+1} - T_m^{i-1}}{2\Delta t} = \frac{1}{3(\Delta x)^2} (k_{m+\frac{1}{2}}^i (T_{m+1}^{i+1} - T_m^{i+1} + T_{m+1}^i - T_m^i + T_{m+1}^{i-1} - T_m^{i-1}) - k_{m-\frac{1}{2}}^i (T_m^{i+1} - T_{m-1}^{i+1} + T_m^i - T_{m-1}^i + T_m^{i-1} - T_{m-1}^{i-1})) \quad (6.4)$$

It is convergent and unconditionally stable. A similar scheme of the form :

$$C_m^i \frac{T_m^{i+1} - T_m^i}{\Delta t} = \frac{1}{(\Delta x)^2} (k_{m+\frac{1}{2}}^i (T_{m+1}^i - T_m^i) - k_{m-\frac{1}{2}}^i (T_m^i - T_{m-1}^i)) \quad (6.5)$$

was used by Allada and Quan (1966), and there is also a Crank-Nicolson version :

$$C_m^{i+\frac{1}{2}} \frac{T_m^{i+1} - T_m^i}{\Delta t} = \frac{1}{2(\Delta x)^2} (k_{m+\frac{1}{2}}^{i+\frac{1}{2}} (T_{m+1}^{i+1} - T_m^{i+1} + T_{m+1}^i - T_m^i) - k_{m+\frac{1}{2}}^{i+\frac{1}{2}} (T_m^{i+1} - T_{m-1}^{i+1} + T_m^i - T_{m-1}^i)) \quad (6.6)$$

A related scheme to equation 6.5 is also given by McAdams (1957, p50).

Another group of solutions exists that uses the enthalpy transformation of Eyres et al (1946) to combine the thermal properties more directly in the difference scheme (Albasiny 1956; Lockwood 1966; Cordell and Webb 1972; Shamsundar and Sparrow 1975; Shamsundar and Sparrow 1976). These use either fully implicit or fully explicit finite difference approximations. They are not as accurate as equation 6.4 or equation 6.6 because of greater truncation errors.

From their study of finite difference schemes Bonacina and Comini (1971) found that the principle advantage of the Lees scheme is that all thermal property approximations

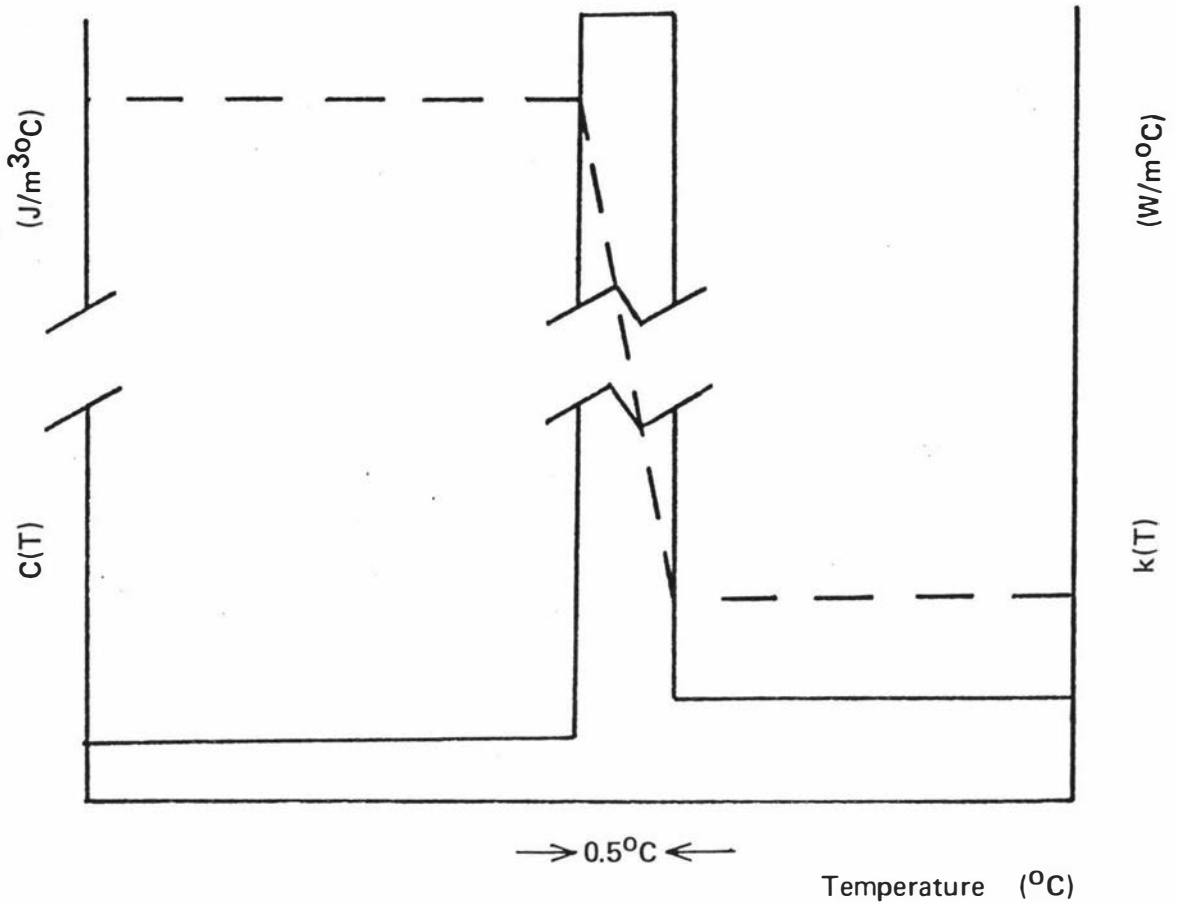


Figure 6.1 Thermal property curves used to approximate freezing at a unique phase change temperature.

- (———) $C(T)$ (refers to left hand scale)
- (- - -) $k(T)$ (refers to right hand scale)

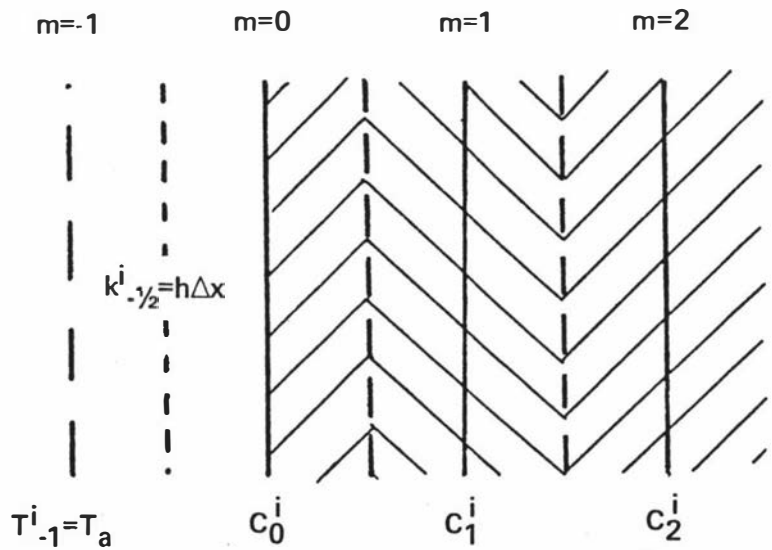


Figure 6.2 The finite difference grid at the surface of a freezing slab.

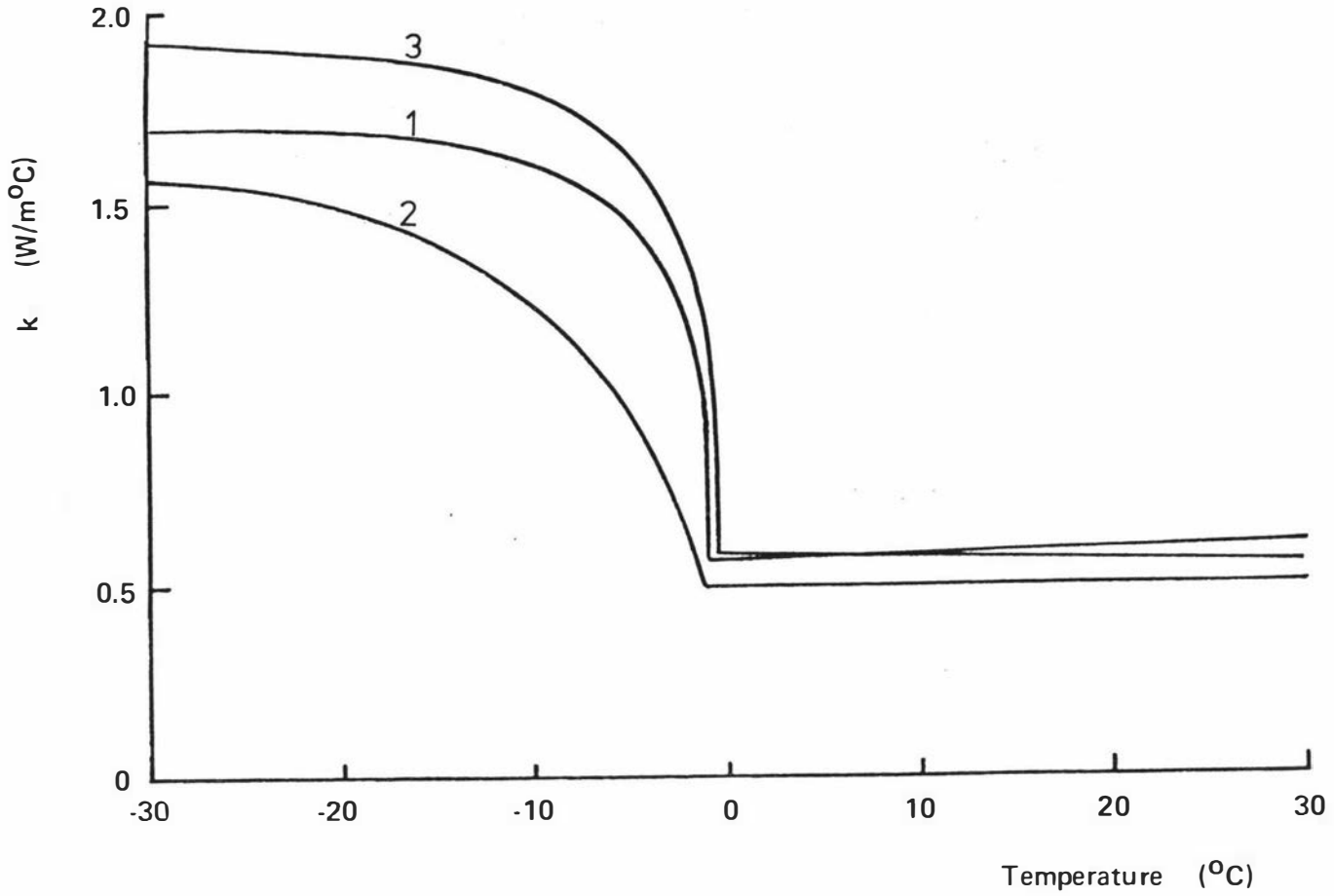


Figure 6.3 Thermal conductivity data. 1 – Karlsruhe test substance. 2 – minced lean beef. 3 – mashed potato.

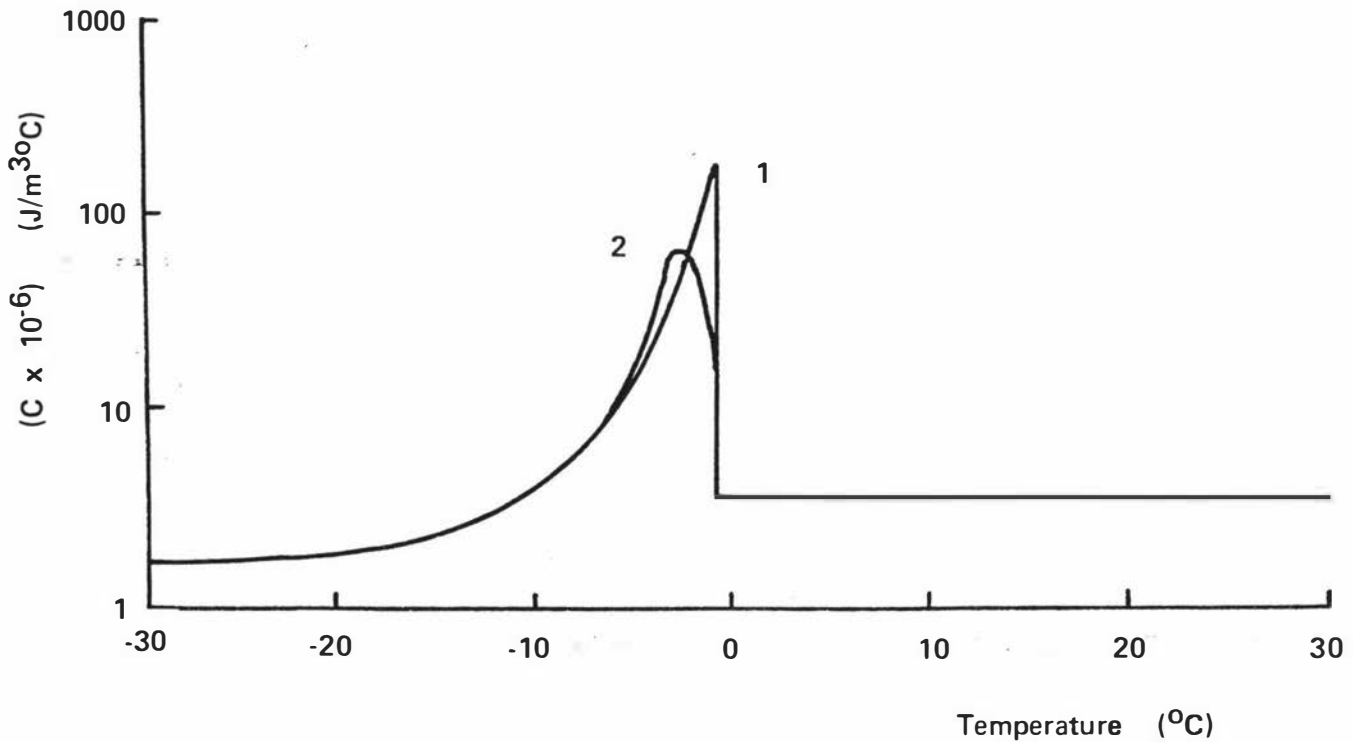


Figure 6.4 Apparent specific heat capacity data for Karlsruhe test substance. 1 – data of Riedel (1960a). 2 – data of Comini (1976).

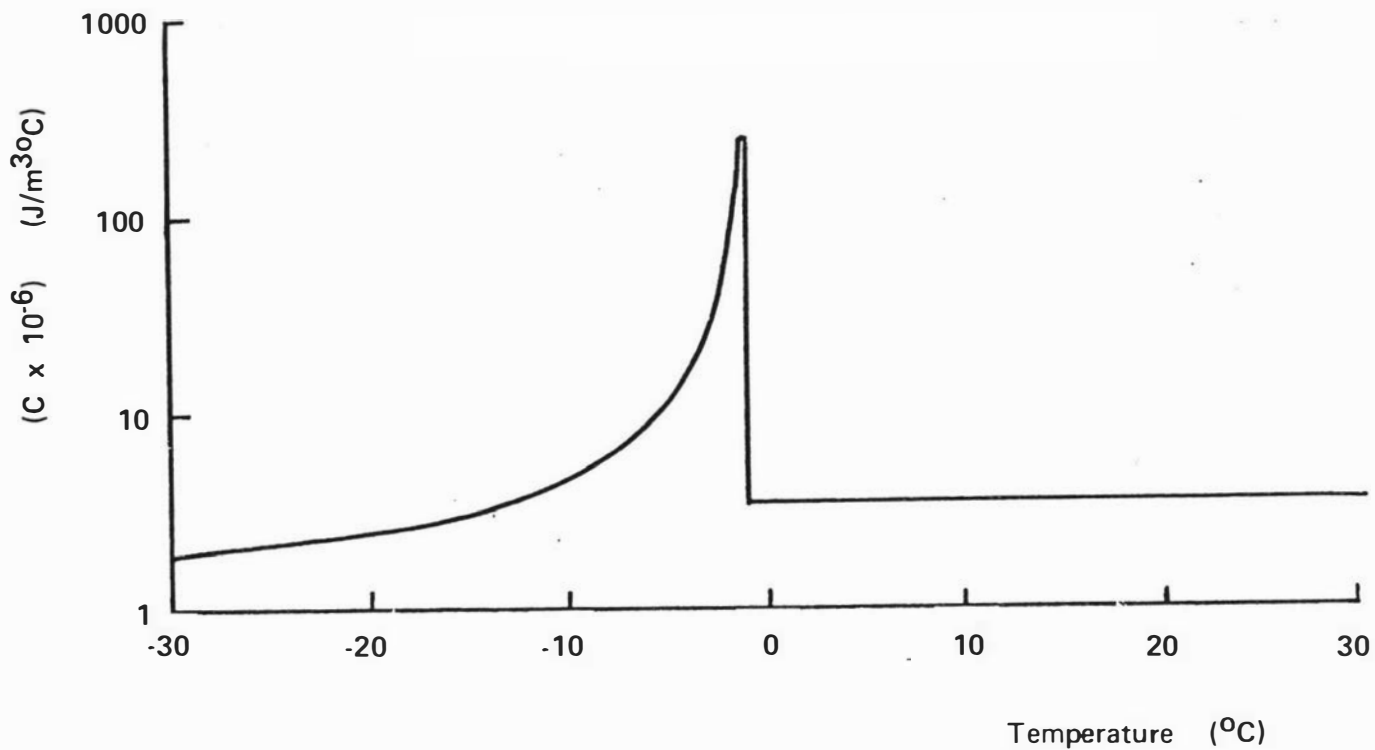


Figure 6.5 Apparent specific heat capacity data for minced lean beef.

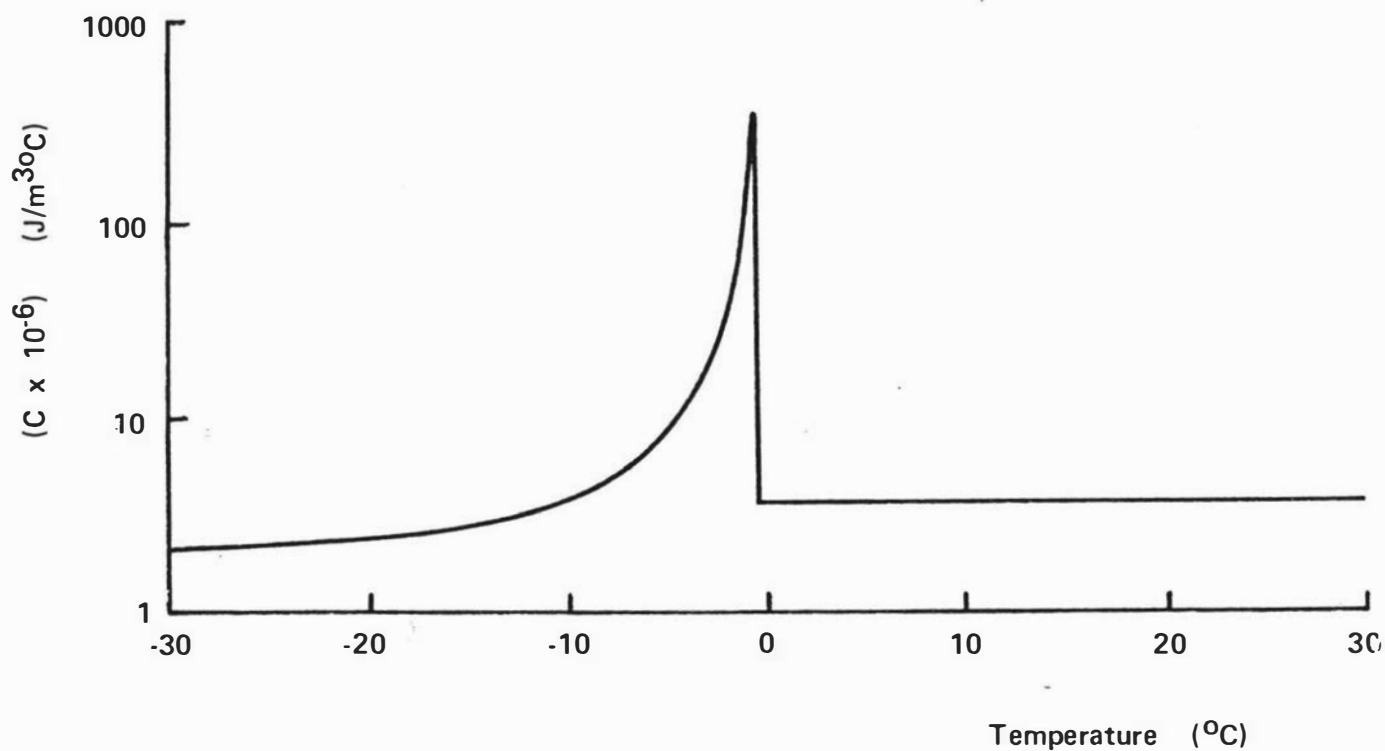


Figure 6.6 Apparent specific heat capacity data for mashed potato.

are at the (i) time level, whereas a Crank-Nicolson type scheme requires evaluation at the $(i+\frac{1}{2})$ time level. As this is an unknown temperature, an iterative loop must be set up at each time step. The other advantage of the Lees scheme is that the approximation to $\frac{\partial T}{\partial t}$ is a more accurate one than that obtainable with a two level scheme. Therefore the three-level scheme is the most accurate available.

Bonacina and Comini (1971; 1973) have discussed application of the fourth and third kinds of boundary condition to this scheme. Application of the third kind of boundary condition has been discussed elsewhere (Cleland and Earle 1977b). Briefly, the third kind of boundary condition is taken into account by setting $m=0$ in equation 6.4; $T_a = T_{-1}^{i+1} = T_{-1}^i = T_{-1}^{i-1}$; and $k_{-\frac{1}{2}}^i = h\Delta x$. This is shown diagrammatically in Figure 6.2. Whereas the internal nodes have the specific heat capacity of a full Δx associated with them, the surface node has the specific heat capacity of only half a space increment.

The functions $C(T)$ and $k(T)$ are shown in Figures 6.3, 6.4, 6.5 and 6.6. The computer programs used can be found in Appendix 2. The Lees scheme is implicit, and requires solution of a set of tridiagonal simultaneous equations at each time step. This is easily done by Gaussian elimination; typical run times for the programs being 25s on a Burroughs B6700 computer.

Because the surface node has the specific heat capacity of only $\frac{1}{2}\Delta x$ associated with it the actual value was halved :

$$c_1^i = c_1^i / 2 \quad (6.7)$$

Freezing times were calculated using this difference scheme but some inconsistent low results occurred. The reason for these is "jumping" of the latent heat peak. Because the peak in $C(T)$ is high and narrow the temperature may jump across this region in one time step if $\frac{\partial T}{\partial t}$ is sufficiently

large. To stop this, Comini (1976) suggested two modifications. When updating at each time step the following should be used :

$$T_m^{i-1} = (T_m^{i+1} + T_m^i + T_m^{i-1}) / 3 \quad (6.8)$$

The apparent specific heat capacity should be calculated from the enthalpy change across the node as follows :

$$C_m^i = \frac{H_{m+\frac{1}{2}}^i - H_{m-\frac{1}{2}}^i}{T_{m+\frac{1}{2}}^i - T_{m-\frac{1}{2}}^i} \quad (6.9)$$

These do substantially reduce the problem, but even use of these measures, and reduction of the time step to very small values did not stop jumping of the latent heat peak completely, especially where the Biot number was large. Because the thermal capacity of the surface node was only half that of the other nodes, and it is the fastest cooling region, it was found that jumping was almost impossible to stop at this node. Hence an alternative approach was sought. Comini et al (1974b) and Tao (1975) have shown that the shape of $C(T)$ in the phase change region is not critical provided the total enthalpy change is preserved. A different set of enthalpy/temperature data to that of Riedel (1960a) was available (Comini 1976), so this was used. It is shown as Curve 2 on Figure 6.4. The shape of the $C(T)$ peak is much flatter (probably because the methyl-cellulose used was different to that of Riedel), and is therefore less likely to be jumped. However jumping still occurred at large Biot numbers.

In the approach just described it was found that because the surface node has only half the heat capacity associated with it cooling was very quick here, and jumping was very likely. Normally Δx is defined as :

$$\Delta x = \frac{D}{2(M-1)} \quad (6.10)$$

where M = number of nodes in the half slab. If Δx is defined as :

$$\Delta x = \frac{D}{2 \left(M - \frac{1}{2} \right)} \quad (6.11)$$

the surface node would have the full specific heat capacity associated with it. This would decrease the likelihood of jumping of the latent heat peak at the surface node, but the estimate of the surface temperature would be poorer because the node most affected would not be on the surface of the material. This approach was tried and found to lead to more consistent results, although the flatter curve for $C(T)$ still had to be used for large Biot numbers.

The freezing times calculated from the two approaches were compared to the experimental freezing times and the percentage differences are shown in Figure 6.7, Typical temperature profiles are shown in Figures 5.1 and 5.2. These are from the first approach because it gives a better estimate of the surface temperature. The freezing times calculated by the second method are given in Table 8.1; this method was adopted as the more accurate approach for calculation of freezing times.

The 95% confidence limits of the percentage differences comparing the calculated freezing times to the experimental results are -8.3% to +10.5% (mean = 1.1%; standard deviation = 4.7%). These limits include error from two sources - experimental error, and errors in the application of the finite difference method. As the time and space steps are reduced in size, the mathematical error in the finite difference results is reduced until in the limit as Δt and Δx tend to zero the exact answer is calculated. Practical limitations on the computation resources available limit the size of the space grid and time step. The larger these steps the greater the error.

Calculations of freezing time were also carried out over the full set of experimental data for Karlsruhe test substance using the enthalpy transformation method of Albasing (1956) with the same space and time grids as were used with the Lees scheme. These showed that the range of

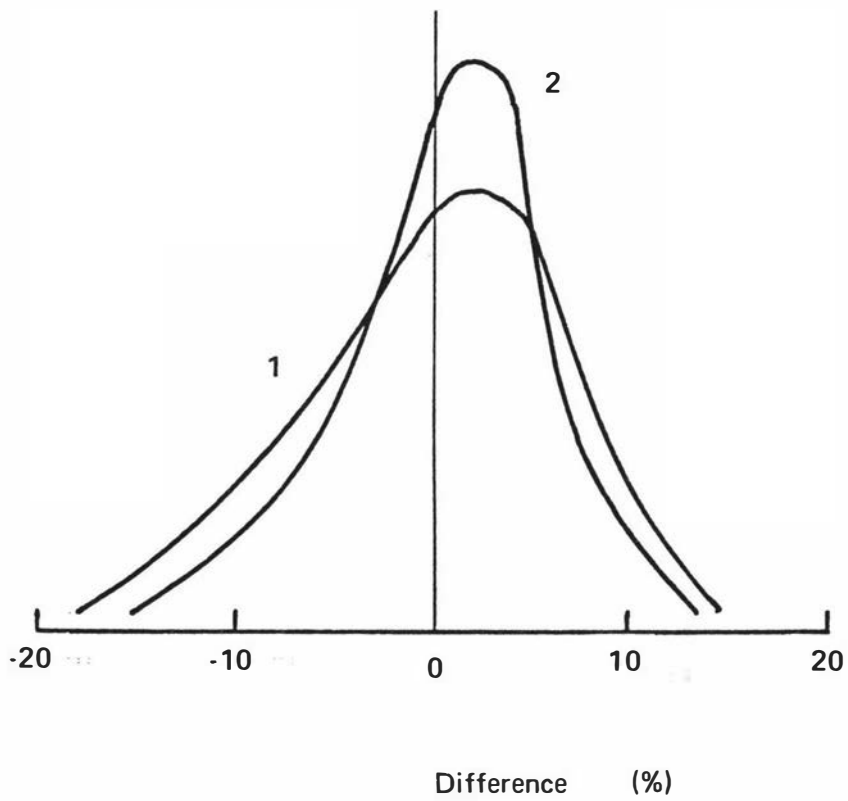


Figure 6.7 Frequency diagram of the percentage differences between experimental freezing times for slabs, and times calculated by finite differences.
1 — using $0.5C_0^i$ at the surface node. 2 — using a modified space grid and the full C_0^i value.

percentage differences between the calculated and experimental freezing times was greater than for the Lees scheme. The mean difference was 4.1% and the standard deviation 6.6%. The larger truncation errors in this scheme affect the accuracy of the results significantly. Therefore, provided jumping of the latent heat peak can be avoided, or reduced by means such as those discussed above, the Lees scheme is the most accurate finite difference scheme available. If the errors introduced by jumping of the latent heat peak in the Lees scheme were greater than the extra truncation errors in the enthalpy transformation method the latter method would be the more accurate. However, for one-dimensional heat transfer jumping has been reduced sufficiently to prevent this situation.

It is impossible to separate the mathematical error from the experimental error. The 95% confidence limits will therefore overestimate the error in the application of the finite difference method, but they do give an indication of the uncertainty in a calculated freezing time when the time and space grids are limited by practical considerations. Errors are higher than for heat conduction with constant thermal properties because the sharp changes in $k(T)$ and $C(T)$ make accurate modelling of these curves very difficult. This is true of any finite difference scheme of this type, not just the Lees scheme.

6.2 CYLINDERS AND SPHERES

6.2.1 Selection of Numerical Method

Solutions to freezing problems in radial geometry that require numerical evaluation are subject to very similar limitations to those discussed in section 6.1.1 for slabs. Problems in radial geometry have received less attention than slabs - only two solutions (Poots 1962a; Selim and Seagrave 1973b) requiring numerical solution exist. These are for the first kind of boundary condition, and hence are of no practical importance.

Consequently the choice of numerical method is limited to finite differences and finite elements. Radial heat transfer in cylinders and spheres can be treated as uni-directional with a regular space grid (Albasiny 1960). In this situation there is no advantage in the finite element technique, therefore the equally accurate finite difference method was used.

6.2.2 Selection of Finite Difference Approach

It has been shown in section 6.1.2 that for slabs the versatile finite difference schemes using the functions $k(T)$ and $C(T)$ to take account of phase change accurately represent the true thermal behaviour of a freezing food material, whereas the schemes that assume that all latent heat is released at a unique freezing temperature do not. Further, the more versatile schemes include the fixed freezing temperature situation as a special case. Because $k(T)$ and $C(T)$ are dependent on the material only, and not its geometric arrangement, this will be true for any shape. Therefore finite difference schemes in radial geometry that assume that a sharp interface exists (Tao 1967; Tao 1968; Morrison 1970; Charm et al 1972; Padmanabhan and Subba Raju 1975) need not be considered further as they will inevitably be of reduced accuracy.

6.2.3 Comparison of Finite Difference Schemes

The general radial heat conduction equation :

$$C(T) \frac{\partial T}{\partial t} = \frac{\partial}{\partial r} \left(k(T) \frac{\partial T}{\partial r} \right) + \frac{a k(T)}{r} \frac{\partial T}{\partial r} \quad (6.12)$$

where $a = 1$ for a cylinder,

$a = 2$ for a sphere,

cannot be simplified if $k(T)$ is a function of position.

This is the case in food freezing problems. Fully explicit, fully implicit and Crank-Nicolson schemes can all be written for equation 6.12, but they are not as accurate as the three-level scheme :

$$\begin{aligned}
C_m^i \frac{T_m^{i+1} - T_m^{i-1}}{2\Delta t} &= \frac{1}{3(\Delta r)^2} (k_{m+\frac{1}{2}}^i (T_{m+1}^{i+1} - T_m^{i+1} + T_{m+1}^i - T_m^i + T_{m+1}^{i-1} - T_m^{i-1})) \\
&\quad - k_{m-\frac{1}{2}}^i (T_m^{i+1} - T_{m-1}^{i+1} + T_m^i - T_{m-1}^i + T_m^{i-1} - T_{m-1}^{i-1})) \\
&\quad + \frac{a k_m^i (T_{m+1}^{i+1} - T_{m-1}^{i+1} + T_{m+1}^i - T_{m-1}^i + T_{m+1}^{i-1} - T_{m-1}^{i-1})}{3m\Delta r \cdot 2\Delta r}
\end{aligned} \tag{6.13}$$

because the three level scheme has smaller truncation errors than the other schemes, as well as the practical advantage of avoiding iteration to find thermal properties at the $(i+\frac{1}{2})$ time level.

At the centre ($m=0$) the method of Albasingy (1960) was used to avoid the singularity :

$$\lim_{r \rightarrow 0} \frac{1}{r} \frac{\partial T}{\partial r} \rightarrow \frac{\partial^2 T}{\partial r^2} \tag{6.14}$$

leading to a finite difference approximation of :

$$C_0^i \frac{T_0^{i+1} - T_0^{i-1}}{2\Delta t} = \frac{(1+a)}{3(\Delta r)^2} (2k_{+\frac{1}{2}}^i (T_1^{i+1} - T_0^{i+1} + T_1^i - T_0^i + T_1^{i-1} - T_0^{i-1})) \tag{6.15}$$

At the surface ($m=M$) the third kind of boundary condition is taken into account by using :

$$h (T_a - T_s) = k_M^i \left(\frac{\partial T}{\partial r} \right)_{M\Delta r} \tag{6.16}$$

and setting $k_{M+\frac{1}{2}}^i = h\Delta r$ and $T_{M+1}^i = T_a$; leading to :

$$\begin{aligned}
C_M^i \frac{T_M^{i+1} - T_M^{i-1}}{2\Delta t} &= \frac{1}{3(\Delta r)^2} (k_{M+\frac{1}{2}}^i (3T_a - T_M^{i+1} - T_M^i - T_M^{i-1})) - \\
&\quad k_{M-\frac{1}{2}}^i (T_M^{i+1} - T_{M-1}^{i+1} + T_M^i - T_{M-1}^i + T_M^{i-1} - T_{M-1}^{i-1})) + \\
&\quad \frac{ah(3T_a - T_M^{i+1} - T_M^i - T_M^{i-1})}{3R}
\end{aligned} \tag{6.17}$$

The region associated with each node is of changing cross-sectional area. The volume of material associated

with each node is $2\pi m(\Delta r)^2$ for cylinders and $4\pi m(\Delta r)^3$ for spheres in the above difference scheme. When this was compared to the actual volume with each node in the real physical situation, it was found that the following correction was necessary for spheres :

$$C_m^i = C_m^i \left(1 + \frac{1}{12m^3}\right) \quad (6.18)$$

The finite difference scheme is implicit and like the scheme for the slab it requires Gaussian elimination of a set of $(M+1)$ simultaneous equations at each time step. The program used is given in Appendix 3.

The scheme agreed well with a known analytical solution for constant thermal properties (Carslaw and Jaeger 1959, p202). When applied to the freezing of Karlsruhe test substance oscillations, leading to a false solution, were found to occur. These were stopped by defining k_m^i as follows :

$$k_m^i = \frac{1}{2} (k_{m+\frac{1}{2}}^i + k_{m-\frac{1}{2}}^i) \quad (6.19)$$

The solution to the problem with constant thermal properties is unaltered.

For application to problems where thermal conductivity is changing it is implicit in the new approximation that k changes linearly in space from position $(m-\frac{1}{2})$ to $(m+\frac{1}{2})$. The real situation is shown in Figure 6.8. The temperature gradient is greater towards the surface of the material. This means that the thermal conductivity changes at an increasing rate towards the surface, leading to the dashed line in Figure 6.8. Therefore the approximation to k_m^i given by equation 6.19 will almost invariably overestimate the thermal conductivity at the node m . This implies that heat can be removed more easily than is physically possible, and ultimately will mean that the calculated freezing time underestimates the real value. This is not just a problem for the scheme given by equations 6.13, 6.15 and 6.17, but must be considered for any scheme where k is a function

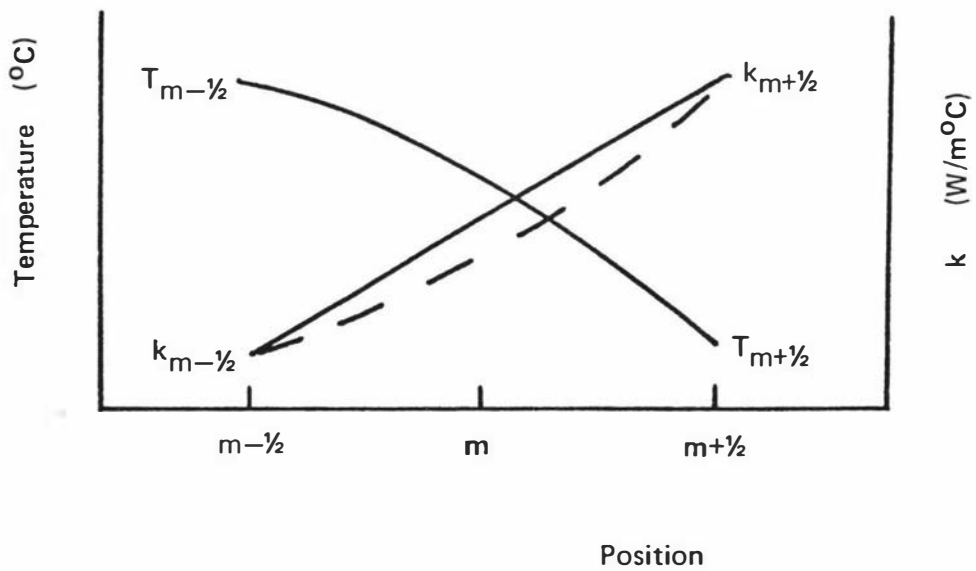


Figure 6.8 Typical temperature and thermal conductivity profiles through a freezing sphere or cylinder showing the effect of a linear approximation of the thermal conductivity.

(- - -) actual thermal conductivity profile.

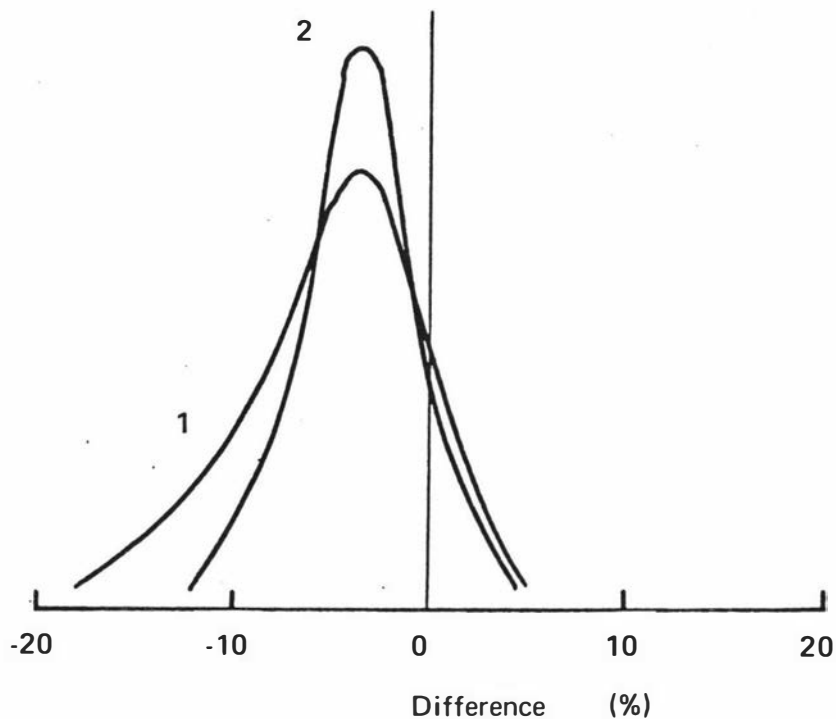


Figure 6.9 Frequency diagram of the percentage differences between experimental freezing times for cylinders, and times calculated by finite differences. 1 – using $0.5C_M^i$ at the surface node. 2 – using a modified space grid and the full C_M^i value.

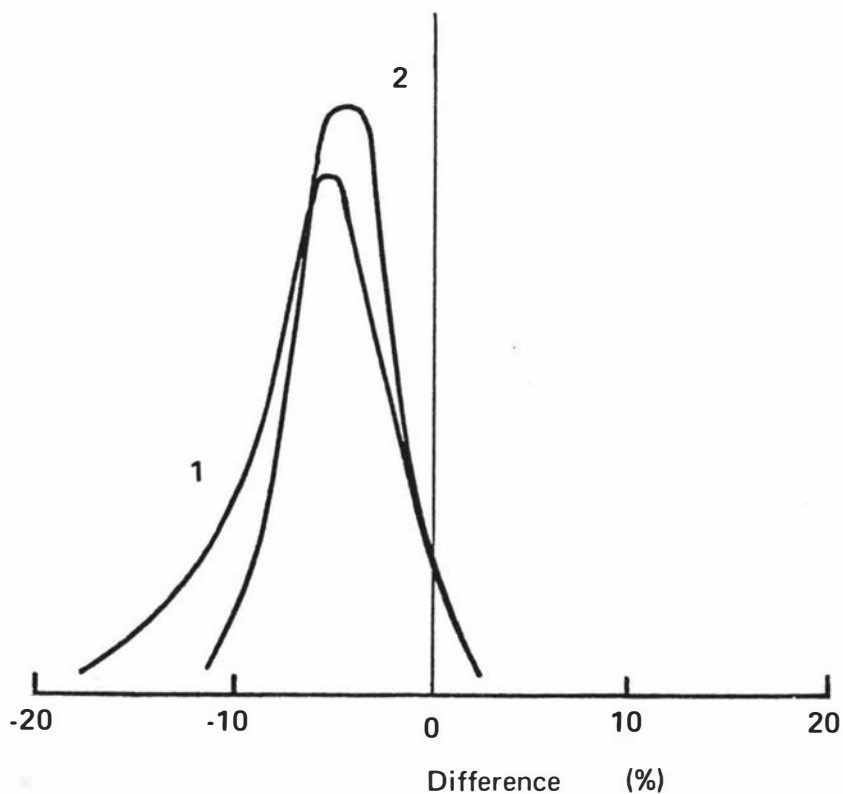


Figure 6.10 Frequency diagram of the percentage differences between experimental freezing times for spheres, and times calculated by finite differences. 1 – using $0.5C_M^i$ at the surface node. 2 – using a modified space grid and the full C_M^i value.

of temperature. In spite of this problem the three-level scheme is still considered the most accurate because it has smaller truncation errors than any other scheme.

At the surface of the body the analogous problem to that found for slabs arises. The surface node has the specific heat capacity of only $\frac{1}{2}\Delta r$ associated with it. The two approaches :

1. Using $\frac{1}{2}C_m^i$.
2. Defining the space grid so that $R/\Delta r = M + \frac{1}{2}$.

were both tried. The frequency diagrams are shown in Figures 6.9 and 6.10. Again, jumping of the latent heat peak is less of a problem with the second approach which was therefore adopted. Full results using this approach are given in Table 8.1. Typical calculated temperature profiles from the first approach can be found in Figures 5.3 and 5.4. Results from this, the less accurate approach, are shown because they give a better estimate of the surface temperature than the second approach. The reasons for this are discussed in section 6.1.3.

The mean values of the percentage difference calculated from the difference between experimental and predicted freezing times are -3.8% for cylinders, and -4.5% for spheres. The standard deviations are 3.1% and 2.5% respectively. The shift in the mean apart, the range of results is very similar to that found for slabs, indicating that the application of finite differences to radial geometry is subject to very much the same limitations as exist for one-dimensional heat transfer in slabs (see section 6.1.3). Freezing times calculated by a scheme using the enthalpy transformation method would be expected to show a greater spread of results than for the three level scheme. This is because jumping of the latent heat peak was reduced to insignificant amounts in the latter method, and the truncation errors in the enthalpy transformation method are greater than those in the three level scheme. Using the enthalpy transformation method a similar mean prediction error to that found for slabs would be expected (approximately 4%).

Therefore the enthalpy transformation method would not be as accurate as the three-level scheme because the offset of the mean from 0% would be similar in size for the two schemes, but a greater spread of results would be expected for the enthalpy transformation method. For these reasons freezing times were not calculated by this method for spheres and cylinders.

Provided the user is aware that the freezing time is likely to be on average 4% low, the three-level finite difference scheme can be used to achieve accurate simulation of freezing in radial geometry over the range of conditions considered, which should cover most practical situations.

6.3 RECTANGULAR BRICKS

6.3.1 Selection of Numerical Method

In spite of the fact that freezing problems where heat is transferred in all three directions occur often in practice, very few numerical solutions have been developed. The great complexity of these problems has limited development of numerical solutions to finite differences and finite elements. For irregular geometry finite elements through the use of isoparametric regions are better suited (Comini et al 1974c), but for regular brick shapes a rectangular grid can be used, and finite differences are equally accurate in this situation.

6.3.2. Selection of Finite Difference Method

Equivalent three-dimensional formulae to equations 6.4, 6.5 and 6.6 can be written, and all have been used (Brian 1961; Earle and Earl 1966; Lazaridus 1970; Fleming 1971a; Cordell and Webb 1972; Bonacina and Comini 1973; Shamsundar and Sparrow 1975). Because the three-level scheme of Lees (1966) was found to be superior for one-dimensional problems, it is reasonable to assume that it

will also be the best scheme for two- and three-dimensional problems.

6.3.3 Use of the Finite Difference Scheme

Bonacina and Comini (1973) have shown how the Lees scheme can be applied to problems in two dimensions by use of standard alternating direction implicit procedures. The extension to three dimensions is straightforward. The general equation of heat conduction :

$$C(T) \frac{\partial T}{\partial t} = \frac{\partial}{\partial x} (k(T) \frac{\partial T}{\partial x}) + \frac{\partial}{\partial y} (k(T) \frac{\partial T}{\partial y}) + \frac{\partial}{\partial z} (k(T) \frac{\partial T}{\partial z}) \quad (2.1)$$

can be approximated by :

$$\begin{aligned} C_{mjk}^i \frac{T_{mjk}^{i+1} - T_{mjk}^{i-1}}{2 \Delta t} &= \frac{1}{3(\Delta x)^2} (k_{m+\frac{1}{2}jk}^i (T_{m+1jk}^{i+1} - T_{mjk}^{i+1} + T_{m+1jk}^i - T_{mjk}^i \\ &+ T_{m+1jk}^{i-1} - T_{mjk}^{i-1}) - k_{m-\frac{1}{2}jk}^i (T_{mjk}^{i+1} - T_{m-1jk}^{i+1} + T_{mjk}^i - T_{m-1jk}^i + T_{mjk}^{i-1} - T_{m-1jk}^{i-1})) \\ &+ \frac{1}{3(\Delta y)^2} (k_{mj+\frac{1}{2}k}^i (T_{mj+1k}^{i+1} - T_{mjk}^{i+1} + T_{mj+1k}^i - T_{mjk}^i + T_{mj+1k}^{i-1} - T_{mjk}^{i-1}) - \\ &k_{mj-\frac{1}{2}k}^i (T_{mjk}^{i+1} - T_{mj-1k}^{i+1} + T_{mjk}^i - T_{mj-1k}^i + T_{mjk}^{i-1} - T_{mj-1k}^{i-1})) + \frac{1}{3(\Delta z)^2} (\\ &k_{mjk+\frac{1}{2}}^i (T_{mjk+1}^{i+1} - T_{mjk}^{i+1} + T_{mjk+1}^i - T_{mjk}^i + T_{mjk+1}^{i-1} - T_{mjk}^{i-1}) - k_{mjk-\frac{1}{2}}^i (\\ &T_{mjk}^{i+1} - T_{mjk-1}^{i+1} + T_{mjk}^i - T_{mjk-1}^i + T_{mjk}^{i-1} - T_{mjk-1}^{i-1})) \end{aligned} \quad (6.20)$$

The three sweeps of the alternating direction implicit method use the following equations derived from the above scheme :

First sweep (in x direction) :

$$\begin{aligned}
& \frac{-2\Delta t}{3(\Delta x)^2} k_{m-\frac{1}{2}jk}^i T_{m-1jk}^{i+1*} + (C_{mjk}^i + \frac{2\Delta t}{3(\Delta x)^2} (k_{m+\frac{1}{2}jk}^i + k_{m-\frac{1}{2}jk}^i)) T_{mjk}^{i+1*} \\
& - \frac{2\Delta t}{3(\Delta x)^2} k_{m+\frac{1}{2}jk}^i T_{m+1jk}^{i+1*} = \frac{2\Delta t}{3(\Delta x)^2} (k_{m+\frac{1}{2}jk}^i (T_{m+1jk}^i - T_{mjk}^i) - \\
& k_{m-\frac{1}{2}jk}^i (T_{mjk}^i - T_{m-1jk}^i)) + \frac{2\Delta t}{3(\Delta y)^2} (k_{mj+\frac{1}{2}k}^i (T_{mj+1k}^i - T_{mjk}^i) - \\
& k_{mj-\frac{1}{2}k}^i (T_{mjk}^i - T_{mj-1k}^i)) + \frac{2\Delta t}{3(\Delta z)^2} (k_{mjk+\frac{1}{2}}^i (T_{mjk+1}^i - T_{mjk}^i) - \\
& k_{mjk-\frac{1}{2}}^i (T_{mjk}^i - T_{mjk-1}^i)) + C_{mjk}^i T_{mjk}^{i-1} + \frac{2\Delta t}{3(\Delta x)^2} (k_{m+\frac{1}{2}jk}^i (T_{m+1jk}^{i-1} - T_{mjk}^{i-1}) \\
& - k_{m-\frac{1}{2}jk}^i (T_{mjk}^{i-1} - T_{m-1jk}^{i-1})) + \frac{4\Delta t}{3(\Delta y)^2} (k_{mj+\frac{1}{2}k}^i (T_{mj+1k}^{i-1} - T_{mjk}^{i-1}) - \\
& k_{mj-\frac{1}{2}k}^i (T_{mjk}^{i-1} - T_{mj-1k}^{i-1})) + \frac{4\Delta t}{3(\Delta z)^2} (k_{mjk+\frac{1}{2}}^i (T_{mjk+1}^{i-1} - T_{mjk}^{i-1}) - \\
& k_{mjk-\frac{1}{2}}^i (T_{mjk}^{i-1} - T_{mjk-1}^{i-1})) \tag{6.21}
\end{aligned}$$

Second sweep (in y direction) :

$$\begin{aligned}
& \frac{-2\Delta t}{3(\Delta y)^2} k_{mj-\frac{1}{2}k}^i T_{mj-1k}^{i+1**} + (C_{mjk}^i + \frac{2\Delta t}{3(\Delta y)^2} (k_{mj+\frac{1}{2}k}^i + k_{mj-\frac{1}{2}k}^i)) T_{mjk}^{i+1**} \\
& - \frac{2\Delta t}{3(\Delta y)^2} k_{mj+\frac{1}{2}k}^i T_{mj+1k}^{i+1**} = T_{mjk}^{i+1*} - \frac{2\Delta t}{3(\Delta y)^2} (k_{mj+\frac{1}{2}k}^i (T_{mj+1k}^{i-1} \\
& - T_{mjk}^{i-1}) - k_{mj-\frac{1}{2}k}^i (T_{mjk}^{i-1} - T_{mj-1k}^{i-1})) \tag{6.22}
\end{aligned}$$

Third sweep (in z direction) :

$$\begin{aligned}
& \frac{-2\Delta t}{3(\Delta z)^2} k_{mjk-\frac{1}{2}}^i T_{mjk-1}^{i+1} + (C_{mjk}^i + \frac{2\Delta t}{3(\Delta z)^2} (k_{mjk+\frac{1}{2}}^i + k_{mjk-\frac{1}{2}}^i)) T_{mjk}^{i+1} \\
& - \frac{2\Delta t}{3(\Delta z)^2} k_{mjk+\frac{1}{2}}^i T_{mjk+1}^{i+1} = T_{mjk}^{i+1**} - \frac{2\Delta t}{3(\Delta z)^2} (k_{mjk+\frac{1}{2}}^i (T_{mjk+1}^{i-1} \\
& - T_{mjk}^{i-1}) - k_{mjk-\frac{1}{2}}^i (T_{mjk}^{i-1} - T_{mjk-1}^{i-1})) \tag{6.23}
\end{aligned}$$

where T^* and T^{**} are intermediate temperatures calculated by the alternating direction scheme that have no physical significance.

The third kind of boundary condition is taken into account in the same way as used for slabs (see section 6.1.3). Because of symmetry only an octant need be considered, with a space grid of $(M+1) \times (J+1) \times (K+1)$ nodes, where $2M\Delta x = D_x$; $2J\Delta y = D_y$; $2K\Delta z = D_z$. For 9 nodes in each direction and 800 time steps a typical computation time for this scheme was 4500s on a Burroughs B6700 computer. The two- and three-dimensional programs are in Appendix 3.

The three-dimensional program was checked against a known analytical solution for the third kind of boundary condition and constant thermal properties (Newman 1936). The results are shown in Table 6.1. The approach using half the specific heat capacity of the surface nodes was used for this run to get the best possible estimate of the surface temperature. Because the program is expensive to run, freezing times were not calculated for all the freezing experiments. Instead, three runs were selected, each with different conditions. Because the accuracy of the results was found to depend on the Biot number for other shapes the three runs chosen had widely differing values of this parameter. Approximately 800 time steps and a $9 \times 9 \times 9$ space grid were used. Practical limitations prevented smaller time and space steps. The results are shown in Table 6.2, and the calculated and experimental temperature profiles are shown in Figures 5.5, 5.6 and 5.7.

For the lowest Biot number (run B72) very good simulation was obtained. For the intermediate Biot number (run B55) simulation was not as good. The calculated centre temperature profile is always low, indicating a probable error in the input data. Because the discrepancy is greater at the end of the freezing run it is possible that some jumping of the latent heat peak may have occurred, but the major error appears to be in the input data. The results for the largest Biot number (run B43) show clearer indications of jumping. The centre temperature profile agrees with the experimental results until it enters the phase

Table 6.1

Comparison of results from the three-dimensional program to a known analytical solution for cooling of a cube
 $Bi = 4.0$; Values of Y , the fractional unaccomplished temperature change, are tabulated.

	Centre of cube		Centre of face	
Fo	Analytical	Numerical	Analytical	Numerical
0	1.000	1.000	1.000	1.000
0.04	0.999	0.999	0.489	0.491
0.08	0.974	0.970	0.387	0.382
0.12	0.897	0.891	0.318	0.309
0.16	0.790	0.782	0.261	0.252
0.20	0.677	0.668	0.215	0.206
0.24	0.570	0.562	0.177	0.170

Table 6.2

Results from the finite difference simulation of the
freezing of rectangular bricks

Run		B43	B55	B72
D_x	(m)	0.135	0.150	0.050
D_y	(m)	0.164	0.150	0.200
D_z	(m)	0.164	0.150	0.200
h	(W/m ² °C)	260	41.0	20.5
T_a	(°C)	-20.3	-20.9	-24.6
T_i	(°C)	26.8	30.8	16.2
Bi		21.3	3.73	0.621
t_{exp}	(hrs)	4.56	6.90	4.10
err	(hrs)	0.21	0.38	0.38
t_{fd}	(hrs)	4.02	6.30	4.14
Difference	(%)	-11.8	-8.7	+1.0

change region. More important, there is a major discrepancy between calculated and experimental surface temperatures which lessens towards the end of the run. If nodes at, or near the surface "jump" the latent heat peak the thermal diffusivity calculated by the program in this region will be higher than the real value. An inflated value of the thermal diffusivity will result in the temperature gradients being underestimated. Therefore the calculated surface temperature will be closer to the centre temperature than the experimental surface temperature. This is what was found to occur. As the region of phase change moves away from the surface this effect slowly disappears.

As the time step and space mesh cannot be altered significantly because of practical limits on the computation time, jumping is an important shortcoming which is almost impossible to avoid for large Biot numbers. This apart, the accuracy obtainable with finite differences in three dimensions appears to be approximately the same as found for other shapes.

A scheme using the enthalpy transformation method can be written for this three-dimensional problem (Shamsundar and Sparrow 1975). It would have larger truncation errors than the three level scheme but the jumping problem would be completely avoided. The accuracy would be, at best, the same as for the equivalent one-dimensional scheme, but probably worse because rounding and truncation errors are greater for three-dimensional schemes. Therefore such a scheme would be expected to have 95% confidence limits of at least +13% on either side of the mean prediction error. The results obtained using the three-level scheme indicate that the 95% confidence limits of the prediction error for this method would probably be no greater than these limits. Therefore the error introduced by jumping of the latent heat peak is probably less than the extra truncation errors involved in the schemes using the enthalpy transformation.

Because three-dimensional finite difference programs

are expensive to write and use, there appeared to be little value in writing a program using the enthalpy transformation when it would not be expected to be any more accurate than the three-level scheme.

6.4 SUMMARY

The Lees finite difference scheme, subject to the limitations imposed by practical constraints, gives accurate prediction of freezing times to within approximately $\pm 9\%$ of experimentally determined freezing times for slabs, cylinders, spheres and rectangular bricks. On average the calculated freezing time for spheres and cylinders was 4% low because of practical difficulties discussed in section 6.2.3. As the space and time grids are reduced all the difference schemes will give greater accuracy, and in the limit converge to the exact answer. Errors arise when constraints on computation resources available mean that relatively coarse time and space grids must be used.

The main problem in this respect is jumping of the latent heat peak. At high Biot numbers the rate of change of temperature with respect to time is large at or near the surface of the freezing material. The peak in $C(T)$ occurs over a very narrow range in temperature, and it is possible that the temperature at a node can "jump" part or all of this region in one time step. For simple shapes the problem can be largely overcome by the use of a smaller time step, and by use of manipulated data with a flatter peak (Comini et al 1974b) at the expense of 1 to 3% additional error. For three-dimensional heat transfer it is not practical to reduce the time step sufficiently, and the problem cannot be resolved as easily.

An alternative method based on the enthalpy transformation of Eyres et al (1946) avoids jumping of the latent heat peak, but introduces additional truncation errors into the calculation. These extra errors were found to be larger than errors introduced by jumping in the three

level scheme for one-dimensional heat transfer in slabs, and would be expected to be similarly larger in practical situations involving three-dimensional or radial heat transfer. Therefore the three-level scheme is the more accurate.

For the design engineer the unreliability caused by jumping is undesirable because he does not want to have to investigate the effect of time and space grids and whether jumping has occurred, especially if he is not completely familiar with the finite difference program.

7 PREDICTION OF FREEZING TIME BY SIMPLE FORMULAE

7.1 THERMAL DATA

Before freezing times predicted by the simple formulae, discussed in Chapter 2, are compared the thermal data used in these calculations must be specified. As has been previously discussed foods, when freezing, release latent heat over a range of temperature, and the thermal properties reflect this gradual change from water to ice.

Most of the simple solutions considered assume that all the latent heat is released at a unique freezing temperature, and that the frozen phase has a constant thermal conductivity. For these solutions the thermal conductivity of the completely frozen phase was used, and the latent heat was obtained by subtracting the sensible heat component from the total enthalpy change between the initial freezing temperature and the final centre temperature. The temperature at which freezing starts was taken as the freezing temperature because this is the temperature at which the well-known "freezing plateau" is found in freezing experiments. These choices fit the concept of the analytical solutions, are not ambiguous, and also use the best known thermal data for foods.

Workers who have suggested empirical modifications or formulae often define the thermal properties differently. Commonly, the full enthalpy change between the initial freezing temperature and the final centre temperature (in this case -10°C) is used instead of the latent heat. Some workers (Mellor 1976) attempt to define an average thermal conductivity. The effect of these definitions will be discussed for each case in later sections. Table 7.1 gives a summary of the data used.

7.2 SLABS

A large number of simple formulae for calculation of

Table 7.1Thermal data for freezing food materials

		Karlsruhe test substance	Minced lean beef	Mashed potato
k_s	(W/m ⁰ C)	1.65	1.55	1.90
k_l	(W/m ⁰ C)	0.55	0.51	0.53
C_s	(J/m ³ °C)	1.90 x 10 ⁶	1.90 x 10 ⁶	1.95 x 10 ⁶
C_l	(J/m ³ °C)	3.71 x 10 ⁶	3.65 x 10 ⁶	3.66 x 10 ⁶
L	(J/m ³)	209 x 10 ⁶	209 x 10 ⁶	235 x 10 ⁶
ΔH	(J/m ³)	226 x 10 ⁶	226 x 10 ⁶	250 x 10 ⁶
k_{ave}	(W/m ⁰ C)	1.20		
T_f	(°C)	-0.6	-1.0	-0.6

ΔH is the enthalpy difference between the initial freezing temperature (T_f) and the final centre temperature (-10°C).

slab freezing times were discussed in Chapter 2. Freezing times were calculated using these methods, and the percentage differences between the calculated results and the experimentally determined freezing times found. From these values a frequency diagram for each method was constructed.

7.2.1 Solutions for the First Kind of Boundary Condition

Solutions that take account of the first kind of boundary condition are considered in Figure 7.1. Stefan's solution (Carslaw and Jaeger 1959, p286) is an exact one, but there are several approximate solutions to the same problem (Hamill and Bankoff 1963; Goodman 1964; Huang and Shih 1975a). The frequency diagrams for these are not significantly different from that for Stefan's solution and are therefore not shown. It is clear from Figure 7.1 that solutions for the first kind of boundary condition do not give useful answers, even when the surface heat transfer coefficient is as high as $400 \text{ W/m}^2\text{C}$. Table 7.2 which gives results for the highest surface heat transfer coefficients obtainable in the experimental plate freezer confirms this. Neither Stefan's solution nor Neumann's solution (Carslaw and Jaeger 1959, p285) gives accurate prediction of the freezing time when the Biot number is less than 20. Use of the average thermal conductivity for the frozen phase (k_{ave}) improved the agreement with the experimental results, but it was still poor. For Biot numbers less than 20 the first kind of boundary condition does not approximate sufficiently well to the practical situation for these solutions to accurately predict the freezing time.

7.2.2 Solutions for the Third Kind of Boundary Condition

Approximate analytical solutions that take account of the third kind of boundary condition are considered in Figure 7.2. Plank (1941), London and Seban (1943), Kreith and Romie (1955), Goodman (1958), Pedroso and Domoto (1973b), and Huang and Shih (1975b) all solved the same problem where there is no initial superheat. The assumptions made

Table 7.2

Comparison of experimental freezing times with times
calculated by Neumann's method

t_{neum} = freezing time from Neumann's method. E = percentage difference.

Run	D (m)	h (W/m ² °C)	T _i (°C)	T _a (°C)	t _{exp} ± err (hrs) (hrs)	t _{neum} (hrs)	E (%)
F23	0.0485	410	11.0	-21.0	1.00 ± 0.05	0.73	-27
F25	0.1000	320	28.0	-21.0	4.28 ± 0.18	4.65	+ 9
F26	0.0250	400	21.6	-22.0	0.32 ± 0.03	0.23	-39
F27	0.0720	410	3.0	-22.0	1.92 ± 0.09	1.28	-33
F30	0.0720	330	10.5	-24.5	1.82 ± 0.09	1.35	-26
F31	0.0250	430	3.0	-19.0	0.34 ± 0.03	0.18	-47
F32	0.1000	310	3.0	-23.0	3.46 ± 0.15	2.36	-32
F33	0.0485	360	3.0	-23.5	0.88 ± 0.05	0.54	-39

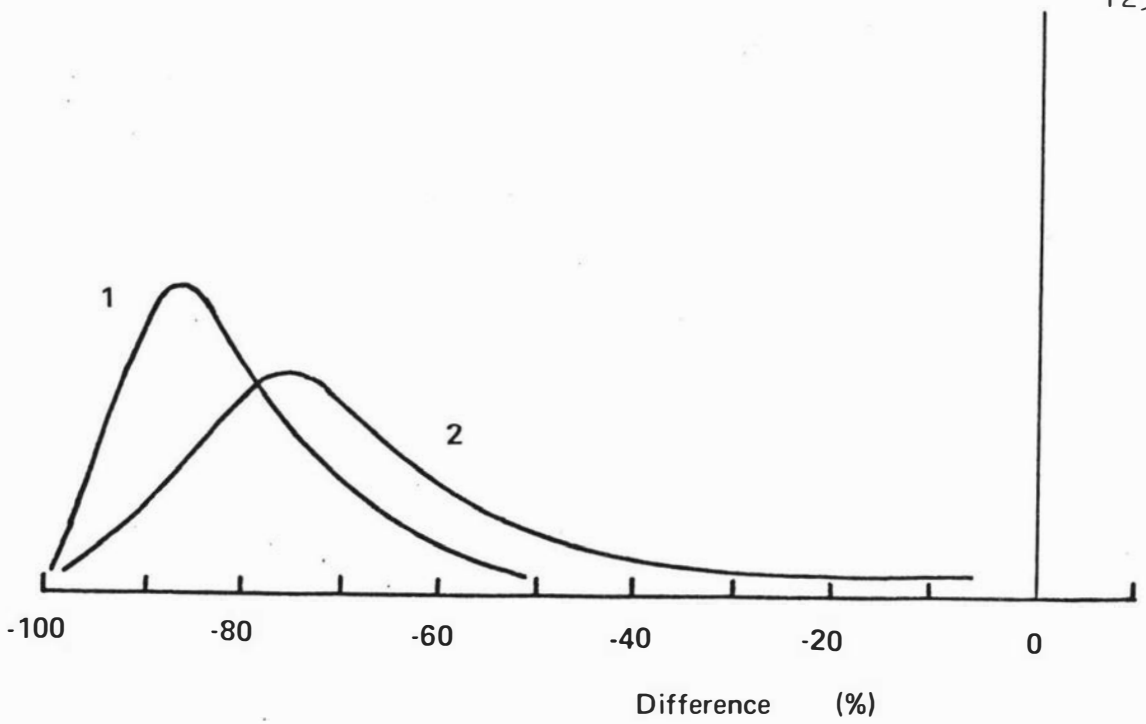


Figure 7.1 Frequency diagram of the percentage differences between experimental freezing times for slabs, and times calculated by solutions with the first kind of boundary condition. 1 – Stefan. 2 – Neumann.

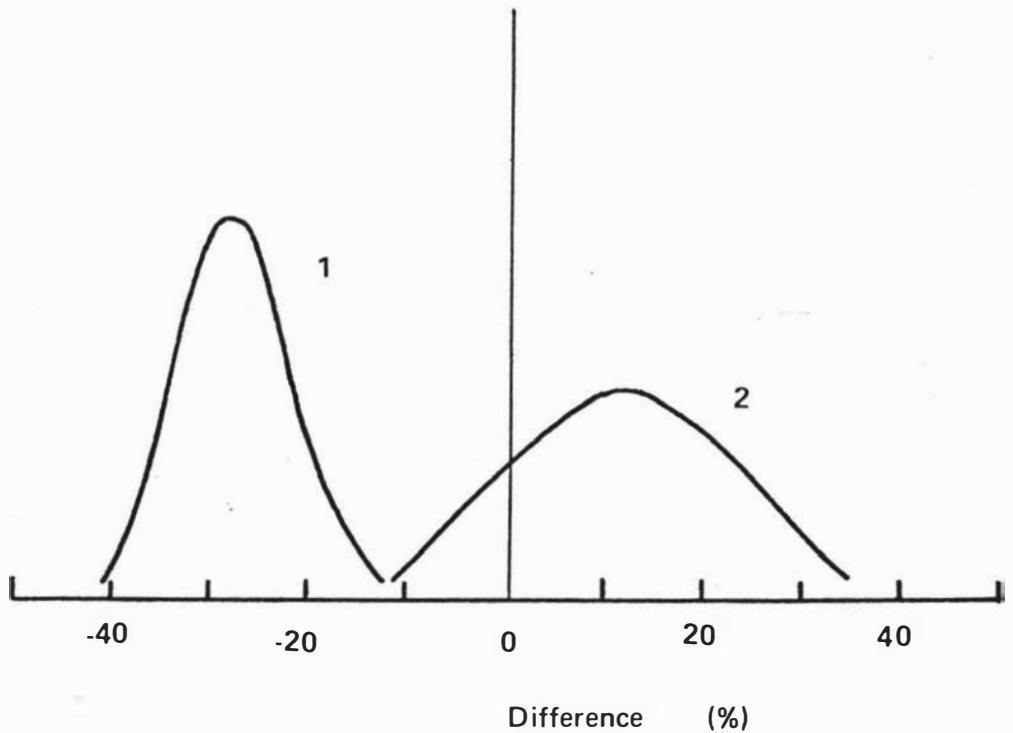


Figure 7.2 Frequency diagram of the percentage differences between experimental freezing times for slabs, and times calculated by solutions with the third kind of boundary condition. 1 – Plank, London and Seban, Kreith and Romie, Goodman, Pedroso and Domoto, Huang and Shih. 2 – Hrycak.

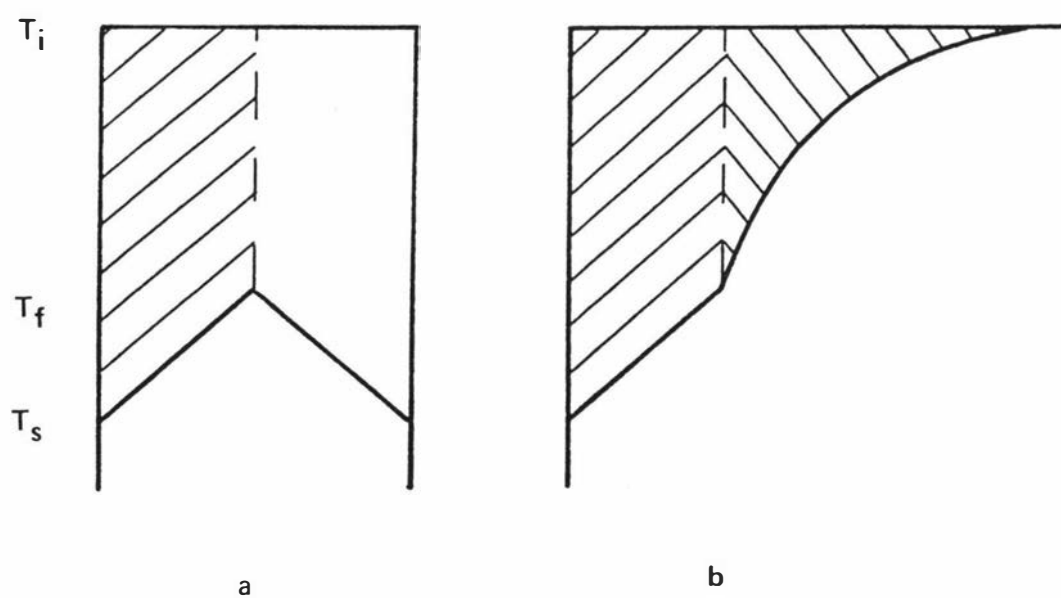


Figure 7.3 Schematic diagram showing the heat to be removed in freezing of slabs. a — finite slab. b — semi-infinite slab. The shaded area represents the heat to be removed in each case.

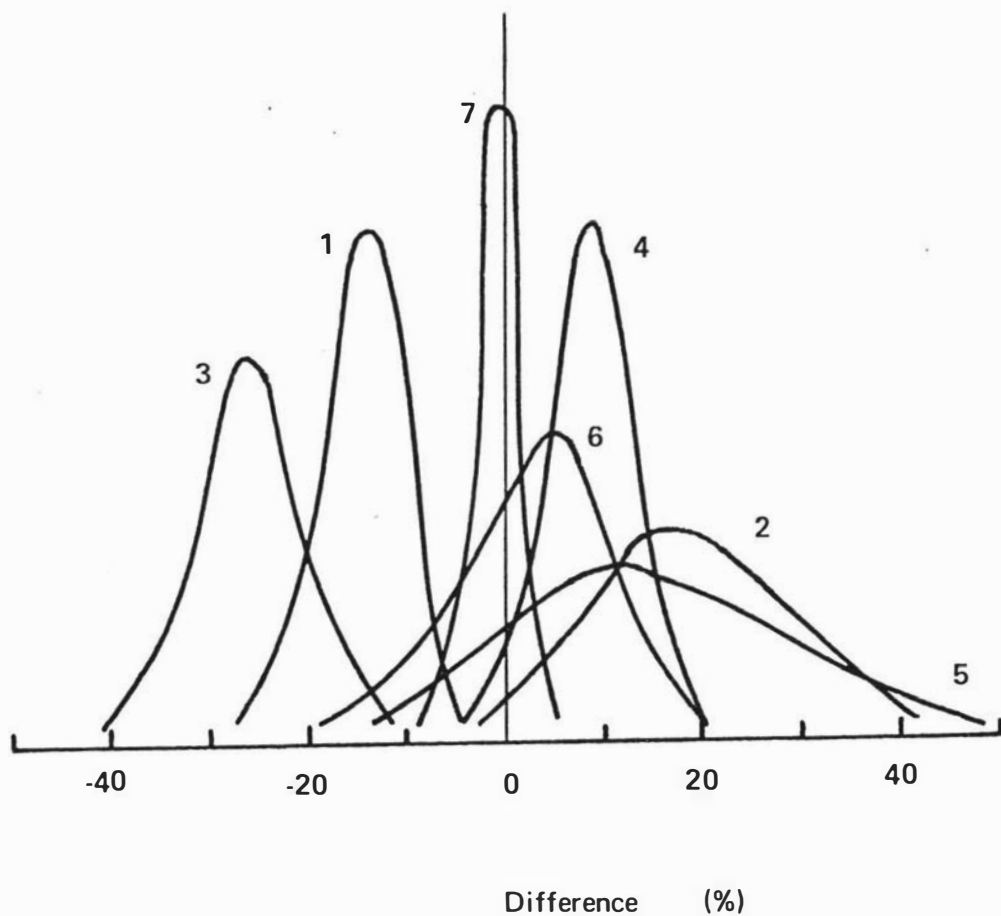


Figure 7.4 Frequency diagram of the percentage differences between experimental freezing times for slabs, and times calculated by empirical modifications and formulae. 1 – Cowell. 2 – Mott. 3 – Rutov. 4 – Mellor. 5 – Nagaoka et al. 6 – modified Plank's equation. 7 – equations 7.4 and 7.5.

in the derivation of these formulae differ (see section 2.2), but the estimates of freezing time are very close to each other. For this reason only a single curve is shown on Figure 7.2 for all these methods - on average the prediction of freezing time was 27% low when compared to the experimentally determined value. This can be attributed to two factors :

1. Neglect of initial superheat. The total heat to be removed can be increased by as much as 50% by the presence of initial superheat. A solution neglecting this will lead to a low prediction of freezing time.
2. Changing thermal conductivity. Phase change occurs over a range of temperature, and the thermal conductivity in the partially frozen region is lower than that of the completely frozen phase which is the value used in the calculation.

Hrycak (1963) has developed a formula for estimation of freezing times of semi-infinite slabs. When applied to finite slabs this formula over-estimates the freezing time, the extent of over-estimation increasing with the amount of superheat. This is shown in Figure 7.3. The 95% confidence limits of this method are -10% to +30%, which makes it the most accurate method in this group.

7.2.3 Empirical Modifications and Formulae

A variety of empirical formulae and modifications to existing formulae have been proposed. The frequency diagrams for the most important of these are given in Figure 7.4.

The formulae of Cowell (1967) and Rutov (1936) consistently under-estimate the freezing time. Those of Mott (1964) and Nagaoka et al (1955) considerably over-estimate the freezing time and are unreliable as witnessed by the wide range of results. Plank's equation using the full enthalpy change in the freezing process ($\Delta H + C_1(T_i - T_f)$)

instead of the latent heat (hereafter referred to as "modified Plank's equation"), on average gives a prediction of the same magnitude as the experimental value, but the 95% confidence limits are -20% to +22%, too great for this modification to be used with confidence. Mellor's formula (1976) gave the best results but the derivation has limitations. The 95% confidence limits are +5% to +20%. Although the formula appears to be accurate it is shown in Appendix 5 that it does not have a sound physical basis. Also, it relies on the estimation of a "mean thermal conductivity" value which may be difficult to estimate for some foodstuffs where data in the region of phase change is not known. These factors detract from the usefulness of this method.

Of the empirical formulae not shown that of Khatchaturov (1958) gave very inaccurate results, and those of Cochran (1955), Baxter (1962) and Tao (1968) gave results very similar to those from the methods that led to Curve 1 on Figure 7.2. This is because they are solutions to the same problem. The solution of Kern (1977) can only be applied to food freezing where there is no initial superheat, and will be as inaccurate as the methods just discussed that also ignore initial superheat. Charm's suggested modification to Neumann's solution so that it can be applied to problems with the third kind of boundary condition (Charm 1971) gave a range of errors of -18% to +630% with a mean of 160% which shows that this modification could be very misleading.

7.2.4 Present Developments

The survey of present methods has shown that that of Mellor (1976) is the most accurate. Because of the problems with this method previously discussed, it may not always be reliable. Hence it was considered worthwhile to seek a better method. Preferably this method would preserve the general form of Plank's equation, the simplest and best known solution, and one with many practical

advantages in terms of physical appreciation of the factors involved. Plank's equation can be written in dimensionless form as :

$$Fo = \frac{P}{Bi Ste} + \frac{R}{Ste} \quad (7.1)$$

where $P = 0.50$ and $R = 0.125$ for a slab.

Introducing the new dimensionless number, the Plank number, to take account of initial superheat :

$$Pk = \frac{C_1 (T_i - T_f)}{\Delta H} \quad (7.2)$$

the functional dependence of the freezing time on the external conditions and the thermal properties of the freezing material is given by :

$$Fo = f(Bi, Ste, Pk) \quad (7.3)$$

To evaluate the functional dependence, an analysis by weighted multiple linear regression was performed on the experimental data obtained using Karlsruhe test substance as the freezing material. Because the data set was non-orthogonal the significance of the input variables and their interactions was evaluated on a trial and error basis to find a model which fitted the data set. This analysis led to the following equations for P and R :

$$P = 0.5072 + 0.2018Pk + Ste(0.3224Pk + \frac{0.0105}{Bi} + 0.0681) \quad (7.4)$$

$$R = 0.1684 + Ste(0.2740Pk - 0.0135) \quad (7.5)$$

Values of P and R calculated from these equations are used in Plank's equation to find the freezing time (note that ΔH is defined as the difference in enthalpy between the initial freezing temperature and the final centre temperature, and not as the latent heat alone). The frequency diagram for this method is shown as Curve 7 on Figure 7.4.

The 95% confidence limits are $\pm 5.4\%$ which is considerably better than $+5\%$ to $+20\%$ for Mellor's formula. In all but three cases the predicted freezing time agreed within the error bounds of the experimental freezing time given in Table 5.3. Full tabulated results can be found elsewhere (Cleland and Earle 1976b).

Applicability to foodstuffs was demonstrated for minced lean beef and mashed potato. The results for this work are shown in Table 7.3. They show that this modification to Plank's equation is as accurate for the real foods tested as it is for Karlsruhe test substance.

Provided accurate data are used the new modification is a substantial improvement on the other methods over the range of experimental conditions it covers, especially in cases where there is initial superheat. Most practical food freezing problems are in this range which is defined by :

$$\begin{aligned} 0.155 &\leq Ste \leq 0.345 \\ 0.2 &\leq Bi \leq 20 \\ 0 &\leq Pk \leq 0.55 \end{aligned} \quad (7.6)$$

7.3 CYLINDERS AND SPHERES

7.3.1 Solutions for the First Kind of Boundary Condition

For slabs it was found that solutions for the first kind of boundary condition do not approximate to the solution of practical freezing problems for Biot numbers up to 20. The highest Biot number used in the experimental work with cylinders and spheres was 4.4. Therefore application of solutions for the first kind of boundary condition to data for radial heat transfer will lead to poor correlation. The solution of Poots (1962a) gave freezing times at least 50% low in all cases. Therefore this solution, and others for the first kind of boundary condition and no initial superheat (Pekeris and Slichter 1939;

Table 7.3

Prediction of freezing times of slabs of minced lean beef and mashed potato by equations 7.4 and 7.5

Experimental conditions are shown in Table 5.4. t_{pl} = predicted freezing time (hours). E = percentage difference between experimental results and the prediction.

Run	t_{exp} (hrs)	\pm	err (hrs)	t_{pl} (hrs)	E (%)
M1	2.32	\pm	0.12	2.24	-3.6
M2	3.84	\pm	0.18	3.69	-3.9
M3	1.68	\pm	0.08	1.68	+0.2
M4	3.30	\pm	0.17	3.40	+2.9
M5	1.54	\pm	0.07	1.58	+2.2
M6	2.34	\pm	0.12	2.23	-4.7
P1	3.20	\pm	0.16	3.16	-2.6
P2	3.72	\pm	0.19	3.92	+5.4
P3	1.58	\pm	0.09	1.54	-2.4
P4	4.48	\pm	0.23	4.63	+3.4
P5	1.76	\pm	0.10	1.71	-3.0
P6	3.02	\pm	0.16	3.13	+3.8

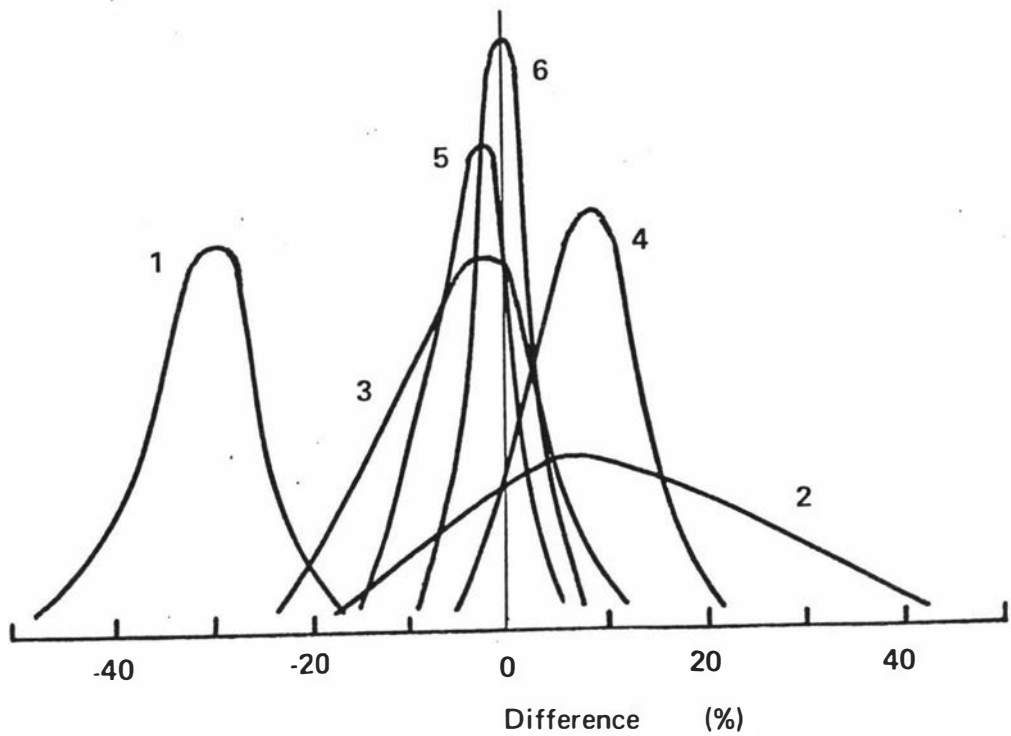


Figure 7.5 Frequency diagram of the percentage differences between experimental freezing times for cylinders, and times calculated by various methods. 1 — Plank. 2 — Nagaoka et al. 3 — modified Plank's equation. 4 — Mellor. 5 — equations 7.4 and 7.5. 6 — equations 7.7 and 7.8.

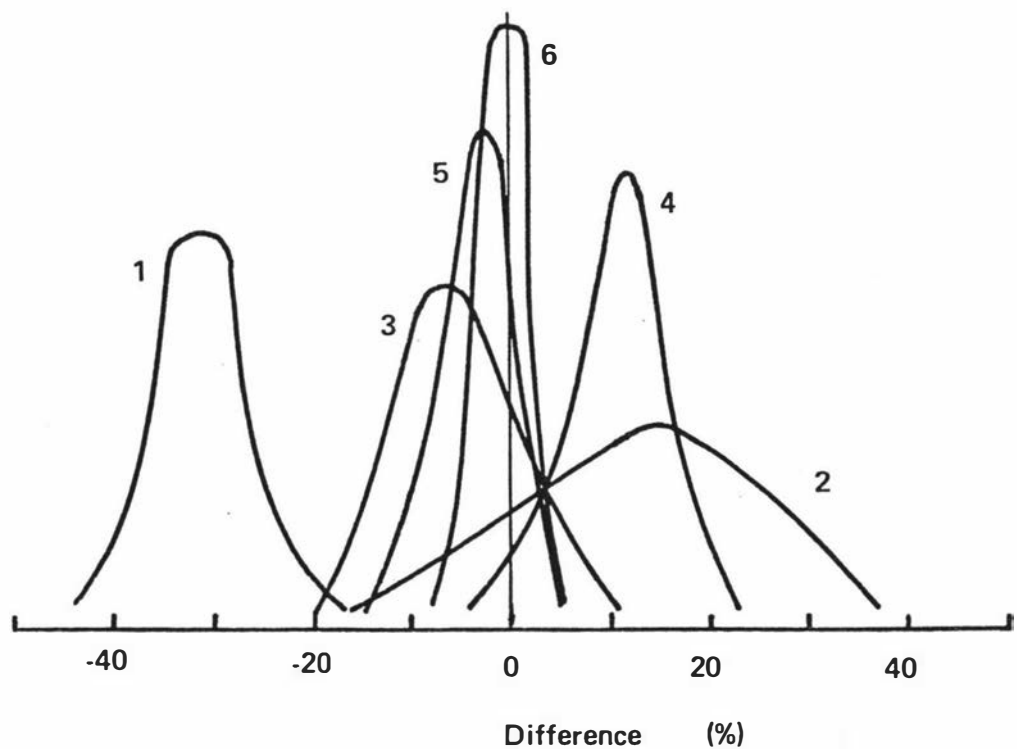


Figure 7.6 Frequency diagram of the percentage differences between experimental freezing times for spheres, and times calculated by various methods. 1 — Plank. 2 — Nagaoka et al. 3 — modified Plank's equation. 4 — Mellor. 5 — equations 7.4 and 7.5. 6 — equations 7.9 and 7.10.

Langford 1966; Cho and Sunderland 1970; Komori and Hirai 1970; Theofanous and Lim 1971; Pedroso and Domoto 1973c; Pedroso and Domoto 1973d; Riley et al 1974) were not considered any further.

7.3.2 Solutions for the Third Kind of Boundary Condition

None of the approximate analytical solutions that exist for the third kind of boundary condition take account of initial superheat. They are all solutions to the same problem which is infrequently met with in practice, and give very similar answers. Therefore the only frequency diagram plotted is for Plank's equation which is shown as Curve 1 on Figure 7.5 for cylinders and Curve 1 on Figure 7.6 for spheres. These will represent approximately results from the solutions of London and Seban (1943), Kreith and Romie (1955), Shih and Chou (1971), Shih and Tsay (1971), and Selim and Seagrave (1973b).

Plank's equation on average predicts the freezing time 31% low compared to the experimental data, and the other solutions will be no better. Initial superheat is clearly an important factor in radial geometry as well as with slabs.

7.3.3 Empirical Modifications and Formulae

7.3.3.1 Cylinders The regression formulae of Baxter (1962) and Tao (1967) which do not take account of initial superheat give results that are almost identical with those from Plank's equation, and are hence represented by Curve 1 on Figure 7.5. All other empirical formulae considered are based on Plank's equation.

Curve 2 is the variation of Nagaoka et al (1955). The 95% confidence limits are -20% to +35% so the method is of limited value because of this wide range of uncertainty.

Curve 3 is the modified Plank's equation - the 95% confidence limits are -20% to +10% which is better than for

the formula of Nagaoka et al.

Mellor's formula (Curve 4) gave 95% confidence limits of +1% to +20% which is a very similar range to that which this formula gave for slabs. The method has the same theoretical limitations when applied to radial geometry as it has for slabs.

Plank's equation implies that a cylinder will freeze in half the time required for the equivalent slab to freeze. The modification to Plank's equation (equations 7.4 and 7.5) derived for slabs was used and the result halved. This led to Curve 5 on Figure 7.5, the mean error is -5.3% and the 95% confidence limits are -13% to +2%. This suggests that a cylinder does not take exactly half the time of the equivalent slab to freeze. The most likely reason for this is that the average thermal conductivity of the semi-frozen phase is different for the two shapes. Because of the radial nature of heat transfer the shape of the temperature profile in the cylinder will be different from that in a slab. Therefore the thermal conductivity gradient will also be different. In these circumstances use of the same thermal conductivity value for both shapes would lead to a difference of a few percent such as was encountered. Use of half the calculated freezing time from equations 7.4 and 7.5 is clearly inadequate.

7.3.3.2 Spheres The empirically modified formulae available for spheres are closely related to those for cylinders. Tao's formula (1967) does not take account of initial superheat, and therefore leads to the same frequency diagram as Plank's equation (Curve 1 on Figure 7.6).

The variation of Nagaoka et al (1955) (Curve 2) is unreliable; the 95% confidence limits are -23% to +40%, very similar results to those obtained for slabs and cylinders.

Curve 3, modified Plank's equation gave 95% confidence

limits of -10% to +21% - very similar results to those obtained with this formula for other shapes.

Mellor's formula (Curve 4) gave 95% confidence limits of +1% to +23%, slightly less accurate results than those for slabs and cylinders.

Curve 5 is the result from the use of equations 7.4 and 7.5. Plank's equation implies that a sphere freezes in one third of the time required for the equivalent slab to freeze, so the results from equations 7.4 and 7.5 were divided by three. The mean value of the error is -3.6% and the 95% confidence limits -12% to +5%. These results are very similar to those found for cylinders; again the deviation from the slab results is probably due to a differently shaped thermal conductivity gradient in the radial case compared to the equivalent slab problem. This would mean that the mean thermal conductivities for slabs and spheres are different, and that the slab formulae (equations 7.4 and 7.5) cannot be applied directly to spheres.

7.3.4 Present Developments

The results of the survey of existing methods showed that none are sufficiently accurate for design purposes. Therefore it seemed worthwhile to seek a new empirical formula similar to that found for slabs. An analysis of the experimental data by weighted multiple linear regression was performed to find modified formulae for the shape factors in Plank's equation. The results are :

Cylinders :

$$P = 0.3751 + 0.0999Pk + \text{Ste}(0.4008Pk + \frac{0.0710}{Bi} - 0.5865) \quad (7.7)$$

$$R = 0.0133 + \text{Ste}(0.0415Pk + 0.3957) \quad (7.8)$$

Spheres :

$$P = 0.1084 + 0.0924Pk + Ste(0.2310Pk - \frac{0.3114}{Bi} + 0.6739) \quad (7.9)$$

$$R = 0.0784 + Ste(0.0386Pk - 0.1694) \quad (7.10)$$

These modifications led to Curve 6 on Figures 7.5 and 7.6 in each case. The 95% confidence limits are $\pm 5.2\%$ for cylinders and $\pm 3.8\%$ for spheres. Because the experimental data was not collected over as wide a range of conditions as the data for slabs the lack of fit of such a simple model will be greater for slabs than in the radial cases. This is why the formulae have narrower 95% confidence limits than equations 7.4 and 7.5 for slabs.

The applicability of these formulae to the freezing of real foodstuffs has not been checked because there is no reason to expect that the correlation of Karlsruhe test substance with real foods will differ between slabs, cylinders and spheres. The fact that the errors found for each calculation method are very similar for all three shapes indicates that the physical behaviour of the three geometries is closely linked.

The range of applicability of equations 7.7 to 7.10 is :

$$\begin{aligned} 0.155 &\leq Ste \leq 0.345 \\ 0.5 &\leq Bi \leq 4.5 \\ 0 &\leq Pk \leq 0.55 \end{aligned} \quad (7.11)$$

7.4 RECTANGULAR BRICKS

7.4.1 Existing Formulae

It has been shown that even when the Biot number is as high as 20, solutions for the first kind of boundary

condition do not approximate sufficiently accurately to the real situation for them to have any practical value. The solution of Riley and Duck (1977) ignores superheat for cases where the boundary condition is of the first kind, and hence need not be considered. Only one approximate analytical solution exists for the third kind of boundary condition, that of Plank (1941). This solution does not take account of initial superheat but has been commonly used, with or without modification.

For a rectangular brick of dimensions $D_x \times D_y \times D_z$ (which can be written as $D \times B_1 D \times B_2 D$) ordinary Plank's equation is used with values of the geometric factors P and R found from :

$$P = \frac{B_1 B_2}{2 (B_1 B_2 + B_1 + B_2)} \quad (7.12)$$

$$R = \frac{Q}{2} ((m-1)(B_1-m)(B_2-m) \ln(\frac{m}{m-1}) - (n-1)(B_1-n)(B_2-n) \ln(\frac{n}{n-1})) + \frac{1}{72} (2B_1 + 2B_2 - 1) \quad (7.13)$$

where

$$\frac{1}{Q} = 4((B_1-B_2)(B_1-1) + (B_2-1)^2)^{\frac{1}{2}} \quad (7.14)$$

$$m = \frac{1}{3}(B_1 + B_2 + 1 + ((B_1-B_2)(B_1-1) + (B_2-1)^2)^{\frac{1}{2}}) \quad (7.15)$$

$$n = \frac{1}{3}(B_1 + B_2 + 1 - ((B_1-B_2)(B_1-1) + (B_2-1)^2)^{\frac{1}{2}}) \quad (7.16)$$

Alternatively they can be obtained from the charts of Ede (1949), although these cannot be read to the accuracy necessary.

Because Plank's equation does not take account of initial superheat it has been found to give a low prediction of freezing time. The most accurate modification to Plank's equation in the literature was found to be that of Mellor (1976). Twelve different boxes were used in the experimental work, these leading to different values of

P and R in each case. These shape factors can be related to the number of "equivalent heat transfer dimensions" W . For a slab $W=1$; for a cylinder $W=2$; for a sphere $W=3$; and for brick shapes $1 \leq W \leq 3$. For each box W can be calculated from :

$$W_1 = \frac{0.5}{P} \quad (7.17)$$

$$W_2 = \frac{0.125}{R} \quad (7.18)$$

Now W_1 and W_2 are not necessarily equal, but they are never very different, and their average gives W , the number of equivalent heat transfer dimensions. For each box the calculated freezing times from Mellor's formula were compared to the experimental values, and the average percentage difference found. This value was plotted against W in Figure 7.7. All the predicted freezing times are low, and the error increases as W is decreased. Yet Mellor's formula always gave a high prediction of the freezing time for other shapes.

Also plotted on Figure 7.7 are results from the use of equations 7.4 and 7.5 after division by W_1 and W_2 respectively. The same trend as found for Mellor's formula occurred.

It is implicit in Plank's equation that a sphere and its escribed cube will freeze in the same time. However use of equations 7.4 and 7.5 (after modification by W_1 and W_2 respectively) led to predictions of the freezing time that were on average 19% low for cubes and 4% low for spheres. Therefore a sphere takes a shorter time to freeze (by about 15%) than its escribed cube. This is in good agreement with the experimental results of Earle and Earl (1966). Also, the exact solutions for heat conduction without change of phase in these shapes generally show a difference in the time for the centre to reach a certain temperature of 5-30% depending on the final centre temperature and the external heat transfer conditions. This

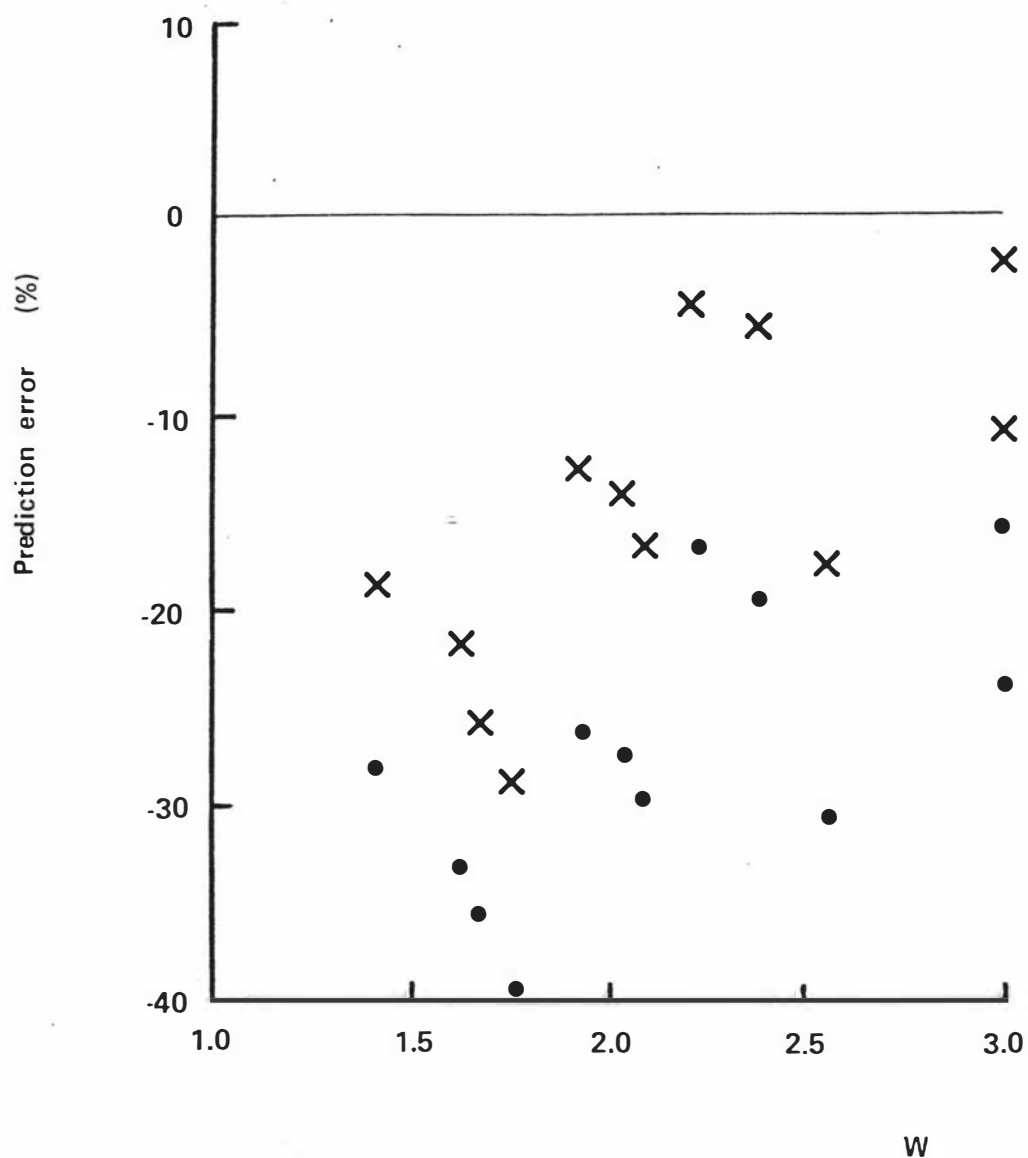


Figure 7.7 Plot of the average prediction error (when comparing calculated freezing times to experimental results for rectangular bricks) versus number of equivalent heat transfer dimensions.

x — from Mellor's formula

• — from equations 7.4 and 7.5 (modified by W_1 and W_2)

is consistent with what was found in the cases where freezing occurred.

Box 12 (runs B67 to B72) had dimensions of 0.200m x 0.200m x 0.050m, and $W = 1.42$. A slab of these dimensions subject to heat conduction without change of phase would have a cooling rate at the centre almost indistinguishable from that of the same slab with heat transfer in only the smallest dimension; that is a one-dimensional slab. When the slab freezing formula (equations 7.4 and 7.5) was applied after modification by W_1 and W_2 the average error was -28%, whereas when it was applied directly the average error was 2% and the range of errors -3% to +5%. Thus, the analogy to heat conduction without change of phase more accurately describes the effect of the other two dimensions on the freezing time than do Plank's geometric factors.

This evidence shows that the assumptions made by Plank in arriving at his geometric factors are not correct, generally becoming more erroneous as W approaches 1. All modifications to Plank's equation that use the geometric factors (Nagaoka et al 1955; Mellor 1976; "modified Plank's equation") will therefore give erroneous results.

7.4.2 Present Developments

It was shown in section 7.3.3 that the freezing times of slabs, cylinders and spheres are closely related in the manner suggested by Plank, although the experimental data does not fit the proposed correlation exactly. The geometric factors proposed for rectangular bricks do not agree with the experimental data. In order to derive a suitable relationship to fit the results of the brick experiments a weighted linear regression was performed to find a general relationship linking slabs, cylinders and spheres, and also a modification to this relationship to fit brick shaped objects.

The final form uses values of P and R from either

Ede's charts or Plank's formulae (see section 7.4.1) in the following general equations :

$$P_1 = P(1.026 + 0.5808Pk + Ste(0.2296Pk + \frac{0.0182}{Bi} + 0.1050)) \quad (7.19)$$

$$R_1 = R(1.202 + Ste(3.410Pk + 0.7336)) \quad (7.20)$$

P_1 and R_1 are intermediate values of the modified geometric factors. These are further modified to find the final values P_2 and R_2 which are used in Plank's equation.

For slabs :

$$P_2 = P_1 \quad (7.21)$$

$$R_2 = R_1 \quad (7.22)$$

For cylinders and spheres :

$$P_2 = P_1 + 0.1278P \quad (7.23)$$

$$R_2 = R_1 - 0.1888R \quad (7.24)$$

For rectangular bricks :

$$P_2 = P_1 + P(0.1136 + Ste(5.766P - 1.242)) \quad (7.25)$$

$$R_2 = R_1 + R(0.7344 + Ste(49.89R - 2.900)) \quad (7.26)$$

P_2 and R_2 are then substituted in Plank's equation (with the enthalpy change between the initial freezing temperature and the final centre temperature used instead of the latent heat) :

$$t_{pl} = \frac{\Delta H}{(T_f - T_a)} \left(P_2 \frac{D}{h} + R_2 \frac{D^2}{k_s} \right) \quad (7.27)$$

The full calculated results from this group of

formulae are given in Table 8.1. Table 7.4 is a summary showing the accuracy of these formulae. The 95% confidence limits closely correlate with the experimental error bounds for each shape. It was found to be impossible to completely generalise the formulae so the arrangement using a common base which is further modified was thought to be the best. The formulae also give good prediction of the freezing time for the potato and meat slabs. This data is shown in Table 8.1. Because the experimental data for Karlsruhe test substance could be correlated over a wide range of shapes, equally good prediction of food freezing times for these shapes would be expected, provided accurate data are used.

The formulae are applicable over a wide range of conditions which should cover most practical food freezing problems. The limits are :

$$0.155 \leq Ste \leq 0.345 \quad (7.28)$$

$$0 \leq Pk \leq 0.55 \quad (7.29)$$

$$0.2 \leq Bi \leq 20 \text{ for slabs} \quad (7.30)$$

$$0.5 \leq Bi \leq 4.5 \text{ for cylinders and spheres} \quad (7.31)$$

$$0.5 \leq Bi \leq 22 \text{ for bricks} \quad (7.32)$$

$$1 \leq B_1 \leq 4 \text{ for bricks} \quad (7.33)$$

$$1 \leq B_2 \leq 4 \text{ for bricks} \quad (7.34)$$

The formulae may be applicable outside this range but at the expense of reduced accuracy. However most practical food freezing situations are covered.

This group of formulae are the most accurate set of simple formulae available to predict freezing times for foods. All other formulae using Plank's geometric factors for bricks gave predictions which deviated too much from the experimental results.

Table 7.4

Means and 95% confidence limits for the applicability of equations 7.19 to 7.27 to the experimental data

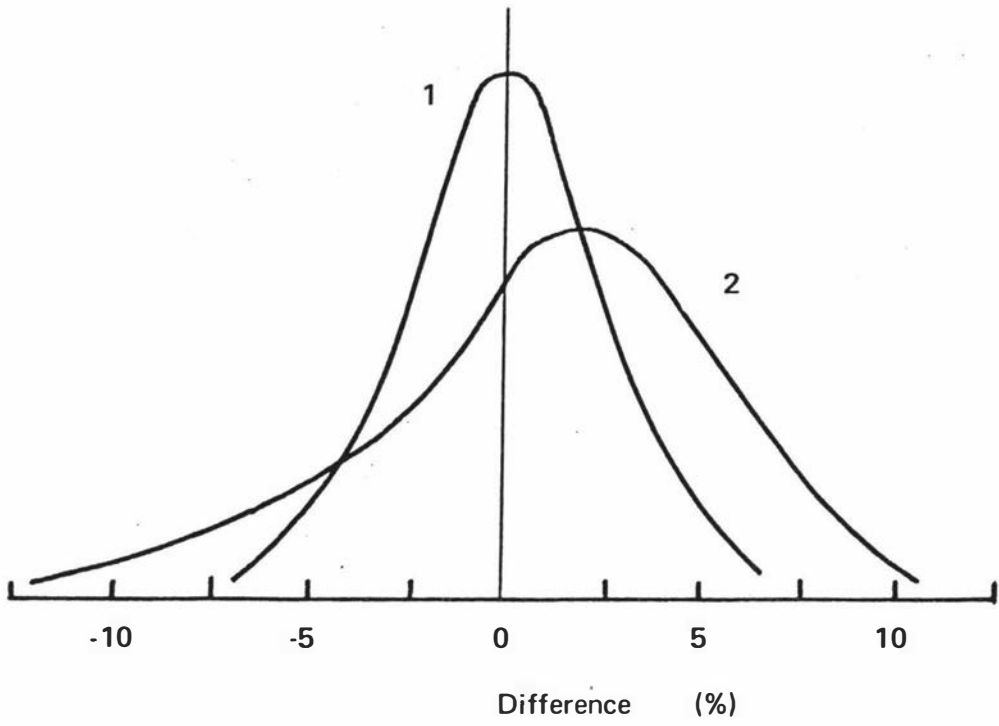
Applicability	Mean (%)	95% confidence limits (%)	Average experi- mental error (%)
Slabs	0.0	-4.8 to +4.8	<u>+4.2</u>
Cylinders	-0.5	-8.1 to +7.1	<u>+6.5</u>
Spheres	0.3	-6.3 to +6.9	<u>+7.0</u>
Bricks	-0.3	-10.4 to +9.8	<u>+8.0</u>
Overall	-0.2	-8.4 to +8.0	<u>+6.6</u>

8 COMPARISON OF NUMERICAL AND SIMPLE METHODS FOR PREDICTING FREEZING TIMES

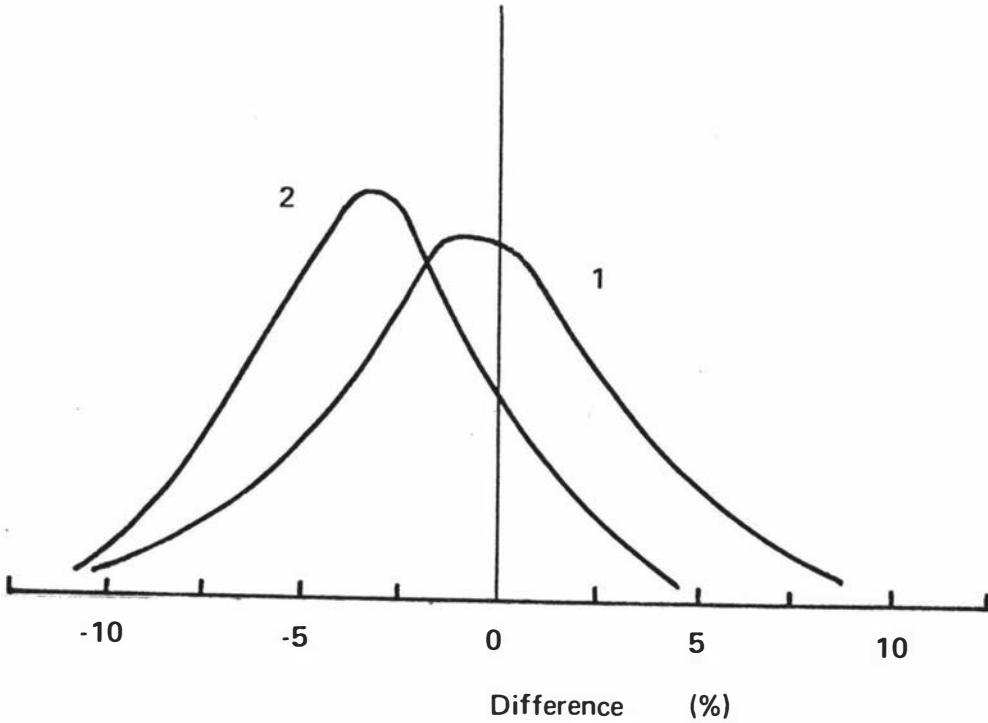
In the previous two chapters methods for predicting the freezing time of foods have been examined to find the best method requiring numerical solution, and the best simple formula for each of slabs, cylinders, spheres and rectangular bricks. The best numerical solution for the different geometries was found to be based on the Lees scheme (Lees 1966; Bonacina and Comini 1971). The examination of simple formulae found that none of the methods in the literature accurately predicted the experimentally determined freezing times. Therefore a new modification to Plank's equation (equations 7.19 to 7.27) is proposed. It was found to be considerably superior to all other simple formulae over the range of data covered. This range should include most practical food freezing problems. The formulae are not perhaps as simple as might have been hoped for, but the complication is the minimum needed to secure sufficient accuracy.

Figure 8.1 shows frequency diagrams for the four geometries investigated. Complete results cannot be shown for brick shapes because the computation time for the three-dimensional finite difference program is large, and practical limitations prevented more than three calculations. Table 8.1 shows the experimental and calculated freezing times for each method. Table 8.2 gives the mean and standard deviation of the percentage differences between calculated and experimental results for each of the shapes and methods.

In a paper (Cleland and Earle 1977a) that considered slabs only, equations 7.4 and 7.5 were compared to finite difference freezing calculations. The final formulae (equations 7.19 to 7.27) include the slab case for which the earlier formulae were derived, and give very similar freezing time predictions to equations 7.4 and 7.5 for slabs. Therefore the conclusions in the paper are equally valid

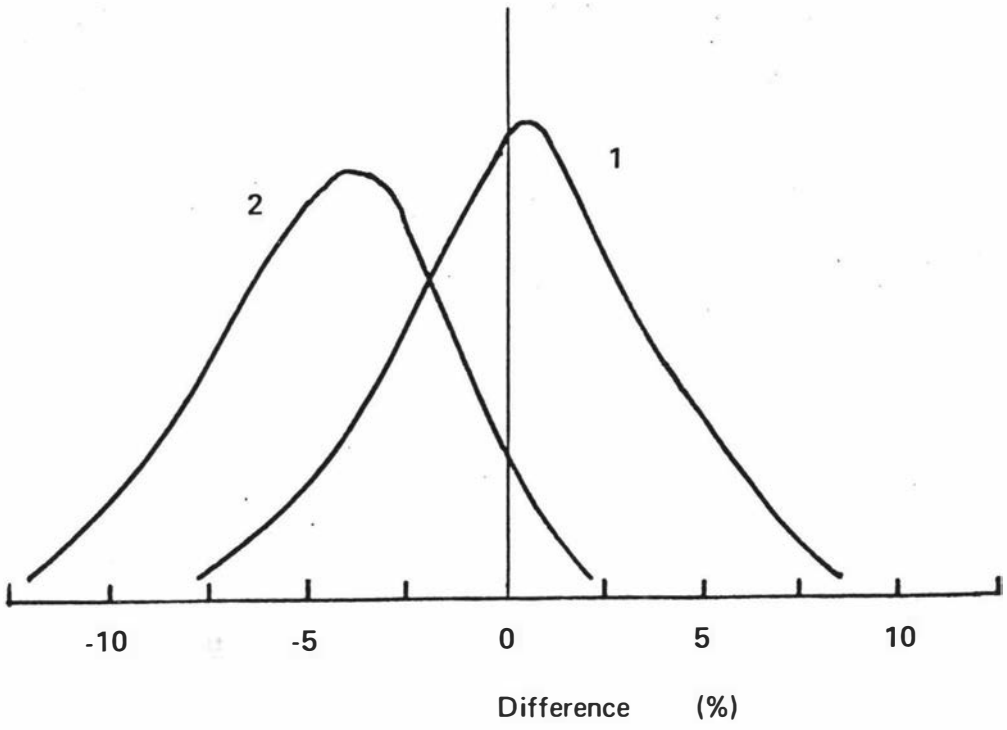


a

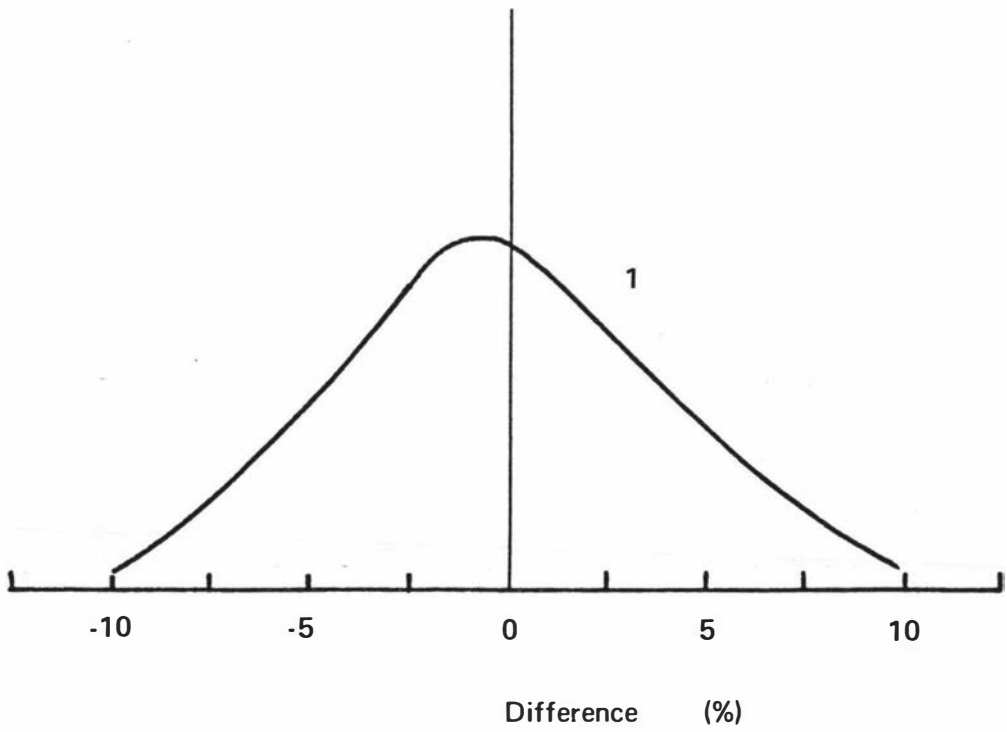


b

Figure 8.1 Frequency diagram of the percentage differences between experimental freezing times, and calculated times. 1 – equations 7.19 and 7.27. 2 – the numerical method.
 a – slabs. b – cylinders. c – spheres. d – rectangular bricks.



c



d

Figure 8.1 continued.

for the prediction of slab freezing times by equations 7.19 to 7.27.

Because of the nature of multiple linear regression the prediction errors from the use of the simple formulae have means very close to 0% for each shape. In radial geometry the mean prediction error from the finite difference results is low by 4%. This low average was expected; the reasons for it are given in section 6.2.3. The mean error in the predicted freezing times for bricks by finite differences cannot be calculated but the results obtained indicate that it would probably be close to 0%, in a manner consistent with the slab results. There is very little difference in the average prediction error between finite differences and equations 7.19 to 7.27, except for the known error in the radial finite difference calculations.

Whilst on average both the simple and numerical methods give accurate answers, reliability is indicated by the spread around the mean value, that is the standard deviation of the percentage differences between calculated and experimental freezing times. For slabs, the simple formulae are better, mainly because of the problem of "jumping" in the finite difference calculations. This is discussed in section 6.1.3. For radial geometry the finite difference results are less spread than those for the simple formulae, but the difference between the standard deviations is small. The reason that the simple formulae are less accurate in this case is that they are based on the overall fit of data for all shapes, and slightly misfit the data for cylinders and spheres. Equations 7.7 to 7.10 which were developed for these shapes on their own gave standard deviations of 2.6% for cylinders and 1.9% for spheres. These values are significantly less than those for the general formulae (3.8% and 3.3% respectively). It would be expected that if full results could be calculated for prediction of brick freezing times by finite differences these would fit the pattern of the rest of the results; with a mean close to 0%, and a standard deviation of about the same size as that

found for the simple formulae (5.1%). However there could well be a tendency to get low calculated freezing times at high Biot numbers where "jumping" has occurred.

Overall there is little difference in accuracy between the two methods; in fact in many instances if one calculation method gives a low prediction the other does also. However special care is needed when applying finite differences to radial shapes because the prediction will be 4% low on average. Table 8.3 compares other aspects of the two types of freezing time calculation.

Because the predicted freezing times are compared with the experimental values in the analysis, the experimental error and the error in the prediction method are confounded together in the difference between the predicted and experimental freezing times. It is impossible to separate these two effects in order to assess the errors in the calculation methods alone. Consequently the average percentage error and the 95% confidence limits represent the additive effect of the two components, and the limits almost certainly overestimate the error in the calculation method alone, but they are the best estimates that can be determined.

Whilst the proposed simple formulae have the advantage of simplicity they cannot handle such a wide range of conditions as the numerical method. Also, changing conditions cannot be handled directly, although by the use of a suitable average the simple formulae can be used to find an approximation to the true freezing time. For practical food freezing problems with constant, or approximately constant, conditions the advantage of simplicity makes equations 7.19 to 7.27 the better method. Problems with non-constant conditions will be considered in the next chapter.

The multiple linear regression used to find equations 7.19 to 7.27 fits the results with a mean error of 0%, but for design purposes it might be desirable to ensure

conservative estimates, that is to allow a safety factor. One useful method for doing this is to adjust the calculated freezing time upwards so that the lower 95% confidence limit is 0%. For example, the 95% confidence limits for slabs are $\pm 4.8\%$. If the calculated freezing time was increased by 4.8% the 95% confidence limits would become 0% to +9.6% which is a more acceptable range than $\pm 4.8\%$ if safety must be ensured for design purposes. This is only a suggested guideline; provided the design engineer is aware of the limitations of the simple formulae he is free to choose his own safety factor.

Table 8.1Experimental and calculated freezing time data for all shapes

t_{pl} = freezing time calculated from equations 7.19 to 7.27.

t_{fd} = freezing time calculated from the three-level finite difference schemes. E = percentage difference between experimental and calculated freezing times.

* indicates a calculated value outside the experimental error bounds

Run	t_{exp} (hrs)	\pm err (hrs)	t_{pl} (hrs)	E (%)	t_{fd} (hrs)	E (%)
F1	0.64	\pm 0.04	0.66	+3.0	0.66	+3.0
F2	2.62	\pm 0.10	2.71	+3.6	2.42	-7.7*
F3	1.42	\pm 0.07	1.38	-2.8	1.44	+1.3
F4	4.74	\pm 0.18	4.77	+0.5	4.70	-0.8
F5	0.56	\pm 0.04	0.57	+1.3	0.55	-2.1
F6	2.22	\pm 0.10	2.30	+3.6	2.01	-9.5*
F7	1.26	\pm 0.07	1.20	-4.8	1.21	-4.4
F8	4.02	\pm 0.17	4.09	+1.8	3.90	-3.0
F9	1.26	\pm 0.07	1.27	+1.1	1.33	+6.2
F10	4.80	\pm 0.22	4.99	+4.0	4.95	+3.1
F11	2.74	\pm 0.14	2.73	-0.5	2.91	+6.2*
F12	8.96	\pm 0.38	9.15	+2.1	9.53	+6.4*
F13	1.12	\pm 0.07	1.11	-1.2	1.16	+3.8
F14	4.50	\pm 0.20	4.36	-3.1	4.27	-4.2*
F15	2.44	\pm 0.13	2.36	-3.1	2.56	+5.0
F16	7.96	\pm 0.34	7.95	-0.1	8.28	+4.0
F17	2.74	\pm 0.12	2.72	-0.6	2.76	+0.6
F18	2.66	\pm 0.12	2.72	+2.4	2.76	+3.8
F19	2.70	\pm 0.12	2.72	+0.8	2.76	+2.2
F20	2.74	\pm 0.12	2.72	-0.6	2.76	+0.6
F21	2.74	\pm 0.12	2.72	-0.6	2.76	+0.6
F22	0.74	\pm 0.04	0.73	-0.7	0.75	+1.4
F23	1.00	\pm 0.05	1.00	-0.2	0.98	-2.1

... continued

Table 8.1 continued

Run	t_{exp} (hrs)	\pm err (hrs)	t_{pl} (hrs)	E (%)	t_{fd} (hrs)	E (%)
F24	3.02	\pm 0.14	3.06	+1.2	3.10	+2.6
F25	4.28	\pm 0.18	4.36	+1.8	4.15	-3.0
F26	0.32	\pm 0.03	0.33	+3.1	0.33	+2.0
F27	1.92	\pm 0.09	1.84	-3.4	1.76	-8.3*
F28	2.04	\pm 0.08	1.95	-4.2*	2.03	-0.6
F29	1.54	\pm 0.07	1.55	+0.6	1.58	+2.4
F30	1.82	\pm 0.09	1.85	+1.5	1.69	-7.1*
F31	0.34	\pm 0.03	0.32	-4.7	0.32	-4.8
F32	3.46	\pm 0.15	3.41	-1.4	3.25	-6.0*
F33	0.88	\pm 0.05	0.87	-0.7	0.81	-8.0*
F34	0.68	\pm 0.04	0.70	+2.3	0.74	+8.1*
F35	2.40	\pm 0.11	2.32	-3.3	2.40	-0.1
F36	5.34	\pm 0.20	5.42	+1.5	5.49	+2.9
F37	8.42	\pm 0.33	8.47	+0.6	8.47	+0.6
F38	2.68	\pm 0.13	2.64	-1.4	2.79	+4.0
F39	5.26	\pm 0.20	5.11	-2.9	5.36	+1.9
F40	3.10	\pm 0.12	3.15	+1.5	3.35	+8.0*
F41	8.50	\pm 0.35	8.38	-1.5	8.64	+1.6
F42	2.32	\pm 0.10	2.40	+3.2	2.42	+5.5
F43	5.82	\pm 0.23	5.78	-0.7	6.04	+3.8
M1	2.32	\pm 0.12	2.40	+3.5	2.32	-0.1
M2	3.84	\pm 0.18	3.68	-4.2	3.81	-0.7
M3	1.68	\pm 0.08	1.75	+4.2	1.82	+8.3*
M4	3.30	\pm 0.17	3.42	+3.6	3.59	+8.8*
M5	1.54	\pm 0.07	1.60	+4.0	1.69	+9.7*
M6	2.34	\pm 0.12	2.29	-2.1	2.41	+2.9
P1	3.12	\pm 0.16	3.19	+2.3	2.97	-4.9
P2	3.72	\pm 0.19	3.76	+1.1	3.66	-1.7
P3	1.58	\pm 0.09	1.53	-3.2	1.46	-7.7*
P4	4.48	\pm 0.23	4.53	+1.1	4.70	+4.9

... continued

Table 8.1 continued

Run	t_{exp} (hrs)	\pm err (hrs)	t_{pl} (hrs)	E (%)	t_{fd} (hrs)	E (%)
P5	1.76	\pm 0.10	1.70	-3.4	1.74	-1.3
P6	3.02	\pm 0.16	2.99	-1.0	3.11	+2.9
C1	8.36	\pm 0.46	8.53	+2.1	8.15	-2.5
C2	6.14	\pm 0.40	6.29	+2.5	6.15	+0.2
C3	2.16	\pm 0.17	2.16	+0.2	2.14	-1.0
C4	8.30	\pm 0.47	8.46	+2.0	8.22	-1.0
C5	5.82	\pm 0.38	5.94	+2.1	5.86	+0.7
C6	1.98	\pm 0.16	2.04	+3.1	2.03	+2.4
C7	7.50	\pm 0.39	7.20	-4.0	7.00	-6.7*
C8	5.30	\pm 0.33	5.29	-0.2	5.09	-4.0
C9	1.84	\pm 0.14	1.83	-0.3	1.79	-3.0
C10	6.10	\pm 0.24	5.66	-7.2*	5.63	-7.6*
C11	4.10	\pm 0.23	3.96	-3.3	3.83	-6.6*
C12	1.28	\pm 0.08	1.32	+2.8	1.27	-1.0
C13	5.56	\pm 0.23	5.17	-7.0*	5.17	-7.0*
C14	3.64	\pm 0.19	3.62	-0.6	3.43	-5.9*
C15	1.18	\pm 0.08	1.24	+4.8	1.19	+0.6
C16	5.48	\pm 0.23	4.95	-9.7*	4.89	-10.8*
C17	3.44	\pm 0.21	3.23	-6.2	3.23	-6.2
C18	1.08	\pm 0.07	1.13	+4.2	1.03	-4.4
C19	8.90	\pm 0.46	8.90	-0.1	8.59	-3.5
C20	9.36	\pm 0.46	8.95	-4.4	8.64	-7.9*
C21	1.06	\pm 0.07	1.11	+4.8	1.03	-3.3
C22	1.04	\pm 0.07	1.10	+6.0	1.01	-3.2
C23	4.56	\pm 0.27	4.72	+3.6	4.60	+0.8
C24	4.74	\pm 0.27	4.69	-1.0	4.54	-4.2
C25	5.86	\pm 0.37	5.88	+0.3	5.49	-6.5
C26	4.14	\pm 0.31	4.14	-0.1	3.94	-4.8
C27	1.34	\pm 0.13	1.40	+4.4	1.34	-0.6
C28	5.70	\pm 0.31	5.51	-3.2	5.41	-5.1
C29	3.96	\pm 0.37	4.01	+1.3	3.80	-4.2
C30	2.10	\pm 0.19	1.96	-6.5	1.98	-5.9

... continued

Table 8.1 continued

Run	t_{exp} (hrs)	\pm err (hrs)	t_{pl} (hrs)	E (%)	t_{fd} (hrs)	E (%)
S1	5.18	\pm 0.33	5.27	+1.8	4.87	-6.0
S2	2.28	\pm 0.18	2.29	+0.3	2.18	-4.4
S3	1.20	\pm 0.11	1.21	+0.6	1.17	-2.5
S4	5.14	\pm 0.32	5.14	+0.1	4.82	-6.6
S5	2.12	\pm 0.19	2.11	-0.3	2.03	-4.1
S6	1.14	\pm 0.11	1.18	+3.2	1.14	+0.3
S7	4.50	\pm 0.28	4.49	-0.3	4.13	-8.2*
S8	1.92	\pm 0.16	1.88	-2.0	1.81	-5.9
S9	0.96	\pm 0.10	1.00	+4.0	0.94	-1.8
S10	3.38	\pm 0.19	3.56	+5.4	3.20	-5.5
S11	1.40	\pm 0.11	1.45	+3.7	1.36	-3.2
S12	0.80	\pm 0.08	0.76	-5.0	0.75	-6.9
S13	3.02	\pm 0.17	3.23	+7.0*	2.97	-1.8
S14	1.30	\pm 0.10	1.31	+0.7	1.25	-3.7
S15	0.74	\pm 0.07	0.70	-5.8	0.69	-7.2
S16	2.70	\pm 0.17	2.87	+6.4	2.68	-0.7
S17	1.22	\pm 0.10	1.25	+2.6	1.18	-3.0
S18	0.68	\pm 0.05	0.65	-4.9	0.62	-8.7*
S19	5.16	\pm 0.33	5.26	+1.9	4.86	-5.8
S20	5.24	\pm 0.33	5.33	+1.8	4.93	-6.0
S21	0.66	\pm 0.05	0.63	-5.2	0.61	-7.7
S22	0.66	\pm 0.05	0.62	-5.3	0.61	-7.8
S23	1.68	\pm 0.13	1.69	+0.5	1.61	-4.3
S24	1.68	\pm 0.13	1.70	+1.5	1.63	-3.3
S25	3.48	\pm 0.24	3.54	+1.7	3.36	-3.6
S26	1.62	\pm 0.17	1.61	-0.9	1.56	-3.5
S27	0.84	\pm 0.10	0.86	+2.7	0.84	-0.2
S28	3.30	\pm 0.24	3.29	-0.3	3.11	-5.9
S29	1.94	\pm 0.19	1.96	+1.1	1.88	-3.5
S30	1.26	\pm 0.15	1.28	+1.7	1.24	-1.6
B1	1.34	\pm 0.10	1.40	+4.1		
B2	1.20	\pm 0.10	1.28	+6.7		

... continued

Table 8.1 continued

Run	t_{exp} (hrs)	\pm err (hrs)	t_{pl} (hrs)	E (%)	t_{fd} (hrs)	E (%)
B3	0.92	\pm 0.07	0.99	+7.4		
B4	0.80	\pm 0.07	0.86	+7.0		
B5	1.28	\pm 0.10	1.32	+3.0		
B6	2.02	\pm 0.16	2.05	+1.5		
B7	3.90	\pm 0.26	3.95	+1.3		
B8	3.40	\pm 0.24	3.45	+1.5		
B9	2.80	\pm 0.15	2.80	+0.1		
B10	2.32	\pm 0.14	2.39	+2.9		
B11	3.32	\pm 0.24	3.17	-4.4		
B12	5.76	\pm 0.46	5.22	-9.4*		
B13	4.10	\pm 0.26	4.02	-2.0		
B14	3.46	\pm 0.24	3.49	+0.8		
B15	3.04	\pm 0.17	2.90	-4.6		
B16	2.32	\pm 0.17	2.49	+7.1		
B17	3.50	\pm 0.27	3.45	-1.3		
B18	5.72	\pm 0.48	5.17	-9.6*		
B19	4.90	\pm 0.26	4.54	-7.3*		
B20	4.24	\pm 0.24	4.08	-3.7		
B21	3.40	\pm 0.16	3.31	-2.5		
B22	2.90	\pm 0.16	2.90	-0.1		
B23	4.02	\pm 0.26	3.80	-5.4		
B24	6.76	\pm 0.52	5.96	-11.9*		
B25	2.44	\pm 0.18	2.52	+3.1		
B26	2.16	\pm 0.17	2.25	+4.2		
B27	1.70	\pm 0.12	1.81	+6.5		
B28	1.48	\pm 0.11	1.58	+7.0		
B29	2.06	\pm 0.16	2.18	+5.8		
B30	3.44	\pm 0.24	3.43	-0.3		
B31	3.06	\pm 0.21	3.14	+2.6		
B32	2.78	\pm 0.20	2.91	+4.7		
B33	2.20	\pm 0.14	2.34	+6.5		
B34	1.94	\pm 0.13	2.05	+5.9		

... continued

Table 8.1 continued

Run	t_{exp} (hrs)	\pm err (hrs)	t_{pl} (hrs)	E (%)	t_{fd} (hrs)	E (%)
B35	2.86	\pm 0.21	2.78	-2.8		
B36	4.30	\pm 0.31	4.19	-2.6		
B37	4.02	\pm 0.25	3.81	-5.3		
B38	3.72	\pm 0.24	3.57	-4.2		
B39	3.02	\pm 0.16	2.94	-2.8		
B40	2.52	\pm 0.15	2.59	+2.8		
B41	3.90	\pm 0.28	3.56	-8.8*		
B42	5.70	\pm 0.48	5.20	-8.7*		
B43	4.56	\pm 0.21	4.50	-1.4	4.02	-11.8*
B44	4.08	\pm 0.19	4.07	-0.2		
B45	3.24	\pm 0.14	3.32	+2.4		
B46	2.82	\pm 0.13	2.78	-1.5		
B47	3.56	\pm 0.20	3.39	-4.8		
B48	5.76	\pm 0.34	5.64	-2.1		
B49	2.32	\pm 0.17	2.30	-0.7		
B50	2.04	\pm 0.15	2.05	+0.6		
B51	1.60	\pm 0.11	1.59	-0.6		
B52	1.36	\pm 0.10	1.35	-0.5		
B53	1.66	\pm 0.13	1.63	-1.7		
B54	2.72	\pm 0.22	2.84	+4.3		
B55	6.90	\pm 0.38	6.52	-5.5	6.30	-8.7*
B56	6.04	\pm 0.32	5.64	-6.6*		
B57	4.88	\pm 0.26	4.51	-7.7*		
B58	4.16	\pm 0.27	3.90	-6.2		
B59	4.84	\pm 0.26	4.45	-8.0*		
B60	7.48	\pm 0.48	7.15	-4.4		
B61	3.30	\pm 0.22	3.39	+2.6		
B62	2.68	\pm 0.20	2.84	+6.0		
B63	2.20	\pm 0.13	2.25	+2.5		
B64	1.86	\pm 0.12	1.98	+6.4		
B65	2.38	\pm 0.19	2.51	+5.4		
B66	3.68	\pm 0.34	3.99	+8.4		

... continued

Table 8.1 continued

Run	t_{exp} (hrs)	\pm err (hrs)	t_{pl} (hrs)	E (%)	t_{fd} (hrs)	E (%)
B67	3.46	\pm 0.26	3.20	-7.6		
B68	2.86	\pm 0.23	2.82	-1.3		
B69	2.30	\pm 0.16	2.24	-2.6		
B70	1.88	\pm 0.13	1.98	+5.5		
B71	2.62	\pm 0.24	2.73	+4.1		
B72	4.10	\pm 0.38	4.05	-1.3	4.14	+1.0

Table 8.2

Means and standard deviations of the percentage differences between experimental freezing times, and times calculated from (a) the three-level finite difference scheme, (b) equations 7.19 to 7.27.

	Numerical method		Equations 7.19 to 7.27	
	Mean (%)	Standard deviation (%)	Mean (%)	Standard deviation (%)
Slabs	1.1	4.7	0.0	2.4
Cylinders	-3.8	3.1	-0.5	3.8
Spheres	-4.5	2.5	0.3	3.3
Bricks			-0.3	5.1

Table 8.3Comparison of methods for prediction of food freezing times

Equations 7.19 to 7.27	Finite differences
Calculations can be done by hand	Calculations require a computer
Quick	Time required to program computer and run program. Package programs rarely available
Minimal cost to use	Cost of computation time and program preparation can be considerable, especially for three-dimensional heat transfer
Minimal knowledge of thermal properties required	Need detailed information on variation of thermal properties with temperature. Jumping of the latent heat peak is a problem
Does not give temperature/time fields	Gives temperature/time fields
Only fundamental knowledge of freezing is needed to use it	Unless a package program is available detailed understanding of finite differences and the freezing process are needed to build a program
Easy to see the effect of all process variables - can differentiate the formula with respect to each one	Effect of process variables can only be determined implicitly by rerunning the program

... continued

Table 8.3 continued

Equations 7.19 to 7.27	Finite differences
Range of applicability is	Applicable in all situations
$0.155 \leq Ste \leq 0.345$	although the basic program may
$0 \leq Pk \leq 0.55$	need modification in some
$0.2 \leq Bi \leq 20$ for slabs	cases, for example, "jumping"
$0.5 \leq Bi \leq 5$ for spheres and cylinders	of the latent heat peak is
$0.5 \leq Bi \leq 20$ for bricks	increasingly difficult to
$1 \leq B_1 \leq 4$ for bricks	avoid as the Biot number is
$1 \leq B_2 \leq 4$ for bricks	increased
These conditions should cover most practical food freezing situations	

9 PREDICTION OF FOOD FREEZING TIMES FOR SITUATIONS WITH NON-CONSTANT CONDITIONS

9.1 INTRODUCTION

In practice conditions in food freezers often vary considerably during the freezing process. This limits the use of the simple formulae, whereas the versatile finite difference and finite element programs can take account of these changes, merely at the expense of writing a more complex computer program. However the simple formulae can still be applied with accuracy in some situations and, at worst, by taking the slowest and fastest freezing conditions they can be used to calculate lower and upper bounds on the food freezing time.

9.2 VARYING AMBIENT TEMPERATURE

In order to carry out an experimental investigation into the effect of varying ambient temperature on the freezing time suitable equipment, that will allow the ambient temperature to be controlled to pre-selected profiles, is necessary. It was found to be impossible to achieve this type of control over the ambient temperature with the equipment available.

If the ambient temperature changes with time this is easily programmed into a finite difference program. To use the simple formulae an average temperature must be used. The two most common ways in which the ambient temperature may vary are cycling around the set point, and an exponential fall (or something approximating to this) towards the set point.

To provide an insight into what would happen in practice, freezing times for one-dimensional heat transfer in a slab were calculated by finite differences, using various ambient temperature profiles. These freezing times were compared to the calculated freezing time for a constant,

average value of the ambient temperature. Detailed results can be found in Appendix 6.

Cycling of the ambient temperature around the mean value of up to $+2.5^{\circ}\text{C}$ led to changes of less than 0.6% in the calculated freezing time when compared to the result using a constant ambient temperature. For an exponential fall in temperature of up to 15°C the use of an average temperature led to results that agreed within 1.2% of each other. The variations in ambient temperature considered here should cover most practical problems. It is unlikely that the ambient temperature will drop by more than 15°C in the freezing process.

Although these results have not been verified experimentally the finite difference calculations generally provide accurate simulation of freezing processes, and should therefore give a good estimate of the error involved in using an average ambient temperature. Errors of a similar magnitude would be expected for other shapes.

Therefore even for substantial changes in the ambient temperature use of an average value introduces little additional error. The simple formulae can often be applied without any significant loss of accuracy in these situations.

9.3 NON-UNIFORM INITIAL TEMPERATURE

Rarely in practice is a food material to be frozen at a uniform temperature throughout prior to the freezing process. A non-uniform initial temperature distribution is easily programmed into a finite difference program - each node is assigned a different starting temperature.

To use the simple formulae the initial temperature distribution must be approximated by a mean value. In order to determine the size of the errors introduced by use of this average an investigation was carried out using finite difference simulation of the freezing process. For

variations within the material of up to 10°C on either side of the mean initial temperature the difference in freezing time was less than 0.5%. The full results are given in Appendix 7. Whilst the investigation was limited to slabs, errors of similar magnitude would be expected for other shapes. Finite differences provide a sufficiently accurate simulation of the freezing process for the value of the error found to represent practical situations.

Therefore it is possible to use the simple formulae (equations 7.19 to 7.27) without any appreciable loss of accuracy for non-uniformities in the initial temperature distribution of up to 10°C around the mean value. For a greater non-uniformity in the initial temperature the error will be higher.

9.4 CHANGING SURFACE HEAT TRANSFER COEFFICIENT

In some freezing problems the resistance to the removal of heat from the surface of the freezing material may alter with time. For example, the air velocity in a blast freezer may be changed, or the object could be transferred to an air blast freezer from liquid immersion, or the surface heat transfer coefficient may depend on the surface temperature of the product. All these changes are easily programmed into a finite difference program.

The simple formulae (equations 7.19 to 7.27) in these situations provide bounds on the freezing time. If the slowest and fastest cooling conditions are taken these can be used to provide the upper and lower bounds on the freezing time. Then, with judgement on the part of the design engineer these bounds can be narrowed. For example, a package of food might be frozen in liquid immersion for 20% of the total freezing time and the rest in air blast. Clearly, the freezing time will be much closer to the upper bound (based on 100% air blast freezing) than the lower bound (based on 100% immersion freezing). This process of narrowing the bounds may, in many cases, be sufficiently

accurate for design. If not, it provides a check on the finite difference method.

The second way in which the surface heat transfer coefficient may vary is variation in space. That is, the surface heat transfer coefficient is not the same on all parts of the surface. This is a common problem in air blast freezing. Finite difference programs can be modified to take this into account without significant loss of accuracy.

The simple formulae are best used to establish bounds on the freezing time. These bounds can then be narrowed using judgement. This is difficult to do because the thermal and geometric centres of the material may not coincide. Depending on the situation sufficient accuracy for design purposes may be achieved in this manner, but at worst it provides a guideline for comparison with the numerical solution.

9.5 IRREGULAR GEOMETRY

Often, food materials to be frozen are not in a regular shape such as a slab, cylinder, sphere or rectangular brick. It is sometimes necessary to find the freezing time of an irregularly shaped object, for example a leg of lamb.

Finite elements are the best numerical method to use in this situation because they easily handle irregular geometry (Comini et al 1974c). The accuracy of a finite element solution is very similar to the accuracy of finite differences (Myers 1971, p339) so a freezing time predicted by the finite element method should have similar 95% confidence limits to a freezing time predicted using finite differences.

The simple formulae cannot be applied directly to irregular shapes, but by use of an estimated value of the number of "equivalent heat transfer dimensions" (see section

7.4.1) values of P and R can be calculated for use in equations 7.19 to 7.27. For example, a leg of lamb has a dimensionality somewhere between that of a cylinder ($W=2$) and a sphere ($W=3$). The design engineer must use his judgement to estimate the actual value - a suitable estimate for a leg of lamb would be $W=2.6$. From this P and R are calculated as $P=0.192$ and $R=0.0481$ for use in the simple formulae for radial heat transfer.

If there is uncertainty over what the value of W should be, then it may be safest to establish lower and upper bounds using two limiting values of W .

These methods allow an estimate of the freezing time to be made from the simple formulae. The extra error introduced may be too great in some cases, and finite elements must be used.

9.6 NON-HOMOGENEOUS FOOD MATERIAL

Food materials to be frozen will often not be homogeneous throughout, and hence the thermal properties will be position dependent as well as temperature dependent. This can be taken into account in a finite difference program but the simple formulae cannot be applied directly. By choosing largest and smallest values of the thermal diffusivity for the material the upper and lower bounds on the freezing time can be calculated. These can be narrowed by the judgement of the design engineer, and by the use of average thermal properties for the material. By these means a sufficiently accurate estimate of the freezing time can be obtained in some cases without need of a finite difference program.

9.7 SUMMARY

For freezing problems that do not fit the restrictions on the conditions imposed by the simple formulae a variety of approximations can be made so that equations 7.19 to 7.27

can be used. In some cases the magnitude of the extra errors introduced may be too great for the simple formulae to be used, and either a finite difference or finite element calculation is necessary. Also, several of the factors discussed above may be important in one problem - the complexity caused by the interaction of these factors may lead to unacceptably wide bounds on the freezing time calculated by the simple formulae.

In spite of these limitations, for many practical food freezing problems the simple formulae (equations 7.19 to 7.27) will give a prediction of the freezing time as accurate as that from either the finite difference or finite element method, and still retain the major advantage of simplicity.

The simple formulae also have an important application in the checking of finite difference and finite element programs. For the freezing of biological materials there is no analytical solution against which the accuracy of a numerical program can be checked. Because the simple formulae (equations 7.19 to 7.27) have been found to respond accurately over a wide range of practical conditions they can be used to check the accuracy of a finite difference or finite element program. This might involve checking to ensure that the difference scheme has been programmed correctly, or a check that jumping of the latent heat peak, leading to a low estimate of the freezing time, has not occurred. Once agreement is good the user can be confident that the temperature/time profiles calculated by the finite difference scheme are accurate. The greater reliability of the simple formulae within their range of applicability is therefore important and useful.

10 CONCLUSIONS

Practical food freezing problems normally involve the third kind of boundary condition and initial superheat. In these cases the non-linear boundary conditions, coupled with the release of latent heat over a range of temperature have prevented the derivation of a general analytical solution. By the use of various simplifying assumptions a number of approximate solutions have been derived, the accuracy of each depending on the assumptions necessary for the derivation of the solution.

For one-dimensional heat transfer in finite slabs the best numerical solution was found to be a three-level finite difference scheme which predicted the freezing time within -8% to +11% of the experimentally determined freezing time with 95% confidence. No approximate analytical solutions or empirical relationships found in the literature predicted the freezing time accurately for slabs. A simple formula, based on that of Plank but with some new modifications to the geometric factors, was found to predict the freezing time to within +4.8% of the experimental value with 95% confidence.

For radial heat transfer in cylinders and spheres a three-level finite difference scheme has been found to be the most accurate numerical solution (-10% to +2% with 95% confidence). None of the existing approximate analytical solutions or empirical relationships gave accurate prediction of the freezing time for these shapes but, in contrast, times predicted by the proposed modification to the geometric factors in Plank's equation are within -8% to +7% of the experimental values with 95% confidence.

Three-dimensional heat transfer in rectangular bricks can be accurately simulated by a three-level finite difference scheme. Existing approximate analytical solutions and empirical relationships based on the geometric factors proposed by Plank are unreliable because the assumptions

in the derivation of these factors are not valid. Incorporating the proposed modification to these factors, Plank's equation predicted the freezing time of rectangular bricks to within $\pm 10\%$ with 95% confidence.

Over the extensive range of experimental conditions, the proposed simple formulae and the three-level finite difference schemes predict the freezing time with similar accuracy. The simple formulae (equations 7.19 to 7.27) have a clear advantage over the finite difference schemes in that they do not require a computer for solution.

For practical problems with changing conditions the finite difference schemes can be applied directly without loss of accuracy. In many of these cases, by use of suitable approximations, the simple formulae will accurately predict the freezing time.

No method will give accurate prediction of freezing time unless accurate data are used. Uncertainties in data, especially the surface heat transfer coefficient, will be much greater than the errors in the two calculation methods in many situations encountered in practice.

NOMENCLATURE

- a - constant for radial geometry
 a_f - amplitude of changing ambient temperature ($^{\circ}\text{C}$)
 A - surface area (m^2)
 Bi - Biot number
 B_1 - ratio of brick dimensions
 B_2 - ratio of brick dimensions
 c_f - length of cycle or time constant in Appendix 6
 $C(T)$ - volumetric specific heat capacity ($\text{J}/\text{m}^3^{\circ}\text{C}$)
 C_1 - volumetric specific heat capacity of unfrozen phase ($\text{J}/\text{m}^3^{\circ}\text{C}$)
 C_s - volumetric specific heat capacity of frozen phase ($\text{J}/\text{m}^3^{\circ}\text{C}$)
 D - thickness or diameter (m)
 D_x - thickness in x direction (m)
 D_y - thickness in y direction (m)
 D_z - thickness in z direction (m)
 err - experimental error bounds (hrs)
 E - difference between calculated and experimental freezing times (%)
 f - arbitrary function
 Fo - Fourier number
 h - surface heat transfer coefficient ($\text{W}/\text{m}^2^{\circ}\text{C}$)
 H - enthalpy (J/m^3)
 ΔH - enthalpy change during freezing (J/m^3)
 i - denotes time level in finite difference schemes
 j - denotes position of a node in y direction in finite difference schemes
 J - denotes number of nodes in y direction in finite difference schemes
 k - denotes position of a node in z direction in finite difference scheme
 $k(T)$ - thermal conductivity ($\text{W}/\text{m}^{\circ}\text{C}$)
 k_{ave} - average thermal conductivity of solidifying phase ($\text{W}/\text{m}^{\circ}\text{C}$)
 k_s - thermal conductivity of frozen phase ($\text{W}/\text{m}^{\circ}\text{C}$)
 K - denotes number of nodes in z direction in finite difference schemes

- L - latent heat (J/m^3)
- m - denotes position of a node in x direction or r direction in finite difference schemes
- m - parameter used in the calculation of geometric factors for Plank's equation
- M - denotes the number of nodes in the x or r directions in finite difference schemes
- M - modulus in equation 4.1
- n - parameter used in the calculation of geometric factors for Plank's equation
- P - geometric factor in Plank's equation
- Pk - Plank number
- P₁ - modified geometric factor in Plank's equation
- P₂ - modified geometric factor in Plank's equation
- Q - surface heat flux (W/m^2)
- Q - parameter used in the calculation of geometric factors for Plank's equation
- r - distance from the centre of the region in radial heat transfer cases (m)
- Δr - space increment in r direction in finite difference schemes (m)
- R - radius (m)
- R - geometric factor in Plank's equation
- R₁ - modified geometric factor in Plank's equation
- R₂ - modified geometric factor in Plank's equation
- Ste - Stefan number
- t - time (s)
- Δt - time step (s)
- t_{el} - elapsed time in finite difference calculations (hrs)
- t_{exp} - experimental freezing time (hrs)
- t_{fd} - freezing time predicted by finite differences (hrs)
- t_{neum} - freezing time predicted by Neumann's method (hrs)
- t_{pl} - freezing time predicted by the proposed modification to Plank's equation (hrs)
- T - temperature ($^{\circ}C$)
- T_a - ambient temperature ($^{\circ}C$)
- T_{ave} - average ambient temperature ($^{\circ}C$)
- T_c - centre temperature ($^{\circ}C$)
- T_f - initial freezing temperature ($^{\circ}C$)

- T_i - initial temperature ($^{\circ}\text{C}$)
- T_s - surface temperature ($^{\circ}\text{C}$)
- T^* - intermediate temperature in finite difference calculations ($^{\circ}\text{C}$)
- T^{**} - intermediate temperature in finite difference calculations ($^{\circ}\text{C}$)
- W - number of equivalent heat transfer dimensions
- W_1 - number of equivalent heat transfer dimensions found from P in Plank's equation
- W_2 - number of equivalent heat transfer dimensions found from R in Plank's equation
- x - distance in the x direction from the surface (m)
- Δx - space increment in the x direction in finite difference schemes (m)
- y - distance in the y direction from the surface (m)
- Δy - space increment in the y direction in finite difference schemes
- Y - fractional unaccomplished temperature change
 $(T - T_a) / (T_i - T_a)$
- z - distance in the z direction from the surface (m)
- Δz - space increment in the z direction in finite difference schemes (m)
- α - thermal diffusivity (m^2/s)
- ϵ - coefficient used in Appendix 1

REFERENCES

- Albasiny, E.L. (1956) The solution of non-linear heat conduction problems on the Pilot Ace. Proc. Inst. Electric Engng 103: Part B, Supplement 1, 158
- Albasiny, E.L. (1960) On the numerical solution of a cylindrical heat conduction problem. Quart. J. Mech. Applied Maths 13: 374
- Allada, S.R. & Quan, D. (1966) A stable explicit numerical solution of the heat conduction equation for multi-dimensional nonhomogeneous media. Chem. Engng Prog. Symp. Ser. 62(64): 151
- Badari Narayana, K. & Krishna Murthy, M.V. (1975) Thermal properties of a model food gel. Ind. J. Technol. 13: 415
- Baerdemaeker, J.De., Singh, R.P. & Segerlind, L.J. (1977) Modelling heat transfer in foods using the finite element method. J. Food Process Engng 1: 37
- Bailey, C., James, S.J., Kitchell, A.G. & Hudson, W.R. (1974) Air-, water-, and vacuum-thawing of frozen pork legs. J. Sci. Food Agric. 25: 81
- Bakal, A. & Hayakawa, K. (1973) Heat transfer during freezing and thawing of food. Adv. Food Res. 20: 217
- Bankoff, S.G. (1964) Heat conduction or diffusion with change of phase. Adv. Chem. Engng 5: 75
- Baxter, D.C. (1962) The fusion times of slabs and cylinders. J. Heat Transfer 84C: 317
- Biot, M.A. (1957) New methods in heat flow analysis with application to flight structures. J. Aeronaut. Sci. 24: 857

- Boley, B.A. (1963) Upper and lower bounds for the solution of a melting problem. *Quart. App. Maths* 21: 1
- Bonacina, C. & Comini, G. (1971) On a numerical method for the solution of the unsteady state heat conduction equation with temperature dependent parameters. *Proc. 13th Int. Congr. Refrig.* 2: 329
- Bonacina, C. & Comini, G. (1973) On the solution of the non-linear heat conduction equations by numerical methods. *Int. J. Heat Mass Transfer* 16: 581
- Brian, P.L.T. (1961) A finite difference method of high order accuracy for the solution of three-dimensional heat conduction problems. *A.I.Ch.E.J.* 7: 367
- Budhia, H. & Kreith, F. (1973) Heat transfer with melting or freezing in a wedge. *Int. J. Heat Mass Transfer* 16: 195
- Carslaw, H.S. & Jaeger, J.C. (1959) Conduction of Heat in Solids, 2nd Ed., Clarendon Press, Oxford.
- Charm, S.E. (1971) Fundamentals of Food Engineering, 2nd Ed., Avi, Westport.
- Charm, S.E., Brand, D.H. & Baker, D.W. (1972) A simple method for estimating freezing and thawing times of cylinders and slabs. *ASHRAE J.* 14: 39
- Chattopadhyay, P., Raychaudhuri, B.C. & Bose, A.N. (1975) Prediction of temperature of iced fish. *J. Food Sci.* 40: 1080
- Cho, S.H. & Sunderland, J.E. (1969) Heat conduction problems with melting or freezing. *J. Heat Transfer* 91C: 421
- Cho, S.H. & Sunderland, J.E. (1970) Phase change of spherical bodies. *Int J. Heat Mass Transfer* 13: 1231

- Cho, S.H. & Sunderland, J.E. (1974) Phase change problems with temperature dependent thermal conductivity. J. Heat Transfer 96C: 214
- Chung, B.T.F. & Yeh, L.T. (1975) Solidification and melting of materials subject to convection and radiation. J. Spacecraft 12: 329
- Chung, B.T.F. & Yeh, L.T. (1976) Freezing and melting of materials with variable thermal properties and arbitrary heat fluxes. AIAA J. 14: 388
- Cleland, A.C. & Earle, R.L. (1976a) A new method for prediction of surface heat transfer coefficients in freezing. Bull. I.I.R., Annexe-1, 361
- Cleland, A.C. & Earle, R.L. (1976b) A comparison of freezing calculations including modification to take into account initial superheat. Bull. I.I.R., Annexe-1, 369
- Cleland, A.C. & Earle, R.L. (1977a) A comparison of analytical and numerical methods for predicting the freezing times of foods. J. Food Sci. 42: 1390
- Cleland, A.C. & Earle, R.L. (1977b) The third kind of boundary condition in numerical freezing calculations. Int. J. Heat Mass Transfer 20: 1029
- Cochran, D.L. (1955) Rate of solidification. Refrig. Engng 63(8): 49
- Comini, G. & Bonacina, C. (1974a) Application of computer codes to phase-change problems in food engineering. Bull. I.I.R., Annexe-3, 15
- Comini, G., Bonacina, C. & Barina, S. (1974b) Thermal properties of foodstuffs. Bull. I.I.R., Annexe-3, 163

- Comini,G., del Guidice,S., Lewis,R.W. & Zienkiewicz,O.C.
(1974c) Finite element solution of non-linear heat
conduction problems with special reference to phase
change. Int. J. Numerical Methods Engng 8: 613
- Comini,G. (1976) Personal communication
- Cordell,J.M. & Webb,D.C. (1972) The freezing of ice cream.
Proc. Int. Symp. Heat Mass Transfer Problems Food
Engng, Part 2, D3.1
- Cowell,N.D. (1967) The calculation of food freezing times.
Proc. 12th Int. Congr. Refrig. 2: 667
- Crank,J. & Nicolson,P. (1947) A practical method for numer-
ical integration of solutions of partial differential
equations of heat conduction type. Proc. Cam. Phil.
Soc. 43: 50
- Cullwick,T.D.C. (1967) Freezing rate studies in blocks of
meat of simple shape. Thesis, M. Tech., Massey
University
- Danckwerts,P.V. (1950) Unsteady-state diffusion or heat con-
duction with a moving boundary. Trans Faraday Soc.
46: 701
- Dusinberre,G.M. (1945) Numerical methods for transient heat
flow. Trans. A.S.M.E. 67: 703
- Earle,R.L. & Earl,W.B. (1966) Freezing rate studies in
blocks of meat of simple shape. Proc. 3rd Int. Heat
Transfer Congr. 4: 152
- Ede,A.J. (1949) The calculation of freezing and thawing of
foodstuffs. Modern Refrig. 52: 52
- Ehrlich,L.W. (1958) A numerical method of solving a heat flow
problem with a moving boundary. Assoc. Comp. Mach. J.
5: 161

- Eyres, N.R., Hartree, D.R., Ingham, J., Jackson, R., Sarjant, R.J. & Wagstaff, J.B. (1946) The calculation of variable heat flow in solids. Trans. Roy. Soc. Lond. A240: 1
- Fleming, A.K. (1971a) The numerical calculation of freezing processes. Proc. 13th Int. Congr. Refrig. 2: 303
- Fleming, A.K. (1971b) The numerical calculation of freezing processes. Thesis, Technical Licentiate Degree, The Technical University of Norway, Trondheim.
- Geuze, C.A., Betten, A. & Touber, S. (1972) Non-steady heat transfer in a freezing model substance. Bull. I.I.R., Annexe-1, 211
- Goodling, J.S. & Khader, M.S. (1974) Inward solidification with radiation-convection boundary condition. J. Heat Transfer 96C: 114
- Goodman, T.R. (1958) The heat balance integral and its application to problems involving a change of phase. Trans. A.S.M.E. 80: 335
- Goodman, T.R. & Shea, J.J. (1960) The melting of finite slabs. J. App. Mech. 27E: 16
- Goodman, T.R. (1964) Application of integral methods to transient non-linear heat transfer. Adv. Heat Transfer 1: 51
- Hamill, T.D. & Bankoff, S.G. (1963) Maximum and minimum bounds on freezing-melting rates with time-dependent boundary conditions. A.I.Ch.E.J. 9: 741
- Hamill, T.D. & Bankoff, S.G. (1964) Similarity solutions of the plane melting problem with temperature-dependent thermal properties. Ind. Eng. Chem. (Fund.) 3: 177

- Hashemi, H.T. & Sliepcevich, C.M. (1967a) A diffusion-analogue method for solving problems of heat conduction with change of phase. Chem. Engng Prog. Symp. Ser. 63(79): 42
- Hashemi, H.T. & Sliepcevich, C.M. (1967b) A numerical method for solving two-dimensional problems of heat conduction with change of phase. Chem. Engng Prog. Symp. Ser. 63(79): 34
- Hills, A.W.D. (1969) A generalised integral-profile method for the analysis of unidirectional heat flow during solidification. Trans Met. Soc. A.I.M.E. 245: 1471
- Hills, A.W.D. & Moore, M.R. (1969) Use of integral-profile methods to treat heat transfer during solidification. p141-171; In Institute Min. Met.. Heat and Mass Transfer in Process Metallurgy. London.
- Hirai, E. & Komori, T. (1971) A proposal to solve Neumann's problem approximately, taking account of bulk dilatation by phase change - a semi-infinite solid. J. Chem. Engng Jap. 4: 96
- Hrycak, P. (1963) Problem of solidification with Newton's cooling at the surface. A.I.Ch.E.J. 9: 585
- Hrycak, P. (1967) Heat conduction with solidification in a stratified medium. A.I.Ch.E.J. 13: 160
- Huang, C-L & Shih, Y-P (1975a) Perturbation solutions of planar diffusion-controlled moving-boundary problems. Int. J. Heat Mass Transfer 18: 689
- Huang, C-L & Shih, Y-P (1975b) Perturbation solution for planar solidification of a saturated liquid with convection at the wall. Int J. Heat Mass Transfer 18: 1481

International Institute of Refrigeration (1972) Recommendations for the Processing and Handling of Frozen Foods 2nd Ed., Paris.

Imber, M. & Huang, P.N.S. (1973) Phase change in a semi-infinite solid with temperature dependent thermal properties. *Int. J. Heat Mass Transfer* 16: 1951

Jackson, F. (1964) The solution of problems involving the melting and freezing of finite slabs by a method due to Portnov. *Proc. Edinburgh Maths Soc.* 14: 109

James, S.J., Bailey, C. & Ono, S. (1976) Determination of freezing and thawing times in the centre of blocks of meat by measurement of surface temperature. *J. Food Technol.* 11: 505

Jiji, L.M., Rathjen, K.A. & Drzewiecki, T. (1970) Two-dimensional solidification in a corner. *Int. J. Heat Mass Transfer* 13: 215

Joshi, C. & Tao, L.C. (1974) A numerical method for simulating the axisymmetrical freezing of food systems. *J. Food Sci.* 39: 623

Kern, J. (1977) A simple and apparently safe solution to the generalised Stefan problem. *Int. J. Heat Mass Transfer* 20: 467

Khatchaturov, A.B. (1958) Thermal processes during air blast freezing of fish. *Bull. I.I.R., Annexe-2*, 365

Komori, T. & Hirai, E. (1970) An application of Stefan's problem to the freezing of a cylindrical foodstuff. *J. Chem. Engng Jap.* 3: 39

Komori, T. & Hirai, E. (1972) Solutions of heat conduction problem with change of phase - a slab. *J. Chem. Engng Jap.* 5: 242

- Kreith, F. & Romie, F.E. (1955) A study of the thermal diffusion equation with boundary conditions corresponding to solidification or melting of materials initially at the fusion temperature. Proc. Phys. Soc. Lond. B68: 277
- Langford, D. (1966) The freezing of spheres. Int. J. Heat Mass Transfer 9: 827
- Lappadula, C. & Mueller, W.K. (1966) Heat conduction with solidification and a convection boundary condition at the freezing front. Int. J. Heat Mass Transfer 9: 702
- Lardner, T.J. & Pohle, F.V. (1961) Applications of the heat balance integral to problems of cylindrical geometry. J. App. Mech. 28E: 310
- Lazaridus, A. (1970) A numerical solution of the multidimensional solidification (or melting) problem. Int. J. Heat Mass Transfer 13: 1459
- Lees, M. (1966) A linear three level difference scheme for quasi-linear parabolic equations. Maths Comput. 20: 516
- Lentz, C.P. (1961) Thermal conductivity of meats, fats, gelatin gels and ice. Food Technol. 15: 243
- Lock, G.H.S., Gunderson, J.R., Quan, D. & Donnelly, J.K. (1969) A study of one-dimensional ice formation with particular reference to periodic growth and decay. Int. J. Heat Mass Transfer 12: 1343
- Lockwood, F.C. (1966) Simple numerical procedure for the digital computer solution of non-linear transient heat conduction with change of phase. J. Mech. Eng. Sci. 8: 259
- London, A.L. & Seban, R.A. (1943) Rates of ice formation. Trans A.S.M.E. 65: 771

- Longwell, P.A. (1958) A graphical method for solution of freezing problems. *A.I.Ch.E.J.* 4: 53
- McAdams, W.H. (1954) Heat Transmission, 3rd Ed., McGraw Hill, Tokyo.
- Mawson, R.F. (1969) A study on ice crystals in frozen meat. Thesis, M. Tech., Massey University.
- Mellor, J.D. (1976) Personal communication
- Morley, M.J. (1972) Thermal properties of meat : tabulated data. Meat Research Institute, Agricultural Research Council, Langford, Bristol. Special Report No. 1
- Morrison, M.E. (1970) Numerical evaluation of temperature profiles and interface position in filaments undergoing solidification. *A.I.Ch.E.J.* 16: 57
- Mott, L.F. (1964) The prediction of product freezing time. *Aust. Refrig., Air Cond. Heat* 18: 16
- Muehlbauer, J.C. & Sunderland, J.E. (1965) Heat conduction with freezing or melting. *App. Mech. Rev.* 18: 951
- Muehlbauer, J.C., Hatcher, J.D., Lyons, D.W. & Sunderland, J.E. (1973) Transient heat transfer analysis of alloy solidification. *J. Heat Transfer* 95C: 324
- Murray, W.D. & Landis, F. (1959) Numerical and machine solutions of transient heat conduction problems involving melting or freezing. *J. Heat Transfer* 81C: 106
- Myers, G.E. (1971) Analytical Methods in Conduction Heat Transfer. McGraw Hill, New York.
- Nagaoka, J., Takaji, S. & Hohani, S. (1955) Experiments on the freezing of fish in an air blast freezer. *Proc. 9th Int. Congr. Refrig.* 4: 105

- Newman, A.B. (1936) Heating and cooling rectangular and cylindrical solid. *Ind. Engng Chem.* 28: 545
- Padmanabhan, T.V. & Subba Raju, K. (1975) Numerical solution for heat conduction problem with freezing. *Ind. J. Technol.* 13: 477
- Patel, P.D. & Boley, B.A. (1969) Solidification problems with space and time varying thermal properties and imperfect mold contact. *Int. J. Engng Sci.* 7: 1041
- Pedroso, R.I. & Domoto, G.A. (1973a) Technical note on planar solidification with fixed wall temperature and variable thermal properties. *J. Heat Transfer* 95C: 553
- Pedroso, R.I. & Domoto, G.A. (1973b) Exact solution by perturbation method for planar solidification of a saturated liquid with convection at the wall. *Int. J. Heat Mass Transfer* 16: 1816
- Pedroso, R.I. & Domoto, G.A. (1973c) Perturbation solution for spherical solidification of saturated liquids. *J. Heat Transfer* 95C: 42
- Pedroso, R.I. & Domoto, G.A. (1973d) Inward spherical solidification by the method of strained co-ordinates. *Int. J. Heat Mass Transfer* 16: 1037
- Pekeris, C.L. & Slichter, L.B. (1939) Problem of ice formation. *J. App. Phys.* 10: 135
- Plank, R. (1941) Beitrag zur berechnung und bewertung der gefriereschwindigkeit von lebensmitteln. *Z. ges Kalteind* 10: Beih Reihe 3; 1
- Poots, G. (1962a) On application of integral methods to the solution of problems involving solidification of liquids initially at the fusion temperature. *Int. J. Heat Mass Transfer* 5: 525

- Poots, G. (1962b) An approximate treatment of a heat conduction problem involving a two dimensional solidification front. *Int J. Heat Mass Transfer* 5: 339
- Rathjen, K.A. & Jiji, L.M. (1971) Heat conduction with melting or freezing in a corner. *J. Heat Transfer* 93C: 101
- Riedel, L. (1957) Kalorimetrische untersuchungen uber das gefrieren von fleish. *Kaltetechnik* 9(2): 38
- Riedel, L. (1960a) Eine prufsubstanz fur gefrierversuche. *Kaltetechnik* 12: 222
- Riedel, L. (1960b) DKV Arbeitsblatt 8-19. *Kaltetechnik* 12
- Riley, D.S., Smith, F.T. & Poots, G. (1974) The inward solidification of spheres and circular cylinders. *Int. J. Heat Mass Transfer* 17: 1507
- Riley, D.S. & Duck, P.W. (1977a) Application of the heat balance integral method to freezing of a cuboid. *Int. J. Heat Mass Transfer* 20: 294
- Riley, D.S. & Duck, P.W. (1977b) An extension of existing solidification results obtained from the heat balance integral method. *Int. J. Heat Mass Transfer* 20: 297
- Rolfe, E.J. (1967) The chilling and freezing of foodstuffs. p137-208. In Blakebrough, N. ed., Biochemical and Biological Engineering Science. Academic, London.
- Rutov, D.G. (1936) Thermal processes involved in the freezing of perishable foodstuffs. *Proc. 7th Int. Congr. Refrig.* : 211
- Savino, J.M. & Siegel, R. (1969) An analytical solution for solidification of a moving warm liquid onto an isothermal cold wall. *Int. J. Heat Mass Transfer* 12: 803

- Seider, W.D. & Churchill, S.W. (1965) The effect of insulation on freezing front motion. Chem. Engng Prog. Symp. Ser. 61(59): 179
- Selim, M.S. & Seagrave, R.C. (1973a) Solution of moving boundary transport problems in finite media by integral transforms. I. Problems with a plane moving boundary. Ind. Engng Chem. (Fund.) 12: 1
- Selim, M.S. & Seagrave, R.C. (1973b) Solution of moving boundary transport problems in finite media by integral transforms. II. problems with a cylindrical or spherical moving boundary. Ind. Engng Chem. (Fund.) 12: 9
- Shamsundar, N. & Sparrow, E.M. (1975) Analysis of multidimensional phase change via the enthalpy model. J. Heat Transfer 97C: 333
- Shamsundar, N. & Sparrow, E.M. (1976) Effect of density change on multidimensional conduction phase change. J. Heat Transfer 98C: 550
- Shih, Y-P & Chou, T-C (1971) Analytical solution for freezing a saturated liquid inside or outside spheres. Chem. Engng Sci. 26: 1787
- Shih, Y-P & Tsay, S-Y (1971) Analytical solutions for freezing a saturated liquid inside or outside cylinders. Chem. Engng Sci. 26: 809
- Siegel, R. & Savino, J.M. (1966) An analysis of the transient solidification of a flowing warm liquid on a convectively cooled wall. Proc 3rd Int. Heat Transfer Conf. 4: 141
- Tanaka, K. & Nishimoto, J. (1959) Determination of time required for freezing of skip-jack. J. Tokyo Univ. Fisheries 45: 205

- Tanaka, K. & Nishimoto, J. (1964) Determination of the time required for contact freezing of whalemeat. J. Tokyo Univ. Fisheries 50: 49
- Tao, L.C. (1967) Generalised numerical solutions of freezing a saturated liquid in cylinders and spheres. A.I.Ch. E.J. 13: 165
- Tao, L.C. (1968) Generalised solution for freezing a saturated liquid in a convex container. A.I.Ch.E.J. 14: 720
- Tao, L.C. (1975) Effect of linear approximation of enthalpy-temperature curve in simulating heat transfer during freezing. J. Food Sci. 40: 1099
- Theofanous, T.G. & Lim, H.C. (1971) An approximate analytical solution for non-planar moving boundary problems. Chem. Engng Sci. 26: 1297
- Tien, R.H. & Geiger, G.E. (1967) A heat transfer analysis of the solidification of a binary eutectic system. J. Heat Transfer 89C: 230
- Tien, R.H. & Geiger, G.E. (1968) The unidimensional solidification of a binary eutectic system with time dependent surface temperature. J. Heat Transfer 90C: 27
- Tien, R.H. & Koump, V. (1968) Unidimensional solidification of a slab - variable surface temperature. Trans A.I. M.E. 242: 283
- Westphal, K.O. (1967) Series solution of a freezing problem with the fixed surface radiating into a medium of arbitrary varying temperature. Int. J. Heat Mass Transfer 10: 195

APPENDIX 1GENERAL DESCRIPTION OF FINITE DIFFERENCE PROGRAMSA1.1 INTRODUCTION

This Appendix describes the five computer programs used for calculation of freezing times by the three-level finite difference schemes. The program listings can be found in Appendices 2 to 4 as follows :

- Appendix 2 - SLAB1 and SLAB2; programs for one-dimensional heat transfer in slabs.
 Appendix 3 - ROD and BRICK; programs for two- and three-dimensional heat transfer in rectangular bricks.
 Appendix 4 - RADIAL; program for radial heat transfer in spheres and cylinders.

A1.1.1 One-Dimensional Heat Transfer in Slabs

The general equation of heat conduction is

$$C(T) \frac{\partial T}{\partial t} = \frac{\partial}{\partial x} \left(k(T) \frac{\partial T}{\partial x} \right) \quad \text{in the region } 0 \leq x \leq D \quad (\text{A1.1})$$

Both constant and non-constant initial conditions are allowed in SLAB1, but SLAB2 can only handle problems with a uniform initial temperature.

In SLAB1 six types of boundary condition can be handled, and the boundary conditions at $x=0$ and $x=D$ may be different. In general, at the boundary $x=b$, the boundary conditions are :

$$\text{Type 1} \quad T_{x=b} = T_a \quad (\text{A1.2})$$

$$\text{Type 2} \quad \left(k(T) \frac{\partial T}{\partial x} \right)_{x=b} = Q \quad (\text{A1.3})$$

$$\text{Type 3} \quad \left(k(T) \frac{\partial T}{\partial x} \right)_{x=b} = h(T_{x=b} - T_a) \quad (\text{A1.4})$$

$$\text{Type 4} \quad T_{x=b} = f(t) \quad (\text{A1.5})$$

$$\text{Type 5} \quad (k(T) \frac{\partial T}{\partial x})_{x=b} = \epsilon ((T_{x=b} + 273)^4 - (T_a + 273)^4) \quad (\text{A1.6})$$

$$\text{Type 6} \quad (k(T) \frac{\partial T}{\partial x})_{x=b} = h(t) (T_{x=b} - T_a(t)) \quad (\text{A1.7})$$

SLAB2 is a specialised program for problems with the third kind of boundary condition only. It incorporates the modification suggested by Comini (1976) to reduce "jumping" of the latent heat peak (see equation 6.9). SLAB1 does not use this modification.

A1.1.2 Two-Dimensional Heat Transfer in Bricks

The general equation of heat conduction is

$$C(T) \frac{\partial T}{\partial t} = \frac{\partial}{\partial x} (k(T) \frac{\partial T}{\partial x}) + \frac{\partial}{\partial y} (k(T) \frac{\partial T}{\partial y}) \quad \text{in the region}$$

$$\begin{aligned} 0 \leq x \leq D_x \\ 0 \leq y \leq D_y \end{aligned} \quad (\text{A1.8})$$

Both uniform and non-uniform initial temperature distributions can be handled. Three types of boundary condition are allowed; the first, third and fourth kinds. As these are symmetrical only a quarter segment of the full region is calculated.

A1.1.3 Three-Dimensional Heat Transfer in Bricks

The general equation of heat conduction is

$$C(T) \frac{\partial T}{\partial t} = \frac{\partial}{\partial x} (k(T) \frac{\partial T}{\partial x}) + \frac{\partial}{\partial y} (k(T) \frac{\partial T}{\partial y}) + \frac{\partial}{\partial z} (k(T) \frac{\partial T}{\partial z})$$

$$\text{in the region} \quad \begin{aligned} 0 \leq x \leq D_x \\ 0 \leq y \leq D_y \\ 0 \leq z \leq D_z \end{aligned} \quad (\text{A1.9})$$

The first, third and fourth kinds of boundary condition can be handled. Because these boundary conditions

are symmetrical only an octant is calculated. Either a uniform initial temperature or a non-uniform initial temperature distribution can be used.

A1.1.4 Radial Heat Transfer in Cylinders and Spheres

The general equation of heat conduction is

$$C(T) \frac{\partial T}{\partial t} = \frac{\partial}{\partial r} (k(T) \frac{\partial T}{\partial r}) + \frac{a}{r} k(T) \frac{\partial T}{\partial r} \quad \text{in the region} \\ 0 \leq r \leq R \quad (\text{A1.10})$$

Uniform and non-uniform initial temperature distributions are allowed. At the boundary $r=R$ four types of boundary condition are allowed; types 1,3,4 and 6 as defined in section A1.1.1. At $r=0$ the boundary condition is

$$\frac{\partial T}{\partial r} = 0 \quad (\text{A1.11})$$

A1.2 INFORMATION REQUIRED TO USE THE PROGRAMS

All programs are written in the FORTRAN IV computing language. The following features are common to all programs.

A1.2.1 Data for $C(T)$ and $k(T)$

Data must be supplied to all programs specifying the relationship between the apparent specific heat capacity and temperature, and thermal conductivity and temperature. In the case of SLAB2 enthalpy data as a function of temperature must also be supplied.

Up to 50 pairs (that is, a value of T associated with a value of either $C(T)$ or $k(T)$) can be used to define each of these functions. Values must be supplied in ascending order of T . The range for which $C(T)$ and $k(T)$ are specified must include all values of T that will occur in the calculation. Linear interpolation is used to link the input pairs into a continuous relationship.

A1.2.2 The Space Region

For SLAB1, SLAB2 and RADIAL the space region is one-dimensional. The number of space increments is one less than the number of nodes needed to define values of T at each division. Up to 50 nodes may be used in each case, but normally 11 nodes in RADIAL and SLAB2, and 21 nodes in SLAB1 give sufficient accuracy.

Up to 50 nodes in ROD and 20 in BRICK are allowed in each direction. Because of the symmetry boundary condition it is unlikely that more than 11 nodes are required in the part of the region considered.

A1.2.3 Initial Temperature Distribution

If the initial temperature is the same throughout the body only a single value need be supplied. Otherwise the temperature at every node at times 0 and $0-\Delta t$ must be read into the program.

A1.2.4 Time Step

To obtain sufficient accuracy without excessive computation time the time step should be adjusted so that 600 to 3000 are necessary. If $k(T)$ and $C(T)$ change rapidly with temperature a larger number may be required.

A1.3 USE OF THE PROGRAMS

Data is entered in free format, values being separated by commas. Each section of the new input must start on a new card or line.

A1.3.1 SLAB1

Section 1 The following must be supplied in the order listed, separated by commas.

(a) an index to indicate whether more input data for

- another run follows. A negative index indicates no more runs, whereas a positive index indicates more data follows.
- (b) run number. Any positive integer less than 99.
 - (c) the number of input pairs defining $C(T)$. A maximum of fifty are allowed.
 - (d) the number of input pairs defining $k(T)$. A maximum of fifty are allowed.
 - (e) the number of nodal points. A maximum of fifty are allowed. The number must be odd if symmetry around the centre line is required.
 - (f) the type of boundary condition at $x=0$. An unsigned integer between 1 and 6.
 - (g) the type of boundary condition at $x=D$. An unsigned integer between 1 and 6.
 - (h) the type of initial condition. an input of 1 indicates a constant initial condition; an input of 2 a non-uniform initial temperature distribution.
 - (i) the size of the space region D .
 - (j) the time step.
 - (k) the frequency of printout. Output will be provided at intervals of this number of time steps.
 - (l) the stopping value. The program stops when the temperature at $x=\frac{1}{2}D$ reaches a settable value. This value must be supplied.
 - (m) the way in which the temperature at $x=\frac{1}{2}D$ approaches the stopping value must be specified. An input of 1 indicates approach from above, whereas an input of -1 indicates approach from below.

Section 2 The initial condition. This depends on the input in section 1(h).

- (a) a single value if 1(h) input was 1
- (b) if 1(h) input was 2 two sets of initial temperatures must be supplied. Each set has the number of values specified in section 1(e). The first set of values are for $t=0$, and the second set for $t=0-\Delta t$. The values are assigned to the nodes starting at $x=0$ and moving towards $x=D$.

Section 3 The boundary condition at $x=0$. A number between

1 and 6 was specified in section 1(f). The input here depends on this number.

1 - only the ambient temperature T_a is required.

2 - the heat flux

3 - the surface heat transfer coefficient and ambient temperature.

4 - values of $f(t)$ must be provided at different values of time. A maximum of 50 pairs are allowed. These must be read in increasing order of t , and are linked by linear interpolation. Preceding these values is an integer on a card or line by itself which defines the number of input pairs.

5 - the coefficient ϵ and the ambient temperature must be supplied.

6 - values of $h(t)$ and $T_a(t)$ must be supplied in ascending order of time. All $h(t)$ values precede the input for $T_a(t)$. The first card must contain only two integers, both less than 51. The first of these defines the number of input pairs for $h(t)$, and the second defines the number for $T_a(t)$.

Section 4 The boundary condition at $x=D$. For each type of boundary condition the inputs are analogous to Section 3.

Section 5 Values of $C(T)$ are read in pairs with the corresponding T value first on the line. These values must be sorted in ascending order of T .

Section 6 Values of $k(T)$ are read in pairs with the associated value of T first on the line. These pairs must be in ascending order of T .

If more than one calculation of freezing time is to be performed all 6 sections must be specified for each run.

A1.3.2 SLAB2

The data input for this program is described on

"Comment" cards in the program listing.

A1.3.3 ROD

Section 1 The following must be supplied in the order given.

- (a) an index as for SLAB1.
- (b) a run number as for SLAB1.
- (c) the number of input pairs defining $C(T)$.
- (d) the number of input pairs defining $k(T)$.
- (e) the number of nodal points in the x direction.
- (f) the number of nodal points in the y direction.
- (g) the type of boundary condition.
- (h) the initial condition as for SLAB1.
- (i) the size of the space region in the x direction D_x .
- (j) the size of the space region in the y direction D_y .
- (k) the time step.
- (l) the frequency of printout.
- (m) the stopping value at the centre of the two dimensional region.
- (n) the approach parameter as for SLAB1.

Section 2 The initial condition.

- (a) a single value if the input in 1(h) was 1.
- (b) values for all the nodes at times 0 and $0-\Delta t$.

Section 3 The values of $C(T)$ and T are read in as for SLAB1.

Section 4 The values of $k(T)$ and T are read in as for SLAB1.

Section 5 The boundary condition. The input is organised in the same way as for SLAB1.

For multiple calculations of freezing time all sections must be repeated.

A1.3.4 BRICK

This program requires very large amounts of computation time and is therefore limited to one freezing time

calculation at a time.

Section 1 The functions $C(T)$ and $k(T)$ are read in as follows:

- (a) a card with two integers defining the number of input pairs for $k(T)$ and $C(T)$.
- (b) the values of T and $C(T)$ as for SLAB1.
- (c) the values of T and $k(T)$ as for SLAB1.

Section 2 The following must be read in the order given.

- (a) the thickness in the x direction D_x .
- (b) the thickness in the y direction D_y .
- (c) the thickness in the z direction D_z .
- (d) the time step.
- (e) the number of nodes in the x direction.
- (f) the number of nodes in the y direction.
- (g) the number of nodes in the z direction.
- (h) the type of initial condition as for SLAB1.
- (i) the type of boundary condition.
- (j) the stopping temperature at the centre of the brick.
- (k) the approach factor as for SLAB1.

Section 3 The initial condition.

- (a) a single value if the input in 1(h) was 1.
- (b) values for all nodes at times 0 and $0-\Delta t$.

Section 4 The boundary condition. Input is organised in the same way as for SLAB1.

A1.3.5 RADIAL

Section 1 The following are read in the order given.

- (a) an index as for SLAB1.
- (b) the run number as for SLAB1.
- (c) the number of input pairs defining $C(T)$.
- (d) the number of input pairs defining $k(T)$.
- (e) the number of nodal points.
- (f) the parameter a ; $a=1$ for a cylinder, and $a=2$ for a sphere.

- (g) the type of boundary condition.
- (h) the type of initial condition.
- (i) the radius of the region R.
- (j) the time step.
- (k) the frequency of printout.
- (l) the stopping temperature at $r=0$.
- (m) the approach factor as for SLAB1.

Section 2 The values of T and $k(T)$ are read in as for SLAB1.

Section 3 The values of T and $C(T)$ are read in as for SLAB1.

Section 4 The initial condition. The input is the same as for SLAB1.

Section 5 The boundary condition. The input is organised in the same way as for SLAB1.

For more than one freezing time calculation all sections must be repeated.

APPENDIX 2ONE-DIMENSIONAL FINITE DIFFERENCE PROGRAMSA2.1 SLAB1A2.2 SLAB2

\$RESET FREE	00000100
FILE 5 (KIND=DISK,TITLE="GENDATA",FILETYPE=7)	00000200
FILE 6 (KIND=PRINTER)	00000300
DIMENSION T(50),TI(50),TT(50),TC(50),TK(50),SPEC(50),COND(50),	00000400
1A(50),BC(50),DC(50),EC(50),KTC(50),CT(50),TIM(50),TS(50),HH(50),	00000500
2TIMHC(50),TIMA(50),TSA(50),HHA(50),TIMHA(50)	00000600
REAL K,KT	00000700
67 READ(5,/) IND,NKUN,NC,NK,NUM,IBC1,IBC2,IC,THIK,DELT,NPRINT,TSTOP,	00000800
1TYPE	00000900
IF(IC .EQ. 2) GO TO 811	00001000
READ(5,/) TIN	00001100
DO 812 I=1,NUM	00001200
TI(I)=TIN	00001300
812 TT(I)=TIN	00001400
GO TO 814	00001500
811 READ(5,/) (TI(I),I=1,NUM),(TT(I),I=1,NUM)	00001600
814 IF(IBC1 .NE. 1) GO TO 815	00001700
READ(5,/) TA	00001800
815 IF(IBC1 .NE. 2) GO TO 816	00001900
READ(5,/) D	00002000
816 IF(IBC1 .NE. 3) GO TO 817	00002100
READ(5,/) H,TA	00002200
817 IF(IBC1 .NE. 4) GO TO 818	00002300
READ(5,/) NFT	00002400
READ(5,/) ((TIM(I),TS(I)),I=1,NFT)	00002500
818 IF(IBC1 .NE. 5) GO TO 819	00002600
READ(5,/) EMISS,TA	00002700
819 IF(IBC1 .NE. 6) GO TO 813	00002800
READ(5,/) NH,NTA	00002900
READ(5,/) ((TIMH(I),HH(I)),I=1,NH)	00003000
READ(5,/) ((TIM(I),TS(I)),I=1,NTA)	00003100
813 IF(IBC2 .NE. 1) GO TO 820	00003200
READ(5,/) TAA	00003300
820 IF(IBC2 .NE. 2) GO TO 821	00003400
READ(5,/) QA	00003500
821 IF(IBC2 .NE. 3) GO TO 822	00003600
READ(5,/) HA,TAA	00003700
822 IF(IBC2 .NE. 4) GO TO 823	00003800
READ(5,/) NFTA	00003900
READ(5,/) ((TIMA(I),TSA(I)),I=1,NFTA)	00004000
823 IF(IBC2 .NE. 5) GO TO 824	00004100
READ(5,/) EMISSA,TAA	00004200
824 IF(IBC2 .NE. 6) GO TO 825	00004300
READ(5,/) NHA,NTAA	00004400
READ(5,/) ((TIMHA(I),HHA(I)),I=1,NHA)	00004500
READ(5,/) ((TIMA(I),TSA(I)),I=1,NTAA)	00004600
825 WRITE(6,826) THIK,IBC1,IBC2	00004700
826 FORMAT(1H0,' SOLUTION OF PARABOLIC PARTIAL DIFFERENTIAL EQUATION I	00004800
1 IN THE REGION 0 < X < D FOR TIME > 0.///',D = ',E16.6,/', AT X = 0 I	00004900
2HE BOUNDARY CONDITION IS OF KIND ',I4,///' AT X = D THE BOUNDARY CO	00005000


```

IF(TP-TK(L)) 22,21,18
18 CONTINUE
21 KT(1)=CUND(L)
GU TO 11
22 IF(L.GT.1) L=L-1
KT(1)=CUND(L)+(CUND(L+1)-CUND(L))/(TK(L+1)-TK(L))*(TP-TK(L))
11 CONTINUE
DO 12 I=1,NUM
DO 25 J=1,NC
IF(TI(I)-TC(J)) 26,27,25
25 CONTINUE
27 CT(I)=SPEC(J)
GU TO 24
26 IF(J.GT.1) J=J-1
CT(I)=SPEC(J)+(SPEC(J+1)-SPEC(J))/(TC(J+1)-TC(J))*(TI(I)-TC(J))
24 IF(1.EQ.1.DR.I.EQ.NUM) CT(I)=CT(I)/2.
12 CONTINUE
DX=THIK/(FLUAT(NUM)-1.)
S=2./3.*DEL1/UX/DX
DO 300 I=2,NUM-1
A(I)=-S*KT(1)
B(I)=CT(1)+S*(KT(I)+KT(I+1))
D(I)=-S*KT(I+1)
E(I)=S*(KT(I+1)*(TI(I+1)+TT(I+1)-TI(I)-TT(I))-KT(I)*(TI(I)+TT(I)
- TI(I-1)-TT(I-1)))+CT(I)*TT(I)
IF(IBC1.NE.1) GO TO 301
T(1)=TA
E(2)=E(2)-A(2)*T(1)
NS=2
GU TO 350
301 IF(IBC1.NE.2) GO TO 302
TA=TI(1)-10.
H=G/(TI(1)-TA)
GU TO 303
302 IF(IBC1.NE.3) GO TO 304
303 KT(1)=H*DX
B(1)=CT(1)+S*(KT(2)+KT(1))
D(1)=-S*KT(2)
E(1)=S*(KT(2)*(TI(2)+TT(2)-TI(1)-TT(1))-KT(1)*(TI(1)+TT(1)-2.*TA
1)+CT(1)*TT(1)+S*KT(1)*TA
NS=1
GU TO 350
304 IF(IBC1.NE.4) GO TO 305
DO 306 I=1,NFT
IF(TIME-TIM(I)) 308,307,306
306 CONTINUE
307 T(1)=TS(I)
309 E(2)=E(2)-A(2)*T(1)
NS=2
GU TO 350

```

```

00010100
00010200
00010300
00010400
00010500
00010600
00010700
00010800
00010900
00011000
00011100
00011200
00011300
00011400
00011500
00011600
00011700
00011800
00011900
00012000
00012100
00012200
00012300
00012400
00012500
00012600
00012700
00012800
00012900
00013000
00013100
00013200
00013300
00013400
00013500
00013600
00013700
00013800
00013900
00014000
00014100
00014200
00014300
00014400
00014500
00014600
00014700
00014800
00014900
00015000

```

308	IF(I .GT. 1) I=I-1	00015100
	T(I)=TS(I)+(TS(I+1)-TS(I))/(TIM(I+1)-TIM(I))*(TIME-TIM(I))	00015200
	GU TO 309	00015300
305	IF(IBC1 .NE. 5) GU TO 310	00015400
	H=EMISS*(CT(I)+273.15)**4-(TA+273.15)**4/(TIC(I)-TA)	00015500
	GU TO 303	00015600
310	DU 311 I=1,NH	00015700
	IF(TIME-TIMH(I)) 313,312,311	00015800
311	CONTINUE	00015900
312	H=HH(I)	00016000
	GU TO 314	00016100
313	IF(I .GT. 1) I=I-1	00016200
	H=HH(I)+(HH(I+1)-HH(I))/(TIMH(I+1)-TIMH(I))*(TIME-TIMH(I))	00016300
314	DU 315 I=1,NTA	00016400
	IF(TIME-TIM(I)) 317,316,315	00016500
315	CONTINUE	00016600
316	TA=TS(I)	00016700
	GU TO 303	00016800
317	IF(I .GT. 1) I=I-1	00016900
	TA=TS(I)+(TS(I+1)-TS(I))/(TIM(I+1)-TIM(I))*(TIME-TIM(I))	00017000
	GU TO 303	00017100
350	IF(IBC2 .NE. 1) GU TO 321	00017200
	T(NUM)=TAA	00017300
	E(NUM-1)=E(NUM-1)-D(NUM-1)*T(NUM)	00017400
	NF=NUM-1	00017500
	GU TO 400	00017600
321	IF(IBC2 .NE. 2) GU TO 322	00017700
	TAA=TI(NUM)-10.	00017800
	HA=QA/(TI(NUM)-TAA)	00017900
	GU TO 323	00018000
322	IF(IBC2 .NE. 3) GU TO 324	00018100
323	KT(NUM+1)=HA*Dx	00018200
	B(NUM)=CT(NUM)+S*(KI(NUM)+KT(NUM+1))	00018300
	A(NUM)=-S*KT(NUM)	00018400
	E(NUM)=S*(KI(NUM+1)*(2.*TAA-TI(NUM)-TT(NUM))-	00018500
	1KT(NUM)*(TI(NUM)+TI(NUM)-TI(NUM-1)-TT(NUM-1)))+CT(NUM)*T(00018600
	2NUM)+S*KT(NUM+1)*TAA	00018700
	NF=NUM	00018800
	GU TO 400	00018900
324	IF(IBC2 .NE. 4) GU TO 325	00019000
	DU 326 I=1,NFTA	00019100
	IF(TIME-TIMA(I)) 328,327,326	00019200
326	CONTINUE	00019300
327	T(NUM)=TSA(I)	00019400
329	E(NUM-1)=E(NUM-1)-D(NUM-1)*T(NUM)	00019500
	NF=NUM-1	00019600
	GU TO 400	00019700
328	IF(I .GT. 1) I=I-1	00019800
	T(NUM)=TSA(I)+(TSA(I+1)-TSA(I))/(TIMA(I+1)-TIMA(I))*(TIME-	00019900
	1TIMA(I))	00020000

	GO TO 329	00020100
325	IF(IBC2 .NE. 5) GO TO 339	00020200
	HA=EMISSA*((TI(NUM)+273.15)**4-(TAA+273.15)**4)/(TI(NUM)-TAA)	00020300
	GO TO 323	00020400
339	DO 331 I=1,NHA	00020500
	IF(TIME-TIMH(I)) 333,332,331	00020600
331	CONTINUE	00020700
332	HA=HHA(I)	00020800
	GO TO 334	00020900
333	IF(I .GT. 1) I=I-1	00021000
	HA=HHA(I)+(HHA(I+1)-HHA(I))/(TIMHAC(I+1)-TIMHAC(I))*(TIME-	00021100
	1TIMHAC(I))	00021200
334	DO 335 I=1,NATA	00021300
	IF(TIME-TIMA(I)) 337,336,335	00021400
335	CONTINUE	00021500
336	TAA=TSAC(I)	00021600
	GO TO 323	00021700
337	IF(I .GT. 1)I=I-1	00021800
	TAA=TSAC(I)+(TSAC(I+1)-TSAC(I))/(TIMAC(I+1)-TIMAC(I))*(TIME-	00021900
	1TIMAC(I))	00022000
	GO TO 323	00022100
400	DO 444 I=NS+1,NF	00022200
	RATIO=-A(I)/B(I-1)	00022300
444	B(I)=B(I)+RATIO*D(I-1)	00022400
	E(I)=E(I)+RATIO*E(I-1)	00022500
	T(NF)=E(NF)/B(NF)	00022600
	KK=NF	00022700
	DO 449 INK=NS+1,NF	00022800
	KK=KK-1	00022900
449	T(KK)=(L(KK)-D(KK)*I(KK+1))/B(KK)	00023000
	NN=NN+1	00023100
	IF(NN .LT. NPRINT) GO TO 33	00023200
	WRITE(6,1000) TIME,(T(I),I=1,NUM)	00023300
1000	FORMAT(10(E12.6,1X))	00023400
1001	FORMAT(1H0) TIME VALUES OF T FROM X = 0 ON THE LEFT,	00023500
	1MOVING TOWARDS X = D'//)	00023600
	NN=0	00023700
33	DO 34 I=1,NUM	00023800
	TI(I)=(TI(I)+TI(I)+I(I))/3	00023900
34	TI(I)=T(I)	00024000
	NIX=(NUM-1)/2	00024100
	IF((T(NIX)-TYPE*TSTUP) .GT. 0.) GO TO 10	00024200
	WRITE(6,1000) TIME,(T(I),I=1,NUM)	00024300
	IF(IND .GE. 0) GO TO 67	00024400
	STJP	00024500
	END	00024600

```

$RESET FREE
FILE 5 (KIND=READER,TITLE="BI0ENG")
FILE 6 (KIND=PRINTER)
C PROGRAM FOR CALCULATION OF FREEZING TIMES FOR FINITE SLABS. SYMMETRY
C BOUNDARY CONDITION APPLIES AT THE SLAB CENTRE. THE PROGRAM IS WRITTEN
C IN BURROUGHS B6700 FORTRAN - A SLIGHTLY MODIFIED VERSION OF FORTRAN
C IV. FILE 6 IS THE LINE PRINTER, AND FILE 5 IS SET TO READ DATA FROM A
C DATA FILE ON DISK CALLED SLABDATA. THE SPECIFICATION OF FILE TYPE IS
C SETTABLE. DOUBLE PRECISION CAN BE USED. VARIABLE DEFINITIONS :-
C
C THIK = SLAB HALF THICKNESS (M)
C H = SURFACE HEAT TRANSFER COEFFICIENT (W/MMC)
C DELT = TIME STEP (S)
C DELX = SPACE INCREMENT (M)
C NUM = NUMBER OF NODAL POINTS IN THE HALF SLAB
C TIME = TIME (S)
C TYME = TIME (HOURS)
C KT = THERMAL CONDUCTIVITY (W/MC)
C CT = VOLUMETRIC SPECIFIC HEAT (J/MMMC)
C T = TEMPERATURE AT TIME LEVEL (M+1) (C)
C TI = TEMPERATURE AT TIME LEVEL (M) (C)
C TT = TEMPERATURE AT TIME LEVEL (M-1) (C)
C TP = TEMPERATURE AT WHICH KT EVALUATED (C)
C NN = COUNT OF TIME STEPS SINCE LAST OUTPUT
C
C A,B,D,E AND RATIO ARE PARAMETERS IN THE GAUSSIAN ELIMINATION SOLUTION
C OF THE SET OF TRIDIAGONAL EQUATIONS.
C
C HRH AND COND DEFINE THE THERMAL CONDUCTIVITY/TEMPERATURE FUNCTION.
C TEMPERATURES ARE PUT IN HRH, AND THERMAL CONDUCTIVITY VALUES IN COND.
C BOSS, SPEC AND ENTH DEFINE THE SPECIFIC HEAT CURVE. BOSS ARE THE TEMP-
C ATURE VALUES, AND SPEC AND ENTH ARE THE SPECIFIC HEAT AND ENTHALPY RE-
C SPECTIVELY. UP TO 50 VALUES CAN BE USED IN EACH CASE. NOTE THAT THEY
C MUST BE LISTED IN INCREASING ORDER OF TEMPERATURE. LINEAR INTERPOLAT-
C ION IS USED. THE DETERMINATION OF THERMAL PROPERTY VALUES COULD BE
C DONE BY SUBPROGRAM BUT I FEEL THAT IT IS EASIER TO FOLLOW IN THE MAIN
C PROGRAM.
C
C NIG IS AN INDEX TO INDICATE THE END OF THE DATA FILE.
C
C
C DIMENSION T(50),TI(50),TT(50),BOSS(50),SPEC(50),HRH(50),COND(50),
C ITP(50),CT(50),KT(50),ENTH(50),A(50),B(50),D(50),E(50)
C REAL KT
C DATA SPEC/1.88,1.92,1.95,2.,2.2,2.3,2.8,3.7,4.2,5.,5.9,7.2,11.,
C 117.,25.,33.,45.,70.,100.,167.,167.,10.,3.69,3.69,3.69/
C DATA BOSS/-40.,-30.,-20.,-18.,-16.,-14.,-12.,-10.,-9.,-8.,-7.,-6.,
C 1-5.,-4.,-3.,-2.5,-2.,-1.5,-1.,-.8,-.7,-.6,0.,20.,40./
C DATA HRH/-40.,-30.,-20.,-15.,-10.,-9.,-8.,-7.,-6.,-5.,-4.,-3.,-2.5
C 1,-2.,-1.5,-1.,-.8,-.7,-.6,0.,20.,40./

```

```

DATA COND/1.67,1.67,1.66,1.64,1.63,1.61,1.60,1.58,1.56,1.52,1.46,
11.35,1.28,1.18,1.04,0.82,0.66,0.55,0.49,0.49,0.557,0.6177
DATA ENTH/0.,19.,38.3,42.3,46.5,51.,56.1,62.6,66.6,71.2,76.6,83.2,
192.3,106.3,127.3,141.8,161.3,190.1,232.0,259.3,276.,284.9,289.,
2362.8,436.6/
C THERMAL DATA FOR TYLOSE HAS NOW BEEN SET
67 READ(S,81) NIG,NRUN,NUM,THIK,DELT,H,TA,TEU,TSTOP
C DATA FOR THE PROBLEM HAS BEEN READ IN
81 FORMAT(3I4,6F8.4)
DU 68 I=1,NUM
TI(I)=TED
68 TI(I)=TED
C INITIAL TEMPERATURE ARRAYS ARE NOW SET
DELX=THIK/(ILUAT(NUM)-0.5)
C NOTE THE WAY THAT DELX IS DEFINED. SEE PUBLISHED PAPER FOR REASONS
TYME=0.
TIML=0.
NN=0
WRITE(6,1002) NRUN,THIK,TA,H,TEU,DELT,NUM
WRITE(6,1000) TYME,IA,(TI(I),I=1,NUM)
C
C
C STATEMENT 10 IS THE FIRST IN THE MAIN PROGRAM LOOP.
10 TIME=TIME+DELT
TYME=TYME/3600.
DU 11 I=2,NUM
11 TP(I)=(TI(I-1)+TI(I))/2.
C TEMPERATURES FOR FINDING THERMAL CONDUCTIVITY HAVE BEEN CALCULATED
C BEGINNING OF LOOP TO FIND THERMAL PROPERTIES
DU 12 I=1,NUM
IF(I.EQ.1) GO TO 24
DU 18 LL=1,50
IF(TP(I)-HRH(LL)) 22,21,18
18 CONTINUE
21 KT(I)=CUND(LL)
GO TO 24
22 L=LL-1
IF(L.LT.1) L=1
KT(I)=CUND(L)+(CUND(L+1)-CUND(L))/(HRH(L+1)-HRH(L))*(TP(I)-HRH
1(L))
24 IF(I.EQ.1.OR.I.EQ.NUM) GO TO 525
VALUE=(TI(I-1)-TI(I+1))*2
IF(VALUE.LT.4.) GO TO 525
C VALUE IS USED AS A CRITERION TO DETERMINE THE METHOD FOR FINDING SPE
C CIFIC HEAT DATA. IF THE DIFFERENCE BETWEEN THE TWO NODAL TEMPERATURE
C S IS MORE THAN 2C THEN ENTHALPY DIFFERENCES ARE USED IN THIS EXAMPLE
C THIS ATTRIBUTE IS SETTABLE.
TB=(TI(I)+TI(I+1))/2.

```

```

00005100
00005200
00005300
00005400
00005500
00005600
00005700
00005800
00005900
00006000
00006100
00006200
00006300
00006400
00006500
00006600
00006700
00006800
00006900
00007000
00007100
00007200
00007300
00007400
00007500
00007600
00007700
00007800
00007900
00008000
00008100
00008200
00008300
00008400
00008500
00008600
00008700
00008800
00008900
00009000
00009100
00009200
00009300
00009400
00009500
00009600
00009700
00009800
00009900
00010000

```

	TF=(TI(I)+TI(I-1))/2.	00010100
	DU 225 JJ=1,50	00010200
	IF(TB=BUSS(J)) 226,227,225	00010300
225	CONTINUE	00010400
227	HH=ENTH(JJ)	00010500
	GU TO 228	00010600
226	J=JJ-1	00010700
	IF(J.LT.1) J=1	00010800
	HH=ENTH(J)+(ENTH(J)-ENTH(J+1))/(BOSS(J)-BUSS(J+1))*(TB-BOSS(J))	00010900
228	DU 245 JJ=1,38	00011000
	IF(TF=BUSS(JJ)) 246,247,245	00011100
245	CONTINUE	00011200
247	HL=ENTH(JJ)	00011300
	GU TO 248	00011400
246	J=JJ-1	00011500
	IF(J.LT.1) J=1	00011600
	HL=ENTH(J)+(ENTH(J)-ENTH(J+1))/(BOSS(J)-BOSS(J+1))*(TF-BOSS(J))	00011700
248	CT(I)=(HH-HL)/(TB-TF)*1.E06	00011800
	GU TO 12	00011900
525	DU 25 JJ=1,50	00012000
	IF(TI(I)=BUSS(JJ)) 26,27,25	00012100
25	CONTINUE	00012200
27	CT(I)=SPEC(JJ)*1.E06	00012300
	GU TO 12	00012400
26	J=JJ-1	00012500
	IF(J.LT.1) J=1	00012600
	CT(I)=SPEC(J)+(SPEC(J+1)-SPEC(J))/(BUSS(J+1)-BUSS(J))*(TI(I)-BUSS(J))	00012700
	CT(I)=CT(I)*1.E06	00012800
12	CONTINUE	00012900
C	SPECIFIC HEAT NOW FOUND. END OF THERMAL PROPERTY LOOP.	00013000
	KT(I)=H*DELX	00013200
C	THIS TAKES ACCOUNT OF THE BOUNDARY CONDITION	00013300
C		00013400
C		00013500
C		00013600
C	PARAMETERS OF THE SET OF TRIDIAGONAL EQUATIONS ARE NOW CALCULATED	00013700
	S=2./3.*DELX/DELX	00013800
	DU 300 I=2,NUM-1	00013900
	A(I)=-S*KT(I)	00014000
	B(I)=CT(I)+S*(KT(I)+KT(I+1))	00014100
	D(I)=-S*KT(I+1)	00014200
300	E(I)=S*(KT(I+1)*(TI(I+1)+TI(I+1))-TI(I)-IT(I))-KI(I)*(TI(I)+TT(I)-TI(I-1)-TI(I-1))+CT(I)*TI(I)	00014300
	A(NUM)=-2.*S*KT(NUM)	00014500
	B(NUM)=CT(NUM)+2.*S*KT(NUM)	00014600
	E(NUM)=S*KT(NUM)*2.*(TI(NUM-1)+TT(NUM-1)-TI(NUM)-TT(NUM))+CT(NUM)*TI(NUM)	00014700
	D(I)=-S*KT(2)	00014800
	B(1)=CT(1)+S*(KT(1)+KT(2))	00014900
		00015000

	$E(I) = S * (KT(2) * (TI(2) + TT(2) - TI(1) - TT(1)) - KT(1) * (TI(1) + TT(1) - 2 * T$	00015100
	$1A)) + CT(1) * TT(1) + S * KI(1) * TA$	00015200
C	BEGINNING OF LOOP TO SOLVE TRIDIAGONAL EQUATIONS	00015300
	DU 444 I=2,NUM	00015400
	RATIO=-A(I)/B(I-1)	00015500
	B(I)=B(I)+RATIO*D(I-1)	00015600
444	E(I)=E(I)+RATIO*E(I-1)	00015700
	T(NUM)=E(NUM)/B(NUM)	00015800
	KK=NUM	00015900
	DU 449 INK=2,NUM	00016000
	KK=KK-1	00016100
449	T(KK)=(E(KK)-D(KK)*T(KK+1))/B(KK)	00016200
C	EQUATIONS SOLVED. BEGINNING OF UPDATING PROCESS FOR NEXT TIME STEP	00016300
	NN=NN+1	00016400
	IF(NN.GT.15) GO TO 33	00016500
C	AT PRESENT PROGRAM PRINTS EVERY 15 TIME STEPS	00016600
	WRITE(C6,1000) TYME,IA,(T(I),I=1,NUM)	00016700
	NN=0	00016800
33	DU 34 I=1,NUM	00016900
	TI(I)=(TI(I)+T(I))/3.	00017000
C	THIS FORM OF UPDATING HELPS AVOID STABLE OSCILLATIONS	00017100
34	TI(I)=T(I)	00017200
	IF(T(NUM).GT.TSTOP) GO TO 10	00017300
C	HAS REQUIRED CENTRE TEMPERATURE BEEN REACHED?	00017400
	WRITE(C6,1000) TYME,IA,(T(I),I=1,NUM)	00017500
	IF(NIG.GE.0) GO TO 67	00017600
C	ARE THERE ANY MORE SETS OF INPUT DATA?	00017700
	CALL EXIT	00017800
1000	FORMAT(F8.3,20F6.2)	00017900
C	NOTE THAT STATEMENT 1000 MUST BE ALTERED IF NUM > 20	00018000
1002	FORMAT(1H1,' CALCULATION OF FREEZING TIME FOR A FINITE SLAB. '//	00018100
	1//,' RUN NUMBER =',I4, '// SLAB HALF THICKNESS (M) =',F8.5, '//	00018200
	2,' AMBIENT TEMPERATURE (C) =',F6.2, '//,' SURFACE HEAT TRANSFER CO	00018300
	EFFICIENT (W/MMC) =',F8.2, '//,' INITIAL TEMPERATURE (C) =',F8.2, //	00018400
	4//,' TIME STEP (S) =',F8.2, '//,' NUMBER OF NODAL POINTS IN HALF SLAB	00018500
	5 =',I4, '//,' TIME TEMPERATURES INTO SLAB ----->', '// (HOURS)	00018600
	6 (DEGREES CELSIUS)', //')	00018700
	END	00018800
		00019000

APPENDIX 3

TWO- AND THREE-DIMENSIONAL FINITE DIFFERENCE PROGRAMS

A3.1 ROD

A3.2 BRICK

\$RESET FREE	00000100
FILE 5 (KIND=DISK,TITLE="TWO D",FILETYPE=7)	00000200
FILE 6 (KIND=PRINTER)	00000300
DIMENSION T(50,50), I(50,50), TT(50,50), TC(50), TK(50), SPEC(50),	00000400
1 COND(50), A(50), B(50), D(50), L(50), KT(50,50), KS(50,50), TB(50,50),	00000500
2 TS(50), TIM(50), CT(50,50)	00000600
REAL KT,KS	00000700
99 READ(5,/) IND, NRUN, NC, NK, NUMX, NUMY, IBC, IC, THIKX, THIKY, DELT, NPRINT,	00000800
1 STUP, TYPE	00000900
IF(IC .EQ. 2) GO TO 811	00001000
READ(5,/) TIN	00001100
DU 812 I=2, NUMX+1	00001200
DU 812 J=2, NUMY+1	00001300
TT(I,J)=TIN	00001400
812 TT(I,J)=TIN	00001500
GO TO 814	00001600
811 DU 631 I=2, NUMX+1	00001700
READ(5,/) (TT(I,J), J=2, NUMY+1)	00001800
631 READ(5,/) (TT(I,J), J=2, NUMY+1)	00001900
814 DU 815 I=1, NC	00002000
815 READ(5,/) TC(I), SPEC(I)	00002100
DU 816 I=1, NK	00002200
816 READ(5,/) TK(I), COND(I)	00002300
IF(IBC .NE. 1) GO TO 817	00002400
READ(5,/) TAA	00002500
817 IF(IBC .NE. 3) GO TO 818	00002600
READ(5,/) H, TAA	00002700
818 IF(IBC .NE. 4) GO TO 819	00002800
READ(5,/) NFT	00002900
DU 820 I=1, NFT	00003000
820 READ(5,/) TIM(I), TS(I)	00003100
819 DELX=THIKX/FLOAT(NUMX-1)/2.	00003200
DELY=THIKY/FLOAT(NUMY-1)/2.	00003300
TIME=0.	00003400
NN=0	00003500
TYME=0.	00003600
AX=2./3.*DELT/DELX/DELX	00003700
AY=2./3.*DELT/DELY/DELY	00003800
WRITE(6,830) NRUN, THIKX, THIKY	00003900
830 FORMAT(1H0, 'RUN NUMBER =', I4, '//	00004000
1 'SOLUTION OF PARABOLIC PARTIAL DIFFERENTIAL EQUATION, IN TWO, SPACE	00004100
2 VARIABLES'//, '0 < X < DX, 0 < Y < DY'//, 'DX =, SPACE	00004200
3E10.6, //, 'DY =, E10.6, //, 'INITIAL TEMPERATURES ...'//)	00004300
DU 832 I=2, NUMX+1	00004400
832 WRITE(6,831) (TT(I,J), J=2, NUMY+1)	00004500
831 FORMAT(10(E12.6, 1X))	00004600
WRITE(6,990)	00004700
990 FORMAT(////)	00004800
IF(IBC .EQ. 1) WRITE(6,833) TAA	00004900
IF(IBC .EQ. 3) WRITE(6,834) H, TAA	00005000

A3.1 ROD

```

IF(IBC .EQ. 4) WRITE(6,836) 00005100
IF(IBC .EQ. 4) WRITE(6,835) ((TIM(I),TS(I)),I=1,NFI) 00005200
833 FORMAT(' FIRST KIND OF BOUNDARY CONDITION.'// ' AMBIENT VALUE = ' 00005300
1,E16.6,///) 00005400
834 FORMAT(' THIRD KIND OF BOUNDARY CONDITION.'// 00005500
1 SURFACE COEFFICIENT H = 'E16.6,/'// ' AMBIENT VALUE = 'E16.6,///) 00005600
835 FURMAT(E16.6,2X,E16.6) 00005700
836 FURMAT(' FOURTH KIND OF BOUNDARY CONDITION.'// ' TIME 00005800
1 F(TIME)',///) 00005900
WRITE(6,335) 00006000
WRITE(6,336) ((TK(I),COND(I)),I=1,NK) 00006100
WRITE(6,337) 00006200
WRITE(6,338) ((TC(I),SPEC(I)),I=1,NC) 00006300
337 FURMAT('///' T (C) C (J/MMMC)'//) 00006400
335 FURMAT('///' T (C) K (W/MC)'//) 00006500
336 FURMAT(E16.6,4X,E16.6) 00006600
IF(IBC .NE. 1) GO TO 840 00006700
NSX=3 00006800
NSY=3 00006900
DO 841 I=1,NUMX+2 00007000
841 T(I,2)=TAA 00007100
DO 842 I=1,NUMY+2 00007200
842 T(2,I)=TAA 00007300
840 IF(IBC .NE. 3) GO TO 850 00007400
NSX=2 00007500
NSY=2 00007600
DO 430 M=2,NUMY+1 00007700
430 KT(2,M)=H*DELY 00007800
DO 440 I=2,NUMX+1 00007900
440 KS(I,2)=H*DELX 00008000
DO 441 I=1,NUMX+2 00008100
TI(I,1)=TAA 00008200
441 TI(1,I)=TAA 00008300
DO 442 J=1,NUMY+2 00008400
TI(1,J)=TAA 00008500
442 TI(1,J)=TAA 00008600
850 DO 851 I=1,NUMX+2 00008700
TI(1,NUMY+2)=TI(I,NUMY) 00008800
851 TT(1,NUMY+2)=TT(I,NUMY) 00008900
DO 852 J=1,NUMY+2 00009000
TI(NUMX+2,J)=TI(NUMX,J) 00009100
852 TT(NUMX+2,J)=TT(NUMX,J) 00009200
185 TIME=TIME+DELT 00009300
NH=NH+1 00009400
IF(IBC .NE. 4) GO TO 500 00009500
DO 860 I=1,NFI 00009600
860 IF(TIME-TIM(I)) 864,863,860 00009700
CONTINUE 00009800
863 TAA=TS(1) 00009900
GO TO 865 00010000

```

864	IF(I .GT. 1) I=I-1	00010100
	TAA=TS(I)+(TS(I+1)-TS(I))/(TIM(I+1)-TIM(I))*(TIME-TIM(I))	00010200
865	DU 866 I=1,NUMX+2	00010300
866	T(I,2)=TAA	00010400
	DU 867 J=1,NUMY+2	00010500
867	T(2,J)=TAA	00010600
	NSX=3	00010700
	NSY=3	00010800
500	DU 410 I=3,NUMX+2	00010900
	DU 410 M=2,NUMY+1	00011000
	TP=(TI(I,M)+TI(I-1,M))/2.	00011100
	DU 18 L=1,NK	00011200
	IF(TP-TK(L)) 22,21,18	00011300
18	CONTINUE	00011400
21	KT(I,M)=COND(L)	00011500
	GO TO 410	00011600
22	IF(L .GT. 1)L=L-1	00011700
	KT(I,M)=COND(L)+(COND(L+1)-COND(L))/(TK(L+1)-TK(L))*(TP-TK(L))	00011800
410	CONTINUE	00011900
	DU 420 M=3,NUMY+2	00012000
	DU 420 I=2,NUMX+1	00012100
	TR=(TI(I,M)+TI(I,M-1))/2.	00012200
	DU 118 L=1,NK	00012300
	IF(TR-TK(L)) 122,121,118	00012400
118	CONTINUE	00012500
121	KS(I,M)=COND(L)	00012600
	GO TO 420	00012700
122	IF(L .GT. 1)L=L-1	00012800
	KS(I,M)=COND(L)+(COND(L+1)-COND(L))/(TK(L+1)-TK(L))*(TR-TK(L))	00012900
420	CONTINUE	00013000
	DU 490 I=2,NUMX+1	00013100
	DU 490 M=2,NUMY+1	00013200
	DU 25 J=1,NK	00013300
	IF(TI(I,M)-TC(J)) 26,27,25	00013400
25	CONTINUE	00013500
27	CT(I,M)=SPEC(J)	00013600
	GO TO 480	00013700
26	IF(J .GT. 1)J=J-1	00013800
	CT(I,M)=SPEC(J)+(SPEC(J+1)-SPEC(J))/(TC(J+1)-TC(J))*(TI(I,M)-TC(J))	00013900
	GO TO 480	00014000
480	IF(I .NE. 2) GO TO 485	00014100
	CT(I,M)=CT(I,M)/2.	00014200
	GO TO 485	00014300
485	IF(M .NE. 2) GO TO 490	00014400
	CT(I,M)=CT(I,M)/2.	00014500
490	CONTINUE	00014600
	DU 670 I=NSX,NUMX+1	00014700
	DU 671 M=NSY,NUMY+1	00014800
	A(M)=-Ax*KS(I,M)/CT(I,M)	00014900
	D(M)=-Ax*KS(I,M+1)/CT(I,M)	00015000

```

B(M)=1.+AX/CT(I,M)*(KS(I,M)+KS(I,M+1))
671 E(M)=AX/CT(I,M)*(KS(I,M+1)*(TI(I,M+1)-TI(I,M))-KS(I,M)*(TI(I,M)-TI
1(I,M-1)))+AY/CT(I,M)*(KT(I+1,M)*(TI(I+1,M)-TI(I,M))-KT(I,M)*(TI(I,
2M)-TI(I-1,M))+TT(I,M)+AX/CT(I,M)*(KS(I,M+1)*(TI(I,M+1)-TT(I,M))-
3KSC(I,M)*(TI(I,M)-TI(I,M-1)))+2.*AY/CT(I,M)*(KT(I+1,M)*(TI(I+1,M)-
4TT(I,M))-KT(I,M)*(TI(I,M)-TT(I-1,M)))
E(NSY)=E(NSY)-A(NSY)*T(I,NSY-1)
A(NUMY+1)=A(NUMY+1)+D(NUMY+1)
DU 672 MM=NSY+1,NUMY+1
RATIO=-A(MM)/B(MM-1)
B(MM)=B(MM)+RATIO*D(MM-1)
672 E(MM)=E(MM)+RATIO*E(MM-1)
TB(I,NUMY+1)=E(NUMY+1)/B(NUMY+1)
KK=NUMY+1
DU 673 II=NSY,NUMY
KK=KK-1
673 TB(I,KK)=(E(KK)-D(KK)*TB(I,KK+1))/B(KK)
670 CONTINUE
DU 674 M=NSY,NUMY+1
DU 675 I=NSX,NUMX+1
A(I)=-AY/CT(I,M)*KI(I,M)
D(I)=-AY/CT(I,M)*KI(I+1,M)
B(I)=1.+AY/CT(I,M)*(KT(I,M)+KT(I+1,M))
675 E(I)=TB(I,M)-AY/CT(I,M)*(KT(I+1,M)*(TI(I+1,M)-TI(I,M))-KT(I,M)*C
1TT(I,M)-TT(I-1,M)))
A(NUMX+1)=A(NUMX+1)+D(NUMX+1)
E(NSX)=E(NSX)-A(NSX)*T(NSX-1,M)
DU 676 MM=NSX+1,NUMX+1
RATIO=-A(MM)/B(MM-1)
B(MM)=B(MM)+RATIO*D(MM-1)
676 E(MM)=E(MM)+RATIO*E(MM-1)
T(NUMX+1,M)=E(NUMX+1)/B(NUMX+1)
KK=NUMX+1
DU 677 MM=NSX,NUMX
KK=KK-1
677 T(KK,M)=(E(KK)-D(KK)*T(KK+1,M))/B(KK)
674 CONTINUE
DU 33 I=1,NUMX+1
DU 34 M=1,NUMY+1
IT(I,M)=(TI(I,M)+TI(I,M)+T(I,M))/3.
34 TI(I,M)=T(I,M)
DU 681 I=2,NUMX+1
TI(I,NUMY+2)=TI(I,NUMY)
681 TI(1,NUMY+2)=TI(1,NUMY)
DU 682 M=2,10
TT(NUMX+2,M)=TT(NUMX,M)
682 TI(NUMX+2,M)=TI(NUMX,M)
IF(CNN.EQ.0) PRINT, GU TO 554
WRITE(6,1012) TIME
DU 331 I=2,NUMX+1

```

```

00015100
00015200
00015300
00015400
00015500
00015600
00015700
00015800
00015900
00016000
00016100
00016200
00016300
00016400
00016500
00016600
00016700
00016800
00016900
00017000
00017100
00017200
00017300
00017400
00017500
00017600
00017700
00017800
00017900
00018000
00018100
00018200
00018300
00018400
00018500
00018600
00018700
00018800
00018900
00019000
00019100
00019200
00019300
00019400
00019500
00019600
00019700
00019800
00019900
00020000

```

331	WRITE(6,1022) (T(I,M),M=2,NUMY+1)	00020100
554	IF((T(NUMX+1,NUMY+1)-TSTOP)*TYPE .GT. 0.) GO TO 185	00020200
	WRITE(6,1012) TIME	00020300
	DU 341 I=2,NUMX+1	00020400
341	WRITE(6,1022) (T(I,M),M=2,NUMY+1)	00020500
	IF(CIND .GT. 0) GO TO 99	00020600
	CALL EXIT	00020700
1012	FORMAT('U TIME = ',E16.0,///)	00020800
1022	FORMAT(10(' E12.6',1X))	00020900
	END	00021000

```

$RESET FILE
FILE 5 (KIND=DISK,TITLE="THREED",FILETYPE=7) 00000100
FILE 6 (KIND=PRINTER) 00000200
DIMENSION T(20,20,20),TI(20,20,20),TT(20,20,20),TM(20,20,20),TN
1(20,20,20),KX(20,20,20),KY(20,20,20),KZ(20,20,20),CT(20,20,20), 00000300
2A(20),B(20),D(20),E(20),TC(50),TK(50),SPEC(50),COND(50),TS(50), 00000400
3TIM(50) 00000500
REAL KX,KY,KZ 00000600
READ(5,/) NK,NC 00000700
READ(5,/) ((TC(I),SPEC(I)),I=1,NC),((TK(I),COND(I)),I=1,NK) 00000800
WRITE(6,40) 00000900
DU 30 M=1,NC 00001000
30 WRITE(6,20) TC(M),SPEC(M) 00001100
20 FORMAT(E16.6,4X,E16.6) 00001200
40 FORMAT(' T (C) C (J/MMHC)' //) 00001300
WRITE(6,70) 00001400
DU 50 M=1,NK 00001500
50 WRITE(6,60) TK(M),COND(M) 00001600
NPRINT=10 00001700
60 FORMAT(E16.6,4X,E16.6) 00001800
70 FORMAT(' T (C) K (W/MC)' //) 00001900
75 READ(5,/) XD,YD,ZD,DELT,NX,NY,NZ,IC,IBC,TSTUP,TYPE 00002000
WRITE(6,80) XD,YD,ZD,NX,NY,NZ,DELT 00002100
80 FORMAT(1H0,' SOLUTION OF PARABOLIC PARTIAL DIFFERENTIAL EQUATI 00002200
1ON IN THREE SPACE VARIABLES. /// DIMENSIONS OF THE BRICK ARE,
2:=' E16.6,' X ' E16.6' X ' E16.6'/// ' GRID SIZE = ' I4' X '
3I4' X ' I4,///' TIME STEP = ' E16.6'///) 00002300
DELT=XD/FLOAT(NX-1)/2. 00002400
DELY=YD/FLOAT(NY-1)/2. 00002500
DELTZ=ZD/FLOAT(NZ-1)/2. 00002600
XX=2./3.*DELT/DELT/VELX 00002700
YY=2./3.*DELT/DELT/VELY 00002800
ZZ=2./3.*DELT/DELT/VELZ 00002900
IF(IC.NE.1) GO TO 140 00003000
READ(5,/) TIN 00003100
DU 90 I=2,NX+1 00003200
DU 90 J=2,NY+1 00003300
DU 90 K=2,NZ+1 00003400
TT(I,J,K)=TIN 00003500
90 TI(I,J,K)=TIN 00003600
GO TO 160 00003700
140 DU 150 I=2,NX+1 00003800
DU 150 J=2,NY+1 00003900
READ(5,/) (TI(I,J,K),K=2,NZ+1) 00004000
150 READ(5,/) (TT(I,J,K),K=2,NZ+1) 00004100
160 IF(IBC.NE.1) GO TO 170 00004200
READ(5,/) TA 00004300
NSX=3 00004400
NSY=3 00004500
NSZ=3 00004600
170 IF(IBC.NE.3) GO TO 180 00004700
00004800
00004900
00005000

```

A3.2 BRICK

	READ(5,/) H,TA	00005100
	NSX=2	00005200
	NSY=2	00005300
	NSZ=2	00005400
180	IF(IBC .NE. 4) GO TO 190	00005500
	NSX=3	00005600
	NSY=3	00005700
	NSZ=3	00005800
	READ(5,/) NFT	00005900
	READ(5,/) ((TIM(I),IS(I)),I=1,NFT)	00006000
190	WRITE(6,210)	00006100
210	FORMAT(' INITIAL CONDITION '///)	00006200
	DO 220 I=2,NX+1	00006300
	WRITE(6,230) (I-2)	00006400
230	FORMAT(' '///' NUMBER OF DELX S IN X DIRECTION = 'I2///)	00006500
	DO 220 J=2,NY+1	00006600
220	WRITE(6,240) (TI(I,J,K),K=2,NZ+1)	00006700
240	FORMAT(' Z -->	00006800
	14X,(11E11,4))	00006900
	WRITE(6,250)	00007000
250	FORMAT(///)	00007100
	IF(IBC .NE. 1) GO TO 260	00007200
	WRITE(6,270) TA	00007300
270	FORMAT(' BOUNDARY CONDITION OF FIRST KIND.'///' AMBIENT VALUE = '	00007400
	1,E16.6,///)	00007500
	GO TO 300	00007600
260	IF(IBC .NE. 3) GO TO 280	00007700
	WRITE(6,290) H,TA	00007800
290	FORMAT(' BOUNDARY CONDITION OF THIRD KIND.'///' SURFACE COEFFICIENT	00007900
	1 = ,E16.6,///' AMBIENT VALUE = 'E16.6,///)	00008000
	GO TO 300	00008100
280	WRITE(6,310)	00008200
310	FORMAT(' BOUNDARY CONDITION OF FOURTH KIND.'///' TIME	00008300
	1 F(TIME),///)	00008400
	WRITE(6,320) ((TIM(I),TS(I)),I=1,NFT)	00008500
320	FORMAT(1X,E12.6,4X,E12.6)	00008600
300	TIME=0.	00008700
	NN=0	00008800
	IF(IBC .NE. 1) GO TO 301	00008900
314	DO 302 I=2,NX+1	00009000
	DO 302 J=2,NY+1	00009100
	TT(I,J,2)=TA	00009200
	TI(I,J,2)=TA	00009300
302	T(I,J,2)=TA	00009400
	DO 303 I=2,NX+1	00009500
	DO 303 K=2,NZ+1	00009600
	TT(I,2,K)=TA	00009700
	TI(I,2,K)=TA	00009800
303	T(I,2,K)=TA	00009900
	DO 304 J=2,NY+1	00010000

	DO 304 K=2,NZ+1	00010100
	TT(2,J,K)=TA	00010200
304	TI(2,J,K)=TA	00010300
	T(2,J,K)=TA	00010400
	GO TO 340	00010500
301	IF(IBC .NE. 3) GO TO 311	00010600
	DO 305 I=2,NX+1	00010700
	DO 305 J=2,NY+1	00010800
	KZ(I,J,2)=H*DELZ	00010900
	CT(I,J,2)=CT(I,J,2)/2.	00011000
	TT(I,J,1)=TA	00011100
305	TI(I,J,1)=TA	00011200
	T(I,J,1)=TA	00011300
	DO 306 I=2,NX+1	00011400
	DO 306 K=2,NZ+1	00011500
	KY(I,2,K)=H*DELY	00011600
	CT(I,2,K)=CT(I,2,K)/2.	00011700
	TT(I,1,K)=TA	00011800
	TI(I,1,K)=TA	00011900
306	T(I,1,K)=TA	00012000
	DO 307 J=2,NY+1	00012100
	DO 307 K=2,NZ+1	00012200
	KX(2,J,K)=H*DELX	00012300
	CT(2,J,K)=CT(2,J,K)/2.	00012400
	TT(1,J,K)=TA	00012500
	TI(1,J,K)=TA	00012600
307	T(1,J,K)=TA	00012700
311	IF(IBC .NE. 4) GO TO 340	00012900
	DO 312 M=1,NFT	00013000
	IF(-TIM(M)) 315,313,312	00013100
312	CONTINUE	00013200
313	TA=TS(M)	00013300
	GO TO 314	00013400
315	IF(M .GT. 1)M=M-1	00013500
	TA=TS(M)+(TS(M+1)-TS(M))/(TIM(M+1)-TIM(M))*(-TIM(I))	00013600
	GO TO 314	00013700
340	TIME=TIME+DELT	00013720
	NN=NN+1	00013740
	DO 330 I=2,NX+1	00013800
	DO 330 J=2,NY+1	00013900
	TT(I,J,NZ+2)=TT(I,J,NZ)	00014000
330	TI(I,J,NZ+2)=TI(I,J,NZ)	00014100
	DO 350 I=2,NX+1	00014200
	DO 350 K=2,NZ+1	00014300
	TI(I,NY+2,K)=TI(I,NY,K)	00014400
350	TI(I,NY+2,K)=TI(I,NY,K)	00014500
	DO 360 J=2,NY+1	00014600
	DO 360 K=2,NZ+1	00014700
	TT(NX+2,J,K)=TT(NX,J,K)	00014800

360	TI(NX+2,J,K)=TI(NX,J,K)	00014900
DO 370	I=2,NX+1	00015200
DO 370	J=2,NY+1	00015300
DO 380	K=3,NZ+2	00015400
	TP=(TI(I,J,K)+TI(I,J,K-1))/2.	00015500
DO 390	L=1,NK	00015600
	IF(TP-TK(L)) 410,400,390	00015700
390	CONTINUE	00015800
400	KZ(I,J,K)=COND(L)	00015900
	GO TO 380	00016000
410	IF(L.GT.1)L=L-1	00016100
	KZ(I,J,K)=COND(L)+(COND(L+1)-COND(L))/(TK(L+1)-TK(L))*	00016200
	1(TP-TK(L))	00016300
380	CONTINUE	00016400
370	CONTINUE	00016500
DO 420	I=2,NX+1	00016600
DO 420	K=2,NZ+1	00016700
DO 420	J=3,NY+2	00016800
	TP=(TI(I,J,K)+TI(I,J-1,K))/2.	00016900
DO 430	L=1,NK	00017000
	IF(TP-TK(L)) 450,440,430	00017100
430	CONTINUE	00017200
440	KY(I,J,K)=COND(L)	00017300
	GO TO 420	00017400
450	IF(L.GT.1)L=L-1	00017500
	KY(I,J,K)=COND(L)+(COND(L+1)-COND(L))/(TK(L+1)-TK(L))*	00017600
	1(TP-TK(L))	00017650
420	CONTINUE	00017700
DO 460	J=2,NY+1	00017800
DO 460	K=2,NZ+1	00017900
DO 460	I=3,NX+2	00018000
	TP=(TI(I,J,K)+TI(I-1,J,K))/2.	00018100
DO 470	L=1,NK	00018200
	IF(TP-TK(L)) 490,480,470	00018300
470	CONTINUE	00018400
480	KX(I,J,K)=COND(L)	00018500
	GO TO 460	00018600
490	IF(L.GT.1)L=L-1	00018700
	KX(I,J,K)=COND(L)+(COND(L+1)-COND(L))/(TK(L+1)-TK(L))*	00018800
	1(TP-TK(L))	00018900
460	CONTINUE	00019000
DO 500	I=NSX,NX+1	00019100
DO 500	J=NSY,NY+1	00019200
DO 500	K=NSZ,NZ+1	00019300
DO 510	L=1,NC	00019400
	IF(TI(I,J,K)-TC(L)) 530,520,510	00019500
510	CONTINUE	00019600
520	CT(I,J,K)=SPEC(L)	00019700
	GO TO 500	00019800
530	IF(L.GT.1)L=L-1	00019900
	CT(I,J,K)=SPEC(L)+(SPEC(L+1)-SPEC(L))/(TC(L+1)-TC(L))*	00020000

	1(TI(I,J,K)-TC(L))	00020100
500	CUNTINUE	00020200
	DU 111 I=2,NX+1	00020300
	DU 111 J=2,NY+1	00020400
111	CT(I,J,2)=CT(I,J,2)/2.	00020500
	DU 112 J=2,NY+1	00020600
	DU 112 K=2,NZ+1	00020700
112	CT(2,J,K)=CT(2,J,K)/2.	00020800
	DU 113 I=2,NX+1	00020900
	DU 113 K=2,NZ+1	00021000
113	CT(I,2,K)=CT(I,2,K)/2.	00021100
	IF(IBC.NE.4) GO TO 540	00021200
	DO 550 M=1,NFT	00021300
	IF(TIME-TIM(M)) 570,560,550	00021400
550	CUNTINUE	00021500
560	TA=TS(M)	00021600
	GO TO 580	00021700
570	IF(M.GT.1)M=M-1	00021800
	TA=TS(M)+(TS(M+1)-TS(M))/(TIM(M+1)-TIM(M))*(TIME-TIM(M))	00021900
580	DU 590 I=2,NX+1	00022000
	DU 590 J=2,NY+1	00022100
590	T(I,J,2)=TA	00022200
	DU 600 I=2,NX+1	00022300
	DU 600 K=2,NZ+1	00022400
600	T(I,2,K)=TA	00022500
	DU 610 J=2,NY+1	00022600
	DU 610 K=2,NZ+1	00022700
610	T(2,J,K)=TA	00022800
540	DU 620 J=NSY,NY+1	00022900
	DU 620 K=NSZ,NZ+1	00023000
	DU 630 I=NSX,NX+1	00023100
	A(I)=-XX*KX(I,J,K)/CT(I,J,K)	00023200
	D(I)=-XX*KX(I+1,J,K)/CT(I,J,K)	00023300
	B(I)=(XX*(KX(I,J,K)+KX(I+1,J,K))+CT(I,J,K))/CT(I,J,K)	00023400
630	E(I)=(XX*KX(I+1,J,K)*(TI(I+1,J,K)-TI(I,J,K))-XX*KX(I,J,K)*(00023500
	1TI(I,J,K)-TI(I-1,J,K))+YY*KY(I,J+1,K)*(TI(I,J+1,K)-TI(I,J,K))	00023600
	2*YY*KY(I,J,K)*(TI(I,J,K)-TI(I,J-1,K))+ZZ*KZ(I,J,K+1)*(TI(I,J	00023700
	3K+1)-TI(I,J,K))-ZZ*KZ(I,J,K)*(TI(I,J,K)-TI(I,J,K-1))+CT(I,J,K	00023800
	4)*TT(I,J,K)+XX*KX(I+1,J,K)*(TT(I+1,J,K)-TT(I,J,K))-XX*KX(I,J	00023900
	5K)*(TT(I,J,K)-TT(I-1,J,K))+2.*YY*KY(I,J+1,K)*(TI(I,J+1,K)-TT(I	00024000
	6I,J,K))-2.*YY*KY(I,J,K)*(TI(I,J,K)-TI(I,J-1,K))+2.*ZZ*KZ(I,J	00024100
	7R+1)*(TT(I,J,K+1)-TT(I,J,K))-2.*ZZ*KZ(I,J,K)*(TT(I,J,K)-TT(I	00024200
	8J,K-1)))/CT(I,J,K)	00024300
	E(NSX)=E(NSX)-A(NSX)*T(NSX-1,J,K)	00024400
	A(NX+1)=A(NX+1)+D(NX+1)	00024500
	DU 640 MM=NSX+1,NX+1	00024600
	RATIO=-A(MM)/B(MM-1)	00024700
	B(MM)=B(MM)+RATIO*D(MM-1)	00024800
640	E(MM)=E(MM)+RATIO*E(MM-1)	00024900
	TM(NX+1,J,K)=E(NX+1)/B(NX+1)	00025000

	KK=NY+1	00025100
	DU 650 MM=NSX,NX	00025200
	KK=KK-1	00025300
650	TM(KK,J,K)=(E(KK)-D(KK)*TM(KK+1,J,K))/B(KK)	00025400
620	CONTINUE	00025500
	DU 660 I=NSX,NX+1	00025600
	DU 660 K=NSZ,NZ+1	00025700
	DO 670 J=NSY,NY+1	00025800
	A(J)=-YY*KY(I,J,K)/CT(I,J,K)	00025900
	D(J)=-YY*KY(I,J+1,K)/CT(I,J,K)	00026000
	B(J)=-YY*(KY(I,J,K)+KY(I,J+1,K))/CT(I,J,K)	00026100
670	E(J)=TM(I,J,K)-(YY*KY(I,J+1,K)*(TT(I,J+1,K)-TT(I,J,K))-YY*KY(I,J,K)*(TT(I,J,K)-TT(I,J-1,K)))/CT(I,J,K)	00026200
1	E(NSY)=E(NSY)-A(NSY)*T(I,NSY-1,K)	00026300
	A(NY+1)=A(NY+1)+D(NY+1)	00026400
	DO 680 MM=NSY+1,NY+1	00026500
	RATIO=-A(MM)/B(MM-1)	00026600
	B(MM)=B(MM)+RATIO*D(MM-1)	00026700
680	E(MM)=E(MM)+RATIO*E(MM-1)	00026800
	TN(I,NY+1,K)=E(NY+1)/B(NY+1)	00026900
	KK=NY+1	00027000
	DO 690 MM=NSY,NY	00027100
	KK=KK-1	00027200
690	TN(I,KK,K)=(E(KK)-D(KK)*TN(I,KK+1,K))/B(KK)	00027300
660	CONTINUE	00027400
	DO 700 J=NSY,NY+1	00027500
	DO 700 I=NSX,NX+1	00027600
	DU 710 K=NSZ,NZ+1	00027700
	A(K)=-ZZ*KZ(I,J,K)/CT(I,J,K)	00027800
	D(K)=-ZZ*KZ(I,J,K+1)/CT(I,J,K)	00027900
	B(K)=ZZ*(KZ(I,J,K)+KZ(I,J,K+1))/CT(I,J,K)+1.	00028000
710	E(K)=TN(I,J,K)-(ZZ*KZ(I,J,K+1)*(TT(I,J,K+1)-TT(I,J,K))-ZZ*KZ(I,J,K)*(TT(I,J,K)-TT(I,J,K-1)))/CT(I,J,K)	00028100
1	E(NSZ)=E(NSZ)-A(NSZ)*T(I,J,NSZ-1)	00028200
	A(NZ+1)=A(NZ+1)+D(NZ+1)	00028300
	DO 720 MM=NSZ+1,NZ+1	00028400
	RATIO=-A(MM)/B(MM-1)	00028500
	B(MM)=B(MM)+RATIO*D(MM-1)	00028600
720	E(MM)=E(MM)+RATIO*E(MM-1)	00028700
	T(I,J,NZ+1)=E(NZ+1)/B(NZ+1)	00028800
	KK=NZ+1	00028900
	DO 820 MM=NSZ,NZ	00029000
	KK=KK-1	00029100
820	T(I,J,KK)=(E(KK)-D(KK)*T(I,J,KK+1))/B(KK)	00029200
700	CONTINUE	00029300
	IF(NN.LT.NPRINT) GO TO 730	00029400
	NN=0	00029500
	WRITE(6,740) TIME	00029600
740	FORMAT(' /// TIME = 'E16.6,///)	00029700
	DO 750 I=2,NX+1	00029800
	WRITE(6,230) (I-2)	00029900
		00030000

	DU 750 J=2,NY+1	00030100
750	WRITE(6,240) (T(I,J,K),K=2,NZ+1)	00030200
	WRITE(6,250)	00030300
730	DU 760 I=1,NX+1	00030400
	DU 760 J=1,NY+1	00030500
	DU 760 K=1,NZ+1	00030600
	TT(I,J,K)=(T(I,J,K)+TI(I,J,K)+TT(I,J,K))/3.	00030700
760	TI(I,J,K)=T(I,J,K)	00030800
	IF((T(NX+1,NY+1,NZ+1)-TSTOP)*TYPE .GT. 0.) GO TO 340	00030900
	WRITE(6,740) TIME	00031000
	DU 780 I=2,NX+1	00031100
	WRITE(6,230) (I=2)	00031200
	DU 780 J=2,NY+1	00031300
780	WRITE(6,240) (T(I,J,K),K=2,NZ+1)	00031400
	IF(IND .GT. 0) GO TO 75	00031500
	CALL EXIT	00031600
	END	00031700

APPENDIX 4

RADIAL FINITE DIFFERENCE PROGRAM

A4.1 RADIAL

	\$RESET FREE	00000100
FILE	5 (KIND=DISK, TITLE="RADDATA", FILETYPE=7)	00000200
FILE	6 (KIND=PRINTER)	00000300
	DIMENSION T(50), TI(50), TT(50), TK(50), TC(50), COND(50), SPEC(50),	00000400
	1A(50), B(50), U(50), E(50), KT(50), CT(50), TIM(50), TS(50), KF(50)	00000500
	1, IH(50), HH(50)	00000600
	REAL K, KT, KF	00000700
67	READ(5,7) INDRUN, NC, NK, NUM, CASE, IBC, IC, THIK, DELT, NPRINT,	00000800
	1TSTOP, TYPE	00000900
	READ(5,7) ((TK(I), COND(I)), I=1, NK)	00001000
	READ(5,7) ((TC(I), SPEC(I)), I=1, NC)	00001100
	WRITE(6,667) ((IK(I), COND(I)), I=1, NK)	00001200
	WRITE(6,668) ((TC(I), SPEC(I)), I=1, NC)	00001300
667	FORMAT(' //, T (C) K (W/MC) '///	00001400
	1(E16.6, 4X, E16.6))	00001500
668	FURMAT(' //, T (C) C (J/MMMC) '///	00001600
	1(E16.6, 4X, E16.6))	00001700
	IF(IC.EQ.2) GU TO 811	00001800
	READ(5,7) TIN	00001900
	DU 812 I=1, NUM	00002000
	TI(I)=TIN	00002100
812	T1(1)=TIN	00002200
	GU TO 814	00002300
811	READ(5,7) (TI(I), I=1, NUM), (TT(I), I=1, NUM)	00002400
814	IF(IBC.NE.1) GU TO 815	00002500
	READ(5,7) TA	00002600
	TT(NUM)=TA	00002620
	T1(NUM)=TA	00002640
	NS=NUM-1	00002700
815	IF(IBC.NE.3) GU TO 817	00002800
	READ(5,7) H, TA	00002900
	NS=NUM	00003000
817	IF(IBC.NE.4) GU TO 818	00003100
	READ(5,7) NFT	00003200
	NS=NUM-1	00003300
	READ(5,7) ((TIM(I), IS(I)), I=1, NFT)	00003400
818	IF(IBC.NE.6) GU TO 551	00003500
	READ(5,7) NH, NTA	00003600
	READ(5,7) ((IH(I), HH(I)), I=1, NH)	00003700
	READ(5,7) ((TIM(I), IS(I)), I=1, NTA)	00003800
551	IF(CASE.EQ.2) GU TO 820	00003900
	WRITE(6,821) NRUN, THIK, (NUM-1)	00004000
821	FORMAT(1H0, ' SOLUTION OF PARABOLIC PARTIAL DIFFERENTIAL EQUATI	00004100
	ION IN CYLINDRICAL COORDINATES. '///, ' RUN NUMBER = 'I4, '///	00004200
	2RADIUS OF CYLINDER = 'E16.6, '///, 'NUMBER OF SPACE DIVISIONS IN R	00004300
	3ADIUS = 'I4, '///)	00004400
	GU TO 822	00004500
820	WRITE(6,823) NRUN, THIK, (NUM-1)	00004600
823	FURMAT(1H0, ' SOLUTION OF PARABOLIC PARTIAL DIFFERENTIAL EQUATI	00004700
	ION IN SPHERICAL COORDINATES. '///, ' RUN NUMBER = 'I4, '///, ' RADIUS	00004800

2	OF SPHERE = 'E16.6,///' NUMBER OF SPACE DIVISIONS IN RADIUS	00004900
	3 = '14,7777)	00005000
822	WRITE(6,825) (TI(I),I=1,NUM)	00005100
825	FURMAT(1H0,///' INITIAL CONDITION.'///' VALUES OF T FROM CENTRE	00005200
	1TOWARDS SURFACE.'//(10E13.6))	00005300
	IF(IBC .NE. 1) GO TO 826	00005400
	WRITE(6,827) TA	00005500
827	FURMAT(1H0,///' BOUNDARY CONDITION OF THE FIRST KIND.'///' SURFA	00005600
	1E VALUE AT (X = R) = 'E16.6,///)	00005700
826	IF(IBC .NE. 3) GO TO 828	00005800
	WRITE(6,829) TA,H	00005900
829	FURMAT(1H0,///' BOUNDARY CONDITION OF THE THIRD KIND.'///' SURFAC	00006000
	1E VALUE AT (X = R) = 'E16.6,///' SURFACE COEFFICIENT = 'E16.6,	00006100
	2777)	00006200
828	IF(IBC .NE. 4) GO TO 830	00006300
	WRITE(6,831) ((TIM(I),TS(I)),I=1,NFT)	00006400
831	FURMAT(1H0,///' BOUNDARY CONDITION OF THE FOURTH KIND.'///'	00006500
	1 TIME F(TIME) '///'(E12.6,4X,E12.6))	00006600
830	IF(IBC .NE. 6) GO TO 552	00006700
	WRITE(6,553)	00006800
	WRITE(6,554) ((TIM(I),TS(I)),I=1,NTA)	00006900
	WRITE(6,445)	00007000
	WRITE(6,555) ((TH(I),HH(I)),I=1,NH)	00007100
553	FURMAT(1H0,'BOUNDARY CONDITION OF SIXTH KIND'///' TIME	00007200
	1 TA(TIME) '///)	00007300
554	FURMAT(' ',(E16.6,4X,E16.6))	00007400
555	FURMAT(' ',(E16.6,4X,E16.6))	00007500
445	FORMAT(' '///' TIME H(TIME) '///)	00007600
552	WRITE(6,832)	00007700
832	FURMAT(1H0,//////' TIME VALUES OF T FROM X = 0 ON THE LE	00007800
	1 FT TO X = R ON THE RIGHT'///)	00007900
	TIME=0.	00008000
	NN=0	00008100
	DELR=THIK/FLOAT(NUM-1)	00008200
	S=2./3.*DELT/DELR/DELR	00008300
835	TIME=TIME+DELT	00008400
	NN=NN+1	00008500
	DO 836 I=1,NUM-1	00008600
	TP=(TI(I)+TI(I+1))/2.	00008700
	DO 837 L=1,NK	00008800
	IF(TP-TR(L)) 839,830,837	00008900
837	CONTINUE	00009000
838	KT(I)=COND(L)	00009100
	GO TO 836	00009200
839	IF(L .GT. 1)L=L-1	00009300
	KT(I)=COND(L)+(COND(L+1)-COND(L))/(TR(L+1)-TR(L))*(TP-TR(L))	00009400
836	CONTINUE	00009500
	DO 840 I=1,NUM	00009600
	DO 841 L=1,NK	00009700
	IF(TI(I)-TC(L)) 843,842,841	00009800

841	CUNTINUE	00009900
842	CT(I)=SPEC(L)*(1.+1./12./(FLOAT(I)**3))	00010000
	GU TO 840	00010100
843	IF(L.GT.1)L=L-1	00010200
	CT(I)=SPEC(L)+(SPEC(L+1)-SPEC(L))/(TC(L+1)-TC(L))*(TI(I)-TC(L))	00010300
	1)*(1.+1./12./(FLUAT(I)**3))	00010400
840	CUNTINUE	00010500
	CT(NUM)=CT(NUM)/2.	00010600
	DU 844 I=2,NUM-1	00010700
	KF(I)=(KT(I)+KT(I-1))/2.	00010800
	A(I)=-S*KT(I-1)+CASE*S*KF(I)/2./FLOAT(I-1)	00010900
	D(I)=-S*KT(I)-CASE*S*KF(I)/2./FLOAT(I-1)	00011000
	B(I)=CT(I)+S*(KT(I)+KT(I-1))	00011100
844	E(I)=CT(I)*TI(I)+S*NT(I-1)*(TI(I-1)+TT(I-1)-TI(I)-TI(I))-S*KT(I)	00011200
	1I)*(TI(I)+TI(I)-TI(I+1)-TT(I+1))+S*KF(I)*CASE/2./FLUAT(I-1)*(00011300
	2TI(I+1)+TT(I+1)-TI(I-1)-TT(I-1))	00011400
	D(I)=-S*2.*(1.+CASE)*KT(I)	00011500
	B(I)=CT(I)+2.*S*(1.+CASE)*KT(I)	00011600
	E(I)=S*KT(I)*(TI(2)+TT(2)-TI(1)-TT(1))*2.*(1.+CASE)+CT(I)*TT(1)	00011700
	IF(IBC.NE.1) GU TO 845	00011800
847	I(NUM)=TA	00011900
	E(NUM-1)=E(NUM-1)-D(NUM-1)*I(NUM)	00012000
	GU TO 850	00012100
845	IF(IBC.NE.3) GU TO 846	00012200
579	KT(NUM)=H*DEL R	00012300
	SA=2.*DEL T*CASE*H/THIK/3.	00012400
	A(NUM)=-S*KT(NUM-1)	00012500
	B(NUM)=CT(NUM)+S*(KI(NUM-1)+KT(NUM))+SA	00012600
	E(NUM)=S*KT(NUM-1)*(TI(NUM-1)+TT(NUM-1)-TI(NUM)-TT(NUM))-S*KT(N	00012700
	1UM)*TI(NUM)+TT(NUM)-2.*TA)-SA*(TT(NUM)+TI(NUM)-3.*TA)+CTC	00012800
	2NUM)*TT(NUM)+S*KT(NUM)*TA	00012900
	GU TO 850	00013000
846	IF(IBC.NE.4) GU TO 571	00013100
	DU 848 L=1,NFT	00013200
	IF(TIME-TIM(L)) 851,849,848	00013300
848	CUNTINUE	00013400
849	TA=TS(L)	00013500
	GU TO 847	00013600
851	IF(L.GT.1)L=L-1	00013700
	TA=TS(L)+(TS(L+1)-TS(L))/(TIM(L+1)-TIM(L))*(TIME-TIM(L))	00013800
	GU TO 847	00013900
571	DU 572 L=1,NH	00014000
	IF(TIME-TH(L)) 574,573,572	00014100
572	CUNTINUE	00014200
573	H=HH(L)	00014300
	GU TO 581	00014400
574	IF(L.GT.1)L=L-1	00014500
	H=HH(L)+(HH(L+1)-HH(L))/(TH(L+1)-TH(L))*(TIME-TH(L))	00014600
581	DU 582 L=1,NTA	00014700
	IF(TIME-TIM(L)) 584,583,582	00014800

582	CONTINUE	00014900
583	TA=TS(L)	00015000
	GU TU 579	00015100
584	IF(L.GT.1)L=L-1	00015200
	TA=TS(L)+(TS(L+1)-TS(L))/(TIM(L+1)-TIM(L))*(TIME-TIM(L))	00015300
	GU TU 579	00015400
850	DU 852 I=2,NS	00015500
	RATIO=-A(I)/B(I-1)	00015600
	B(I)=B(I)+RATIO*D(I-1)	00015700
852	E(I)=E(I)+RATIO*E(I-1)	00015800
	T(NS)=E(NS)/B(NS)	00015900
	KK=NS	00016000
	DU 854 INK=2,NS	00016100
	KK=KK-1	00016200
854	T(KK)=(E(KK)-D(KK)*I(KK+1))/B(KK)	00016300
	IF(NN.LT.NPRINT) GU TU 33	00016400
	WRITE(6,1000) TIME,(T(I),I=1,NUM)	00016500
1000	FORMAT(10E13.6)	00016600
	NN=0	00016700
33	DU 34 I=1,NUM	00016800
	TI(I)=(TI(I)+FI(I)+I(I))/3.	00016900
34	TI(I)=T(I)	00017000
	IF((T(I)-TSTOP)*TYPE.GT.0.) GU TU 835	00017100
	WRITE(6,1000) TIME,(T(I),I=1,NUM)	00017200
	IF(INU.GT.0) GU TU 67	00017300
	CALL EXIT	00017400
	END	00017500

APPENDIX 5

DERIVATION OF MELLOR'S FORMULA

For freezing of a body where all latent heat is released at a unique freezing temperature the temperature profiles within the body are of the form shown in Figure A5.1. This schematic diagram shows typical temperature profiles in a freezing slab at two different times.

For the freezing front to move from position 1 to position 2 the heat to be removed is approximately

$$L + \frac{1}{2} C_l (T_i - T_f) + \frac{1}{2} C_s (T_f - T_a) \quad (A5.1)$$

Treating this as a lump sum and integrating by the method of Plank (1941), the freezing time is given by :

$$t = \frac{1}{T_f - T_a} (L + \frac{1}{2} C_l (T_i - T_f) + \frac{1}{2} C_s (T_f - T_a)) (P \frac{D}{h} + R \frac{D^2}{k_{ave}}) \quad (A5.2)$$

Mellor uses the mean thermal conductivity k_{ave} , and defines L as the latent heat component of the enthalpy change between the initial freezing temperature and the ambient temperature.

The weaknesses in the derivation are in the manner in which the lump sum is found. Immediately after the onset of cooling the simplified situation of Figure A5.1 does not apply because phase change may not start for some time. As the freezing front nears the centre of a finite body the unfrozen region will be at or near the initial freezing temperature. In this instance the simple lump sum given by equation A5.1 considerably overestimates the heat to be removed, and therefore the formula will overestimate the freezing time. Also, the derivation of the lump sum assumes that the surface of the body is at the ambient temperature which is not true where the boundary condition is of the third kind.

In fact, the derivation given above is more valid for

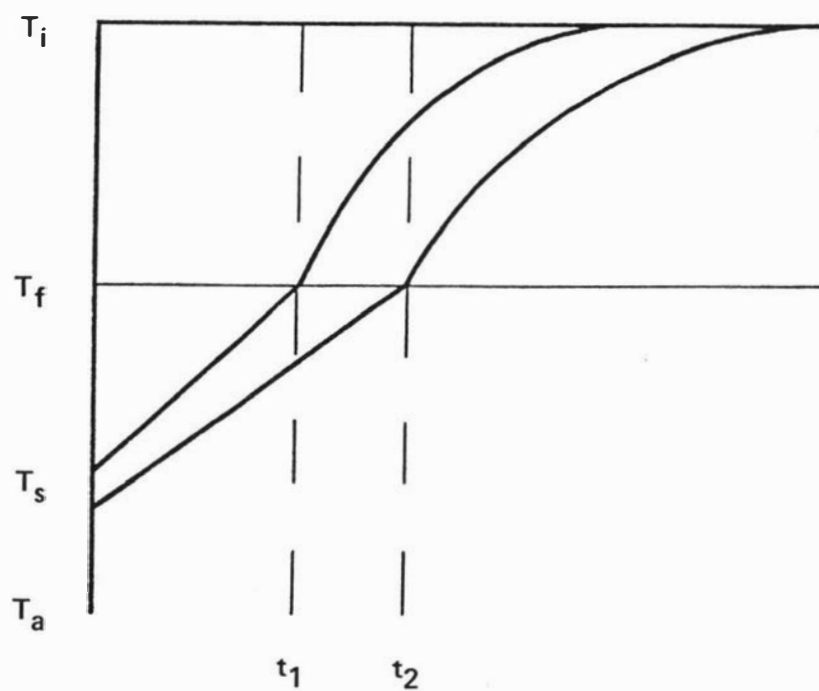


Figure A5.1 Schematic representation of typical temperature profiles within a freezing material where freezing occurs at a unique phase change temperature T_f .

freezing of a semi-infinite body, and therefore will approximate to the solution of Hrycak (1963). The calculated results confirm this, although the range in the results is greater for Hrycak's method.

The physical basis of Mellor's formula cannot be established for a finite body, although it does approximate to freezing of a semi-infinite body.

APPENDIX 6INVESTIGATION OF CHANGING AMBIENT TEMPERATURE

Because of the limitations of the experimental apparatus it was not possible to investigate the effect of a changing ambient temperature on the freezing time experimentally. Simulation by finite differences was used to investigate ambient temperature changes of two types - cycling and an exponential decrease. This simulation should provide an indication of the effect of ambient temperature/time profiles, that could be found in practice, on the freezing time.

A6.1 CYCLING AMBIENT TEMPERATURE

The ambient temperature was assumed to behave in the manner shown in Figure A6.1a. The conditions investigated are given in Table A6.1, and the calculated freezing times for different ambient temperature profiles are given in Table A6.2. The results show that cycling of up to $\pm 2.5^{\circ}\text{C}$ around the mean ambient temperature does not lead to significantly different freezing times to those calculated using a constant average value of T_a . It is therefore valid to use the average ambient temperature in this situation without introducing a significant error.

A6.2 EXPONENTIAL DECREASE IN AMBIENT TEMPERATURE

In many food freezing situations the ambient temperature in the freezer is considerably higher than the set point prior to the freezing process. Once the refrigeration is turned on the ambient temperature falls in some manner until it reaches the set point. An exponential fall will approximate many of these situations.

Figure A6.1b shows the ambient temperature profile used. The calculated freezing times are shown in Table A6.3. The difference between the results obtained using

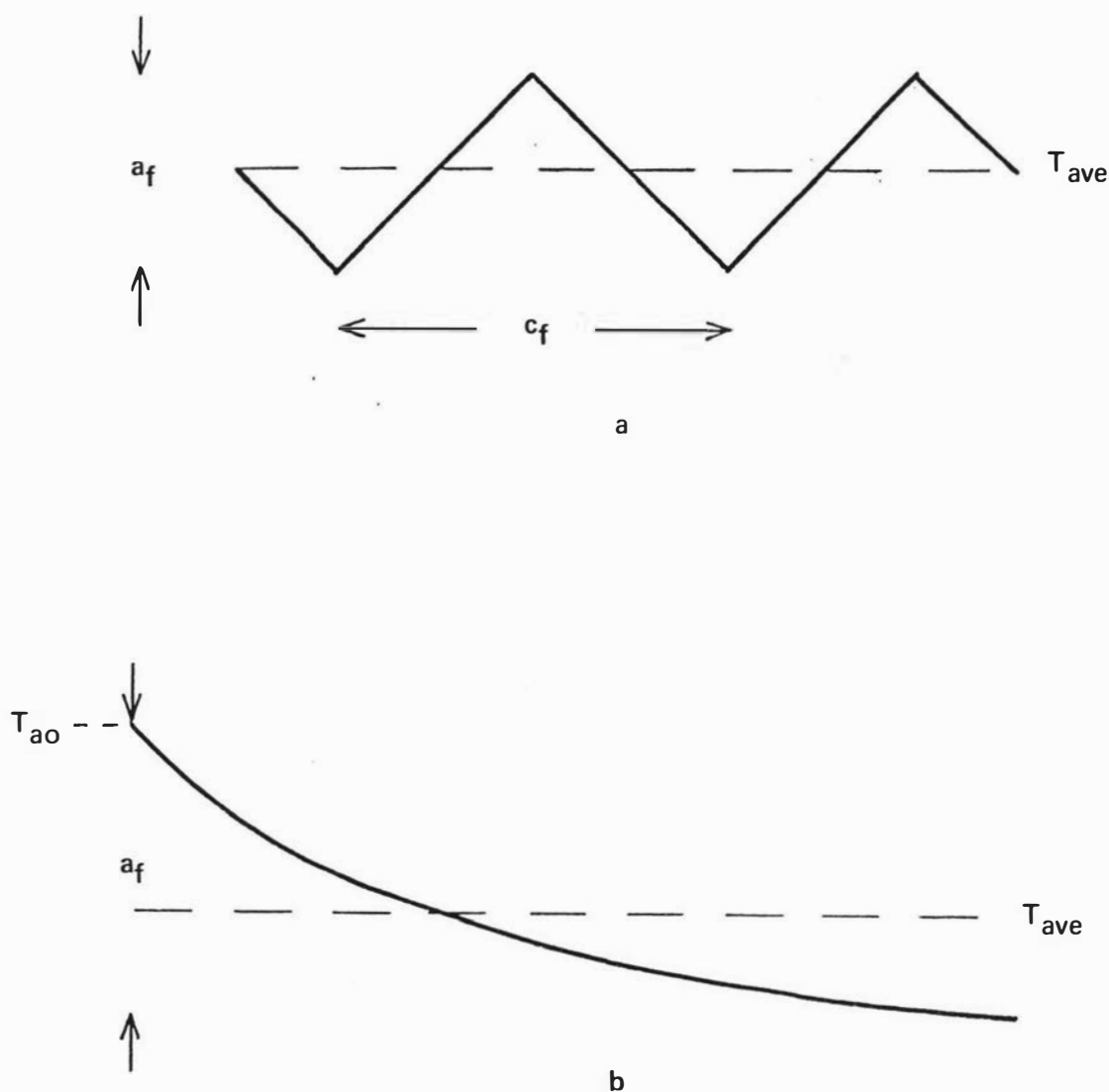


Figure A6.1 Ambient temperature profiles. a – cycling temperature. b – exponential decrease of the form.

$$T_a = T_{ao} - a_f e^{-(t_{el}/c_f t_{fd})}$$

where t_{el} = elapsed time (hrs)

t_{fd} = predicted freezing time for a constant ambient
temperature T_{ave} (hrs)

c_f = relative cycle size

T_{ave} = average ambient temperature ($^{\circ}\text{C}$)

the average ambient temperature and those obtained for an exponential decrease in T_a is small (less than 1.2%), even for cases where the ambient temperature changes by 15°C .

Whilst this analysis does not cover all types of changing ambient temperature that will occur in practice it does indicate that errors introduced by using an average ambient temperature will be small, even for relatively large changes in ambient temperature.

Table A6.1

Conditions used for the investigation of the effect of
changing ambient temperature on freezing time

T_{ave} = average ambient temperature. t_{fd} = freezing time
 calculated by finite differences for constant conditions.

Run	D (m)	h (W/m ² °C)	T_i (°C)	T_{ave} (°C)	t_{fd} (hrs)
1	0.0250	51.9	10.0	-40.0	0.548
2	0.0720	51.9	10.0	-20.0	4.27
3	0.0485	30.6	20.0	-30.0	2.76

Table A6.2

Results of the finite difference simulation of freezing
of a slab subject to a cycling ambient temperature

		Run 1	Run 2	Run 3
$\frac{c_f}{t_{fd}}$	a_f (°C)	t_{fd} (hrs)	t_{fd} (hrs)	t_{fd} (hrs)
0.005	1.0	0.548	4.29	2.76
0.005	5.0	0.548	4.27	2.76
0.10	1.0	0.551	4.28	2.77
0.10	5.0	0.550	4.29	2.76
0.05	3.0	0.549	4.28	2.77

Table A6.3

Results of the finite difference simulation of freezing of a slab subject to an exponential fall in ambient temperature

		Run 1	Run 2	Run 3
c_f	a_f ($^{\circ}\text{C}$)	t_{fd} (hrs)	t_{fd} (hrs)	t_{fd} (hrs)
0.1	3.0	0.549	4.28	2.76
0.5	3.0	0.548	4.30	2.76
0.3	9.0	0.549	4.23	2.77
0.1	15.0	0.548	4.22	2.74
0.5	15.0	0.553	4.22	2.74

APPENDIX 7INVESTIGATION OF NON-UNIFORM INITIAL TEMPERATURE

The effect of a non-uniform initial temperature distribution on freezing time could not be investigated by experiment because of limitations on the equipment available. Therefore an investigation was carried out using simulation by finite differences. This should give a close approximation to the real situation.

The calculations of freezing time were carried out for a slab of Karlsruhe test substance ($D = 0.072\text{m}$; $h = 21.6\text{ W/m}^2\text{C}$; $T_a = -20.0^\circ\text{C}$) with a mean bulk initial temperature of 30.0°C . A linear initial temperature gradient from the surface of the slab to the centre was assumed. The freezing times calculated for the different initial temperature distributions are shown in Table A7.1. The results show that as the degree of non-uniformity increases there is a greater error in approximating the initial temperature by the mean bulk temperature. However the error is small, for a range of 20°C in the initial temperature distribution the difference in calculated freezing times compared to the calculation using the mean bulk temperature is less than 0.5%.

Similar results would be expected for other shapes. Approximation of a non-uniform initial temperature distribution by the mean bulk initial temperature to allow easier calculation of freezing time introduces only very small errors. Whilst this analysis has been carried out using finite difference simulation very similar results would be expected if an experimental investigation was carried out.

Table A7.1

Results from the finite difference simulation of freezing of a slab of Karlsruhe test substance with non-uniform initial temperature

$D = 0.072\text{m}$; $h = 21.6 \text{ W/m}^2\text{°C}$; $T_a = -20.0\text{°C}$.

T_s = initial surface temperature. T_c = initial centre temperature. t_{fd} = calculated freezing time

T_s ($^{\circ}\text{C}$)	T_c ($^{\circ}\text{C}$)	t_{fd} (hrs)
30.0	30.0	10.03
35.0	25.0	10.01
40.0	20.0	9.99
25.0	35.0	10.06
20.0	40.0	10.08